Tesis Doctoral

Ingeniería de Telecomunicación

Self-contained microfluidic platform for general purpose Lab-on-Chip using PCB-MEMS technology

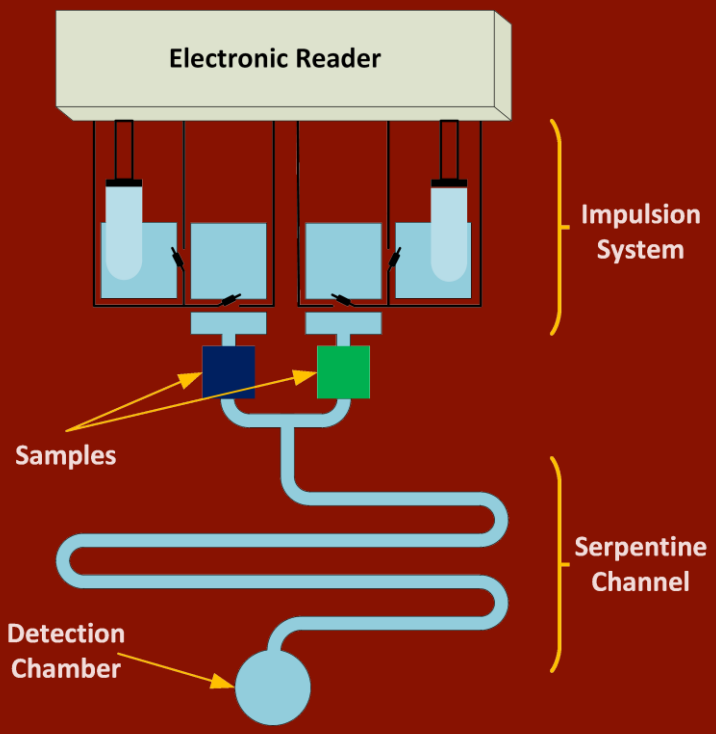

Autora: Guadalupe Flores Salado

Directores: José Manuel Quero Reboul

Francisco Antonio Perdigones Sánchez

Dept. Ingeniería Electrónica

Escuela Técnica Superior de Ingenieros

Universidad de Sevilla

2017

Tesis Doctoral
Ingeniería de Telecomunicación

Self-contained microfluidic platform for general purpose Lab-on-Chip using PCB-MEMS technology

Autor:

Guadalupe Flores Salado

Directores:

José Manuel Quero Reboul

Francisco Antonio Perdigones Sánchez

Dept. de Ingeniería Electrónica

Escuela Técnica Superior de Ingenieros

Universidad de Sevilla

Sevilla, 2017

To Paco and my parents. Thank you for your unconditional support.

Contents

List of Figures

Tables Index

AGRADECIMIENTOS

La realización de una tesis doctoral es una carrera larga y llena de dificultades que no sería posible sin el apoyo desinteresado de mucha gente a la que me gustaría agradecer. Una tesis doctoral implica un sacrificio profesional y personal en el que entra mucha gente en juego, directamente e indirectamente. Es por eso que me gustaría hacer una mención especial a todos aquellos que han formado parte de este trabajo. Estos cinco años no hubiesen podido ser posibles sin ellos.

En primer lugar me gustaría agradecer a quien va dedicada esta tesis, Paco y mis padres, ellos han sido el mejor apoyo que podría haber tenido nunca. Papa y mama, habéis estado ahí desde el principio, siempre apoyándome en todas mis decisiones, aconsejándome y ánimandome. Habéis vivido esta tesis conmigo y por tanto, también es un poco vuestra. Gracias de todo corazón. Gracias a ti también Paco, me conoces, me entiendes, me apoyas y sabes mejor que nadie lo que ha supuesto esta tarea. Has celebrado mis triunfos durante esta tesis, pero también has estado ahí para darme ánimos en los momentos que más lo necesitaba. No tengo palabras para agradecerte lo que has supuesto para esta tesis y estoy segura, que sin tí esto no hubiese sido posible. Gracias por estar siempre ahí, por ser mi compañero de vida.

También me gustaría agradecer esta tesis a mi familia, por su apoyo incondicional. A mis hermanos, tías, tíos y abuelos, siempre interesándose por mí trabajo. También quiero agradecer a mi nueva familia, que también han estado apoyándome e interesándose, muchas gracias Amalia.

Me gustaría agradecer también a todos mis amigos, no hace falta que los nombre, ellos saben quiénes son. Muchas gracias, por escucharme, animarme a luchar y comprender mis momentos de ausencia. Saber que siempre los tengo al lado me ha ayudado a seguir para delante.

También quiero dar las gracias a mis directores de tesis José Manuel Quero Reboul y Francisco Perdigones Sánchez. Sus directrices, consejos, apoyo, dedicación y experiencia han sido fundamentales en este trabajo. Ellos han hecho posible que este trabajo llegue a buen término. Gracias.

No quisiera olvidarme de mis compañeros de grupo, mis compañeros de batallas en las horas de laboratorio. Vuestra ayuda ha sido crucial para realizar este trabajo. Gracias Antonio, por darme la oportunidad de entrar en el grupo. Blas, Miguel, Juan muchas gracias por siempre estar ahí, el compañerismo que he tenido ha sido envidiable. Y especialmente gracias Carmen y de nuevo Fran, ha sido un proyecto en el que hemos ido muchas veces a la par, muchas horas de laboratorio y de artículos escritos juntos. Sé que me llevo más que compañeros de trabajo.

No quería dejar de agradecer al Profesor Stefan Gassmann su ayuda en esta tesis. Gracias por darme la oportunidad de pasar un tiempo en la Universidad de Jade y por dedicarme su tiempo desinteresadamente. Durante la estancia allí aprendí muchas técnicas de fabricación que han sido muy útiles para esta tesis. Además, tuve la suerte de trabajar con un gran profesional, el Ingeniero Helmut Schütte, muchas gracias por la dedicación y consejos.

Finalmente, me gustaría agradecer a los compañeros del Departamento de Ingeniería Electrónica, de un modo u otro han contribuido durante mis años de tesis.

ACKNOWLEDGMENT

A doctoral thesis is a long and difficult career that would not be possible without the disinterested support of many people whom I would like to thank. A doctoral thesis involves a professional and personal sacrifice in which many people come into play, directly and indirectly. For this reason, I would like to make a special mention to all those who have been part of this work. These five years could not have been possible without them.

First of all, I would like to thank those who this thesis is dedicated, Paco and my parents. They have been the best support I could ever have. Dad and mum, you have always been there, supporting me in all my decisions, advising and encouraging me. You have made this possible and therefore, this is also yours. Thanks from the bottom of my heart. Thanks to you Paco, you know me, you understand me, you support me and you know better than anyone what a thesis means. Together we have celebrated my triumphs, but you have been also there for the bad moments, to encourage me. I have no words to thank you and I am sure that without you this would not have been possible. Thank you for always being there, for being my life partner.

I would also like to thank this thesis to my family for their unconditional support. To my brothers, aunts, uncles and grandparents, always concerning about my work. I also want to thank my new family, who have been also there, thank you very much Amalia.

I would like to thank all my friends, it is no necessary to name them, they know who they are. Thank you very much, for listening, for encouraging me and for understanding my absences. Having them nearby helped me to stay ahead.

I also want to thank my thesis directors José Manuel Quero Reboul and Francisco Perdigones Sánchez. Their guidelines, advice, support, dedication and experience have been crucial in this work. Thank you very much.

I would like not to forget my colleagues, my co-combatants during lab hours. Your help has been fundamental to this job. Thanks Antonio, for giving me the opportunity to join the group. Blas, Miguel, Juan many thanks for always helping me, I have found a great environment and fellowship. Especially I want to thanks Carmen and again Fran, it has been a project in which we have worked together many times, many hours in the laboratory and many articles written together. I know I have found more than a working relationship.

I wish also to thank Professor Stefan Gassmann for his help in this thesis. Thank you for giving me the opportunity to spend some time at Jade University and for your time. During the stay there, I learned many manufacturing techniques that have been very useful for this thesis. In addition, I was fortunate to work with a great professional, the Engineer Helmut Schütte, many thanks for the dedication and advice.

Finally, I would like to thank the colleagues of the Department of Electronic Engineering, in one way or another they have contributed during my thesis years.

RESUMEN

El presente trabajo está centrado en la investigación de una nueva plataforma microfluídica autónoma para propósito general fabricada en PCBMEMS. En la vista de la proliferación en los últimos años de los sistemas microfluídicos Lab on Chip (LoC) y la multitud de aplicaciones en las que tienen cabida, surge la necesidad de creación de un sistema portable, autónomo y con una fabricación orientada hacia la producción masiva.

En este contexto, se presenta el trabajo de esta tesis dentro de los proyectos de investigación de financiación nacional ISILAB (TEC2011-29045-C04-02) y BIOLOP (TEC2014-54449-C3-2- R). La tesis se encuentra organizada para cubrir los aspectos previamente propuestos. Primeramente, se presenta una introducción donde se explican los motivos para el desarrollo de este trabajo y cuáles son los objetivos específicos que se quieren cumplir. Seguidamente, se hace un breve estudio del arte. En este estudio se presenta la tecnología MEMS, los principios básicos de la microfluídica, que son los fundamentos de los sistemas LOCs y por último, se detalla un estudio de los principales elementos activos en la literatura que componen una plataforma microfluídica.

Después de la introducción y revisión literaria del marco de esta tesis, se explican los resultados obtenidos. Esta tesis está desarrollada en dos fases principales: el desarrollo de todos los componentes que hacen un lab on chip autónomo de propósito general y el desarrollo de una tecnología basada en estándares para una producción masiva. En la primera fase se detallan los principales componentes que forman parte de una plataforma autónoma multifunción: microválvula, sistema de impulsión, circuito microfluídico y plataforma de sensado. Todos estos componentes son diseñados como un prototipo y están fabricados en SU-8 y PCB-MEMS. El PCB permanece como sustrato y los canales y cámaras microfluídicas

están fabricados en SU-8. La microválvula diseñada presenta una activación termoeléctrica, es de un solo uso y tiene una rápida activación y un consumo bajo de energía. Además, el diseño está pensado para ser altamente integrable en una plataforma microfluídica. El siguiente componente descrito es una sistema de impulsión basado en cámaras presurizadas, este sistema está integrado con la microválvula y su principal característica es la activación en el momento de uso, asegurando la ausencia de pérdidas. Para probar la validez de los componentes anteriores, se desarrolla un circuito microfluídico de propósito general. El circuito está diseñado para mezclar dos muestras y transportarlas a una cámara de detección. Finalmente, se desarrolla una plataforma para la detección de glucosa, integrable en el circuito microfluídico.

Una vez desarrollado el prototipo, el siguiente objetivo de la tesis es el paso de la tecnología de prototipado hacía una de producción masiva. Para ello los materiales utilizados son el PMMA y el PCB. La tecnología PCBMEMS es conocida por su versatilidad para la integración de la electrónica, por lo que lo hace idóneo para la conexión con el exterior. El PMMA es un material también muy extendido en las aplicaciones microfluídicas, debido a su transparencia, bio compatibilidad y su fácil modelado. La unión de los dos componentes representa un desafío en el desarrollo de la tesis, debido a sus diferentes propiedades químicas. El proceso de fabricación se desarrolla integrando la microválvula y el sistema de impulsión, como partes de una plataforma microfluídica. Para terminar, se ha diseñado un pequeño circuito microfluídico para probar la viabilidad del sistema propuesto hacia una tecnología de gran escala.

Finalmente, se exponen las conclusiones de la investigación, las posibles líneas futuras de este trabajo y los apéndices que complementan el trabajo de la tesis.

ABSTRACT

The work presented is focused on the investigation of a new autonomous microfluidic platform manufactured using PCBMEMS technology for general purpose. With the proliferation of the microfluidic platforms, Lab on Chip (LoC), and the multitude of applications which have placed in the market, there is a need to create a self-contained microfluidic platform for general purpose with mass production-oriented manufacturing.

Within this framework, the work of this thesis is presented. This is part of two national research project ISILAB (TEC2011-29045-C04-02) and BIOLOP (TEC2014-54449-C3-2- R). The thesis is organized to cover the aspects previously explained. Firstly, an introduction is presented with the motivation and objectives of this work. Subsequently, a study of the art is done. This study presents the MEMS technology, the basics principles of microfluidics, which are the pillars of the lab on chips and finally, a study of the main active elements presented in the literature.

After the introduction and the literary revision of the framework of this thesis, the results obtained are presented. This thesis is developed in two main phases: the development of all components that make an autonomous general purpose lab on chip and the development of a standards-based technology for mass production. The first phase details the main components of an autonomous multifunction platform: microvalve, impulsion system, microfluidic circuit and sensing platform. All of these components are designed as a prototype and are manufactured in SU-8 and PCBMEMS. The PCB remains as a substrate, and the microfluidic channels and chambers are manufactured in SU-8. The microvalve developed is a single use thermoelectrical microvalve with fast activation and low power consumption. In addition, the design is thought to be highly integrable in a microfluidic plat-

form. The next component is a impulsion system based on pressurized chambers. The system is integrated with the microvalve and its main characteristic is the activation at the moment of use, ensuring the absence of losses. To test the validity of the above components, a general purpose microfluidic circuit is developed. The circuit is designed to mix two samples and transport those to a detection chamber. Finally, a platform for the detection of glucose, integrable in the microfluidic circuit, is developed.

Once the prototype is achieved, the next objective of the thesis is the migration from prototyping technology to mass production. To this end, the materials used are PMMA and PCB. PCBMEMS technology is known for its versatility for the integration of electronics, making it suitable for electrical connection. PMMA is also widely used in microfluidic applications due to its transparency, bio compatibility and easy modeling. The union of the two components represents a challenge in the development of the thesis due to its different chemical properties. The manufacturing process is developed by integrating the microvalve and the drive system, as parts of a microfluidic platform. In conclusion, a small microfluidic circuit is designed by testing the feasibility of the proposed system towards large-scale technology.

Finally, the conclusions of the research, the possible future lines of this work and the appendices that complement the work of the thesis are presented.

1

INTRODUCTION

1.1 Motivation

Over the past decades MEMS has demonstrated a big number of miniaturized sensors, actuator and microstructures with performances exceeding those of their macroscale equivalents. Fields as microfluidics and the concept of lab on chip (LoC) has been growing up in areas from chemical synthesis, biological analysis, optics and informatics. Lab on chips addresses a big number of capabilities in comparison to big scale systems: the ability of use small quantities of samples and reagent, high resolution, short times analysis and low cost. However, the lab on chips are still at an early stage of development and there is much works until reaching the commercialization in mass productions of LoCs. In order to reach the market the are two main approach to overcome: it must provide functionalities of macro level and it must follows the technology that is now available. To address the first approach, the lab on chips must be an autonomous system able to integrate a total sequence of lab processes to perform chemical analysis. In addition, the lab on chips must adjust to the downstream technologies, it must follows standards and interconnectivity to provide a cheap and simple system. The lab on chips developed so far do not fulfill the two requirements explained above, there are LoCs which contains high functionalities but with very complex design and no interfaces or on the other hand, these are highly integrable in a manufacturing scale but without many capabilities. Because of this, research turns towards a new lab on chip platform where all the elements work in an autonomous way, without external sources and in a mass production technology, which standards in the fabrication process and in the outlet ports.

The Microsystem Group of University of Seville is working inside this research. Several doctoral thesis of different microfluidic components have been developed, among them flow focusing systems [1], micropumps [2], microvalves [3–6] and Lab on Chips platforms [7]. Those thesis are the results of different public funding projects in R&D. Among these projects ISILAB (TEC2011-29045-C04-02) is found, a national funding project in collaboration with the National Center of Microelectronics of Barcelona from CSIC institution for the development of a microfluidic platform for the analysis of wine components. Inside the target of this project this work thesis is developed. The main goal of this thesis is the development of a self-contained general purpose Lab-on-Chip highly integrable and low cost. The key part will be the use of the PCB as part of the Lab on chip platform, providing standards and interfaces in the integration between other components.

With this background, it will be necessary to define the requirements and hypothesis of this lab on chip platform in order to identify restrictions in the systems and can contribute with new approaches.

1.2 Hypothesis

The goal of this thesis is the fabrication of a lab on chip platform for the management of fluids in a controlled way and, without any external source. Furthermore, this platform will be designed to be manufactured into mass production, in order to achieve a low cost device. On this basis, the main hypothesis of this thesis are detailed:

Reliability This is a mandatory objective in any device, the lab on chip must fulfill its purpose, the transport of fluids in a controller way without zero losses. In addition, it must assure the tightness of channels and chambers at high pressure.

Self-contained The designed lab on chip must be autonomous, either at the electrical level and pneumatic level. The system must be able to drive the fluids without any external pump or valve. Moreover, the electronic monitoring of the platform must be integrated, becoming a portable lab on chip.

Adaptability and interconnectability The design and fabrication of the system must be simple to be customize to the desired requirements. In addition, the materials and technology used will be adapted to industrial fabrication. The fluidic and electrical interfaces will be designed following standards, developing and interconnectable system.

Low cost Finally, the last objective is the development of a low cost lab on chip. This objective is highly linked with the simplicity of the fabrication process and the used materials. The fabrication process must be focused towards the mass production.

1.3 Outline - structure of the thesis

The presented thesis is organized in five chapters and three appendices in which the developed work, and the obtained results are explained. In addition, a state of

the art related to the field with the different fabrication techniques and the most representative developed systems are included. Finally, there is a bibliography with the most representative references.

The different chapters and appendices are structured as follows:

Introduction The first chapter is the introduction of this thesis where the motivation, objectives and framework of this thesis are described.

State of the art A review of the literature of the thesis is done. The chapter is organized in two parts: a general study of MEMS, microfluidics and materials used and a review of the main microfluidic devices in the literature.

Components of a Lab on Chip In this chapter is described the prototype lab on chip developed in this thesis. A self-contained platform for multipurpose applications. The different components which are part of the LoC are explained in detail.

Towards Mass Production This chapter covers the migration of the prototyped developed platform towards a mass production technology. The fabrication process developed and the implementation of the active components of the prototype.

Conclusions The last chapter encompasses all the conclusions of the main achievements of this work. In addition, the future open lines of this work are described.

Appendix A: Fabrication process developed in Jade university This appendix described the fabrication technologies learnt during the stay in Jade University.

Appendix B: Publications The scientific contribution in journals and conferences upon the frame of this thesis are included in this appendix.

1.4 Framework

This work presented herein has been developed in the Microsystem group of Universidad de Sevilla. It is encompassed into the ISILAB project titled 'Integración de Sensores Inteligentes en Lab-on-Chip para Aplicaciones Biomédicas', which

was funded by the Secretary of State of Investigation, Development and Innovation of the Ministry of Economy and Competitivity of Spain.

Additionally, concerning the PhD student, author of this thesis, her work has been funded by the Ministry of Economy and Competitivity under a FPI (Formación del Personal Investigador) grant BES-2012-054329.

2

STATE OF THE ART

2.1 Introduction

The aim of this chapter is to gather information about the microfluidic systems for management of fluids in the state of the art. The first section provides an overview over the MEMS, definition of the Microelectromechanical Systems, history of MEMS and aspect such as characteristics and fabrication techniques. Secondly, it is introduced the main concepts of Microfluidics, the equations that govern the systems, the dimensionless numbers and the simplification for laminar flow. In addition, it is addressed the main materials used for microfluidics devices. Finally, it is analyzed the work reported by other research groups in the main devices gather in this thesis work, such as microvalves, impulsion systems and lab on chip systems. The different types of microvalves based on its working principle are described, focusing in the thermoelectrical single use microvalves. Moreover, impulsion systems are explained and the chapter ends with the Lab on Chip systems. The main components that may form a lab on chip are summarized and some examples of the devices presented so far.

2.2 Microelectromechanical Systems (MEMS)

Micro-Electro-Mechanical Systems, or MEMS, is a technology that miniaturize mechanical and electro-mechanical elements. The critical physical dimensions of MEMS devices can vary from one micron to several millimeters. Likewise, the types of MEMS devices can vary from relatively simple structures having no moving elements, to extremely complex electromechanical systems with multiple moving elements under the control of integrated microelectronics. These devices (or systems) have the ability to sense, control and actuate on the micro scale, and generate effects on the macro scale [8–10].

MEMS is an original acronym from the United States, but in Europe are also known as Mycrosystem Technology and in Japan Micromachines. An schematics illustrations of MEMS components is detailed in Fig. 2.1. MEMS can be composed of mechanical microstructures, microelectronics, microsensors or/and microactuators.

The history of MEMS dates back to 1950's where Richard Feynman gave the famous lecture 'There's Plenty of Room at the Bottom' [11]. In this lecture he spoke about the 'Tiny Machines' a first approach towards the nanotechnology. In 1960's the first pressure sensor is presented, and Westinghouse developed the

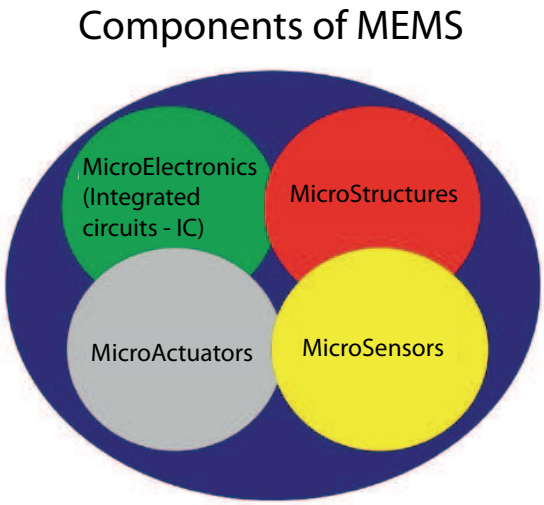

Figure 2.1: MEMS components.

Resonant Gate Field Effect Transistor, in which is described the use of a sacrificial layer to free mechanical parts of a silicon wafer. Besides, in 1970's the first micromachined inkjet nozzle and the first silicon accelerometer were developed. In 1980's the MEMS became more popular, several industries began doing experiments. A disposable blood pressure transducer is manufactured. In the research area paper like 'Silicon as a Mechanical Material', 'Silicon-to-silicon direct bonding method' and 'Graphical piezoresistance coefficient in silicon' were reported [12–14]. In addition, in 1990's the MEMS technology was rising and the methods of micromachining were more accurate towards the improvements of the sensors. A Multi-User MEMS Process is developed by Defense Advanced Research Project Agency, the first surface micromachined accelerometer is sold by Analog Devices (ADXL50). Moreover, the Ion Etching is patented and the Bio MEMS and the Optical MEMS become rising. Finally, in 2OOO's the MEMS technology is totally integrated in the industry and in the Research Centers and, numerous applications have been developed, as can be observed in the Table 2.1 [15, 16]. Moreover, the massive fabrication reduces the fabrication costs. In Fig. 2.2 is shown the MEMS market evolution [17].

Table 2.1: Applications of MEMS

Applications of MEMS				
Automotive	**Electronics**	**Medical**	**Communications**	**Defence**
Internal navigation sensors	Disk drive heads	Blood pressure sensor	Fiber-optic network components	Munitions guidance
Air conditioning compressor sensor	Inkjet printer heads	Muscle stimulators drug delivery systems	RF Relays switches filters	Surveillance
Brake force sensors suspension control	Projection screen televisions accelerometers	Implanted pressure sensors	Projection displays in portable communications devices	Arming systems
Fuel level and vapor pressure sensors	Earthquake sensors	Prosthetics	Voltage controlled oscillators (VCOs)	Embedded sensors
Airbag sensors	Avionics pressure sensors	Miniature analytical instruments	Splitters and couplers	Data storage
Intelligent tires	Mass data storage systems	Pacemakers	Tuneable lasers	Aircraft control

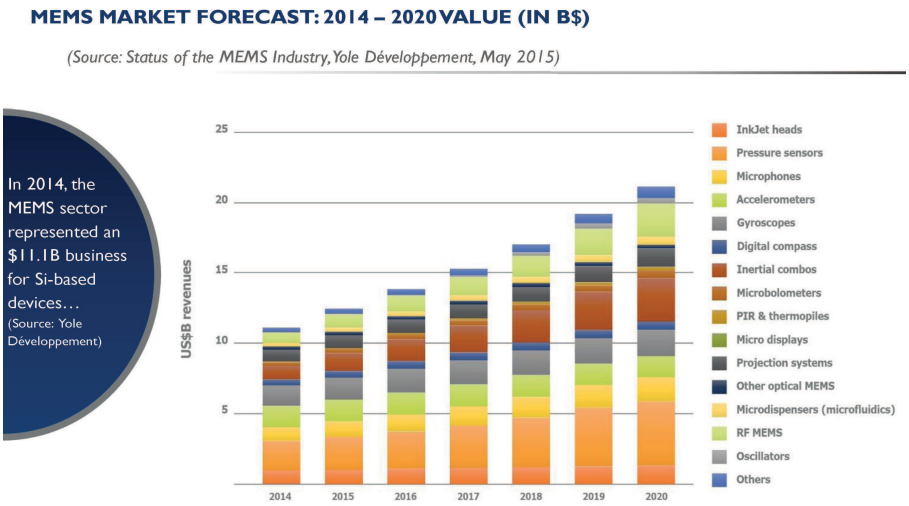

Figure 2.2: MEMS market forecast.

2.2.1 MEMS characteristics

MEMS is a technology that miniaturize mechanical and electro-mechanical elements and the dimensions can be from one micron to milimiters, as it was defined. Consequently, the basic physics and principles of the microlevel need to be understood [18]. The main principles are:

- Friction is greater than inertia. Forces like capillarity, electrostatic and atomic are dominant in micro-level systems.
- Heat dissipation is greater than heat storage.
- Fluidic or mass transport properties are extremely important.
- Material properties (Young's modulus, Poisson's ratio, grain structure) and mechanical theory (residual stress, wear and fatigue, etc.) may be size dependent.
- Miniature device packaging and testing is not straightforward. Certain MEMS sensors require environmental access as well as protection from other external influences. Testing is not rapid and is expensive in comparison with conventional IC devices.

- Cost for the success of a MEMS device, it needs to leverage its IC batch fabrication resources and be mass-produced. Hence mass-market drivers must be found to generate the high volume production.

2.2.2 Fabrication process

The fabrication method for MEMS are based on the techniques for the integrated circuit as oxidation, diffusion, ion implantation, LPCVD, sputtering, etc., and combines these capabilities with highly specialized micromachining processes. MEMS are divided into three basic classification: bulk micromachining, surface micromachining and high-aspect-ratio micromachining (HARM) [19–21].

2.2.2.1 Photolithography

Photolithography is a fabrication technique used to transfer a master pattern onto the surface of a substrate material by UV light. The substrate could be light sensitive or not, if is it not, this is covered with a photoresist to act as a medium to pattern the desired structure. For instance, Integrated Circuits are designed by means of mask and with the deposition of a photoresist over the copper of the Printer Circuit Board (PCB). After UV exposure, the photoresist change its properties and can be eliminated by means of a photoresist developer. As consequence, the copper remains without photoresist in the places that the UV light has reached. Finally, this PCB is introduced in an acid solution, defining the copper tracks. Despite, this technology is commonly used for Integrated Circuit, in MEMS fabrication process there are plenty of application of the photolitography. MEMS wafers are patterned with the deposition of a photoresist for pattering the structure [20, 22, 23]. The PCB are often used as substrate for MEMS devices and many photoresists are used into manufactures 3D structures, like the SU-8 negative photoresist.

2.2.2.2 Bulk Micromachining

Bulk micromachining is the oldest micromachining technology. The fabrication technique is based on the removal of a layer in order to create mechanical parts. The removal can be done by chemical etching or by physical means [24].

The chemical wet etching is the most used in MEMS industry because it provides a high-aspect resolution. There are two types of wet etching: isotropic wet

etching and anisotropic wet etching. In isotropic wet etching the rate does not depend on the crystallographic orientation of the substrate, the etching is carried out in all directions. Normally, this wet etching is proceeded with a mask to isolate the parts that remains. However, a lateral etching is produce under the mask of the same rate of the normal etching, producing a non rectangular profile. Isotropic wet are normally used in MEMS to remove sacrificial layers to control beams or cantilevers [25, 26] and, to micromachined arrays of silicon field emission tips by etching pillar of silicon down to sharp points [27]. The anisotropic wet etching consists on immersing the substrate in a chemical solution where the etching rate depends of the crystallographic orientation of the substrate. Wet anisotropic chemical etching is typically described in terms of etch rates according to the different normal crystallographic places, usually <100>, <110>, and <111>. Several approaches have been developed as pressure sensors [28], accelerometer [29], gas-flow sensors [30], actuators [31], nanowires [32]and micromirros [33] among others.

The dry etching is used with a bombardment of ions, normally plasma, that remove the parts of the wafer that are exposed. The dry etching is an anisotropic etching, because the etching is directional. The most common ions bombardment are reactive ion etching (RIE). RIE is considered a high-aspect-ratio technology due to the smoothly of the walls, as explained below [34, 35].

2.2.2.3 Surface Micromachining

Surface micromachining is a very common technique in MEMS devices [36]. There are several techniques of doing surface micromachining but the most common is based on the use of a sacrificial layers to release structures [37]. This technique is very popular because it provides a high accuracy in the vertical direction. The sacrificial layers used has a precise thickness. Moreover, another important benefit is the wide range of structures that can be defined. However, the main disadvantage of this technology is the stress produced to the layers in the release of the sacrificial layers. Residual stress is created and stiction effect can appear. The most common material for this structures is polysilicon and for the sacrificial layer silicon dioxide.

2.2.2.4 Wafer Bonding

Wafer bonding is a MEMS technique to attach two or more wafers to create a multiwafer stack [38]. There are different types of wafer bonding, but it can be:

direct bonding, surface activate bonding, plasma anodic bonding, eutectic bonding, glass frit bonding, adhesive bonding, thermocompression bonding, reactive bonding and transient liquid phase diffusion bonding. Direct bonding is used to bond two silicon wafers together without any intermediate layer [13]. The silicon direct bonding is based on intermolecular interactions including van der Waals forces, hydrogen bonds and strong covalent bonds. This fabrication technique can be really useful for creating thicker structures where the mass has to be higher or for creating several layers structures [39]. Surface activated bonding (SAB) is a wafer bonding doing under low temperature and activated surfaces by fast atom bombardment. This activation is used to clean the surfaces and improve the bonding without high temperature. The bombardment removes dirtiness and native oxides in the surfaces. Moreover, the activation create direct bonding between the surfaces. This bonding is used to attach metal, semiconductors and dielectrics and, it is carried out in ultra-high vacuum (UHV) of 10^{-7} Pa [40, 41]. Plasma activate bonding is a derivative for surface activate bonding but the activation is carried out with plasma [42, 43]. Anodic bonding is also another bonding technique by means of ionic glass [44]. This is accomplished with the application of a electrostatic field. Finally, another wafer bonding technique is based on the used of an intermediate layer to bond wafers. Among the intermediate bonding layers can be found epoxy resins, photoresist, polyamides, silicones and polymers [45, 46].

2.2.2.5 High-Aspect Ratio Micromachining

High-Aspect Ratio Micromachining (HARM) consist on micromachining an structure that requires micromachining as part of the fabrication process for the creation of microstructures by mouldering. Different materials can be used since electroformable metals to plastics and thermoplastics as acrylate, policarbonate, polyimide and styrene. It is a very promising technology at a high performance-to-cost ratio and several techniques as LIGA or Hot embossing are included in this category.

LIGA is a German acronym for 'Lithographue Galvanoformung Adformung'. The fabrication technique involves the exposition of PMMA to X-ray synchrotron radiation under a lithographic mask. The areas which are exposed are developed and the structure pattern by the mask is defined with a high resolution and nearly perfectly vertical walls. Afterward, the PMMA developed acts as a mold, it is inserted into a electroplatting bath and a metal is is placed into the open areas. Finally, the PMMA is removed and the structure in metal remains [47–50].

Hot Embossing is another HARM technique for creating structures by molding [51, 52]. The main difference between hot embossing and LIGA is the non use of X-ray. A mold is fabricated using an appropriate fabrication method (for instance micromachining, LIGA). This mold is placed with the polymer substrate into a hot embossing system, consisting in two hot plates and pressure source. The mold and the polymer are pressured and heated above the glass transition temperature of the polymer substrate. Later on, the polymer is cooled down and the structure is de-embossed. The main advantage is the cost of non using X-ray for every structure built.

2.3 Microfluidics

In this section is going to be studied the microfluidics, due to the repercussions it has in the thesis work. Microfluidics studies the behaviour of fluids through microchannels. This involves a multidisciplinar field containing physics, engineering, chemistry, biochemistry, nanotechnology and biotechnology. The microlevel means in microfluidics volumes lower than μL and physical behaviour where the surface tension, energy dissipation and fluidic resistance dominate the system [53]. Many components such as injector, nebulizers, Lab on a Chip, Micropumps or fuel cells have been developed in this technology. Having a great repercussion the inkjet printheads and the DNA chips. Moreover, this field has not been totally developed yet, there is plenty of research non studied [54].

The main advantages of working in microscale fluidics are:

- Low production cost. Due to the microlevel, the cost of materials decreases.
- Low volumes of samples and reagents. Despite using less volume of samples and reagents, the residual waste is also lower.
- Higher speed in reactions and analysis. As flow become laminar the mixing of fluids is higher.
- Biocompatibility. Due to the polymers arising, many of the microfluidics devices are manufactured being biocompatible.
- Working in an aseptic environment. Many of the microfluidics components are manufactured in clean rooms where the amounts of particles are controlled. This feature together with the biocompatible materials, makes the microfluidic suitable for bio chips.

- Transparency. The transparency of polymers makes those very versatile for optical sensing. Moreover, it helps in the visualization of the fluids through the microchannels.

- Parallelization. Due to the new fabrication techniques, parallelization provides an opportunity for the fabrication of massive devices with the same features. Moreover, it helps in the parallelization of distinct device operation and/ or the reliability through redundancy.

- Portability. Due to the miniaturization, the devices can be easily portable which can be a great approach in the bio applications for the patient user.

- Low cost in the analysis of samples. Due to the low volume of samples and to the portability, the microfluidics leading to significant cost saving in comparison with traditional detection systems.

The physical behaviour of the microfluidics is based on the Navier-Stokes equations [55]. The motion of a fluids can be seen as Newton's second law of motion for fluids. This equations assumes the mass conservation, also called continuity equation (2.1), the conservation of momentum, the equations of motion (2.2), and the conservation of energy, the energy equation(2.3):

$$\frac{\partial \rho}{\partial t} + \nabla \cdot (\rho \vec{v}) = 0 \tag{2.1}$$

$$\rho(\frac{\partial \nu}{\partial t} + \vec{v} \cdot \nabla \vec{v}) + \nabla p = \nabla \cdot \tau + \rho \vec{f_m} \tag{2.2}$$

$$\rho(\frac{\partial \varepsilon}{\partial t} + \vec{v} \cdot \nabla \varepsilon) = \nabla \cdot (k \nabla T) - \rho \nabla \cdot \vec{v} + \Phi_\nu + Q_r + Q_q \tag{2.3}$$

where ρ is the fluid density, $\vec{v}$ is the velocity vector field, p is the pressure, τ is the stress tensor, $\vec{f_m}$ is the vector of the mass forces per unit volume, ε is the thermodynamic internal energy, k is the temperature coefficient, T is the temperature, Φ_ν work of forces in the deformation of a particle, Q_r is the radiative heating and Q_q is the viscous heating. These equations are the theoretical bases of fluid flow modeling, solving them gives the flow rate and the pressure in a channel. However, due to his complexity there are ways to simplify the equations depending the flow regime of interest. This simplifications are characterized by dimensionless numbers, the most typical are: Reynolds Number, Péclet Number, Capillary

Number and Weber Number. These numbers are going to be explained in details and the flow regimes of applications:

- **Reynolds Number**

  Reynolds number is the ratio between the inertia force and the viscous force (2.4) [56]:

$$Re = \frac{\rho v L}{\mu} \tag{2.4}$$

  where ρ is the density, v the velocity, L is the characteristic length and μ is the viscosity of the fluid. However, for a flow in a pipe or a tube, the characteristic Length L is normally replaced by the hydraulic Diameter D_h which is defined by the perimeter and the area (2.5):

$$D_h = \frac{4A}{P} \tag{2.5}$$

  This number is used to determine if the flow is laminar, transient or turbulent. If $Re < 2300$ is a laminar flow, whereas $2300 < Re < 3000$ is a transient flow and in case $Re > 3000$ is a turbulent flow. In microfluidics most of the time the regime is laminar, due to small dimensions of channels.

- **Péclet Number**

  Péclet Number is the ratio of the contributions to mass transport by convection to those by diffusion (2.6) [57]:

$$Pe = \frac{vL}{D} \tag{2.6}$$

  where v is the velocity, L is the characteristic length and D is the diffusion coefficient. Péclet number is proportional to system size, in the microscale it is lower than one. This means that diffusion contributes more efficiently to mass transfer, so the mixing can be achieved without mixing.

- **Capillary Number**

The Capillary Number is the ratio between the viscous force and the surface tension in an interface between a liquid and a gas, or between two immiscible liquids(2.7) [58]:

$$Ca = \frac{v\mu}{\sigma} \tag{2.7}$$

where v is the velocity, μ is the viscosity and σ is the surface or interfacial tension between the two fluid phases. If Ca < 10^{-5}, the regime is dominated by capillary forces, on the contrary, if it is bigger than 10^{-5}, capillary forces are negligible in comparison with viscous forces. In microfluidics, the surface tension is dominant.

- **Weber Number**

  Weber number is the ratio between deforming inertial force and the surface tension force for a fluid (2.8) [59]:

$$We = \frac{\rho v^2 L}{\sigma} \tag{2.8}$$

  where ρ is the density, v is the velocity, L is the characteristic and length and σ is the surface or interfacial tension between the two fluid phases. The Weber Number indicate which force is dominant the kinetic force or the surface tension. The lower the Weber number is the mire dominant is the surface tension and vice versa. The Weber Number is very useful for the analyzing of droplets and bubbles.

There are another dimensionless numbers that has not been explained because it has been only considered the most significant for the developed system. Among these can be found: Strouhal Number, Mach Number, Euler Number, Froude Number and Prandtl Number [55].

The Navier-Stokes equations are very complicated to solve in a closed form. However, under some cases this equations can be simplify. For the thesis background, some assumptions can be admit and the flow regime can be solved by the Hagen-Poiseuille Law (2.9) [60]:

$$\Delta P = R_f \cdot Q \tag{2.9}$$

where ΔP is the increased pressure in the channel, Q is the flow rate in the channel and R_f is the fluidic resistance in the channel. The fluidic resistance depends of the geometry of the channel, for instance for a circular shape channel is defined by (2.10) and for a square channel (2.11).

$$R_f = \frac{128\mu L}{\pi D^4} \tag{2.10}$$

$$R_f = \frac{28.4\mu L}{L^4}. \tag{2.11}$$

The different assumptions for these simplifications are:

- Incompressible fluids. The density remains constant, so it implies the continuity equation is equal to zero: $\nabla \cdot (\rho \vec{v}) = 0$.
- Steady flow. There is not variation in time and the flow is unidirectional, laminar flow.
- Newtonian fluid. The fluid is incompressible and the viscosity is constant ($\nu = 0$).
- The forces responsible for the fluids are related with the pressure and the gravitation acceleration.
- Entrances and exits effects are negligible. The length of the channel is big enough.

Morever, the goal in this thesis work is the monitorization of fluids in a LoC platform. Fluids are going to transported in a controller way from one point of the microfluidic circuit to another. Applying the Ideal gas Law in a close circuit, the system can be solved under two conditions: the particles have no forces acting among them and the volume occupied by the molecules themselves is entirely negligible relative to the volume of the container [61]. The equation states (2.12):

$$PV = nRT \tag{2.12}$$

where P is the pressure in the system, V is the volume, n is the number of moles, R is the gas constant (8.31441 $JK^{-}1mol^{-}1$) and T ins the temperature. The Ideal gases Law is the simplification of the fourth Gas Laws: Boyle's Law, which relates the pressure with the volume, Charles' Law, which relates the temperature with the volume, the Gay-Lussac's Law, which relates the pressure with

the temperature, and the Avogadro's Law, which relates the volume with amount of gas [62]. For the development of this thesis, the goal is focusing in the volume transport in steady state, as it was commented. Consequently, the fluid is going to be driven by controlling the pressure for a constant temperature by means of the Boyle's Law (2.13):

$$P_1 V_1 = P_2 V_2 = k \tag{2.13}$$

Boyle's Law states that the volume of a given amount of gas held at constant temperature, is inversely proportional to the applied pressure when the temperature and mass are constant. For a close system, the product of the initial pressure and volume (P_1, V_1) is equal to the product of the pressure of volume after a change (P_2, V_2) under constant temperature.

2.4 Materials for microfluidic devices

The MEMS fabrication techniques was discussed in the section (2.2.2), in this section the importance of the silicon was commented. Silicon was the first material used in microfluidics, due to the inherit of microfabrication in the semiconductor industry. It presents a great advantages over other materials, the high accuracy in the fabrication and the mass production. On the contrary, the fabrication for a single chip is very expensive, the needed cost needed for prototyping a chip are very high due to the equipment and the clean environment and, because of the silicon is not a permeable material, it is not suitable for long term cell culture. These reasons, motivate the development of other materials more suitable for microfluidics [63, 64]. Among this materials can be found the polymers, which can be divided at the same time in three groups: elastomers, thermoplastics and thermosets [65].

In the development of this thesis, the technology used to manufactured the Lab on Chips are the polymers and the PCB-MEMS. In particular SU-8 and PCB for the prototype and PMMA and PCB for the industry prototype. As a result, this section is going to be focused in the description of the three fabrication materials used in this thesis.

2.4.1 SU-8

SU-8 is defined as high contrast, epoxy based photoresist designed for micromachining [66] and other microelectronics applications where a thick, chemically

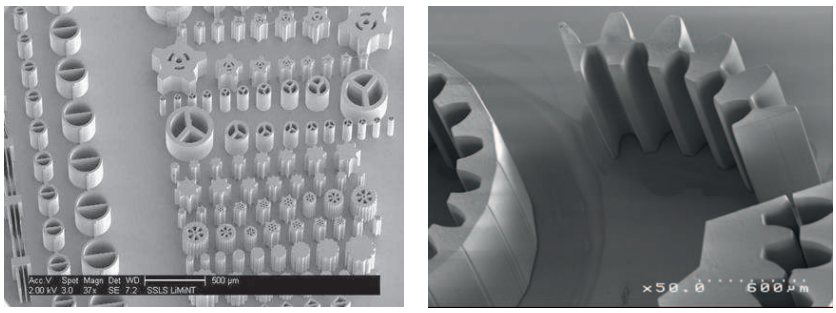

Figure 2.3: Examples of microstructures in SU-8.

and thermally stable image is desired, Fig. 2.3. The reason for the use of this polymer is the fast and easy fabrication process for rapid prototyping and the high-aspect ratio in the fabrication. Moreover, the material is optically transparent that makes it very convenient for fluidics applications. SU-8 was developed and patented by IMB-Watson Research Center and it is one of the most used polymers in MEMS fabrication [67, 68], due to the interesting technical properties of the material, Table. 2.2.

In addition to the technical properties of the SU-8, there are other advantages for using the SU-8 as a polymer for microfluidics system:

- SU-8 is a biocompatible material, this characteristic is very suitable in LoC platforms for working with bio samples [69].

- SU-8 is a hydrophobic material, this property is really important for microfluidics devices, because it avoids that fluids adhere to the walls of channels [70].

- It is a transparent material, which is very suitable for observing the liquids and for the possibility of inserting light sensors.

- SU-8 presents a good mechanical and chemical strength. This is stiffer than others polymers, the risk of deformation is lower [71].

- It is low cost, the material is very suitable in the fabrication of prototypes and single used devices like most of the microfluidics chips.

Table 2.2: SU-8 properties

Properties	**SU-8 2000**
Tone	Negative
Max Single Coat Thickness (μm)	250
Aspect Ratio	10 : 1
Storage Condition / Life	$15 - 30^{\circ}C$/ 1 year
Softening point, DMA (°C)	210
Young's Modulus (GPa)	2.0
Coeff. of Thermal Expansion, CTE (ppm/°C)	52
Tensile Strength (MPa)	60
Elongation at Break (%)	6.5
Thermal Conductivity (W/m·K)	0.3
Dielectric Constant, 1 GHz, 50% RH	4.1
Dielectric loss, 1 GHz	0.015
Dielectric Strength (V/μm)	112
Volume Resistivity ($\Omega \cdot$ cm)	$2.8{\cdot}10^{16}$
Surface Resistivity ($\Omega \cdot$ cm)	$1.8{\cdot}10^{17}$

2.4.1.1 SU-8 Fabrication Process

SU-8 fabrication process is based on photolitography, SU-8 is a negative epoxy photoresist which is exposed with conventional UV light (350-400 nm) meanwhile a mask to create the desire 3D structures. The SU-8 fabrication process start over a substrate, where the SU-8 is deposited in coats. The typical substrates used for SU-8 are Silicon, Glass, Quartz and FR4. Despite Quartz and Silicon are the most common used in MEMS, FR4 is growing in recent years due to the low cost and the possibility of the integration of electronics in a microfluidic platform. The process flows is summarized in Fig. 2.4 and it is going to be explained in detail following the datasheet provided by the manufacturer [72].

1. **Substrate Pretreat**. Firstly, like most fabrication process, the substrate should be cleaned to eliminate any dirtiness. In this particular case, for FR4, the substrate is clean with Acetone to eliminate any rest of organic material and with Isopropanol (C_3H_8O) to clean the surface. Moreover, the surface should be dried before the deposition of SU-8. In some cases, the surface can be pretreat with an adhesion promoter, but in FR4 with the SU-8 2000 series Microchem [66] is not necessary.

2. **Coat**. The next step is the deposition of the SU-8 coat. The coat is deposited with the help of a spin coater. The viscosity of the SU-8 and the revolution per minute of the spin coater will give the thickness of the coat. The SU-8 manufacturer company gives the curves of thickness versus revolution per minute (r.p.m.), in this thesis work, Microchem Co, Fig. 2.5. The procedure for the coat deposition starts by dispensing 1 ml of resist for each 25 mm of substrate diameter, the dispensed of the SU-8 is accomplish directly from bottle to avoid bubbles. Secondly, the substrate is spinned at 500 r.p.m. for 10 seconds. Finally, the spin coater is set to the desire r.p.m depending the SU-8 thickness desired.

3. **Edge Bead Removal (EBR)**. During the deposition of the coat, an accumulation of SU-8 may occur on the edge of the substrate. This should be eliminated with a solvent to assure that the photomask can be placed into close contact with the surface, improving the resolution and the aspect ratio.

4. **Soft Bake**. This step is used to eliminate the solvent of the SU-8 and leaves the coat solidified. This task is accomplished heating the SU-8 at a certain temperature. The heating is carried out in a hot plate, because it is necessary

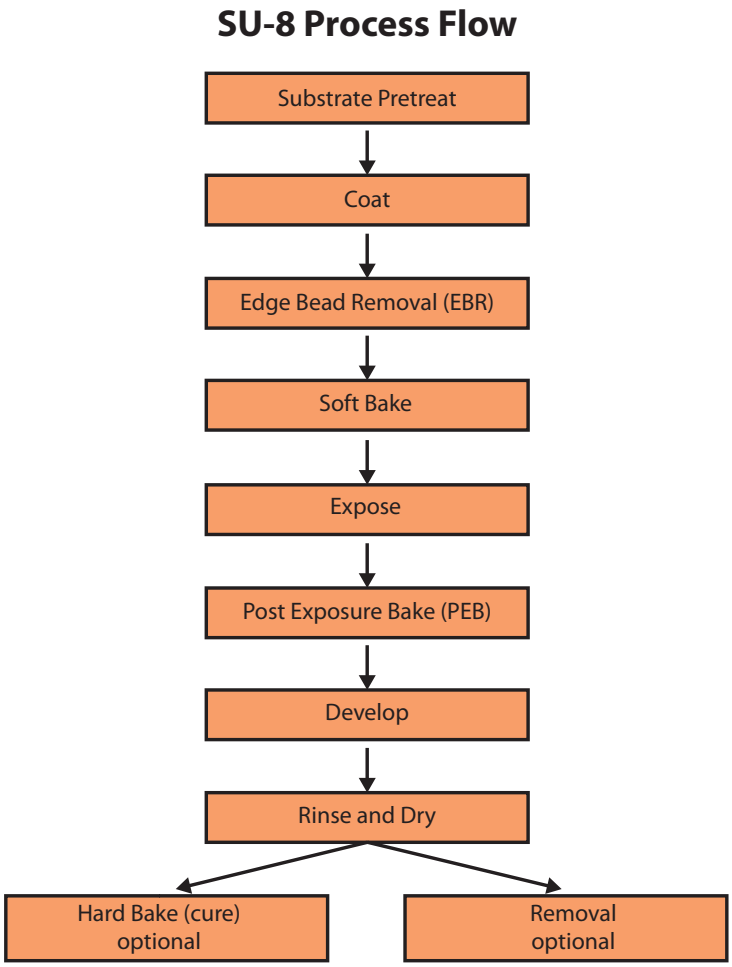

Figure 2.4: SU-8 Fabrication Process Flow.

to release the gas produced by the evaporated solvent leaves. In convection ovens, a skin may form on the surface, inhibiting the solvent evaporation. Moreover, it is also very important that the flatness of the hot plate, a small tilt may cause the deformation of the coat. The manufacturer suggests the temperature and the time relay on the thickness of the coat, Fig. 2.6. It is important to highlight that this temperatures and times are design for a silicon substrate, in this thesis work, the substrate is FR4 and the characterization is done in our labs.

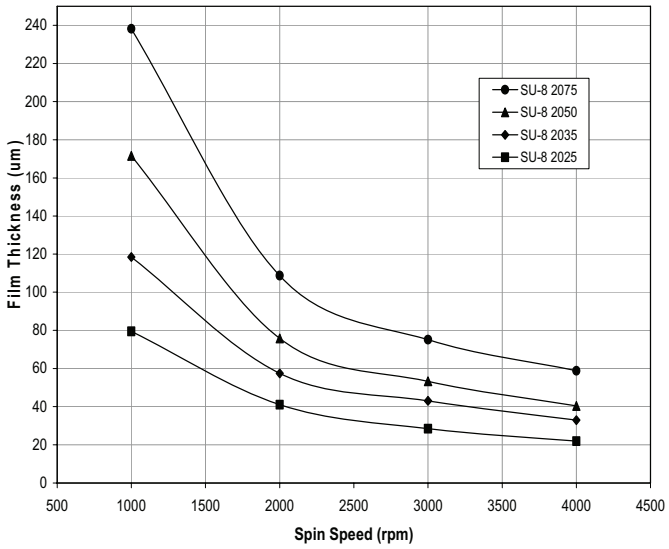

Figure 2.5: SU-8 2000 Microchem Co. Spin speed vs thickness

THICKNESS	SOFT BAKE TIMES	
microns	(65°C) minutes	(95°C) minutes
25 -40	0 - 3	5 - 6
45 - 80	0 - 3	6 - 9
85 - 110	5	10 - 20
115 - 150	5	20 - 30
160 - 225	7	30 - 45

Figure 2.6: SU-8 2000 Microchem Co. Soft Bake temperatures and time vs thickness.

5. **Exposure**. The exposure consists on illuminating the photoresist with UV through a mask to remove or leave parts of the deposition. To obtain vertical side walls, a filter to eliminate the UV radiation below 350 nm is needed. Depending the thickness the exposure energy is different. The Fig. 2.7 shows the different exposure energies according to the thickness of the coat.

6. **Post Exposure Bake (PEB)**. The Post Exposure Bake is the step in which the illuminated SU-8 is crosslinked. This is performed at 95 °C for a certain time depending the thickness of the coat, Fig. 2.8. This should be also

THICKNESS microns	EXPOSURE ENERGY mJ/cm^2
25 - 40	150 - 160
45 - 75	150 - 215
80 - 110	215 - 240
115 - 150	240 - 260
160 -225	260 - 350

Figure 2.7: SU-8 2000 Microchem Co. Exposure energy vs thickness.

THICKNESS	PEB TIMES	
microns	(65°C) minutes	(95°C) minutes
25 -40	1	5 - 6
45 - 80	1 - 1	6 - 7
85 - 110	2 - 5	8 - 10
115 - 150	5	10 - 12
160 - 225	5	12 - 15

Figure 2.8: SU-8 2000 Microchem Co. PEB temperatures and time vs thickness.

performed in a flat hot plate. After the that, the wafer with the SU-8 must be cooled down slowly, to avoid possible stress that may occur.

7. **Development**. The development is the step in which the non illuminated SU-8 parts are removed. The development can be accomplished by immersion, spray or spray-puddle processes with SU-8 developer. The developer is PGMEA, propilen glicol metil eter aceton, however, other solvent based developer, as diacetone alcohol and ethyl lactate may be used. In structures with high aspect ratio or thick coats, the wafer should be stirred. Microchem and Co. gives a recommended development times, Fig. 2.9, but these times are approximate, since these depend on the agitation.

8. **Rise and Dry**. After the developing, the wafer must be cleaned with fresh solution for 10 seconds, to eliminate any remain of uncrosslinked SU-8. Later on, the wafer should be cleaned with Isopropyl Alcohol (IPA) for another 10 seconds. Finally, it must be dried with nitrogen.

THICKNESS microns	DEVELOPMENT TIME minutes
25 - 40	4 - 5
45 - 75	5 - 7
80 - 110	7 - 10
115 - 150	10 - 15
160 -225	15 - 17

Figure 2.9: SU-8 2000 Microchem Co. Developing time vs thickness.

9. **Hard Bake (cure)**. This step is optional, and it is applied when the final manufactured SU-8 wafer is going to be exposed to thermal processing. Hard Bake cure consists in adding a hard bake to ensure that the mechanical properties of SU-8 do not change. Depending of the application a bake between 150 °C to 250 °C is proceed for a time of 5-30 minutes.

10. **Removal**. This step is also optional, SU-8 is design as a permanent material and it is very difficult to remove it. Using a remover could lift off minimally crosslinked SU-8. However, if a coat of OmniCoat (30-10 nm) (referencia) has been applied, the SU-8 can be removed with a bath at 50-80 °C in Remover. The time will depend on the thickness and crosslinked density.

In summary, SU-8 fabrication process has been explained in detail for the coat of 0.5-200 μm thickness. However, for thicker coats, several layers must be deposited. In this case, the fabrication process must be adapted for each application. In this thesis work, the fabrication process will be explained in detail.

2.4.2 PCB-MEMS

PCB-MEMS technology is based on the PCB and its technology for creating MEMS devices. It was developed in Rostock University in 1998 and it is increasing due to it is a low cost process and the high integration of fluidics and electronics [73, 74]. Normally, it is used as a substrate and it is composed by FR4 and a layer of copper. FR4 is a composite material made of woven fiberglass cloth with an epoxy resin binder that is flame resistant. The layer of copper can be of several microns, depending on the manufacturer, typical are 18, 35 or 70 μm, Fig. 2.10.

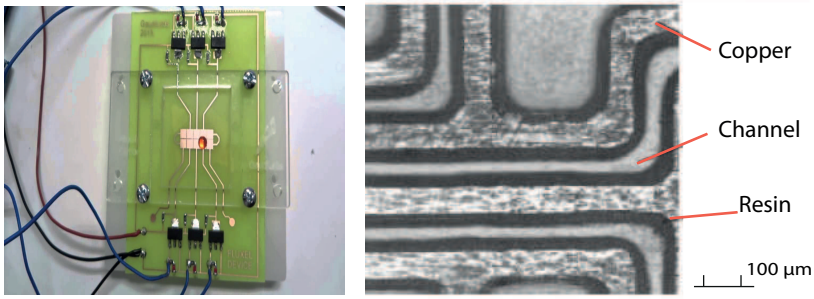

Figure 2.10: Examples of microfluidics systems in PCB.

One advantage of being used as a substrate are the good adhesion to most of the photoresists, due to the properties of the FR4 epoxy resin. Materials as SU-8 makes more versatile the use of PCB as substrate than silicon, because of the ease of manipulation. Furthermore, the low thermal conductivity makes the substrate isolating to heat which is very convenient for heat transfer applications.

Many applications have raised using PCB as a substrate, the Printed Circuit Boards open the possibility to manufacture only with tracks of copper over the FR4 channels, electrics pads, heaters, pressure sensors and flow sensors [75–78]. Moreover, it gives the chance of manufacturing more complex microfluidics structures as pumps, valves, sensors and LoC systems [79–84]. Pumps and valves can be manufactured with the use of auxiliary chambers, a track of copper is used to to heat the chamber and increasing the pressure in the chamber, releasing volume. Sensors are manufactures using the copper lines as electrodes.

Moreover, the PCB MEMS applications are not closed only to the use as a substrate. Using two glued PCBs, the tracks can create channels of different thickness [85], depending the PCBs of copper thickness used, pumps [86] and sensors [87]. The glue to bond the two PCBs is an epoxy glue with a very low viscosity, the PCB is immersed in the glue, leaving a thin layer of glue deposited in the PCB (between 2-10 μm). Later on, the PCBs are joined with heat and pressure and the PCB are sealed with the microchannel inside.

For all this characteristics mentioned, the ease of handling, fabrication and the low cost, PCBs are being developed by many research groups in the manufactured of microfluidics and MEMS devices.

2.4.3 Thermoplastics

Thermoplastics are macromolecular substances comprised of thousands of monomeric units linked in molecular chains [64, 88]. Thermoplastics usually are amorphous and from the point of view of the fabrication are defined by the the glass transition temperature, the melt temperature and thermal expansion coefficient [63]. The glass transition temperature (T_g) is the temperature where the viscosity changes and the thermoplastic change from a rigid material to a soft material, this is the temperature in which those became processable. The melt temperature is the temperature at which the material change from solid to liquid state, it is normally much higher than the glass transition temperature. Finally, the thermal expansion coefficient link the change in length or volume with the change of temperature. This property is very important to highlight due to his influence in the fabrication process of the thermoplastic and in the bonding with other material. Typical thermoplastics for MEMS applications are: Polymethylmethacrylate (PMMA), Polycarbonate (PC), Polystyrene (PS), Polypropylene (PP), and Cycloolefine copolymer (COC). Thermoplastics are very suitable for sealing chambers and channels because these are barely permeable to gas. Moreover, the good optics properties of the plastics make them very suitable for optical detection systems. In addition, other properties as density modulus, thermal conductivity and water absorption are important to consider. Depending the desired application one are more suitable than others, in Table 2.3 can be observed the main mechanical and physical properties of those thermoplastics.

The development of microfluidic microstructures in thermoplastics is carried out by six fabrication process: mechanical micromachining, injection molding, hot embossing, soft lithography, laser ablation and X-ray lithography. However, the most popular are the replication techniques: hot embossing [52] and injection molding [89]. Hot embossing was first developed in 1990s [90–92] and consist in the use of a stamp as imprinting tool for the fabrication of polymer devices, as it was previously commented in 2.2.2.5. These process start with the fabrication of the master that will be used for the replication, normally these are manufactured in in silicon by means of LIGA or etching but, the stamp may also be manufactured in metal by micromachining. The next step in the procedure is cleaning and drying the plastic material. Then, the master and the thermoset is placed in a hydraulic press and it is pressed at a certain pressure and temperature. The temperature must be closed to the glass transition temperature of the plastic. However, the mold can be done at room temperature by increasing the pressure applied. The results at

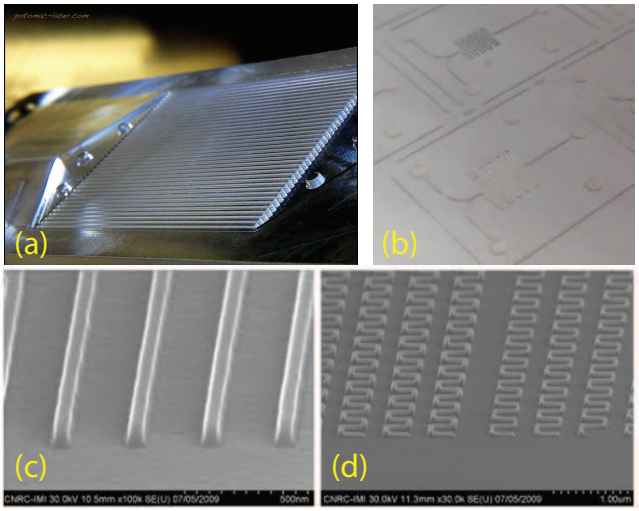

Figure 2.11: Hot Embossing in Thermoplastics. a) High aspect ratio channels in PMMA. b) Nickel Microfluidic Mold for Hot embossing. c) and d) Channels in a polymer of 50 nm and 10 μm width by hot embossing.

room temperature are more critical and dependable of several parameters than at high temperature. On the contrary, at room temperature the structures devices can be reproduced in less than 2 min. The most popular plastics for hot embossing are PS, PMMA, PVC and PC [51, 52]. In Fig. 2.11 can be seen some examples of structures fabricated with hot embossing. Injection molding was introduced in microfluidics in 1997 by ACLARA Bioscience Inc. [93]. The injection molding consist in injecting a viscous plastics into an evacuated master at high temperature and cooled down below the glass transition temperature of the material. The control of the time and temperature is very demanding to achieve the same features as the mold. Furthermore, the cooled down is critical for taking out the polymer from the mold without any stress. The main advantages of injection molding from hot embossing is the possibility to create 3D structures, Fig. 2.12.

Thermoplastics has been used for the fabrication of MEMS devices for a range of applications [65, 94]. Most of them are focused in microfluidics and micro optics. However, there are other applications in electrical and mechanical field. In microfluidics a great variety of applications have been developed, like ink jets, capillary electrophoresis systems, cells culture systems, pumps, valves, flow sensors and pressure sensors. Microchannels are very easily replicable with micro molding techniques, from simple channels configuration to more compli-

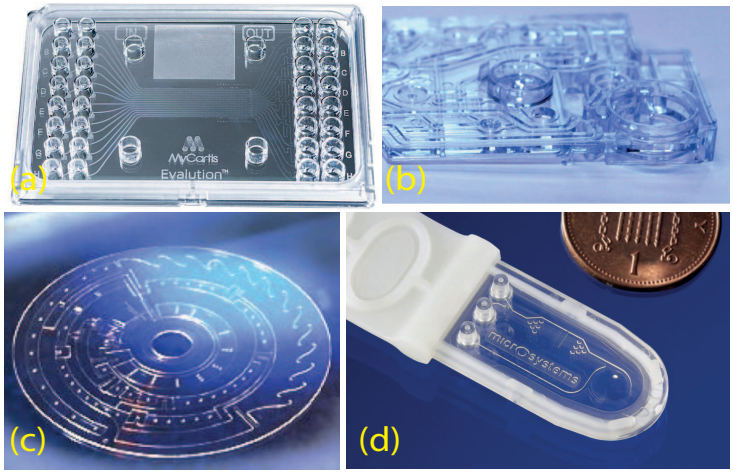

Figure 2.12: Different microfluidic cartridge developed by injection molding.

cated structures integrating different elements. In addition, in fluorescence detection application, thermoplastics shows better autofluorescence than glass, notably PMMA and PC. Additional benefits of the thermoplastics for fluidic applications include low cost of substrate material, the price of thermoset in comparison with boro-float glasses, boro-silicate glasses and photostructurable glasses is approximately 10 time less. Moreover, the steps involve in glass fabrication are very expensive due to the reagents and instrumental needed. In addition, the etching process are restricted in the aspect ratio, wall angle and high, which can be desired in many applications. Another important aspect is the contamination from the point of view of the samples and the environment. In chemistry or bio diagnostics, the devices must be disposable and thermoplastics are a good alternative due to his low cost. Finally, rewarding the environment contamination, the etching process implies several chemical reagents which involves waste disposal, which is much less in thermoplastics fabrication process.

Table 2.3: Thermoplastics mechanical and physical properties.

Properties	**PMMA**	**PC**	**PS**	**PP**	**COC**
Density (gm^{-3})	1.17-1.20	1.20	1.05	0.896-0.915	1.01-1.02
Glass Transition Temperature(°C)	106	150	80-100	0-32	138
Elasticity Modulus (Gpa)	3.1-3.3	2.0-2.4	3	1.1-1.6	3.1
Linear Thermal Expansion Coefficient ($10^{-6}K^{-1}$)	70-90	65	70	100-200	60
Thermal Conductivity ($Wm^{-1}K^{-1}$)	0.186	0.192-0.21	0.18	0.22	0.16
Tensile strength (MPa)	48-76	62.1-65.5	40	40	66
Water absorption (%)	0.3-0.4	0.35	0.05	0.02	<0.1
Refractive Index	1.49	1.586	1.51	1.51	1.53
Transparency	High Transparency	High Transparency	Medium Transparency	Mechanical Properties	High Transparency

2.5 Microlvaves

In this section a state of the arts of microvalves in MEMS applications is presented. There are many types of microvalves, but it can be divided into two main groups focusing in their actuation: actives and passives microvalves. Moreover, those two groups are categorized in different subgroups relying on the physics applied. In Table 2.4 can be observed the main classifications [95].

Active microvalves are those which need the external energy for their actuation, these are divided into three subgroups using mechanical and non mechanical moving parts and with the help of external systems. Active mechanical microvalves are traditionally coupled a flexible membrane connected to a magnetic, electric or thermal stimulus. These microvalves are manufactured using MEMS-based bulk or surface micromachining technologies. Magnetics, mechanical, active microvalves are carried out using a solenoid connected to a magnetic membrane [96]. Magnets can be integrated in order to reduce the power consumption [97, 98]. Moreover, instead of a membrane, a spherical metal ball can be used [99]. Within the active microvalves, electrostatic microvalves has been reported as an alternative. Most of these are employed for gas flow instead of liquids due to high voltage applied for its activation. Rigid or flexible membrane are used for its activation [100, 101]. Piezoelectric materials are widely used in microvalves, applying an electric field the material is stressed, producing small displacements [102–104]. Between the mechanical active microvalves, the thermally actuated microvalves are very attractive due to its simplicity. These are divided into three groups: bimetallic [105], thermopneumatic and shape memory alloy actuation [106], being the most popular thermopneumatic active microvalves. These microvalves operation is based on volumetric thermal expansion links to a flexible membrane [107–109]. Finally, Bistables microvalves are those who do not need a continuous source of energy for its activation. These use a bistable actuation that requires power in the switching between the two states [110–112].

The non-mechanical active microvalves are microvalves without mechanical moving parts, among them it can be found electrochemical, phase change and rheological microvalves. Electrochemical microvalves are based on the gas or bubble generation based on electrolysis [113,113,114]. Phase change microvalves employ material as hydrogel [115], sol-gel [116], paraffins [117] and ice [118] for its operation. These phase change microvalves are of particular interest due to its simplicity structure, low cost and for being cheap. Moreover, rheological microvalves have also particular interest, it can be found using electro-rheological

Table 2.4: Microvalves

Active	Mechanical	Magnetic
		Electric
		Piezoelectric
		Thermal
		Bistable
	Non-Mechanical	Electrochemical
		Phase Change
		Rheological
	External	Modular
		Pneumatic
Passive	Mechanical	Flap
		Membrane
		Spherical ball
		In-line mobile structure
	Non-Mechanical	Diffuser
		Capillary

and ferro fluids [119, 120]. Another type of active microvalves needs external systems for its operation. This involves bigger and complex structures but, at the same time, these microvalves assure no leakage flows and withstand high pressure. Among these can be found modular microvalves [121, 122] and pneumatic [123, 124].

Passive microvalves are a type of valve which does not need external energy for its operation. Likewise in the active microvalves classification, these are also divided in mechanical and non-mechanical passive microvalves. Mechanical passive microvalves are only open by the forward pressure. Since check microvalve does not use external energy, it can be cantilever-type flaps made of silicon, metal or polymers [125–127]. Moreover, membrane check valves have been developed, being formed with holes, bumps or bridges [85, 128, 129]. Spherical ball microvalves are very popular, due to its used in human hearts [130].

Non-mechanical passive microvalves, also called valveless micropumps, make used of nozzle [131], diffuser [132] or Tesla [133] elements. Some of these microvalves combine channels with nozzle with sharp entrance and a tapered angle. Moreover, capillary effects: abrupt, burst and hydrophobic channels are used as microvalves [134, 135].

2.5.1 Single use thermoelectrical microvalves

The desired characteristics of one microvalve range from: flow control, on/off switching and sealing. All the microvalves explained respond to a certain requirement inside the flow control, there is not any microvalve that favor all the requirement, indeed, the characteristics of the microvalve will depend on the application. Single use microvalves are growing in the recent years thanks to the bio and chemical applications. Inside this type of microvalves, thermoelectrical microvalves are becoming popular due to its simplicity in the activation. The most relevant single use thermoelectrical microvalves are going to be describe in order to do a comparison at the end of the thesis with the developed microvalve.

In 1998 in Institute for Microsystem in the Ecole Polytech of Lausanne, Switzerland, one-shot microvalve with thermoelectric activation was developed by Guerin et al [136]. The microvalve is manufactured using glass, copper and PE / PET (Polyethylene / Polyethylene Terephthalate). The glass is used as substrate of the microvalve, it contains a hole made with electrochemical discharges, this is closed by a membrane of PE / PET with a layer of copper. The layer of copper is patterned as a resistor. The mechanism of operation is applying electrical current,

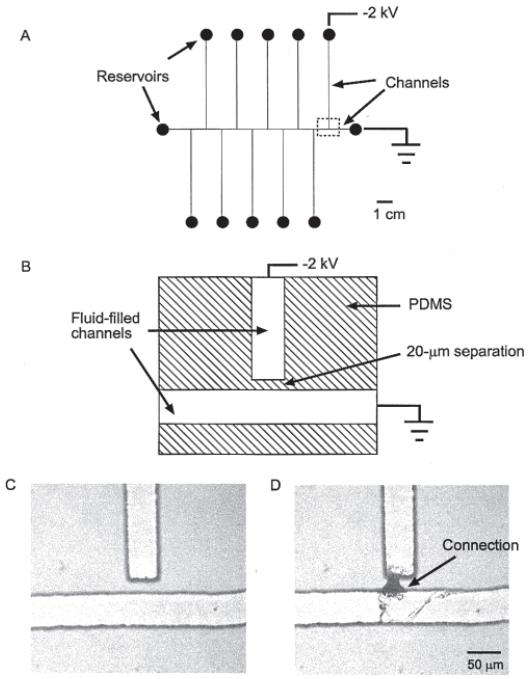

Figure 2.13: Single use microvalve in PDMS. A) Schematics of the microvalve: one main channel and 10 perpendicular channels separated 20 μm of the main channel. B) Schematic of the gap between channels. C) Microscope picture of the microvalve without activated and D) activated.

heating the resistor and melting the PE membrane. The power required to open the microvalve is 400 mW, and the activation time is 1.2 s.

McDonald et al. from the Department of Chemistry and Chemistry Biology in the University of Harvard, Massachusetts, developed in 2001 a single use microvalve made of PDMS [137]. The microvalve operation is found on the connection of microfluidic channels. These microchannels are separated by a wall of 20 μm of PDMS. The idea is to apply the rupture voltage of the PDMS (21 V / μm) and open a path in the wall between the channels, connecting those. The microvalve and the operation can be seen in Fig. 2.13. The applied voltage varies from 1 to 5 kV in a time of 1 s or less.

In 2004, Ahn et al. from the University of Cincinnati developed a LoC system in COC for clinical diagnosis [138]. The system is formed by a microfluidic circuits, with passive microvalves and an active microvalve. The active microvalve consists of a gas pressurized in a chamber of COC, with a Ni resistance performed

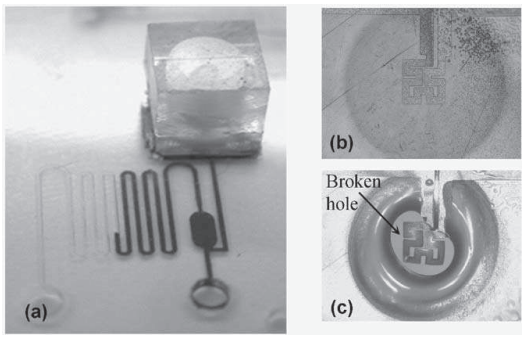

Figure 2.14: Schematic of Ahn microvalve.

with electroplating techniques. The microvalve has an activation time of 1 s and a power of 50 mW. The microvalve can be seen in Fig. 2.14.

Much work has been also done in microvalves in silicon. One example is the array of microvalves created by Cardenas-Valencia et al. in 2007 [139]. The proposed device contains a membrane in SiNx with a metal resistor in Gold or Platinium. The membrane is done via dry etching and the resistor via lit-off. The membranes were able to withstand pressure up to 5 bar for 3 μm membrane thickness. The time of activation of the microvalves is of 0.1 s with an energy consumption of 140 mJ.

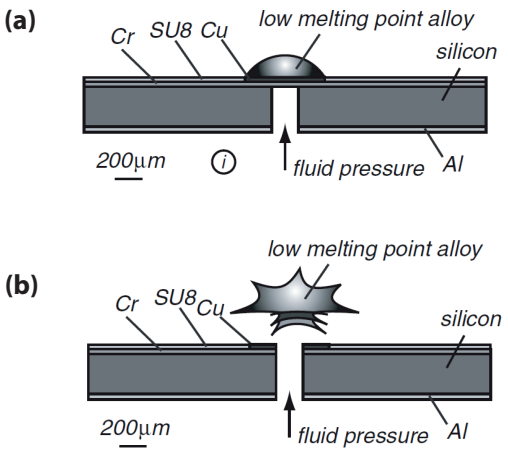

Figure 2.15: Microvalve developed by Debray: a) Close microvalve b) Open microvalve.

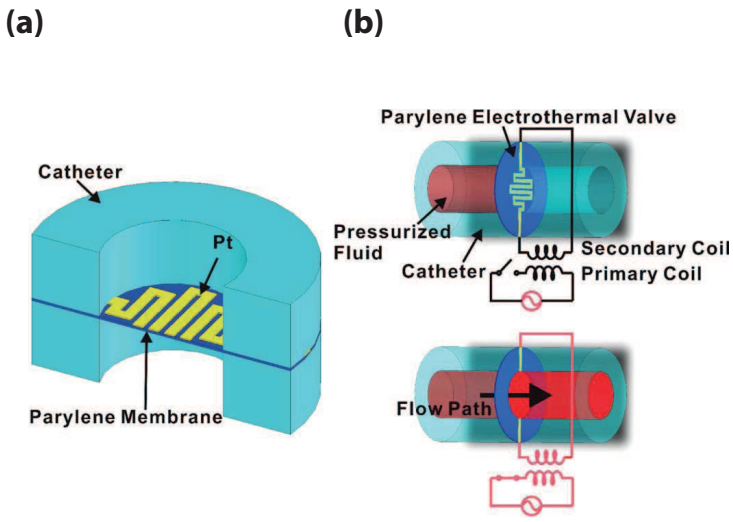

Figure 2.16: Microvalve developed by Li: a) Scheme of the microvalve. b) Operation principle of the microvalve.

Low melting point alloys are commonly used in single use microvalves. Debray et al. from the University of Tokyo, Japan developed a one-shot microvalve [140] in 2007. A microchannel fabricated in a silicon wafer is created all through the wafer by deep-RIE. This microchannel is sealed by a low melting point alloy of 370 nm, in this case 47°C. The microvalve is passive, there is not heating for the activation. When the atmosphere temperature rises until the melting temperature of the alloy, the pressure applied in the channel open the microvalve, in Fig. 2.15 the working of the microvalve can be seen. The main problem with this microvalve is the time in reaching the melting temperature, around 500 s.

Li et al. from the Department of Biomedical Engineering of the University of the South California developed a single use solenoid microvalve made in Parylene [141]. The valve consists of beams in the form of resistance of Platinum embedded in a 10 μm Parylene membrane, Fig. 2.16. The fabrication process is quite simple, because it is made of a membrane in Parylene and a platinum structures made by Lift-off techniques. However, the integration in a microfluidic platform is low. The activation is based on melting the membrane applying current. The membrane is capable of withstanding a maximum pressure of 1034 mbar and the activation time of the microvalve is several seconds for a current of 7 mA with a power consumed of 22 mW.

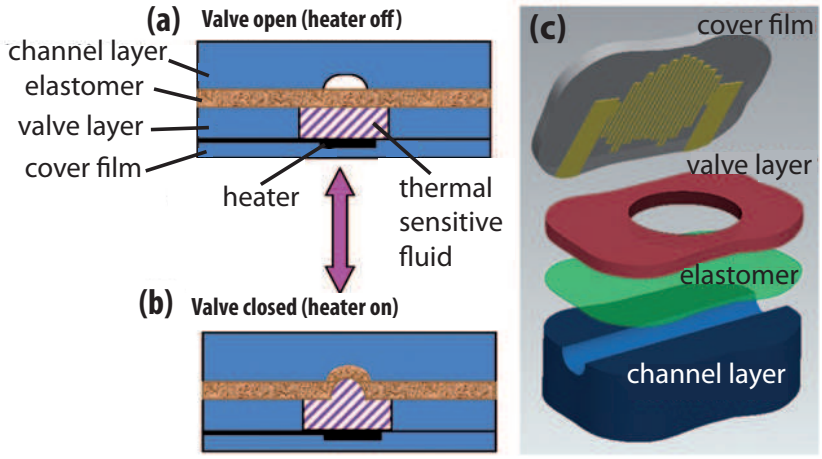

Figure 2.17: Schematic of the microvalve developed by Pitchaimani.

At the University of Florida, the Microsystems group developed in 2009 a plastic valve with thermal activation by Pitchaimani et al.[142]. The valve is developed in COC using molding procedures. The microvalve is made of 4 layers of plastic, as shown in Fig. 2.17. The first layer contains the microfluidic channel, the second one contains the elastomer, the third one contains the tank where the fluid to be impulsed will be located, and the last layer contains the heaters. The microvalve is operated by means of the heaters, the fluid is heated and expanded and consequently, the layer of elastomer is also expanded. This expansion closed the microfluidic channel. The operation of the micro-valve is produced in a time of 7-80 s with a consumption between 50-90 mW.

The group of Microsystems of the University of Seville, headed by José Manuel Quero, has a wide experience in MEMS and Microfluidics. As a results, several microvalves have been developed. One of them was developed in 2009 [5] and consists of a SU-8 membrane traversed by a gold resistive element on a PCB substrate, Fig. 2.18 (a). The membrane is located between a chamber and a microchannel. The membrane comes under a pressure, responding to a mechanical stress. When an electrical current is supplied to the resistor, the resistor is heated. This heat together with the mechanical stress lead to the rupture of the membrane. The membrane is able to withstand 0.8 MPa. The microvalve has an activation time of 3 s and an energy consumption of 0.7 J. In 2010 a new microvalve was developed in SU-8 and PCB [4]. This valve is compound of a SU-8 membrane with a gold wire embedded, Fig. 2.18 (b). The microvalve has sufficient inherent

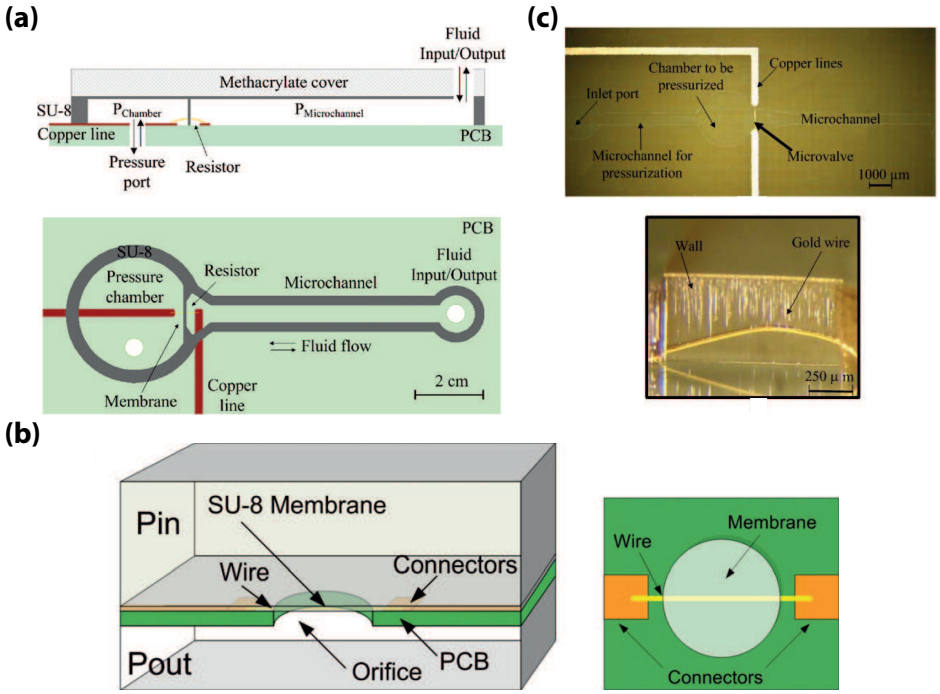

Figure 2.18: Schematic of the microvalves developed by the group of Microsystems of University of Seville: (a) Moreno microvalve, (b) Aracil microvalve and (c) Perdigones.

rigidity to cope with pressures of 400 kPa. The activation time is 2.5 s and the energy consumption is 350 mJ. Perdigones in 2014 [6] developed a new microvalve based on the previous microvalves developed. This microvalve combines the design of the first microvalve with the disposition of the wire in the membrane of the second, Fig. 2.18 (c). With this new design, the activation time and the required energy was reduced to 1 s and 188 mJ.

Other interesting technology used in microfluidics and microvalves is high-temperature co-fired ceramic (HTCC) due to its high-temperature and chemical sustainability. Khaji et al. from Uppsala University, Sweden developed a single use opening microvalve in HTTC [143]. The microvalve consists of a membrane with a heater and a cavity stack, Fig. 2.19. Three different heaters configuration were considered and the membranes thickness were from 40 - 120 μm. The cavity was made of three layers with a hole via milling. The membrane tolerates a

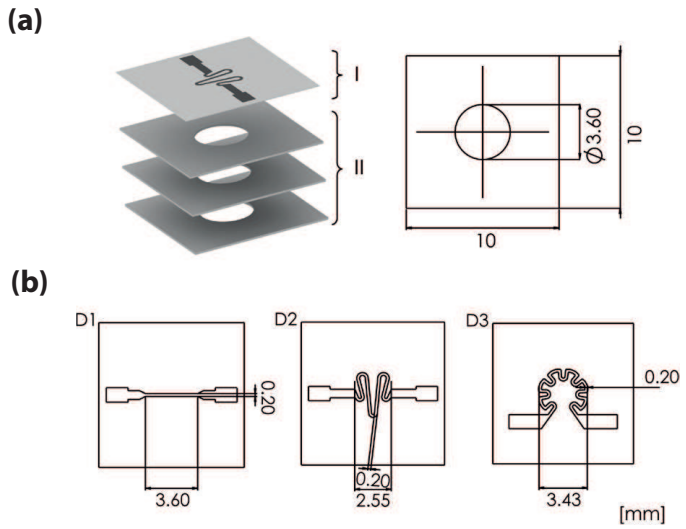

Figure 2.19: Schematic of the microvalve developed by the Uppsala University: (a) the different parts that compound the microvalve and the dimensions (b) Different shapes for the heater.

maximum pressure of 8 bar and the energy consumption to open the microvalve was in the range of 250-560 mJ.

Finally, in Table 2.5 is shown a summary of the main characteristics of the microvalves mentioned previously. For each microvalves the operation principle has been explained, the used materials and its characteristics, focusing in the consumption energy and the activation time, the most critical parameters of a single use thermoelectrical microvalve.

Table 2.5: Characteristics of the main single use thermoelectrical microvalves.

Microvalve	Body Material	Thermal Resistive Material	Activation Time (ms)	Energy consumption (mJ)	Complexity of fabrication	Integrability
Guerin	PE / PET	Cu	1200	400	Medium	Medium
McDonald	PDMS	Pt	1000	150	Low	High
Ahn	COC	Ni	700	28	Medium	High
Cardenas-Valencia	SiNx	Pt/Ti	100	140	High	Medium
Debray	Silicon	NS	5e5	NS	Medium	Medium
Li	Parylene	Pt	100	2.5	Medium	Low
Pitchaimani	COC	Au	7000	350	Medium	Low
Moreno	SU-8	Gold	2000	350	Medium	High
Aracil	SU-8	Gold	2500	700	Low	High
Perdigones	SU-8	Gold	1000	188	Medium	High
Khaji	HTTC	Pt	5000	250	Low	Medium

2.6 Impulsion Systems

Impulsion systems play a pivotal role in the Lab on Chip systems, the handling of small volumes of liquids is a difficult task with the conventional pumps or actuators. The large sizes and the complex mechanical components of these devices make them non appropriate for the LoC systems, where accuracy is linked to integrability and low cost. However, micropumps are presented as an alternative to those macro pumps, offering integrability due to the small sizes, accuracy, in a way these are developed for a certain application, and low cost. Thought there are many types of impulsion systems in the nano-scale, these can be roughly divided according to its working principle in Solid Chemical Propellant, Electrolytic Gas Generator, Electrowetting on Dielectrics (EWOD), Surface Acoustic Wave Droplet Manipulation (SAW), Dielectrophoresis and Pressurized Chambers.

Solid chemical propellant are based on a chemical substance that is heated in a controlled manner, producing pressurized gas that is used for displacement of fluids. The chemical substance is normally Azobisisobutyronitrile (AIBN) which formula is $[(CH_3)_2C(CN)]_2N_2$, and heated at 70°C it releases nitrogen. The typical configuration of this impulsion system consists in a chamber where the substance is placed and a microheater under the AIBN, the liquid to be impulsed is placed in a microchannel connected to the microchamber. When a current passes through the heater and it reaches the 70°C, the pressure of the chamber increases and the sample is moved. Several devices have been developed [144], but one representative is the Micro-Injection System for Localized Drug Delivery reported by the School of Electrical Engineering and Computer Science from Seoul National University, South Korea [145]. As can be seen in Fig. 2.20, there is a chamber where the heater and the AIBN is placed and the drug is connected to the chamber and to the microneedles. The system injects between 2.29-2.9 μl sample during 6 second with a voltage applied of 30.4 V and a current of 164 mA.

Electrolytic gas generation is another chemical principle that can be used for the movement of fluids. For the implementation of this technique is necessary a power source, a liquid solution and two electrodes. In these systems the reaction is, likewise in the previous system, in a chamber connected to a microchannel where the sample to be impulsed is located. Moreover, this actuator needs a flexible membrane to isolate the liquid solution. After applying the electrical current and the reaction occurs, the gas generated deform the membrane, moving the sample, Fig. 2.21. One application of this technology is developed in [146], it is composed a low pressure chemical vapor deposition silicon nitride membrane,

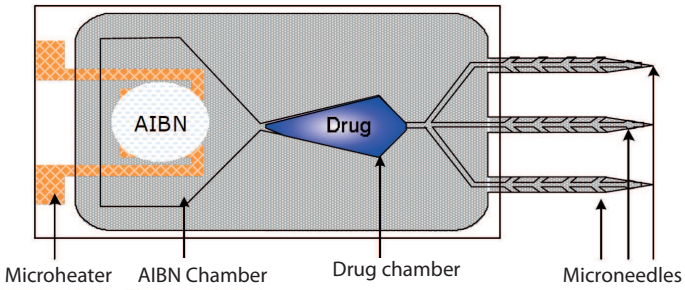

Figure 2.20: Schematic of the Impulsion System developed by the University of Seul.

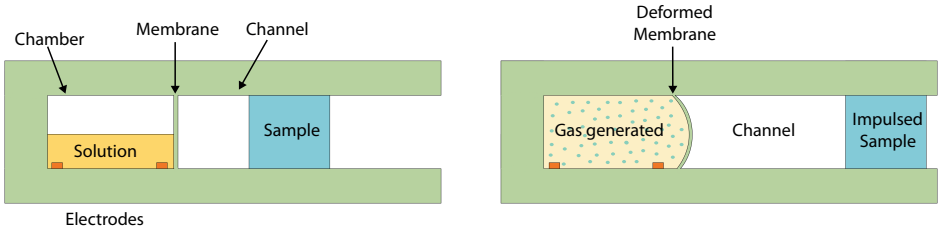

Figure 2.21: Schematic of the Impulsion System based on Electrolytic gas generation.

a solution of copper sulphate and electrodes made of copper and Platinium. The microdevice reachs a pressure of 2kPa with a power of 7 μW during 100s.

Digital microfluidics is another technology for handling small volume of liquids, the most significant method is Electrowetting on Dielectrics (EWOD). In this case, droplets are moved due to a electric field that changes the contact angle of the droplet. Droplets are in contact with a hydrophobic layer under a electrodes, insulating those, Fig. 2.22 . The voltage applied between the droplet and the electrode causes a electric field in the hydrophobic layer, acting as a dielectric, which decreases the surface tension between the droplet and the dielectric following Lippman-Young equation. The application of this physics in an array of electrodes results in the displacement of the droplet. There are two kind of EWOD, using one plate or two plates. There is a plenty of applications of EWOD technology, in the work presented by [147] EWOD technology is used to transport droplets with proteins or peptides. Moreover, digital microfluidics has been used

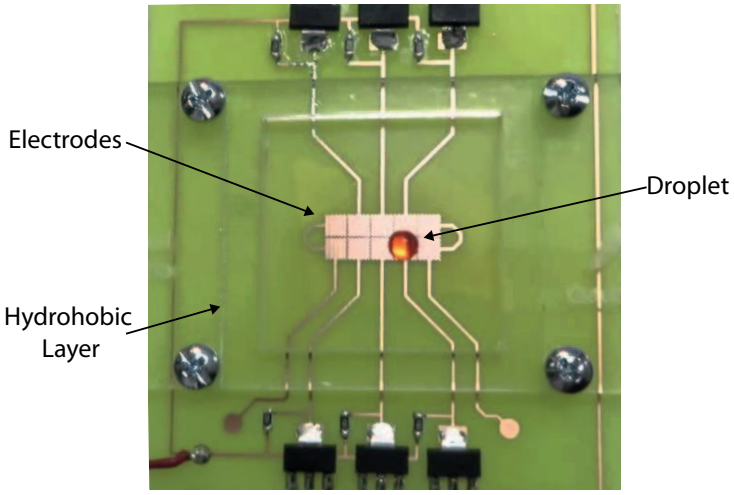

Figure 2.22: Example of the Electrowetting on Dielectrics (EWOD). These systems are composed of electrodes, one hydrophobic layer and the droplet to be handle.

for primary cell growth in [148] and as a microfluidic platform for point care of testing [149].

Another droplet handling technology is the Surface Acoustic Wave (SAW). This technology is based on the use of the piezoelectric behaviour of some materials like zinc oxide or quartz to convert electrical energy in mechanical energy in form of acoustic waves. The impulsion systems based on SAW technology need an interdigitated transducer (IDT) and the piezoelectric substrate. An electrical signal is applied to the IDT, so the piezoelectric substrate is contracted and expanded, generating acoustics waves, and consequently, the droplet is displaced. There has been reported several devices, in the work developed in [150] a LoC prototype is designed for protein/peptides analysis as can be shown in Fig. 2.23, and in the work reported in [151] a microfluidic device which detects the Leiden Factor V syndrome in human blood.

Dielectrophoresis is the motion of a dielectric particle when it is subjected to a non-uniform electric field. In microfluidics, the dielectric particle is a droplet of water, and the electric field polarizes the particle, and the poles of that particle suffer a force a long the electric field. This force is attractive or repulsive depending on the orientation on the dipole. Since the field is non-uniform, the electrostatic attraction is bigger where the electric field is stronger and the particle will move. There are two types of dielectrophoresis, positive DEP (pDEP) when

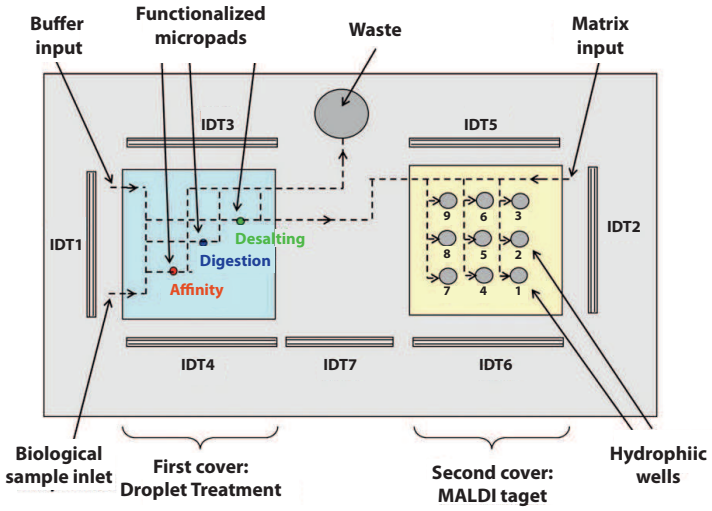

Figure 2.23: Schematic of the LoC prototype for protein/peptides analysis based on SAW technology.

the particle is moved to maximum electric field region, or negative DEP (nDEP) when the particle moves away from the maximum electric field. In Fig. 2.24(a) is shown the principle of working of droplet handling by dielectrophoresis and in Fig. 2.24(b) is an example of application, in this case the manipulation is refer to proteins and cells [152].

Pressurized chambers is a technology widely used in LoC systems for the displacement of liquids. A chamber at high pressure is open by means of a microvalve and the released gas impulsed the sample downstream the microvalve until a balance of pressure is achieved. The microvalve is normally a membrane connected to a microheater, so due to the temperature and the pressure the membrane is broken, releasing the air of the chamber, as it was reported by Ahn's group [153], Fig. 2.25(a) . Nevertheless, the configuration could be different as it will be shown. The high pressure of the microchamber can be obtained during the fabrication process or connecting an external source. Many devices have been developed with the pressurized air integrated in the fabrication process, in the work reported by Ahn's group the high pressure in the chamber is carried out with a nitrogen source before the packaging, as can be observed in Fig. 2.25(b). Other example of pressurized microchamber with the pressurized air integrated in the fabrication process is the one reported by [154], uncrosslinked SU-8 is introduced in a channel connected to the microchamber and is pushing the air and

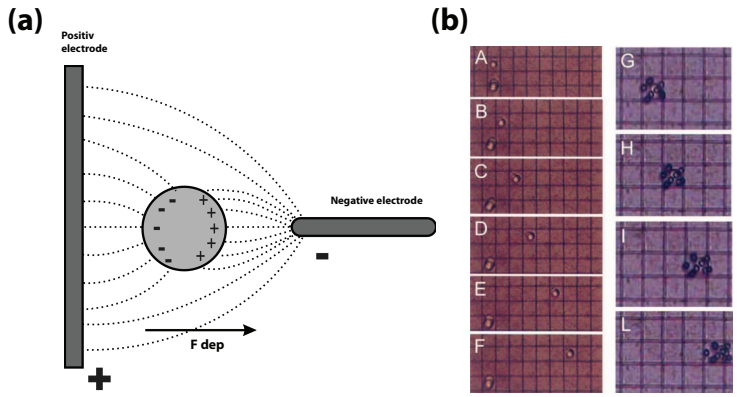

Figure 2.24: (a) Working principle of dielectrophoresis, (b) Application of cell and protein manipulation using dielectrophoresis phenomenon.

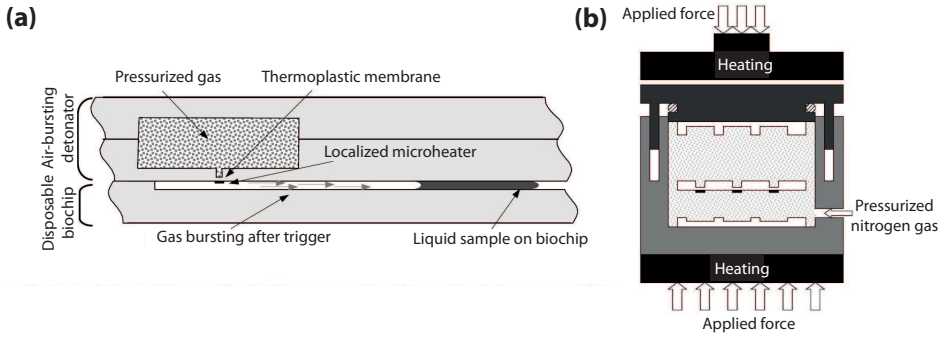

Figure 2.25: Example of the impulsion system based on pressurized chamber developed by Ahn: (a) Cross view of the complete system, (b) Fabrication process of the nitrogen at high pressure introduced in the pressurized chamber.

pressurizing the chamber following Boyle's Law. This method assures a total control of the volume and the pressure achieved, Fig. 2.26. However, these portable devices have a disadvantage, the losses of pressure as a function of the time due to the permeability to gases of the plastics materials, COC in [153] and SU-8 in [154]. The use of an external source overcome these problems at the expense of the portability and the integrability [5].

Despite being focused in these methods, there are other methods of fluids motion in the state of the art. Among them it can be found the optoelectrowetting technique, very similar to electrowetting on dielectrics with an additional pho-

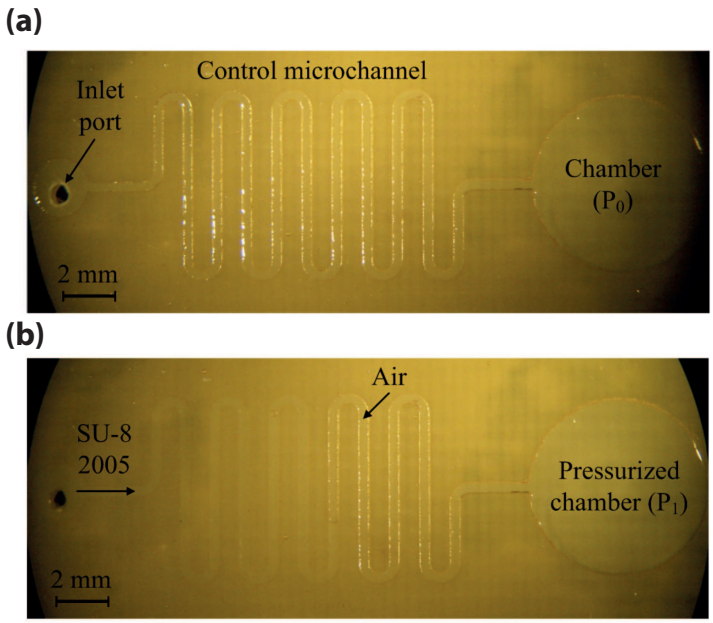

Figure 2.26: Example of the impulsion system based on pressurized chamber developed by Moreno: (a) Top view of the fabricated microdevice before pressurization, (b) Fabricated microdevice after pressurization, the crosslinked SU-8 fills part of the microchannel raising the pressure in the microchamber.

toconductive layer [155, 156]. An alternative technique is the use of centrifugal force to impulse liquids [157,158]. This technology has the advantage of involving functions of valving, mixing, switching and separation without any external actuator. Multiphase flows are another technique of droplet handle [159] and Paraffin pumps present a very large volume expansion with low melting temperature [160, 161].

2.7 Microfluidics Platforms, Lab on Chip

Lab-on-chips systems (LoC) or micro total analysis systems (μTAS) can be defined as a miniaturized portable device that integrates synthesis and analysis of chemical substances. The miniaturization of chemical processes normally managed in a laboratory presents several benefits such as cost efficiency, parallelization, low fluids volumes consumption, faster analysis and responses, and sensitiv-

ity. The main challenge of the lab-on-chip systems is being able to integrate onto a single chip several biochemical operations to get a precise diagnosis of possible diseases into a drop of blood collected from a patient. Unfortunately, this technology is far from that, but many advances have been done in the recent years and in a future chemical diagnosis will be different from the way the diagnosis are done now.

The history of the LoC dates back to 1979 where a gas chromatographic analyzer was presented [162]. This device manufactured in silicon was able to separate a simple mixture of compounds in seconds. However, it was not until 1990 where the concept of μTAS was developed by Manz et al. [163] and these group also presented a chip containing an open-tubular column and a conductometric detector connected to a pump and valve [164]. At that moment, there were published several papers related to μTAS, the chip were implementing several functions as integration of reactor chamber for continuous precolumn reactions [165], separation of oligonucleotides [166], DNA [167] and cell manipulation by electrical field [168]. The LoC systems were also focused in optical and electrochemical detection [169]. In the following years, new approaches were developed until the present, where several LoC systems have been developed but there is a plenty of thing still to cover [54].

Though depending on the application, the features that must accomplish a lab on chip will be different. The laboratory functions that a complete lab on chip must perform are sample handling, sample and reagent mixing, separation and detection [170]. To fulfill these functions the lab on chip must be composed of some components: injector, preparator, transporter, mixer, reactor, separator, detector, controller and power supply, Fig. 2.27. In this section these components will be described in detail.

- **Injectors**: Injectors are components which manage the volume of sample introduced in the system for the analytical process. Those can be external parts connected to the controller, as syringe pumps and robotic pipettes [171], or internal parts of the lab on chip [172].

- **Transporter**: Also called impulsion systems are the component in charge of the motion of fluids from one point of the circuit to the other. These can be active or passive, but it was extensively described in section 2.6.

- **Preparator**: The sample are exposed to a treatment of isolating the interested part from the rest of the sample before analysis, its reduces the pro-

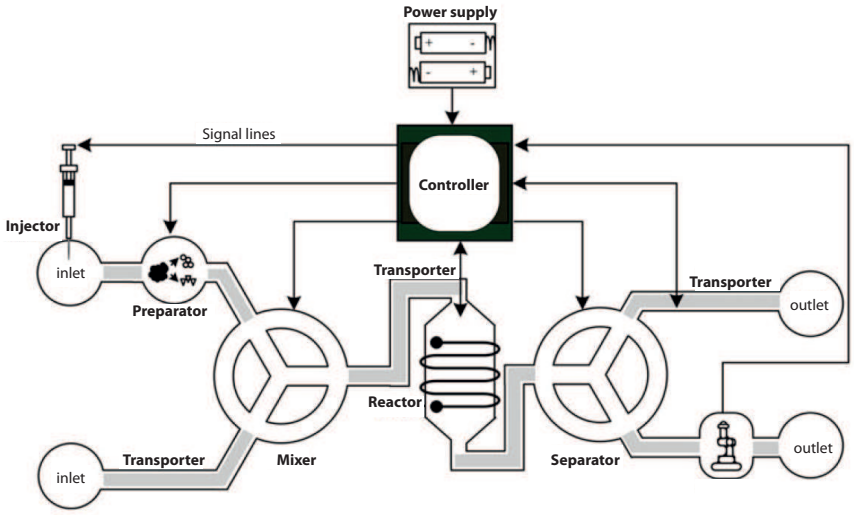

Figure 2.27: Scheme of a complete lab on chip from a component view via [170].

cessing time. This step is crucial in molecular analysis like DNA/RNA amplification. The common protocol of preparation are filtration, pre-concentration, cell lysis and derivatization. Filtration is used to separate the analyte of interest from the rest of the sample [173,174]. Pre-concentration is used to increase the concentration and improving the sensitivity in the detector [175]. Cell lysis refers to the breaking down of a cell, often by viral, enzymic, or osmotic mechanisms that compromise its integrity [176]. Finally, derivatization is a protocol used to convert the sample in a very similar chemical structure, this is also used to improve the sensitivity [177].

- **Mixer**: A mixer is the component which mixes two or more fluids in a microfluidic circuit. The mixing is carried out under laminar flow, due to the low Reynolds numbers of the fluids in the microchannels. The mixers are divided into two groups: active and passive micromixers. Active micromixers needs external source to perform the mixing. Among these it can be found magnetics using external magnets and magnetic particles [178], and ultrasonic vibrations, creating a turbulence that mixes the fluids [179]. Passive micromixers do not need external forces to perform the mixing, which

make them more stable and robust. The way to carried out the mixing is by spiral channels, secondary flow and vortex [180, 181].

- **Reactor**: Reactors are devices which control and contain chemical or biological reactions. These are composed of heaters, sensors and actuators to control the reaction. The integration of reactor in lab on chips is a great step forwards, as it provides heat and mass transfer reducing volume of sample and reagent and cost. Reactors can be found in three different groups: gas phase, liquid phase and packed bed [182–184].

- **Separator**: Separators separate fluids and solids after mixing or reaction processes. This component is commonly used to select a particular cell for analysis or to isolate some particles that can not be identify and manipulate. The most used technique is capillary electrophoresis (CE) but other techniques such as dielectrophoresis (DEP), isotachophoresis, chromatography, optical tweezers, magnetics and laminar flow based filters can be found [185, 186].

- **Detectors**: Detectors are the part of the lab on chip where the sample is identify and measured. The detection is carried out by transducers that transform physical signals in electrical signals. In lab on chips there are different methods of detection as optical, electrochemical, mass spectrometry, capacitance and magnetic. Optical detection is the most commonly used because of its integration and simplicity. One method of optical detection is measuring the fluorescence of cells which are excited with a light source [187]. Moreover, absorption spectroscopy is widely applied, a beam of light pass through the sample and one photodetector read the measurement [188]. In these fields fiber optics present a great potential. In electrochemical detection three electrodes are used to detect a sample under a conductive environment [189]. Mass spectrometry is a technique that allows to determine the molecular weight and its structural information [190]. Finally, capacitive detectors measure the capacitance of a sample and converts it into frequency signal [191].

- **Controller**: Controller are the brain of the lab on chip, it is responsible for the control of the system, data acquisition and signal processing operation. Normally it consists of a microcontroller with a communication interface, control circuit, signal processing circuit and the power electronics. Normally this module is outside the lab on chip and connected to it via ports

[192], but some lab on chips have been reported with the controller integrated inside [193].

- **Power supply**: Power supply provides the electrical energy to the active components of the lab on chip including transducer, actuator and any electronic circuit. For portable lab on chips, the power supply are normally batteries. On the other hand, system based on electrophoresis or dielectrophoresis technique needs higher energy and makes use of power supply connected to electrical network.

The components described are those which should be integrated in an ideal multipurpose lab on chips. However, it is far from that, there is any lab on chips that fulfill these requirements. Moreover, researchers do not agree in how many components must be a lab on chip contains. For instance, the preparator is performed normally off-chip because the complexity in the sample treatment. On the other hand, researchers usually agree in integrate components as transporters, mixers, reactors and detectors. Other important aspect in the integration of the components in a lab on chip is the fabrication process. There is not any standardization in lab on chips, its depends on the used materials and the standard of fabrication for these materials. In conclusion, the degree of integration of the components depend on the intended analysis, the application and the fabrication process.

2.7.1 Representative integrated lab on chips

In this subsection is going to be described some examples of LoC. There has been chosen the most representative in several technologies, including the PCB-MEMS [194]. The different LoC are described, focusing in characteristics described above and, in the materials used, dimmensions and application. At the end of the section a table is shown summarizing the LoCs described with the main characteristics.

The first work described is the lab on chip developed by Ahn's group from the University of Cincinnati in 2004 [138]. The lab on chip developed is a disposable biochip with a control and detection module. The disposable bio chip is made of COC and has a dimension of 2.5 x 2.5 x 0.6 cm. This is composed of air bursting detonators as transporter, a smart passive microfluidic control system as multiplexer, and an array of electrochemical detection sensors. The air bursting detonator is an eletropneumatic micropump, a chamber with pressurized air with

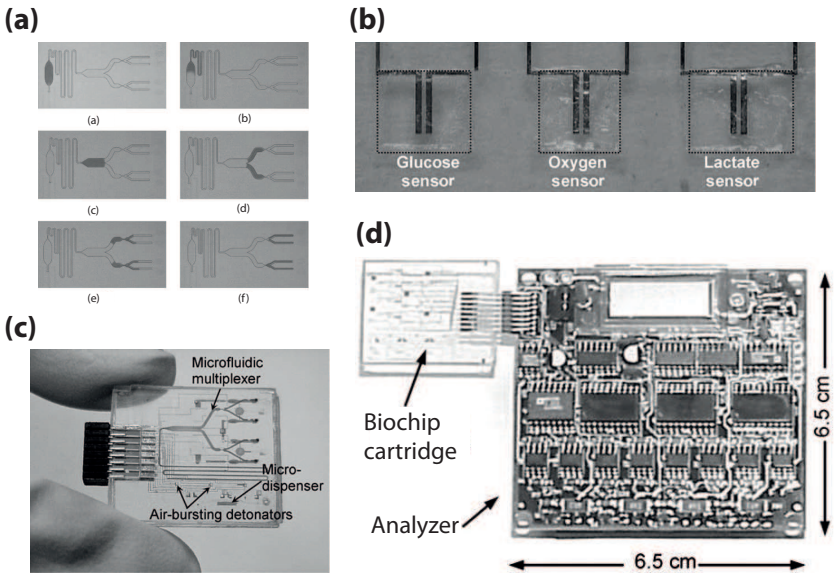

Figure 2.28: Lab on chip developed by Ahn. (a) sPROMs technology based on passive microvalves for the separation, (b) bio sensors array for electrochemical detection, (c) complete biochip and (d) complete picture of the proposed lab on chip.

a membrane with microheaters, as it was explained in section 2.5.1. The smart passive microfluidic control systems is based in the technology developed by the authors called sPROMs. This technology is based on a series of microchannels with passive microvalves situated in strategic locations, Fig. 2.28(a). The sensing systems are based on electrodes to detect Glucose, Oxygen and Lactate of blood, Fig. 2.28(c). The complete microfluidic biochip is shown in Fig. 2.28 (c). Moreover, the system contains an electronic control device for the detection of the sensors and for the activation of the air bursting detonators. The circuit is a Printed circuit Board (PCB) of 6.5 x 6.5 x 13.8 cm and contains a detection circuit, a pulse drive circuit and a control circuit a LCD for showing the results. The system has a total power consumption of 0.4 W and contains batteries, which makes it portable, Fig. 2.28(d).

Another example of lab on chip system is the work reported by Liu in 2008 from the University of Cheng Kung, Taiwan [195]. The lab on chip is developed for the detection of urinary proteins, and contains a microfluidic control module and a electrochemical detection module. The microfluidic control module presents a novel two-ways spiral shape micropump which transports the samples to the de-

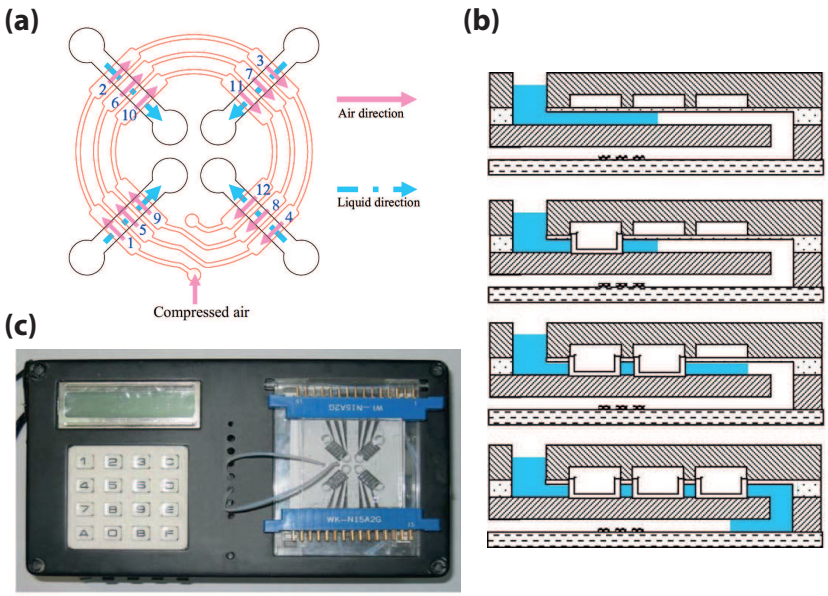

Figure 2.29: Lab on chip developed by Liu. (a) Top view of the peristaltic pump, (b) cross view of the complete microfluidic system, (c) complete picture of the proposed lab on chip.

tection module. This pump is manufactured in PDMS and it is a peristaltic pneumatic micropump manufactured in three levels. In the first level the electrodes are located, the second level contains four channels and on top of those, in the third level, separated by a membrane, there is a four spiral channel where compressed air flows, Fig. 2.29(a). When the pressurized air passes through the spiral channel, the membrane is compressed, impulsing the liquid of the channel, Fig. 2.29(b). The sensing part is done by three electrodes and it is able to detect lysozyme and albumin protein. In addition, the systems contains a controller system connected to a compressor, Fig. 2.29(c).

The following work reported is a portable lab on chip for use in immunosensing systems by Park et al. [196]. The system incorporates two steps: reaction and washing process. The reaction sample is detected electrochemically by electrodes. The lab on chip is manufactured in PDMS and glass, Fig. 2.30(a). The analyte sample is loaded into analyte sample inlet and reaches the reaction channel by capillarity. The buffer solution is loaded in the buffer reservoir. Then, the buffer liquids reach the reaction channel by pushing the reservoir cap, and the ana-

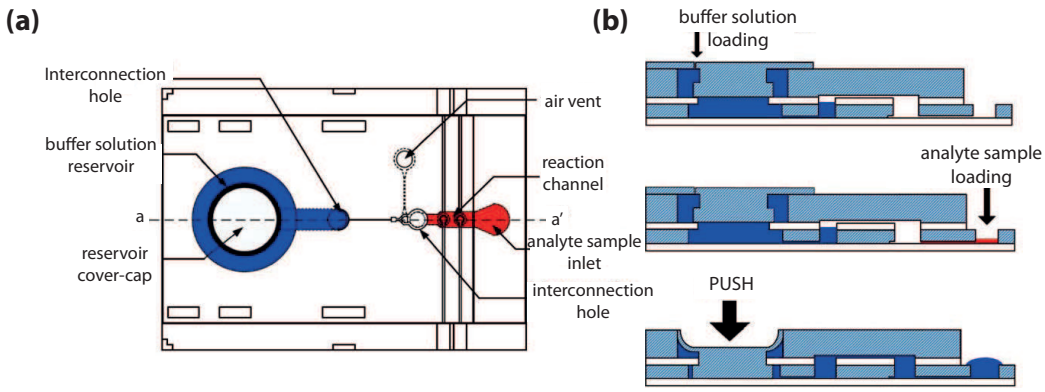

Figure 2.30: Lab on chip developed by Park. (a) Top view of the lab on chip, (b) cross view of the complete microfluidic system and operation mechanism.

lyte sample is washed out, Fig. 2.30 (b). This microfluidic chip does not need any external source or controller for the activation, only a PC for reading the electrochemical sensors. However, if the analyte sample and the buffer solution need to be mixed, it can be done connecting one pump to the buffer solution with a speed under 5 μL/min. The application of the lab on chip was for the detection of DNP antibody.

Lee et at. [197] developed a lab on chip for the detection of dengue virus infection. The microfluidic systems is very comprehensive, it includes a sample chamber, a four membrane-type micromixer, microchannels, two ways micropumps, a circular array of micro coils, a sample loading/mixing chamber, a sample purification chamber, two sample detection chamber and a waste collection chamber. The four membrane-type micromixers are used for mixing, the two ways micropumps for transportation and the microcoils arrays for separator. An optical detection chambers measures the fluorescence signals of the immunoglobulin G (IgG) and immunoglobulin M (IgM), responsible of dengue virus. The microfluidic system is developed in PDMS and glass. In spite of the entire microfluidic functions of the system, it presents one disadvantage the portability, the systems need an external source of pressure, controller system and power supply for the operation.

One representative example of lab on chip for multiparameter analysis is the "Fraunhofer ivD-platform" developed by seven Fraunhofer institutes in Postdam, Germany by Schummacher et al. [198]. The proposed lab on chip presents a low cost microfluidic cartridge in combination with an automated controller. The car-

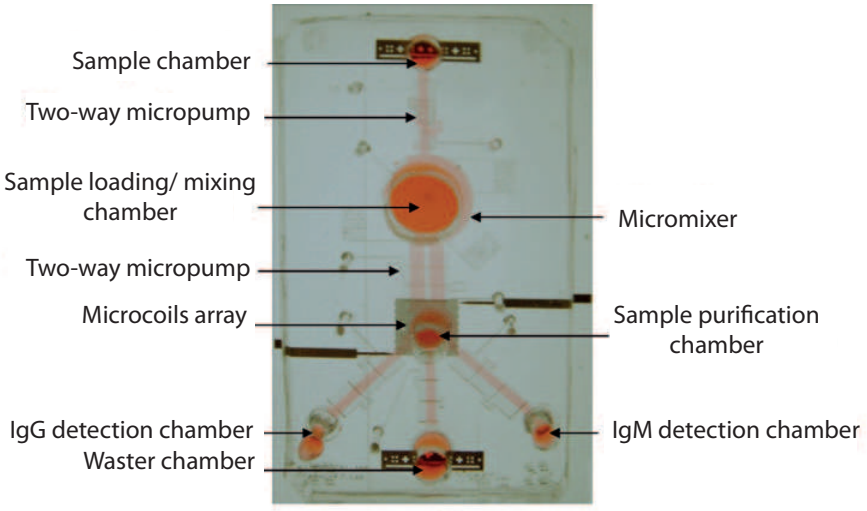

Figure 2.31: Picture of the lab on chip developed by Lee.

tridge is designed in COC and PCB, the microfluidic channels and the reservoirs are fabricated in COC and the contacts for pumps and valves are fabricated in the PCB, Fig. 2.32. The principle of working of pumps is the electrolytic gas generation, using the membrane in COC and the contacts in the PCB. One of the goals of the system is the modularity and integration. On this basis, the system is designed for different assays types with the possibility of choosing between an optical or electrochemical detection sensors, Fig. 2.32(b). The sensors are easily assembled in the cartridge. The controller read-out contains the electronics necessary for the cartridge control and the different sensing. Several applications have been developed proving the feasibility of the systems in nucleic acid and protein markers detection as DNA assay.

Finally, the last lab on chip described in the work presented in 2013 by Yu et al. [199] described an electrowetting on dielectric (EWOD) based lab on chip. The system integrates an electrochemical detection for ferrocenemethanol (FcM) and dopamine (DA). The chip is manufactured in two parallel-plate EWOD made of a layer of glass as substrate, a SU-8 layer as dielectric, a Teflon layer as hydrophobic layer and the electrodes are made of gold. The configuration of the digital microfluidic is designed for merging, mixing, transporting, sensing and recycling droplets, as can be seen in Fig. 2.33. The digital control of the EWOD

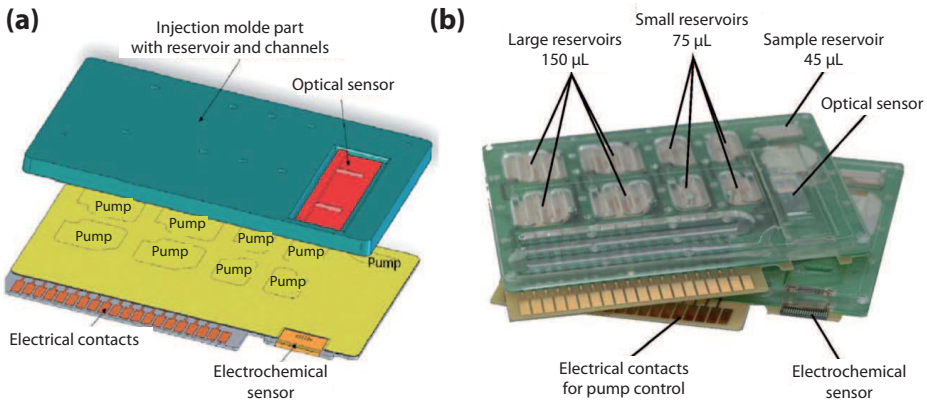

Figure 2.32: Picture of the lab on chip developed in Fraunhofer institutes.(A) Schematic of the iv-Dcartridge. (b) Picture of two cartridges with different sensor configuration: electrochemical and optical sensor.

is carried out by the LABVIEW software. Although the lab on chip offers less possibilities than other works reported, the main contributions of the device are the integrability, low consumption and the minimal consumption of reagents.

In Table 2.6 the main characteristics of the lab on chips described in this section is summarized.

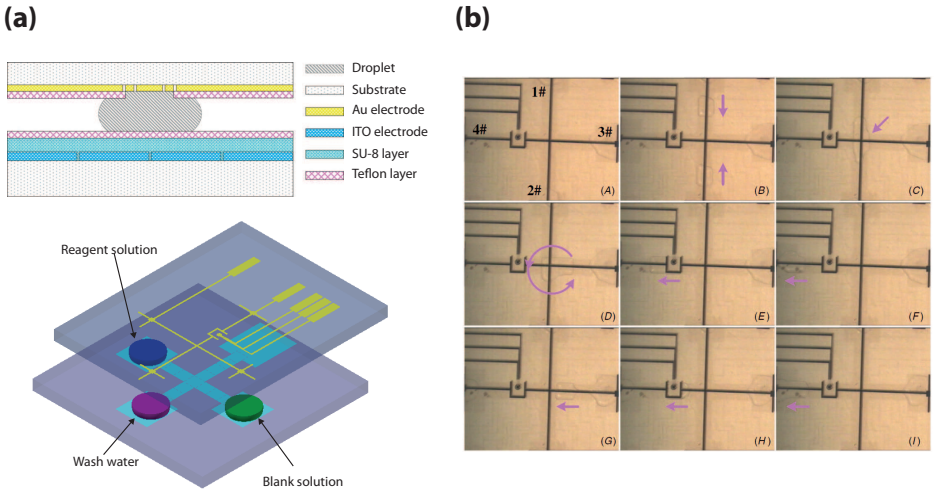

Figure 2.33: Picture of the lab on chip developed by Yu.(A) Schematic of the EWOD based lab on chip. (b) Picture of the complete process of droplet manipulation: (A)-(C) merging, (D) mixing, (E) transporting, (F) collecting effluent droplet and washing the electrodes (G)-(I).

Table 2.6: Summary of the main characteristics of the described lab on chip systems.

Characteristics	**Ahn (2004)**	**Liu (2008)**	**Park (2008)**	**Lee (2009)**	**Schumacher (2011)**	**Yu (2013)**
Transporter	Thermo pneumatic	Electro static	Hand pump	Two way pump	Thermo pneumatic	EWOD
Mixer	Passive microvalves	-	Pump	Four membrane	-	EWOD
Separator	-	-	-	Microcoils	Flushing	EWOD
Detector	Electro chemical	Electro chemical	Electro chemical	Optical	Optical Electroch.	Electro chemical
Controller	Reader	Reader	PC	PC	Reader	PC
Power S.	Portable	Compressor	No need	PC	Portable	PC
Material	COC	PDMS	PDMS Glass	PDMS Glass	PCB COC	Glass/ SU-8 Teflon /Au
Application	Glucose, lactose	Urine	DNP	IgM, IgG	DNA, PCR	FcM, DA
Integrability	Medium	Low	Medium	Low	High	High

3

COMPONENTS OF A LAB ON CHIP

3.1 Introduction

In this chapter a prototyping Lab on Chip platform for multipurpose applications is presented. The main challenge of the platform is the autonomy. The microfluidic platform is designed with its own impulsion system, without the need of an external pump. Moreover, the platform works in a controlled manner, this provides a smart electronics system that is able to monitor the system without the interaction of the user, which makes the platform useful for non expert users. In addition, this electronic system is also electrically autonomous. Therefore, all the power of the system is given by batteries. Regarding this aspect of the electrical autonomy, the whole system is developed to have a low consumption. The system is composed by two impulsion systems with an electronic microvalve, a serpentine for mixing and a detection chamber for sensing. The different components are going to be developed taking into account the purpose of being integrable between each other and also to other platforms. The used fabrication process is based on PCB and polymers (SU-8 and PDMS), the reason is their low cost and versatility in the fabrication of structures and their integration with other technologies. Despite of using these materials, the fabrication process would be the more simple as possible with the idea of migrating towards other more industrial technology, like thermoplastics.

The chapter is developed in four main sections. Firstly, the microvalve that handle the impulsion system would be developed. Secondly, the chapter deals with an autonomous pump system, integrated with a microvalve. Thirdly, a microfluidic circuit with a mixing system and a detection chamber is implemented together with the impulsion system and the microvalve. To sum up, an application for the detection chamber of the system is built. A glucose sensing platform is manufactured being totally compatible with the created LoC platform.

3.2 Fuse Microvalve

3.2.1 Introduction

In this chapter a single-use and unidirectional microvalve, with low consumption of energy for PCB-based microfluidic platforms is presented. Its activation is simple and effective because it works as a fuse. The procedure of fabrication of the device is based on the PCB technology and the typical process of SU-8, using

the PCB as a substrate and SU-8 for the microfluidic channels and chambers. The microvalve is intended for being used to impulse small volume of fluids and it has been designed to be highly integrable in PCB-based microfluidic platforms. The proposed actuator is composed by a pressurized chamber as an inlet, the microfuse as actuator and the outlet chamber.

3.2.2 Structure and working

The main purpose in this section is the manufacturing of a microvalve with low consumption, highly integrable in a microfluidic platform and low cost. The proposed microvalve is single-use, and it is fabricated using PCB and SU-8. The PCB acts as a substrate and the SU-8 as a polymer in the definition of the microvalve structure. The main reasons for using PCB as a substrate are its low cost and versatility for integrating electronic control. The copper layer of the PCB is used to construct the microvalve and the electronic connections at the same time. The microfluidic circuit is manufactured using SU-8 over the PCB. The SU-8 is a good photoresist for rapid prototyping, low cost and has a good adherence to the PCB.

The microvalve structure is shown in Fig. 3.1. As previously said, it is composed of an inlet chamber, an outlet microfluidic circuit and a microfuse. The microfuse consists on a thin copper line working as a fuse. In addition, this copper line separates the inlet chamber from the rest of the microfluidic circuit. The inlet chamber is set to high pressure. The method of operating consists on applying electric energy between the pads of the thin layer of copper until reaching the meting point of copper, opening the fuse. When the fuse is destroyed, the pressurized air leaves the inlet chamber and drives the fluids through the outlet chamber.

The three main parts that compose the microvalve are reported in detail, focusing in the physical phenomena behind each part and the design before explaining the fabrication process.

3.2.2.1 Inlet Chamber

The inlet chamber is in charge of the displacement of the fluids from the inlet chamber to the outlet chamber. It is set to a higher pressure than the rest of the microfluidic circuit. The amount of volume moved depends on the volume and pressure of the chamber following the Boyle's law (3.1). Where P_i and V_i are the pressure and volume set to a high pressure, and P_o and V_o are the volume and

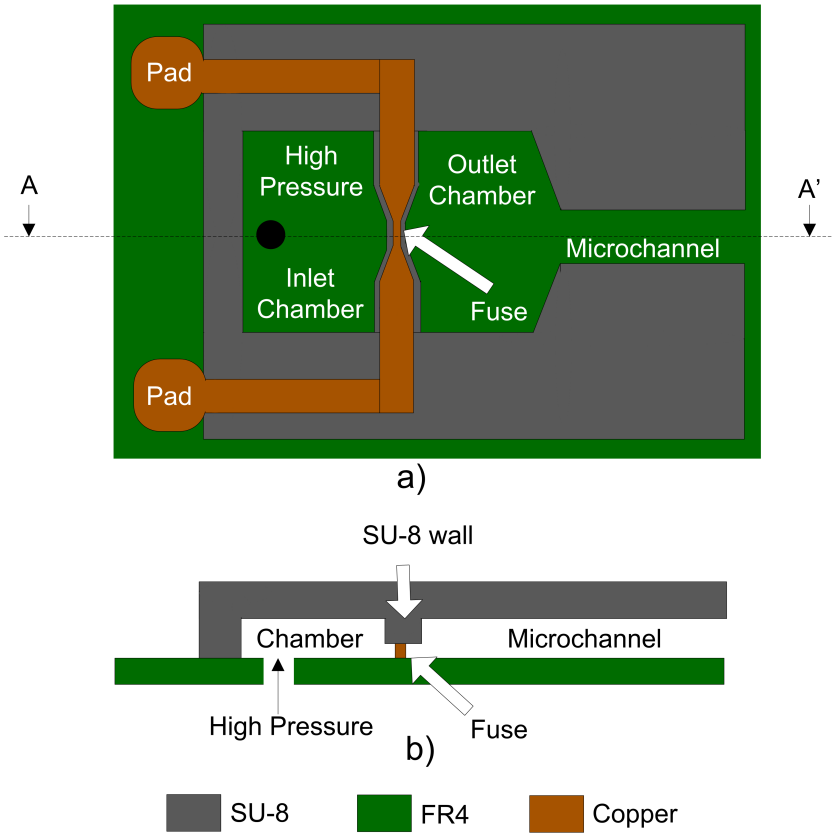

Figure 3.1: a) Top view. Microvalve integrated with a microchannel and a chamber set at high pressure. b) Cross section view (AA') of the microvalve.

pressure at steady state when the microvalve is open. Furthermore, the pressure inside the channel is going to affect to the flowrate. The flow rate is related to the increment of pressure by the fluidic resistance of the system under laminar flow (3.2). The microfluidic resistance of the microfluidic circuit is defined by the resistance in the microactuator, which is the biggest one in the circuit as will be explained later. The pressure system of the inlet chamber will be carefully explained in section 3.3.

$$P_i \cdot V_i = P_o \cdot V_o \tag{3.1}$$

$$\Delta P = R_f \cdot Q \tag{3.2}$$

The chamber has to withstand a high pressure and avoid any leakage during the time it is pressurized. For this purpose, the SU-8 has been chosen for fabrication, due to his low porosity to gases and good adhesion to the FR4.

3.2.2.2 Outlet Chamber and microfluidic circuit

The outlet chamber is the microvalve exit and the beginning of the microfluidic circuit that is going to be driven by the microvalve. For the microvalve working out it is not influential. The parameters that define the microvalve, the flow rate and the activation time, depends on the pressure in the inlet and the resistance of the microfuse, as it will be commented subsequently. In this particular case, the chamber has the same size than the inlet chamber for a better view of the experimental results.

3.2.2.3 Actuator microfuse

The microactuator is responsible for the activation of the microvalve. It is encharged of the flow from the inlet chamber to the outlet chamber. It is a single use microactuator. Its physical behavior is based on a fuse melting. An electric current passes through a conductor, releasing heat. The amount of heat released H is proportional to the square of the current following Joule's law (3.3), where I is the current that pass through the conductor, R_f the resistance of the conductor and t is the time.

$$H = I^2 \cdot R_f \cdot t \tag{3.3}$$

A SU-8 wall is located over the fuse, separating the two microfluidic chambers. The adhesion between SU-8 and copper is robust enough to support the difference of pressure and to avoid leakages between high and low pressure chambers of the circuit. Also, this wall works as a link between the microfluidic and electrical circuits to achieve the complete integration between SU-8 and PCB parts of the microvalve.

In order to activate the device, it is connected to a power supply to melt the copper fuse. The fuse demands a short-circuit current, destroying the fuse in a very short time. The consumption of energy takes place during this short melting time. The melting time is an important parameter in the design of the microvalve and depends on the current and the resistor which likewise depends on the fuse section. In this particular case, the fuse section is rectangular with the height fixed

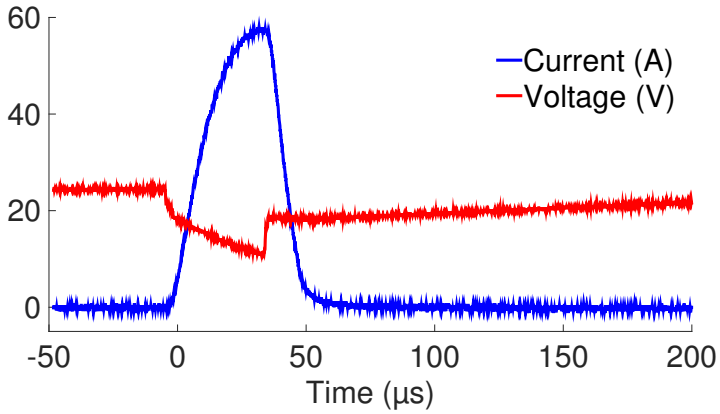

Figure 3.2: Capture from the Oscilloscope during the melting time. The blue line represents the current in Ampere and the red line represents the voltage.

by the copper layer of the PCB. The smaller the section is, the lower the time and the Energy is (3.4). For this reason, a PCB copper layer with a thickness of 5 μm has been chosen. The width of fuse is a parameter to be characterized subsequently, this will depend on the fabrication process. It will be design in order to minimized the fuse section and assuring the adhesion between the SU-8 and the copper for minimizing losses. This electrical energy can be applied by a battery or using a power supply. The electrical behaviour can be seen with an oscilloscope, in Fig. 3.2.

$$E = \int (I^2 \cdot R_f) dt \tag{3.4}$$

3.2.3 Microfluidic behavior of the microvalve

Once the working and the different components that define the microvalve have been explained, the microfluidic behavior is analyzed. The main fluidic parameters which define the microvalve are the fluidic resistance and the flowrate. The flowrate relies on the microfluidic resistance and the pressure increase. Likewise, the microfluidic resistance depends on the geometry of the microchannel when the microvalve is open. For this particular case, the microfluidic resistance in the microactuator is going to predominate in the microvalve due to the small aperture height of the microfuse, 5 microns. However, although the height and the

length is constant by design, the width is not, it is related to the electric breakage during the melting. In order to characterize the flowrate of the microvalve, the resistance is assumed to be constant and it is only dependent on the pressure of the inlet channel. In the evaluation of the complete system, the possible widths of the microfuses are assumed.

To solve the microfluidic study, the microvalve can be seen like a reservoir with an initial pressure that is being discharged through the microfuse channel. This problem can be solved by the equation of Hagen-Poiseuille (3.5). The equation relates the pressure drop (ΔP) with the flow rate (Q), where R_f is the fluidic resistance of the channel created when the microfuse is melted. The section of the microchannel is square-shape and the dimension are L=150 μm, w=100 μm, h=5 μm. The resistance of a square section has the expression (3.6), where L is the length of the microchannel, h is the height, w is the width and μ is the air viscosity. The problem is solved assuming laminar flow, doing a calculation of the Reynold number. If the Reynold number is higher than 2300, the flow is turbulent and the problem will be solved in a different way.

$$\Delta P = Q \cdot R_f \tag{3.5}$$

$$R_f = \frac{12\mu L}{1 - 0.63(\frac{h}{w})} \frac{1}{h^3 w} \tag{3.6}$$

$$Re = \frac{\rho \cdot Deq \cdot v}{\mu} \tag{3.7}$$

Firstly, the resistance and the flow rate are calculated. The resistance is calculated following (3.6) and using this resistance, the flow rate is calculated for every pressure. In the Fig. 3.3 the different initial flow rates of the microvalves for a range of pressure drop from 10000 Pa to 200,000 Pa (100 mbar to 2000 mbar over the atmospheric pressure) is presented. For this flow rate ranges the Reynold Numbers following (3.7) where ρ is the air density, Deq is a hydraulic diameter for a rectangular section and v is the speed. The different Reynold Numbers are shown in Fig. 3.4. It can be observed than the biggest number is 68 for a pressure of 200000 Pa(2 bar) over atmospheric pressure. In conclusion, the assumption of laminar flow is correct. Moreover, this low Reynold Number makes the microfluidic design bear more than 2 bar of pressure drop.

A transient analysis of the pressure is realized to evaluate the behavior of discharge. The analysis is made in Scilab software and the block diagram is presented

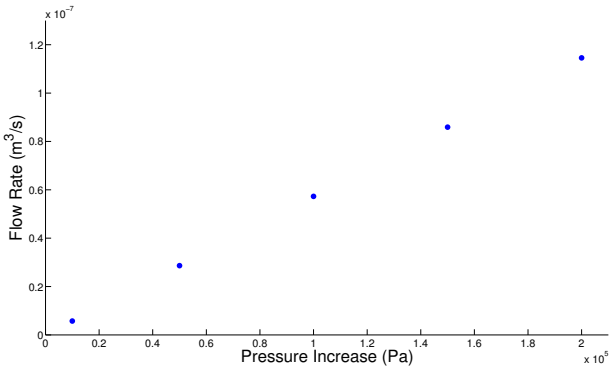

Figure 3.3: Flow rate of the microvalve as a function of the pressure applied in the inlet chamber.

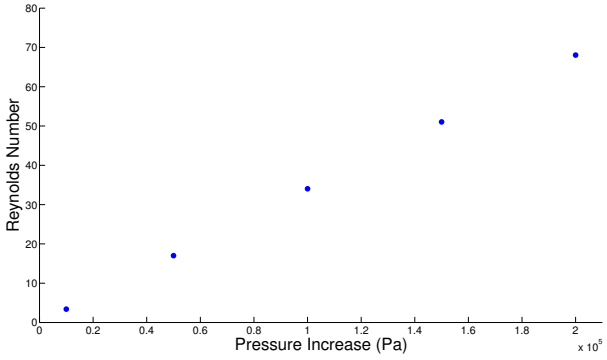

Figure 3.4: Reynold Number of the microvalve as a function of the pressure applied in the inlet chamber.

in Fig 3.5. The pressure over time when the microvalve is open follows equation (3.8). Where P_a is the atmospheric pressure, $P_0(0)$ is the pressure before open the microvalve and t_0 is the characteristic time of discharge. The design is made setting constant density. Initial parameters are set: pressure, inlet chamber volume and the fluidic resistance. The same values of pressure used for calculating the Reynolds number and the flow rate are used as initial parameters to see the discharge in time. The results are shown in Fig 3.6. The values show an exponential discharge, as it was defined previously in equation(3.8). The higher the initial pressure is, the longer it takes to discharge the tank, as it was expected. The time

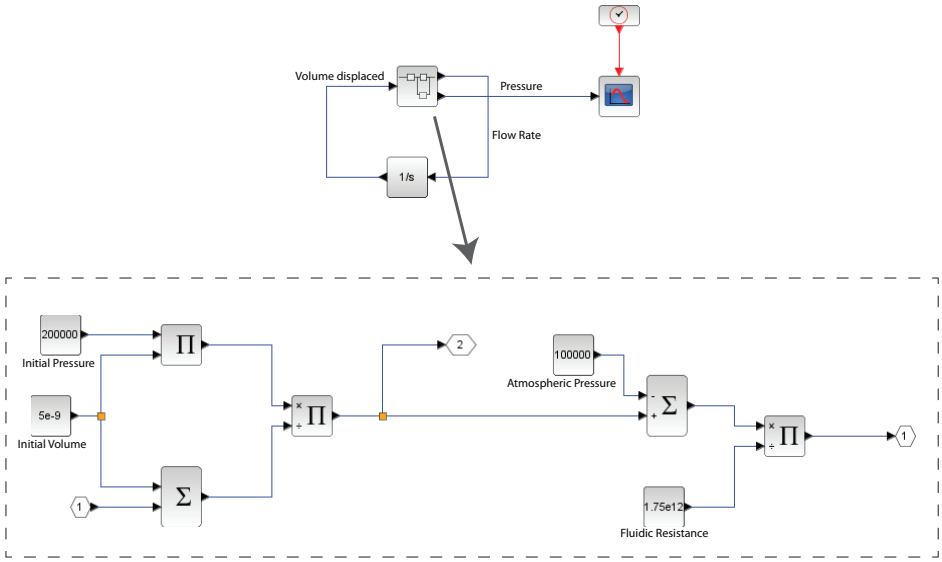

Figure 3.5: Block diagram for the evaluation in time of the pressure.

is lower than 1 s for the worst case, it emphasizes the low activation time of the microvalve.

$$P(t) = P_a + (P_0(0) - P_a)e^{\frac{-t}{t_0}} \tag{3.8}$$

3.2.4 Fabrication process

In this section the fabrication process for the fuse microvalve is presented. The fabrication process starts from the design microvalve adapting the dimensions to the technology. The main goal is to implement a versatile fabrication process capable of being integrated with other microfluidic devices and transferred to other technology.

The process is manufactured in PCB, SU-8 and PDMS in one particular step. The microfluidic structure is SU-8 due to his versatility for rapid prototyping and his accuracy for microstructures. The design is carried out by means of masks, as in any photolithographic fabrication process. In the mask, the dimensions are defined for the chambers and the microactuator. The PCB is manufactured by wet etching and the SU-8 by photolithographic process. The microvalve is developed

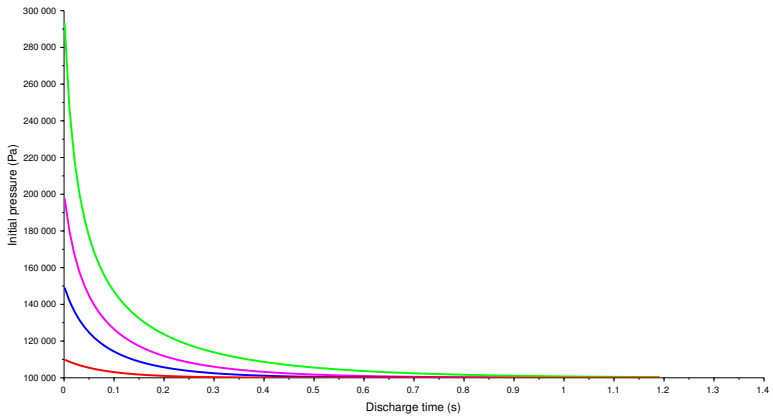

Figure 3.6: Discharge of the inlet chamber over the time for different pressures.

in the Clean Room of the Microsystems Group of the Electronic Department in University of Seville.

3.2.4.1 Masks

The photolithographic mask will define the resolution of the structures. The masks are designed using L-Edit software and developed with a photoplotter FP-8000 XL. The photoplotter has a resolution up to 8192x8600 dpi. However, the resolution of our design is fixed by the microfuse width and the wall of SU-8 over the copper track. The width of the fuse is defined by the amount of power needed for its activation and the SU-8 wall is defined by the amount of pressure able to withstand.This issue will be studied later on, in Section 3.2.5.

In the fabrication process, there have been different designs, one design for the electrical test of the microvalve and another design for the complete behavior of the microvalve. Each design is composed of three masks, one mask for the copper tracks, another for a seed layer of SU-8 which is used for improving the SU-8 fabrication process, and the last one is used for the microfluidic circuit in SU-8.

The copper mask consists on tracks of copper where the fuse is located, it has the same design for both test. The fuse has a size of 200 μm length, 150 μm width, and a thickness of 5 μm due to the PCB copper layer thickness. The PCB is manufactured by etching using a positive photoresist, so the mask is designed in this way, the black part of the mask will stay and the rest is removed. However, in

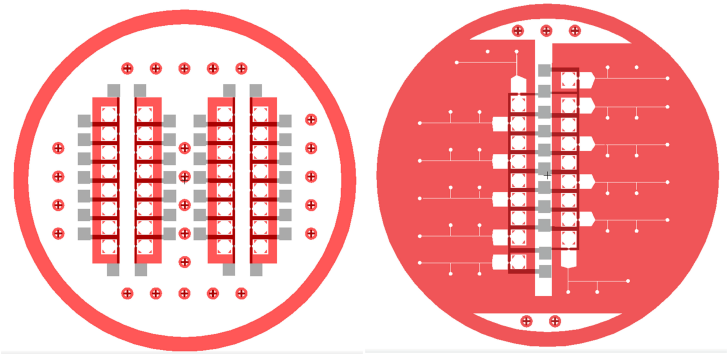

Figure 3.7: Designed masks for the electronic and the complete test of the microvalve.

the other hand, the SU-8 is a negative photoresist and the mask must be designed taking into account that the black parts of it will be released and the rest will stay. The SU-8 seed layer is a simple mask, this mask is designed for improving the adhesion of the next SU-8 layers and the PCB. It is a 5 μm-thick layer that covers the whole PCB with exception of the electric pads of the microfuse. The third mask is used for fabricating the SU-8 circuit, it is designed to contain the wall on the top of the microfuse. To characterize the electrical behavior, the mask contains the inlet chamber and the wall of SU-8. For the complete behavior, the SU-8 mask contains the outlet chamber with a microfluidic circuit. The size of the inlet chamber is set to contain a volume of 5 μl, but it can be modified easily, just for the application requirement. The wall over the fuse has a width of the same size of the copper fuse. When the copper fuse is melted the part is released and the liquid flows. If the wall of SU-8 is much wider than the copper fuse width, the melting of the fuse does not peel off the SU-8 wall and the fluid inside the inlet chamber is not released. However, if the wall of SU-8 is less width or a few microns wider than the copper fuse, in the melting, the energy releases is able to peel off the SU-8 wall. In addition, the wall of SU-8 has to withstand the pressure of the inlet chamber.

In order to improve the alignment between the different fabrication process, crosses are used as alignment marks. The design masks could be seen in Fig. 3.7. The red part is the SU-8 mask and the grey is the copper mask. The red is manufactured in negative because as it was said, the colour part stays and the transparent releases. The fabricated masks can be seen in Fig. 3.8. The masks have been man-

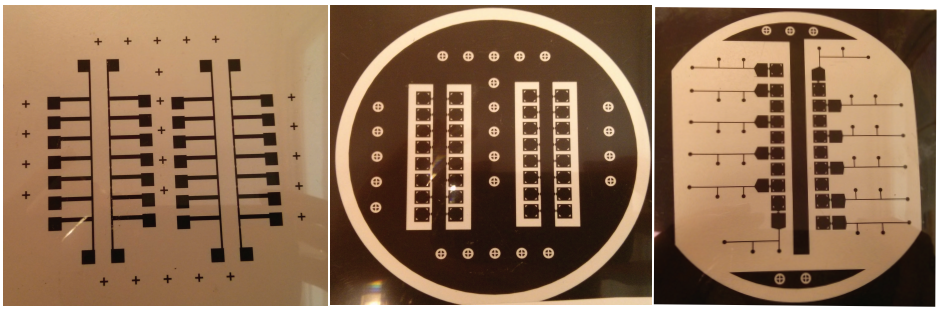

Figure 3.8: Fabricated masks. From left to right the mask for the copper track, the SU-8 mask for the electrical test and the SU-8 mask for the complete test.

ufactured with a resolution of 4064x8600 dpi. This resolution is high enough for the considered dimensions.

3.2.4.2 Process flow

The process flow is reported in this section. The fabrication process is focused on the reliability, the highly integration in a Lab on Chip and the low cost point of view. As previously said, the microvalve is manufactured in PCB and SU-8. The fabrication process for PCB and SU-8 is explained in detailed for this microvalve. However, it would be mostly the same for the other components which form the Lab on Chip. For this reason, the PCB and SU-8 process is explained in deep and would work for the rest of the components of the Lab on Chip. The fabrication process is carried out in the Clean Room of the Microsystem Group from University of Sevilla.

The process starts over a virgin Printed Circuit Board (PCB) where the tracks for the microfuse and the electric connections are placed. The PCB has 5 μm-thick copper layer and a FR4 layer with a thickness of 1.5 mm, Fig 3.9. The copper tracks are transferred to the PCB with the typical copper etching process. A positive photoresist is deposited over the copper layer by spin coating, and with the help of the copper mask, the PCB is exposed to UV light for 40 s in a UV light mask aligner using 7mW/cm^2. The UV light would change the properties of the exposed parts of the photoresist. The PCB is immersed in developer for positive photoresist for 1 min, and the exposed parts of the photoresist would be removed. The PCB is cleaned with water. Later on, the PCB is immersed in an acid mixture composed of hydrogen peroxide (H_20_2), hydrochloric acid (HCl) and distilled water (H_2O) in a proportion 1:1:2. The parts of copper with no photoresist would

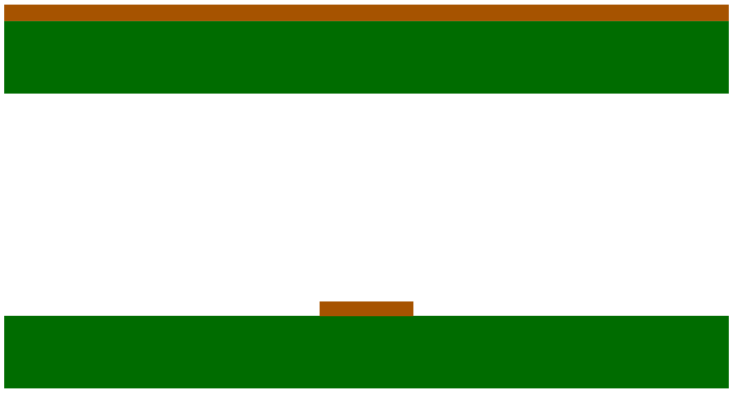

Figure 3.9: First step in the fabrication process: copper etching.

be removed and the parts with photoresist will stay. When the no desired copper is released, the PCB is introduced in water and cleaned with acetone to eliminate the photoresist of the tracks.

The next step is the fabrication of the microstructures in SU-8. SU-8 is a negative photoresist very used in MEMS. The physical and chemical properties of SU-8 makes it very suitable for microfabrication. The process starts with a 5 μm-thick layer of SU-8 which is deposited in order to created a seed layer to improve the adhesion between the SU-8 and PCB, Fig 3.10. SU-8 2005 (Microchem Corp.) is deposited using a spin coater at 3000 r.p.m for 50 s with a previous ramp at 700 r.p.m for 10 s for achieving a thickness of 5 μm. The layer of SU-8 is baked at 65 ^{o}C for 5 min and at 95 ^{o}C for 15 min. Then, it is exposed to UV light with a light source of 7mW/cm^2 for 2 min in steps of 20 s. A post exposure bake is carried out for 2 min at 65 ^{o}C and for 3 min and at 95 ^{o}C min and the desired SU-8 remains crosslinked. In order to remove the non crosslinked SU-8 the board is immersed in developer mr. 600 (Microchem Corp.) for 40 s.

The following step is the fabrication of the chambers, the wall over the fuse and the microfluidic circuit. The thickness of the chambers and channels are 300 μm. To achieve this thickness, two layers of 150 μm are developed. A first deposition of SU-8 2050(Microchem Corp.) is spinned to 700 r.p.m. for 50s with a previous 10 s at 400 r.p.m. This layer is baked for 5 min to 65 ^{o}C and for 15 min to 95 ^{o}C. In this step the solvent is not completely eliminated but the layer is hard enough to can withstand another deposition. When the board is at room temperature, a second deposition with the same parameters is carried out. The bake is done for 5 min at 65 ^{o} and for 2 h at 95 ^{o}C. The exposure is taken for 2

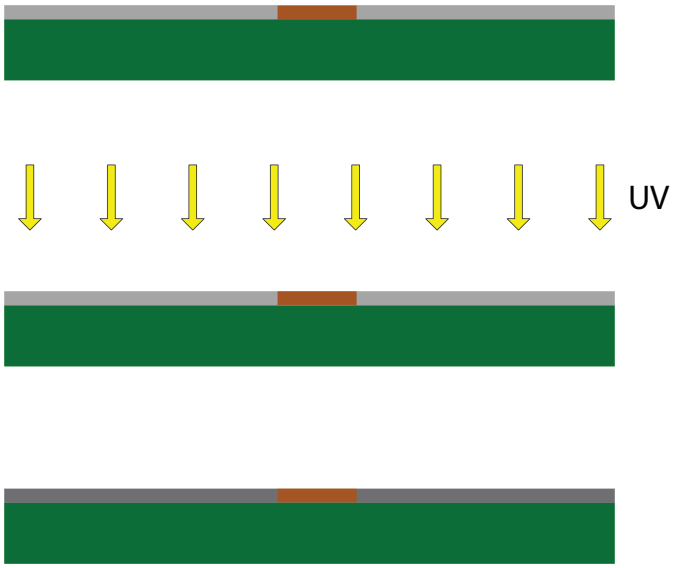

Figure 3.10: Second step in the fabrication process: SU-8 seed layer.

min in steps of 20 s. This exposure time is the same than the time previously used for the seed layer of 5 μm. The reason is the substrate, in one case is PCB and in other is SU-8 and the adhesion changes completely. Then, the board is developed for 7 min. This process can be seen in Fig. 3.11 and the fabricated microfuse and the microvalve can be seen in Fig. 3.12 and Fig. 3.13.

Finally, the last step is the fabrication of the cover of the microvalve. Before the cover is manufactured, the inlets and outlets ports are drilled. The copper is manufactured using BETTS technique [200]. The process consists on the fabrication of a SU-8 layer. The fabrication starts preparing Polydimethylsiloxane (PDMS). The PDMS is prepared by mixing the prepolymer and curing agent in a relation of weight of 10:1. This mixture is stored in a vacuum chamber for 1 hour. In this time the bubbles that appears during the mixing are removed. This mixture is deposited over an acetate film cleaned with acetone and isopropyl alcohol. The deposition is made at 400 r.p.m. for 50 s with a previous ramp at 400 r.p.m. for 10 s. The width achieved is 200 μm. The width of PDMS is not a critical point, it is only important to ensure there is a flat deposition as it would be explain later. The PDMS is cure at 80 ^{o}C for 20 min. Once the deposition of PDMS is ready, a layer of SU-8 is going to be deposited on the PDMS. This layer is going to bond with the microstructure of the microvalve. A layer of about 50 μm is obtained doing a

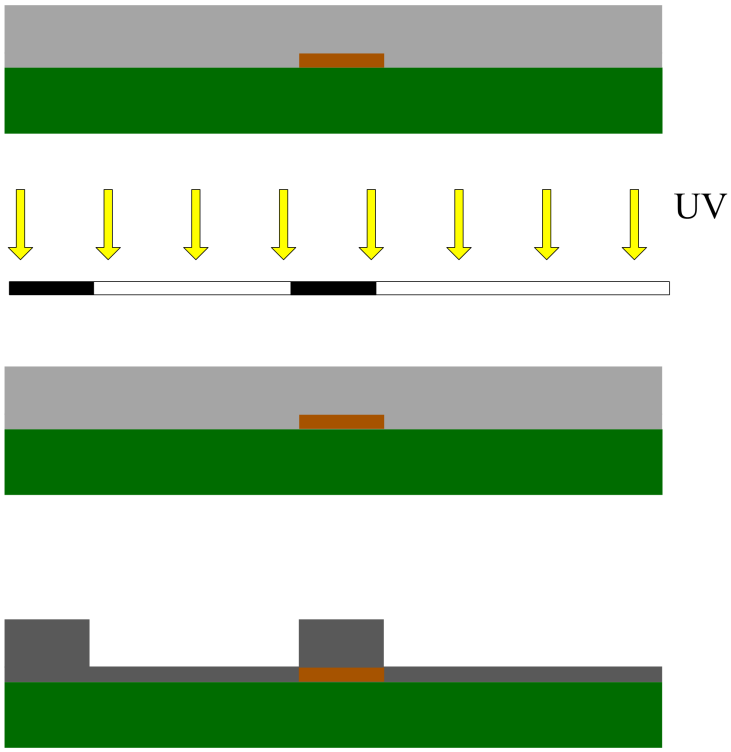

Figure 3.11: Third step in the fabrication process: fabrication of the microfluidic circuit in SU-8.

deposition of SU-8 2025 (Microchem Corp.) at 2800 r.p.m. with a previous ramp of 500 r.p.m. The different height of SU-8 can be seen in this graphic Fig. 3.14. This acetate with the PDMS and the layer of uncrosslinked SU-8 is placed over the rest of the microdevice. The process is accomplished by bonding the side with the uncrosslinked SU-8 with the SU-8 structure of the microvalve. This task is made manually and a slightly pressure is applied with a stick to help the uncrosslinked SU-8 spreading through the microstructures. This process is very critical in the fabrication process, if the SU-8 layer is too thick, when the SU-8 is being spread it could collapse the microchannel. However, if the deposition is too thin, and the surface of the fabricated structure is not totally flat, some parts could result unglued. Under several experiments and for our design parameters, between 40 and 50 μm of width there is not problem in the BETTS process for the 300 μm-thickness channels. Once the acetate with the PDMS and the SU-8 is place in the

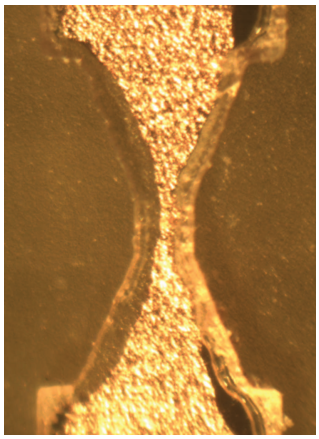

Figure 3.12: Fabricated microfuse. The SU-8 wall above the fuse is wider than the copper fuse. It is designed in this way to help the adhesion and when the fuse is open, the strength in the melting is able to unglued the SU-8 wall.

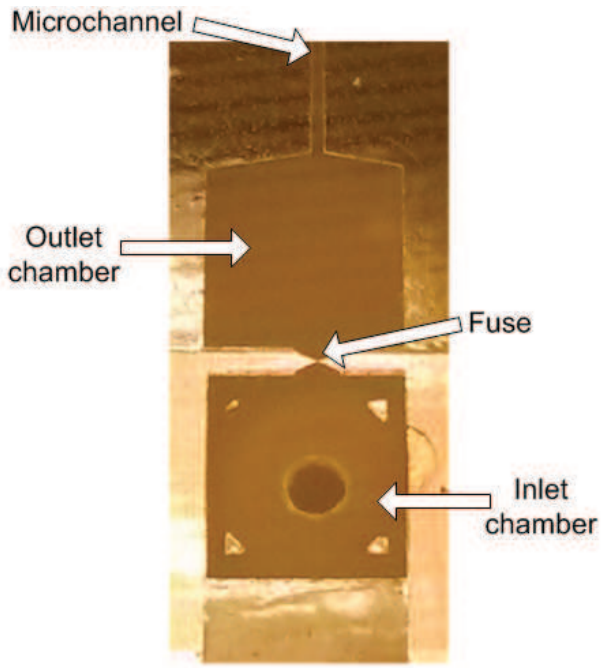

Figure 3.13: Fabricated microvalve without the BETTS cover.

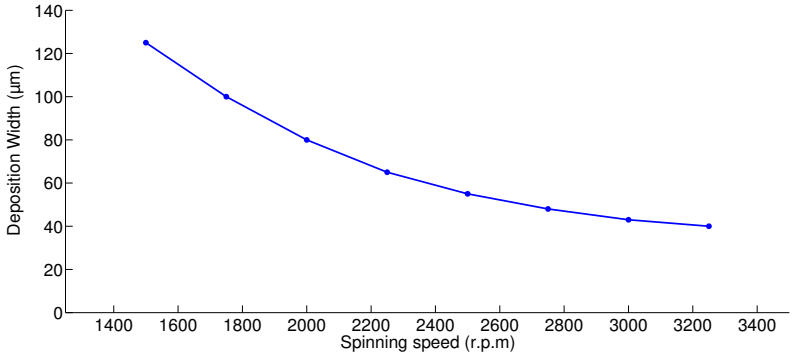

Figure 3.14: Deposition width of a layer of SU-8 over a PDMS sustrate.

structure, this is exposed to UV light for 1 min and later a post exposure bake is done during 3 min at 75 ^{o}C.

To finish the process, the acetate and the PDMS are peeled off from the SU-8 cover. The bad adhesion between PDMS and SU-8 simplify the task and the microvalve is finished. A detailed scheme of the cover step can be seen in Fig. 3.15 and the fabrication result of the complete microvalve is shown in Fig. 3.16

3.2.5 Characterization of the microvalve

This section is focused in the experimental behavior of the microvalve. The microvalve has been tested from two different point of view, from the electrical and consumption and also from the complete working of the microvalve. The working of the microvalve is based on an electrical activation that open the valve and a fluid can pass through it. It is necessary an impulsion source to move the fluids. Nevertheless, the consumption of the microvalve is only electrical. To evaluate the electrical behavior of the microvalve the dimensions of the microfuse are 200 μm length and the width is between 150 and 50 μm, the height is fixed by the PCB. These dimensions are designed taking into account the fabrication process to assure the sealing of the chambers. To fully achieve this task, the set up for activation is shown in Fig 3.17. A power supply and a pressure source is used for the operation of the microvalve and a camera is used to record the process. Moreover, the electrical characterization is analyzed using an oscilloscope, to observe the current and the voltage during the melting point.

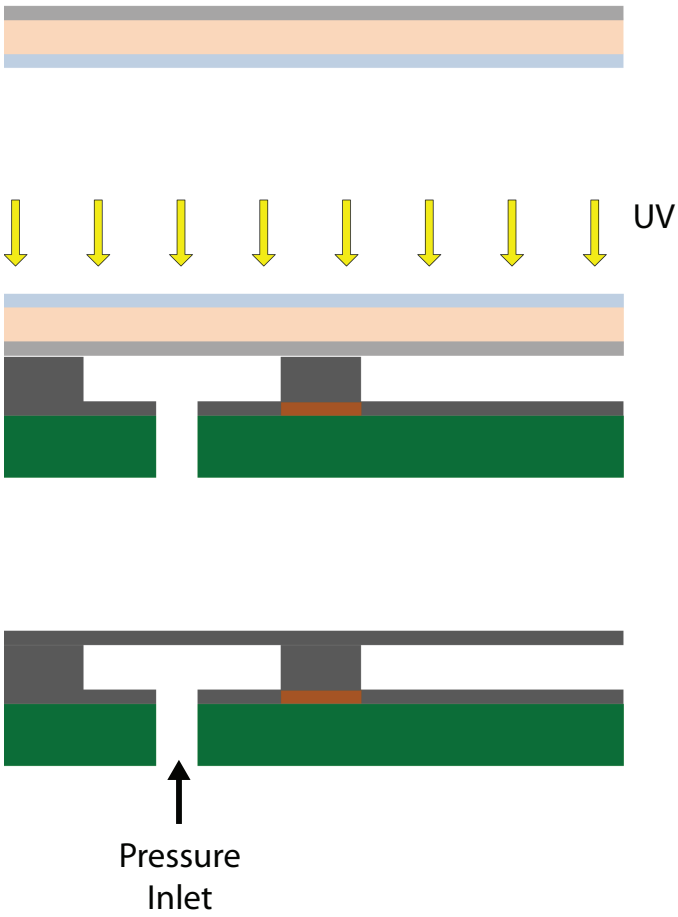

Figure 3.15: Last step in the fabrication process: top cover of SU-8 by means of BETTS technique.

3.2.5.1 Activation test: electrical working

To test the electrical opening of the microvalve, a set of different microfuses are manufactured. Different voltages are applied between the pads of the microfuse and evaluating the breakage. It is important to evaluate the microfuse without SU-8, to obtain what is the minimum voltage applied between the pads to melt the microfuse. This would be a first approach to evaluated the microvalve before being fabricated with SU-8. Forty-three experiments were carried out to evaluate the area of copper melted. The amount of area melted leaves a space that defines

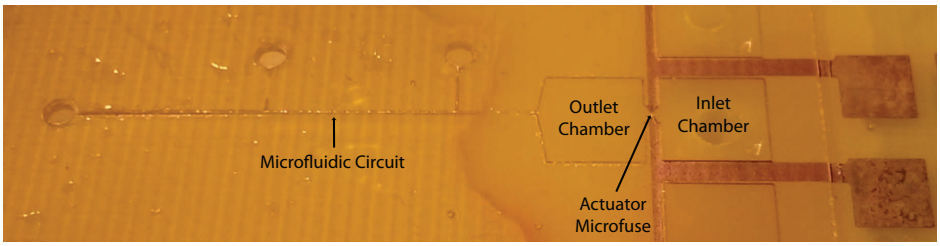

Figure 3.16: Final fabricated microvalve.

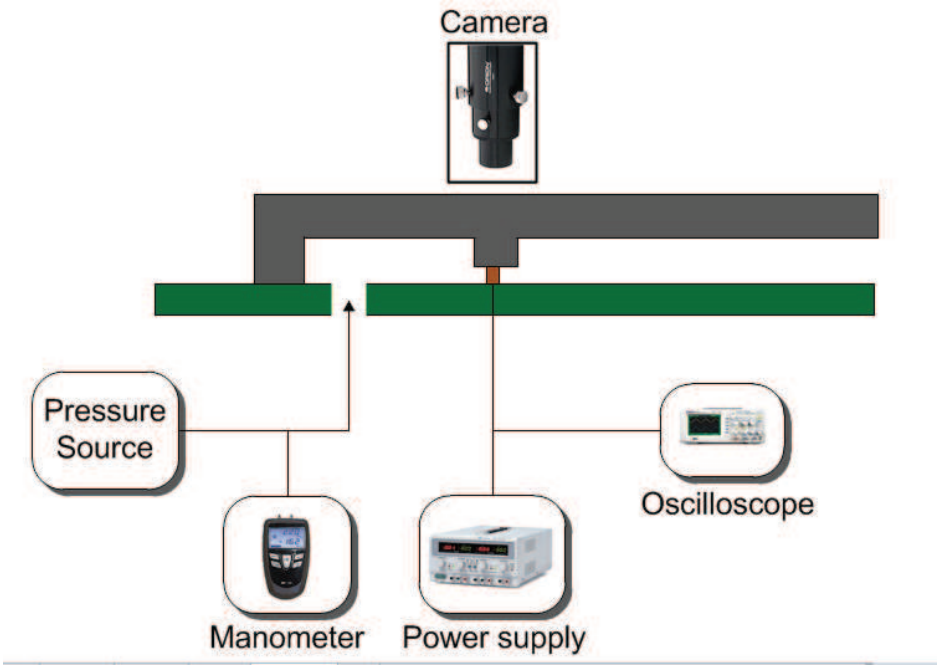

Figure 3.17: Set up for the microvalve characterization.

the fluidic resistance of the microvalve, and this fluidic resistance affects directly to the flow rate as commented previously. The tests were made with an applied voltage from 1 V to 40 V. The results can be seen in the Table 3.1. It is important to highlight that with only 1 V applied between the pads the fuse was open. However, with these results, the conclusion achieved is that it is possible to melt a copper fuse without need of a great voltage between the pads. The next step would be the characterization of the fabricated microfuse with the wall of SU-8 in terms of opening and energy consumption.

Table 3.1: Voltage applied between the pads of different microfuses and maximum width able to melt.

Applied Voltage (V)	Melted area of the microfuse (μm^2)
1	3375.10
1.5	3858.76
2	4117.18
3	4910.16
5	6462.71
10	6824.92
15	7724.66
20	8180.62
30	8988.80
25	9477.32
30	12976.13
40	12976.13

3.2.5.2 Characterization of the microvalve: energy consumption

In the previous section, the goal was focused in the opening of the microvalve. For that reason, it was only consider the track of copper, that is the microfuse. However, it was observed that the microfuse were easily melted due to his low volume of copper. Consequently, the next step in the characterization would be the opening of the microfuse with the wall of SU-8 over it. Several microfuses of different width of copper have been tested and the results obtains are satisfactory, Fig 3.18, as it was expected. So, after the results given with the microvalves and the easy of breakage, the final device was decided to have a width of copper of 150 μm. This was the maximum evaluated and the best solution in terms of sealing. With these premises, the energy at the moment of melting was calculated with the current that passes through the copper track and the applied voltage. The results of the voltage and the current were captured with an oscilloscope as it was shown in Fig 3.2 and the energy was calculated following (3.4) with the help of Matlab software. The energy consumption has been calculated for a set of 5 microvalves of the same dimensions, the results are shown in Table 3.2. The energy of the microvalves is in the range of 14 mJ to 31 mJ for a applied voltage of 24 V. This difference is directly related with the breakage of the microfuse and

Table 3.2: Energy consumption for a set of 5 microvalves of the same characteristics.

	Energy consumption in the opening (mJ)
1	14.1
2	31.3
3	25.9
4	17.9
5	25.8

the tolerances in the fabrication process. Nevertheless, the energy consumption is low in comparison with the state of the art that will be evaluated later.

3.2.5.3 Complete characterization: pass of a fluid

Once the electrical phenomena and the energy consumption have been characterized, the complete activation of the microvalve is carried out. The purpose is to move a fluid due to a pressure difference. A color liquid is injected in the inlet chamber and subsequently a pressure source is connected to the inlet chamber, pressurizing the chamber. The stiffness of the top cover of the microdevice allows the chamber can be pressurized up to 3 bar over the atmospheric pressure. When the microvalve is open, the fluid inside the inlet chamber would be displaced to a particular flow rate. That flow rate will depend on the value of the selected pressure and also of the fluidic resistance of the microvalve. It is important to highlight that the pressure chamber is not depending on the activation time. This depends of the applied Voltage, as explained before. In spite of the fluid to be impulsed is placed in the inlet chamber, it is not mandatory, in this case is placed there because of the ease of watching the experiment. In fact, for further applications, the idea is to impulse the liquid located downstream the microvalve, in the microfluidic circuit.

The process starts inserting the colored liquid inside the inlet chamber, Fig 3.19. Later on, the pressure source is connected to the inlet chamber and with the help of a manometer the pressure is set to 1.3 bar, Fig 3.20 a). The next step is the opening of the microvalve. In order to do so, the voltage is applied between the pads of the microfuse and the microvalve is open. Due to the pressure difference between the inlet and the outlet chamber, the colored liquid is impulsed and moves from the inlet chamber through the outlet chamber, reaching the microfluidic circuit,

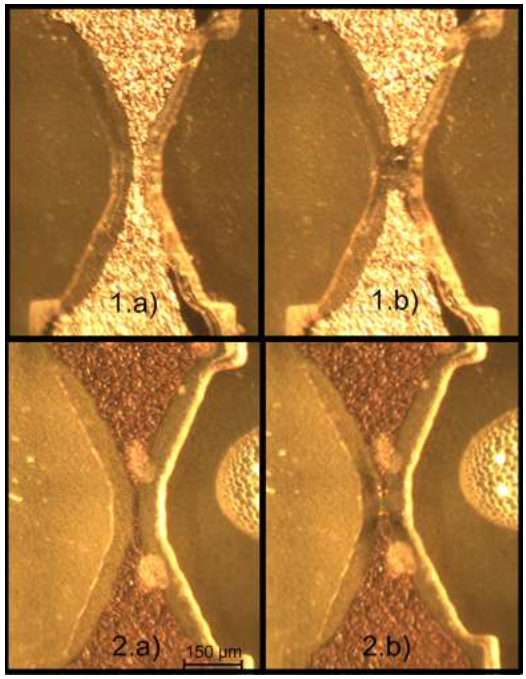

Figure 3.18: Microvalves before and after activation. The difference between a) and b) are the width of the copper fuse.

Fig 3.20 b) and c). It is remarkable the non abrasive breakage of the microvalve, the electric copper fuse is melted but the wall of SU-8 remains.

The displaced volume of fluid has not been considered for this characterization, because this consideration depends on the pressure of the inlet chamber with would be explain in detail in the next section. The goal was the creation of a microvalve with low consumption, highly integrable and fast enough to control the displacement of fluids.

3.2.5.4 Comparation with the State of the Art

After having experimentally characterized the microvalve, it is going to proceed to do a comparison with similar devices is in the state of the art, Table 3.3. It will be compared the main characteristics of these devices for being integrated in microfluid platforms. Firstly, it should be pointed out the activation time, it is essential to have a control in the activation time. The improvement consists on a time 1000 time shorter than the previous Li work. The second aspect to consider

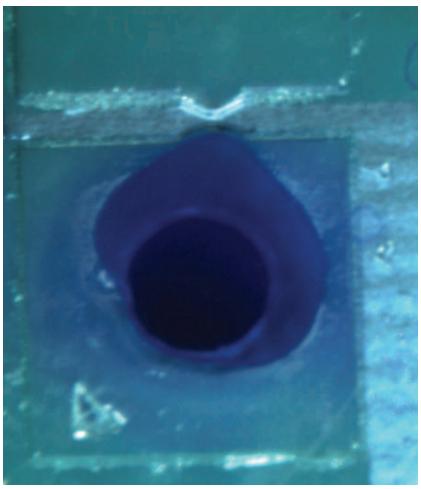

Figure 3.19: Inlet chamber.

is the energy consumption, which is closely linked with the activation time. This paper presents an energy of 30 mJ, approximately equal to consumption of Ahn microvalve, and slightly larger than the one of Li, even thus, in comparison with the rest of the microvalves, the improvement is larger than an order of magnitude. Finally, another important parameter, less related with the operation of the microvalve, but not least, the fabrication and integration of the device on a microfluidics platform. Although the Li's microvalve is very good in consumption and the activation time is acceptable, its fabrication process makes it difficult for integrating in a LoC platform. Nevertheless, the proposed work, due to its simplicity in the design, shows a high integrability in a microfluidic platform. As a result, the microvalve presented is up to date and provides a new approaches in the state of the art. Improving the autonomy of the Lab on Chip platforms and providing another step towards the point of care testing.

3.3 Impulsion System

3.3.1 Introducction

In this section, a pressurization method for manufacturing an independent impulsion system for the microfuse valve is proposed. The method consists in inserting a deformable material filling the inlet microchamber (auxiliary chamber

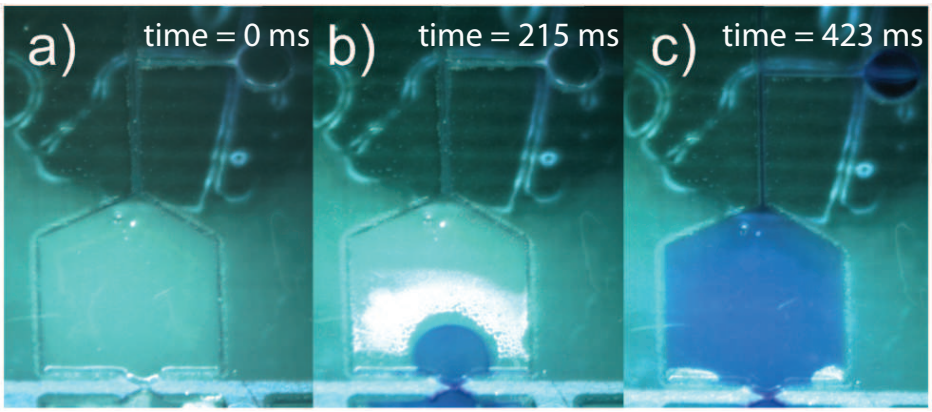

Figure 3.20: Activation process: for t=0 the microvalve is closed, for t= 215 ms the liquid inside the inlet chamber moves through the outlet chamber by the pressure difference and in t=423 ms the liquid has reached the microfluidic circuit.

in Fig 3.21), leading to its pressurization, which will be leading the pressurization and the resulting impulsion of the fluids. The reached pressure involves a wide range of positive values which match well for its application in microfluidic systems, such as Lab on a Chip. It has to be highlighted that the portability of microfluidic platforms is improved due to the fact that the use of external pumps to impulse the fluids can be avoided. So, the section is focused on the displacement of fluid from one part of the microfluidic circuit to another, with the minimum error, in steady state. The control on the impulsion of liquids only depends on the volume of material which has been inserted in the auxiliary microchamber. This method is used together with the microvalve, in order to perform the impulsion of fluids in a controllable manner. The permeability of the system has also been studied. The experiments have shown good impermeability during 1 hour, time enough to perform the subsequent activation after pressurization. A microfluidic circuit, including the pressurized system, has been implemented for testing and as an example of a certain application.

3.3.2 Working Principle

The concept of pressurization is based on the Boyle's Law

$$P_1 V_1 = P_2 V_2 = \text{constant} \tag{3.9}$$

Table 3.3: Comparative of the single used microvalves in the state of the art.

Microvalve	Activation Time(ms)	Energy (mJ)	Fabrication complexity	Integrability
Guerin [136]	1200	400	Medium	Medium
McDonald [137]	1000	150	Low	High
Ahn [138]	700	28	Medium	High
Li [141]	100	2.5	Medium	Low
Pitchaimani [142]	7000	350	Medium	High
Moreno [5]	2000	350	Medium	High
Aracil [4]	2500	700	Low	High
Perdigones [6]	1000	188	Medium	Very high
This work	**0.1**	**30**	**Low**	**Very high**

This expression states that, the absolute pressure exerted by a given mass of an ideal gas is inversely proportional to the volume it occupies if the temperature and amount of gas remain unchanged within a closed system. Where P_1 and V_1 are the initial pressure and volume, and P_2 and V_2 are the pressure and volume in final conditions. Boyle's Law explains how the volume of a gas varies with the surrounding pressure. Applying this concept, the difference of initial and final volume brings about a change of pressure. Consequently, the pressure of a chamber can be controlled by means of the change of volume and vice versa.

An scheme of the proposed system is in Fig 3.21. The impulsion system is based on a chamber which is pressurized by means of an auxiliary chamber connected through a small microchannel. This pressurized chamber is connected to a valve and when the microfuse is activated, the pressure is released moving the fluids downstreams the microvalve. The auxiliary chamber contains the air of the pressurized chamber when a deformable material is inserted. The microchamber to be pressurized will be connected to the auxiliary chamber through the small microchannel, this microchannel would filter the amount of volume inserted. When the pressure of this chamber is released, by means of the actuator, the impulsed volume is the same than the injected one. The auxiliary chamber is designed for contain the desired volume that wants to be delivered. Therefore, the proposed system is completed with the fuse microvalve to activate the system in a controllable manner. This method is designed to be single-use. Even thought

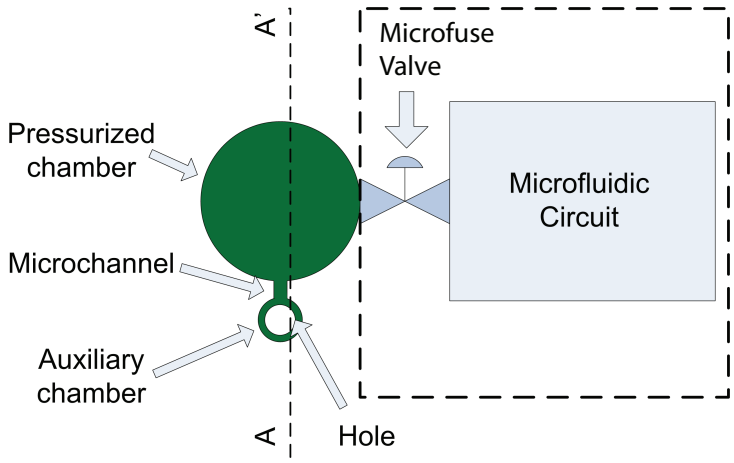

Figure 3.21: Microfluidic structure. The parts of the microfluidic structure can be seen.

the advantages of continuous operation devices are wider in general applications, single-use devices provide interesting advantages on biological and chemical applications. These devices are disposables, low-cost and highly integrable due to the fact that these do not need a cleaning circuit that assure its sterilization.

The method is summarized in Fig. 3.22, where a cross-sectional view of the Fig. 3.21 is detailed. Firstly, before activating the pressurize system, the initial pressure is the atmospheric one (P_1) (step a). The procedure consists in inserting a putty-like modeling material as a filler in the auxiliary chamber through a hole in the substrate. During the process, the pressure increases meanwhile the material is been inserted (step b). Finally, the auxiliary chamber is filled and the final pressure is reached (step c). The dimensions of the auxiliary chamber and the hole of the FR4 has to be designed to contain the desired volume to be displaced. Moreover, the microchannel acts as a filter defining the amount of putty injected.

3.3.3 Design

As it was commented before, the pressure on the pressurized chambers depends on the volume of those chambers and the injected material following (3.9), where P_1 is the atmospheric pressure, P_2 is the final pressure on the pressurized chamber, V_1 is the total initial volume (auxiliary chamber, pressurized chamber, microchannel and hole substrate) (3.10) and V_2 is pressurized chamber volume, $V_2 = V_{pc}$. The

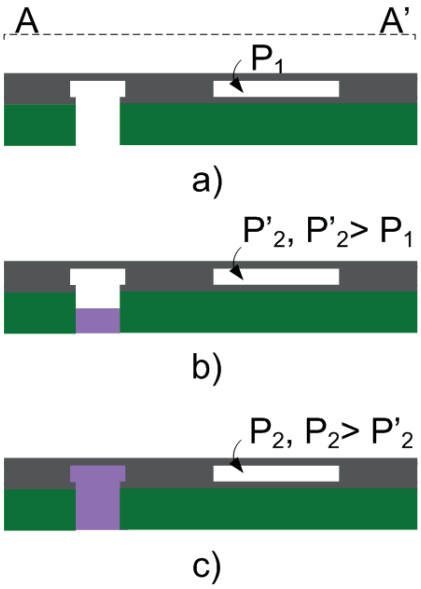

Figure 3.22: Pressurization method, step by step, from the cross view AA' of Fig. 3.22.

theoretical inserted volume V_{ha} is the sum of the volumes of hole substrate, V_H, the auxiliary chamber, V_{aux}, and the volume of the microchannel, V_{mc}, that will be the impulsed volume after the activation.

$$V_1 = V_{aux} + V_{pc} + V_{mc} + V_H \tag{3.10}$$

Consequently, the design parameters are the diameter of the hole, the substrate thickness and the chambers dimensions because the volume of the microchannel is designed to be negligible if compared with V_{ha}. Finally, the expressions of V_{ha} and P_2 can be written as a function of the chambers and hole dimensions as follows:

$$V_{ha} = \frac{\pi D^2 H_{substrate}}{4} + V_{aux} \tag{3.11}$$

$$P_2 = P_1 \frac{V_1}{V_2} = P_1 \frac{V_{ha} + V_{pc}}{V_{pc}} \tag{3.12}$$

where D is the diameter of the substrate hole, $H_{substrate}$ is the substrate thickness, V_{aux} is the auxiliary chamber volume and V_{pc} is the pressurized chamber

one. The volume of the microchannel, V_{mc} has been neglected, as it will be commented in the characterization of the impulsion system.

The ratio (inserted volume/total volume) has to be less than one because the inserted one has to be always smaller than the volume of the circuit. Otherwise, the samples would be transported out the device. The inserted volume has to be designed as a function of the volume to be moved, in order to transport the samples towards the desired place in the device. Therefore, this ratio depends on the designer.

The minimum inserted volume depends on the machining of the substrate, that is, on the diameter of the drilling tool used to perform the hole through a PCB substrate of 1.5 mm. The diameter has to be large enough to insert the filler material manually filling the chamber and to avoid the tool breaking. In our case, the minimum drilling tool has a diameter of 600 μm, to fulfill these issues. Therefore, the minimum volume is 0.42 μL, if the volume of the auxiliary chamber is reduced to zero.

Regarding the minimum pressure, it has to be enough to move the samples, that is, higher than the one due to the friction with the walls. In the proposed approach, the sample is colored water and the material is SU-8. The friction on the circuit can be considered negligible due to the hydrophobic nature of the SU-8.

The design is based on the steady state regime of the system. However, some transient parameters could be necessary if the application requires. These parameters depend on the connected microvalve, an exhaustive study of the transient parameters was done in 3.2.3. It was observed that from pressurized chambers of 1.1 atm to 3 atm, the responses time varies from 0.25 s to 1.2 s.

Despite being design for the microfuse valve, the method can be readily integrable with other thermo-mechanical microvalves[4–6, 139, 201] to achieve a portable pneumatic system. For this purpose, the storage of air is easily done in a controlled manner. The flow process of working with any particular microvalve can be seen in Fig. 3.23. It is explained in phases from the time when the pressurized chamber is set to the desired high pressure (step 1), after the activation of the microvalve when the pressure is decreasing and the sample after the microvalve is moved (step 2), and the steady state where the chamber has been depressurized and the sample has moved to the desired position (step 3).

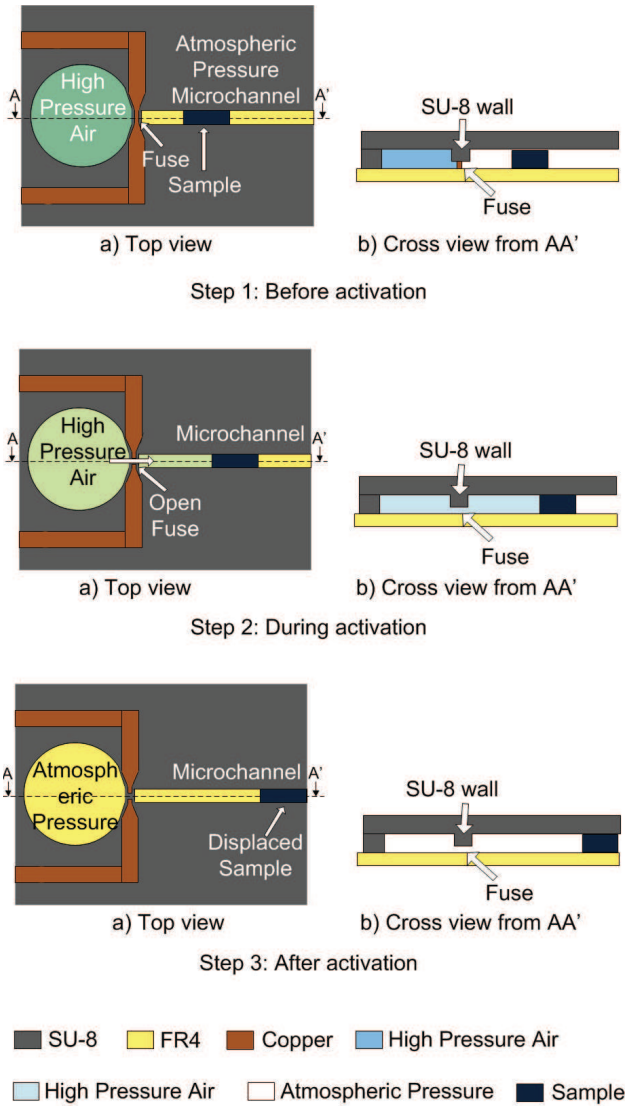

Figure 3.23: Working of the microvalve.

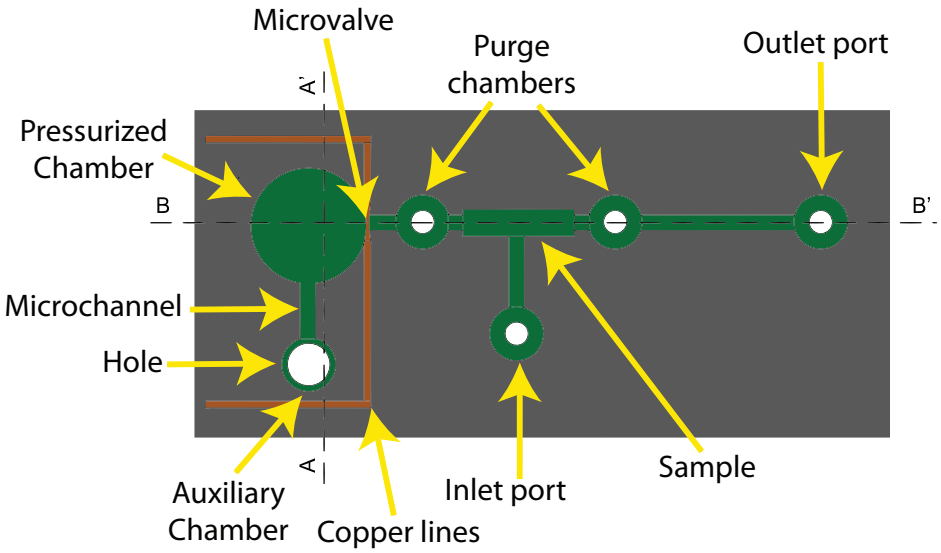

Figure 3.24: Complete system composed by a pressurized chamber, the auxiliary chamber, the selected microvalve and microfluidic circuit for testing.

3.3.4 Fabrication process

To test the impulsion system, a microfluidic circuit with the impulsion system and the microfuse valve have been designed, Fig. 3.24. The system includes the pressurization chamber, the microfluidic circuit, and the microvalve between them. In this case, the microfluidic circuit is very simple, it is composed of a microchannel with a sample, an inlet port to insert the sample, two purge chambers and an outlet port. The goal was to test the impulsion system, the more simplicity of the circuit, the easier to check the results. However, it can as complex as desired.

The fabrication process is shown in Fig. 3.25, from the cross view AA' of Fig. 3.24. It is going to be briefly explained, because the fabrication process is very similar to the microvalve in previous section. As a rapid prototyping, it is going to be manufactured in PCB and SU-8. In addition, as being implemented with the microfuse valve, the fabrication process is intended to be continued.

It starts from the manufactured microvalve in copper, (step a). Later on, the SU-8 structure is manufactured. A 5 μm of SU-8 2005 (Microchem Corp.) is deposited by spin coating in order to improve the adherence between the SU-8 and the FR4 substrate (step b). After that, the SU-8 is baked for 5 min at 65 °C and for 15 min at 95°C in a hotplate and it is exposed to UV light for 40 s (step c).

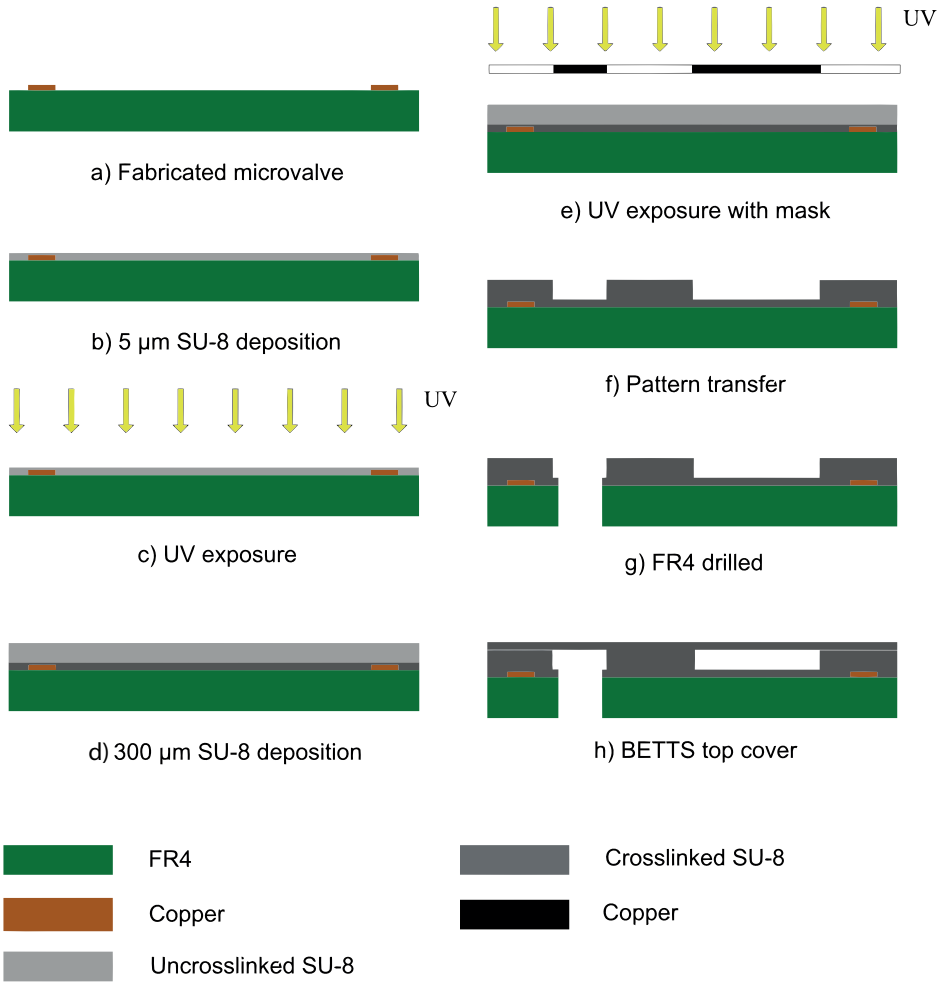

Figure 3.25: Fabrication process step by step to fabricate the general purpose microfluidic circuit.

Then, a post exposure bake step (PEB) is carried out, baking for 2 min at 65 °C and for 3 min at 95 °C in order to achieve the crosslinking of the SU-8 layer. The next step, (step d) is the deposition of a 300 μm SU-8 layer over the last deposited layer. Then, the softbake of this SU-8 layer is performed baking for 5 min at 65 °C and for 120 min at 95 °C. This SU-8 layer is exposed to UV light for 2 min with a mask that defines the microfluidic structure (step e). After that, a PEB step is performed for 3 min at 65 °C and for 5 min at 95 °C.

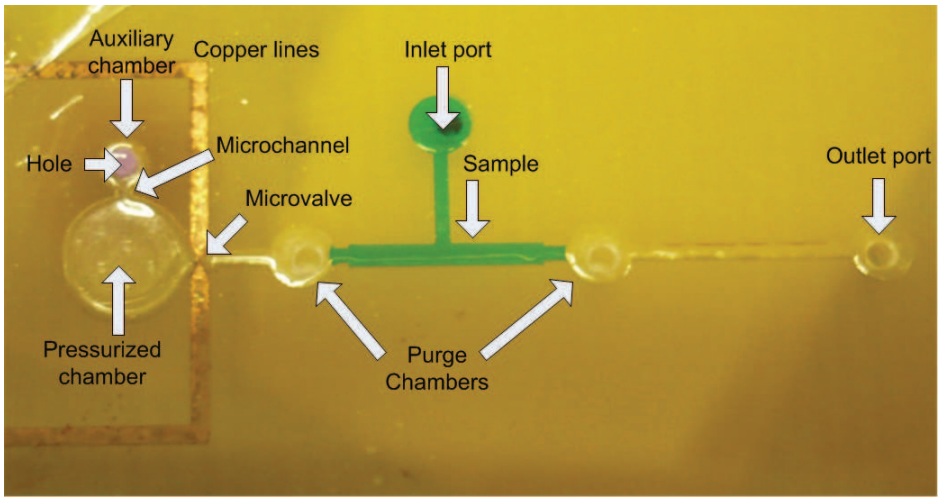

Figure 3.26: General purpose microfluidic circuit for impulsion. It can be seen, that the sample that will be used in the operation is already inserted in the center of the microchannel.

When the SU-8 is crosslinked, the developing is performed to achieve the desired structure. It consists in removing the uncrosslinked resist by immersion in Mr 600 Developer (Microchem Corp.) for 5 min and then, the SU-8 is carefully rinsed in isopropyl alcohol (IPA) (step f). Once the structure has been cleaned, the substrate is drilled through the FR4. The corresponding hole for the auxiliary chamber with a diameter D, and the rest of the orifices are drilled to perform the outlet and inlet ports port with a diameter of 800 μm (step g). After that, the structure is cleaned with N_2 in order to remove the dust due to the drilling. Then, a 50 μm layer (SU-8 2025) is transferred as top cover by BETTS process [200], (step h) where the acetate used in this process is not removed.

The results of fabrication can be seen in Fig. 3.26 where the inlet and outlet ports, and the chambers are shown. The sample is already inserted in the center of the microchannel and the pressurization is already done.

3.3.5 Characterization and results

Once the microdevice for testing, the impulsion system has been manufactured, a characterization is carried out in two phases. In a first phase, the set up used to test the system is described. The goal is to test the displacement of the fluids,

Table 3.4: Theoretical impulsion parameters.

Experiment	Hole diameter (μm)	Aux. chamber volume (μL)	Theor. volume introduced (μL)
A	600	0.46	0.88
B	800	0.60	1.35
C	1500	1.25	3.90

analysing the error in volume from the designed volume to the displaced volume. In the second phase, the goal is focused on the permeability of the microdevice, that is, the air leakages of the chamber, and how long does it take to reach the atmospheric pressure and the validity in time in terms of pressure. This is going to be studied for this particular configuration and for these materials, to have a global view of the proposed system.

3.3.5.1 Impulsion system

To validate the impulsion system, three experiments with different inserted volumes are going to be made for analyzing the results of the displaced volume. The microvalve is activated by electrical current and the stored air is released, impulsing the sample until reaching the atmospheric pressure. The volume which leaves the pressurized chamber should be the same than the one injected through the drilled hole of the auxiliary chamber. It is important to highlight that after the impulsion, the behavior of the putty material was correct, there is not any change in the material.

The impulsed volume can be easily measured with the microscope, and P_2 will be deducted by (3.9) using the experimental impulsed volume. This pressure is not measured by a sensor, in this case, since the value of the total volume will be modified by the sensor volume. This change of volume implies that the pressure reached would not be the same than in the original system. Because of that the pressure P_2 is deduced. Three different experiments are made, as can be seen in Table 3.4.

The microchannel volume, 0.02 μL, has not been considered in the calculated parameters, as previously said in Section 3.3.3, because it is negligible in comparison with the impulsed volume. The percentage of extra volume added to the theoretical impulsed volume taking into account the microchannel would be 2.55

Table 3.5: Comparison of the values obtained experimentally with the theoretical.

Experiment	Theor. volume introduced (μL)	Exper. volume displaced (μL)	error (%)
A	0.88	0.91	3.4
B	1.35	1.4	3.7
C	3.90	4.30	10.3

%, 1.66 % and 0.5753 % in case A, B, C respectively. The volume of the sample to impulse is 0.68 μL in case A and 1.35 μL in cases B and C. The total volume for the experiments is 10.41 μL in case A, 13.58 μL in case B and 18.5 μL in case C. The ratio between the inserted volume and the total volume of the system is 8.4 %, 9.94 % and 21.08 % for the three cases respectively. However, as previously said, these parameters depend on the design of the circuit, and they do not affect to the pressurization.

The results of the experiments can be seen in Fig. 3.27 for the impulsions described on Table 3.4. The experiment A, the Fig. 3.27-A1 corresponds to the circuit before the impulsion, and Fig. 3.27-A2 is the same circuit after a theoretical impulsed volume of 0.88 μL. In this case, the experimental impulsed volume is 0.91 μL, and therefore the error in this impulsion is 3.4 %. The experiment B, the Fig. 3.27-B1 and Fig. 3.27-B2 corresponds to the circuit before and after a theoretical impulsed volume of 1.35 μL, respectively. The experimental impulsed volume is 1.4 μL, and the error is 3.7 %. Finally, the experiment C, the Fig. 3.27-C1 and Fig. 3.27-C2 corresponds to the circuit before and after a theoretical impulsion of 3.9 μL. The experimental impulsed volume is 4.3 μL, and the error is 10.3 %. These results are summarized in Table 3.5. The errors appear between the theoretical and the experimental behavior are due to tolerances of the fabrication process. The main error is due to the drilling. The adhesion of the putty in the wall of the drill is not good enough because the FR4 is a rough material. The higher diameter of the hole implies the higher value of tolerance.

Taking into account that the volume of the pressurized chamber is 3.77 μL, the values of pressures obtained from the measured impulsed volume are 0.02 MPa, 0.04 MPa and 0.11 MPa for experiments A, B and C, respectively. These values of pressure only affect to the dynamic behavior of the system. However, the impulsed volume is independent of that pressure, it depends only on the volume of the injected material in both, the auxiliary chamber and the drilled hole. Therefore,

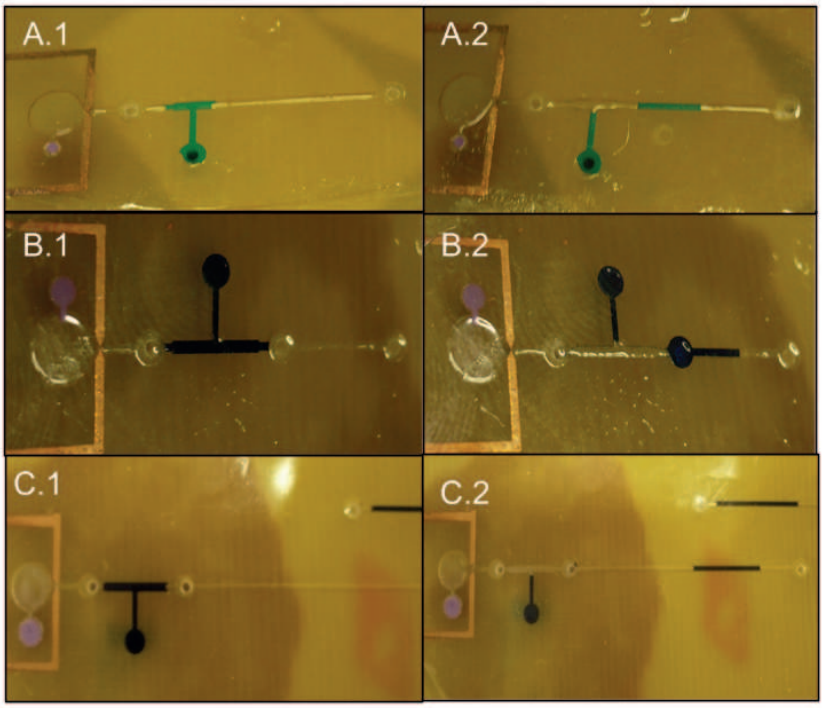

Figure 3.27: Experimental results for three different impulsions.

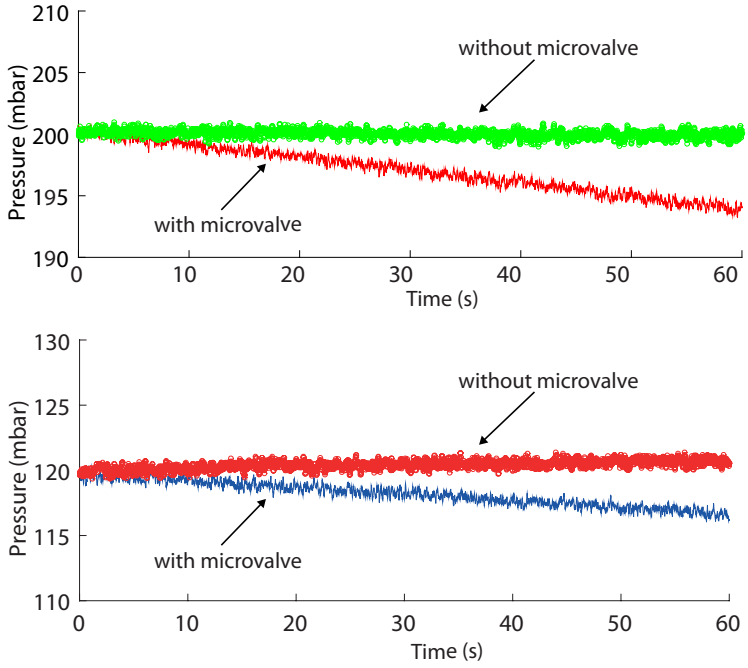

Figure 3.28: Pressurized microsystem in time with and without microvalve.

the impulsed volume of air which pushes the liquid sample has the same steady state independently of the pressure for a fixed volume.

In this section, the characterization of the impulsed volume for Lab on Chip applications was searched. The volume of the proposed system involves microliters range, like the most microfluidic applications. However, if a larger value is required, different strategies can be performed. One possible approach is to enlarge the auxiliary chamber diameter. Other strategy consists on designing several systems (chamber-microvalve) in series, that is, the impulsions performed sequentially. And finally a combination of both of them.

3.3.5.2 Permeability of the impulsion system

After being studying the experimental behavior of the proposed impulsion system, a study of the permeability of the system is made. Polymers are several orders of magnitude more permeable to gas leakage than other materials like glass or metals. However, the epoxy resins are characterized by low gas permeability and therefore can be used for packaging [202–204]. A study of the permeability

of the pressurized chamber is performed due to the porosity of the polymers, it is important specially in the long-term. The aim is to assure that there are not enough leakages to reduce the pressure during the operation time. The system is designed for being pressurized at the moment of using. Nevertheless, the study of permeability is made for 1 hour. This time should be enough to proceed with the experiment.

The method for measuring the leakages of the system in time is based on the control of the pressure inside the pressurized chamber. The impulsion system is composed of SU-8 chambers and a microactuator, the employed microvalve. In addition, the method is designed to be integrable with other components. As a result, there are two different experiments, the first one studies the permeability of the chamber with no microvalve, and the second one studies the complete system chamber-microvalve.

In this section, the measurement of pressure inside the chamber is carried out by the pressure sensor (40PC015G1A from Honeywell) because it is necessary to monitor the value of the pressure along the time. The target is to validate that the pressure keeps stable enough to perform the impulsion. The results are plotted in Fig. 3.28.

As can be seen, there are two plots, each plot corresponds to a couple of experiments with microvalve and without microvalve for a particular pressure. In this case 200 mbar and 120 mbar have been used. As a result, the experiment shows that the leakages of the complete system, chamber-microvalve, are considerably higher than the ones with no microvalve. The main leakage is due to the thin wall of the SU-8 microvalve. The decrease of pressure in the first case lies from 185 to 180 mbar for 1 h, and in the second one from 120 to 117 mbar. That means a leakage of 2.7 % and 2.5% in both cases. These leakages are low enough to perform the activation after 1 hour from the pressurization.

To sum up, it is important to highlight that this method is independent of the selected microvalve and the manufactured materials. The results can improve with materials with lower porosity. This experiment has been done with the main purpose of showing the reliability of the proposed system, even using a polymer.

3.4 Microfluidic Circuit for the developed impulsion system

In this section, a generic microfluidic circuit is developed for the management of fluids that is design to be integrated with the impulsion system. The microfluidic circuit is composed by microchannels, a serpentine channel and chambers to store the fluidic samples. Besides, the microfluidic circuit is controlled by an electronic platform making the system a Lab on Chip platform, where all the monitoring is doing, autonomous and in a controllable manner. The system is thought to mix two fluids and reach a detection chamber for sensing. However, the versatility of the integrated components, the materials and the fabrication process, make the LoC very versatile for other applications in the LoC state of art.

3.4.1 Design

In this part the design of the microfluidic circuit where the impulsion system and the microvalve are integrated is described. The system is designed as a general sensing platform. However, it can be redesigned for different applications, due to the high integrability of the active components, the microvalve and the impulsion system. The complete design of the microfluidic is shown in Fig. 3.29. The active components are located in the first part of the circuit, the two impulsion system which are connected to each other through a microvalve. As, it was described in Fig. 3.21, the impulsion system consists of an auxiliary chamber, a pressurized chamber and a microvalve, in this case the fuse microvalve. Then, the passive components of the circuit and the samples are connected in the second part of the circuit. The samples are the non active components, the serpentine that acts as a micromixer and a sensing chamber. The system has two phases, in the first phase an impulsion is carried out and the samples are moved towards the serpentine, where the samples are mixed and heated if necessary. In the second phase, the samples, already mixed, are impulsed towards the detection chamber for being sensed. Depending on the application, the requirements of the sensing chamber would be different and the chamber would be designed with these specifications. In this case, a circular chamber has been used for testing the circuit.

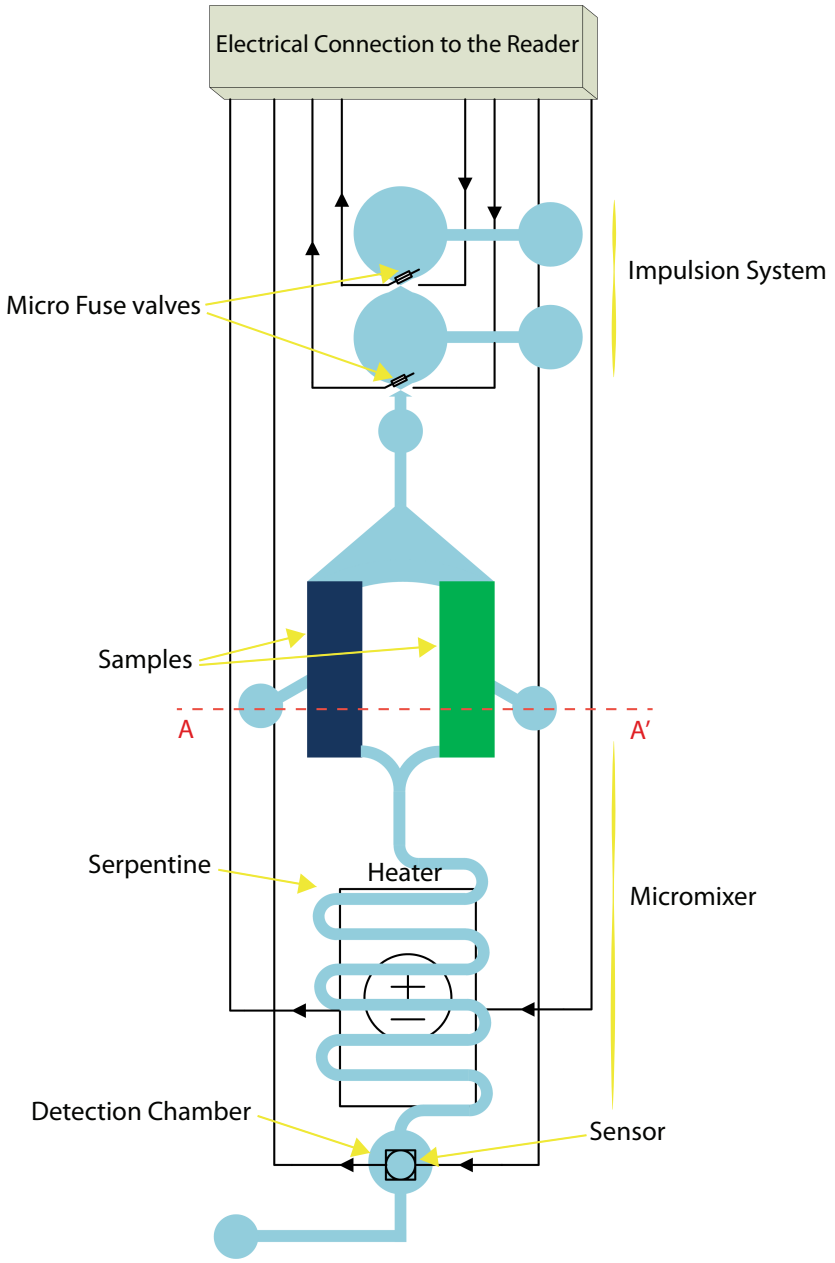

Figure 3.29: General outline of the LoC developed.

Table 3.6: Fluidic resistance of the main components of the microfluidic circuit

	Microfluidic Resistance
Microvalve	$2.89 \cdot 10^{12}$
Serpentine with air	$1.81 \cdot 10^{8}$
Serpentine with water	$9.29 \cdot 10^{10}$

3.4.1.1 Active components of the Microfluidic Circuit: Double Impulsion System

In the definition of the design parameters, a model in Simulink is used. The model is based on the previous simulation model used for the impulsion system and the microvalve.There are some parameters that are defined in a theoretical study. However, other parameters need to be defined by means of a simulation of the model. The fixed parameters are the width of channels that is fix to 500 μm and the samples have a volume of 10 μl. To do a fluidic simulation, it is necessary to know the fluidic parameter, fluidic resistance, of all of its components, to see in which conditions it would be modeled. As previously commented in section 3.2.3, the fluidic resistance of the microvalve is very high due to the low height of the cross section left when the fuse is melted, 5 microns. The rest of the components are the chambers for the samples, the serpentine and the sensing chamber. As can be seen in Fig. 3.29, the samples chambers and the sensing chamber can be neglected, due to their large cross-sectional area. Consequently, the microfluidic parameter is going to be calculated only for the microvalve and the serpentine. In the serpentine, there are two possible options, being full of air or full of water. As can be seen in the Fig. 3.29, in the first impulsion the serpentine would be full of air but, in the second it would be full of liquid. The liquid has been considered water because the possible samples for the sensing are water-based. The calculation can be seen in Table 3.6. It is worth stressing that the fluidic resistance of the microvalve is much higher than the two cases of the serpentine. As a result, it is going to be the dominant in the evaluation of the system.

The fluidic circuit for simulation is designed in Simulink, Fig. 3.30. The mathematical model is based on the conservation of the mass and in the Boyle's Law (3.13),(3.14) considering constant temperature at all times and variable density. Where me is the total mass stored in the second pressurized chamber, m_{c2} is the mass of air that leaves the second chamber and m_{c1} the mass of air that leaves the

first pressurized chamber. With this premise, the equation that follow the circuit can be expressed, as follows.

$$me = m_{c2} + m_{c1} \tag{3.13}$$

$$PiVi = PoVo = cte \tag{3.14}$$

A detailed analysis is made for the the different blocks that compound the system. For the second impulsion chamber block, the pressure of the the chamber is proportional to the initial pressure and volume and inversely proportional to volume that leaves the chamber, whererho_e is the density of the air.

$$Po_{c2}(t) = \frac{Pi_2 Vi_2}{\frac{m_e}{rho_e} + Vi_2} \tag{3.15}$$

The mass of air that passes through the second microvalve resistance, mo_{c2}, can be calculated from the the volume of air that leaves. This volume is calculated from the pressure inside the microchamber $Po_{c2}(t)$ and from the pressure of the total system through the first microvalve, Po_{c1}.

$$Q_{c2} = \frac{Po_{c2} - Po_{c1}}{Rf_2} \tag{3.16}$$

$$V_2 = \int Qc_2 dt \tag{3.17}$$

$$\rho_2 = \frac{mo_2}{Vi_2 + V_2} \tag{3.18}$$

$$mo_{c2} = V_2 \rho_2 \tag{3.19}$$

The mass of air that flows to the first chamber impulsion, m_{c2}, is the sum of the mass of air from the second impulsion system,mo_{c2} and the air that leaves the first chamber impulsion m_{c1}.

$$m_{c1} = mo_{c2} + m_{c1} \tag{3.20}$$

The pressure that leaves the first chamber impulsion from the second impulsion chamber pressurization, Po_{c1}, is proportional to the initial pressure inside the chamber, in this case the atmospheric pressure $Pi_1 = 102400Pa$ and the current

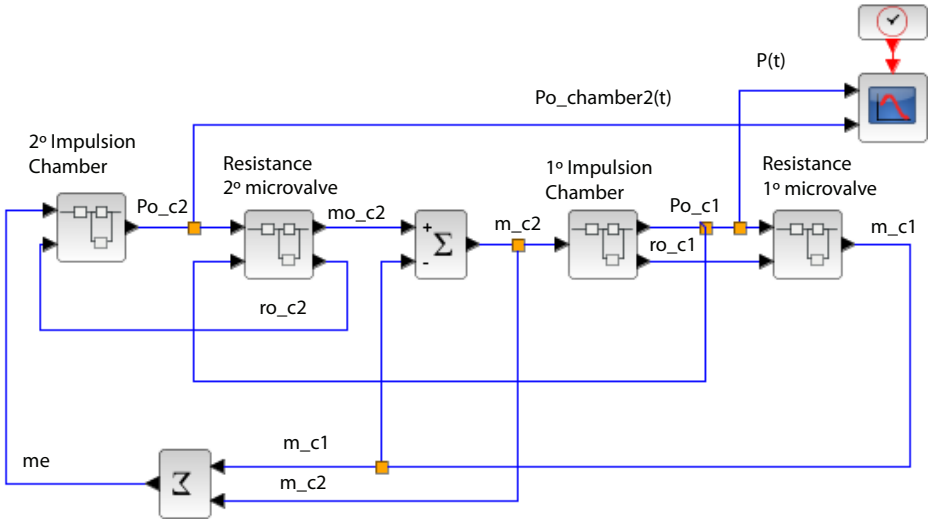

Figure 3.30: Mathematical simulation model for the double impulsion system.

density of air in the chamber, and inversely proportional to the initial density of air. This is the actual impulsion pressure from the second impulsion system that leaves the circuit towards the samples and the serpentine.

$$\rho_1 = \frac{mo_1 + m_{c2}}{Vi_1} \tag{3.21}$$

$$P(t) = Po_{c1} = \frac{Pi_1 \rho_1}{\rho_{i1}} \tag{3.22}$$

The mass of air that leaves the first impulsion chamber is calculated in the second chamber, calculating the flow rate that leaves the chamber.

$$Q_{c1} = \frac{P(t) - Pi_{c1}}{Rf_1} \tag{3.23}$$

$$m_{c1} = \int Q_{c1} \rho_1 dt \tag{3.24}$$

To sum up, this mass m_{c1} and the mass of air that leaves the second chamber m_{c2} is the total mass in the system *me* following (3.13).

Once the model has been designed, the parameters that define the system are set. There are different parameters fixed by design and another can vary over a

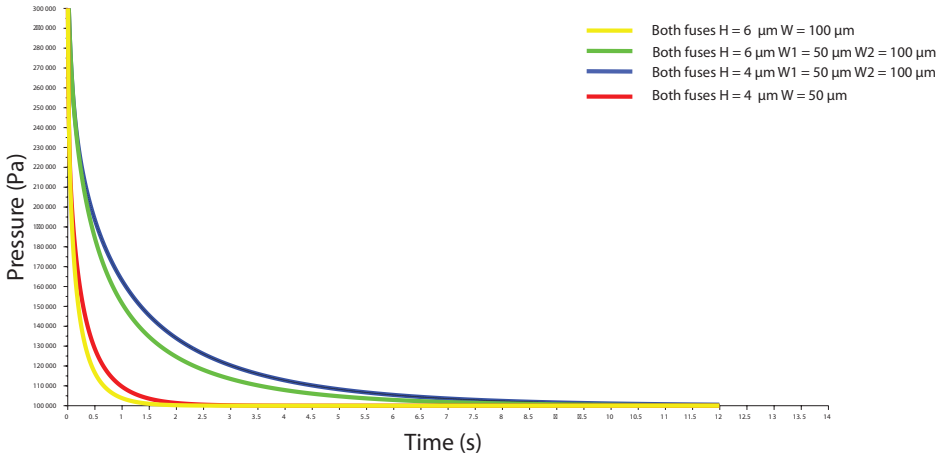

Figure 3.31: Mathematical simulation of the discharge of the LoC system with double pressurized system. The impulsion is carried out through double microvalve. The four graphics correspond to four cases with different microfluidic resistance.

range. The fixed parameters are: the volume to be impulsed, 10 μl as it was said, the pressure for the pressurized chamber which is set to 2 atm over atmospheric pressure and the volume of the pressurized chambers, 5 μl. The only parameter which can vary is the fluidic resistance of the microvalve. The resistance is defined by the length, width and thickness. The thickness is 5 μm with 20 % tolerance (P.W. Circuits Ltd.), the length is set by design to 150 μm and the width depends on the copper melting. Numerous experimental tests proved that the width of melting is set between 50 and 100 μm. Taking into account this premises, the simulation has been developed for four cases. The two extreme cases with the lowest and the highest fluidic resistance while the other two graphics assume that the height of the copper fuses is the same and the widths are different. After observing the results, Fig. 3.31 it is remarkable the high influence of the height of the copper fuse in the fluidic resistance, with differences in time of 10 s in the discharge of the complete system. However, for the applications which are designed, point of Care Testing [205], a total set up time of seconds is more than acceptable.

3.4.2 Passive components of the Microfluidic Circuit: Micromixer and Detection Chamber

3.4.2.1 Micromixer

The function of this component is to mix two different samples. The samples are water based. These two liquids are inserted into two chambers of the microfluidic circuit, between the impulsion system and the serpentine, as can be observed in Fig. 3.29. As it was commented before, there are two impulsions. The first impulsion is in charge of the mixing of the fluids and the storage in the serpentine. The second impulsion drives the mixed liquids towards the detection chamber.

In the design of the micromixer, there is an important issue to take into account, the asymmetries. As can be seen in the picture Fig. 3.29, the two chambers for storing the colored liquid samples are connected to the pressurized chamber above, and below to the serpentine. If there is any asymmetry of the fabrication process or in the insertion of the liquids, when the microvalve is opened the air would only follow the path of the smallest microfluidic resistance. As a result, only one sample would be impulsed. It is not an easy problem to overcome because there are always asymmetries due to the fabrication process tolerances. To resolve the issue, the geometrical design and operation of the circuit must be approached to absorb any tolerance.

Taking into account these concerns, various tests were carried out to evaluate a good working of the circuit. The final structure can be seen in the Fig. 3.29. A triangle-shaped chamber is placed between the impulsion system and the samples. The samples are stored in chambers which are connected to the serpentine. The volume of the chambers to store the liquids is 4.83 μL each, they have rectangular shape with dimensions of 2.3 mm x 7 mm. These wide chambers help the movement of the liquids when the valves are opened. This is due to the high transversal area where the pressure is exerted (w = 2.3 mm x h = 0.3 mm). Therefore, the force over the colored liquid samples is high enough to push them, making the dimensional tolerances negligible. On the other hand, the triangle-shaped geometry is a divergent nozzle used for reducing the kinetic energy of the air, avoiding preferred ways of flow towards the chambers of the liquids. The serpentine has a length of 65 mm and a width of 500 μm, being its volume 9.75 μL.

3.4.2.2 Detection Chamber

The detection chamber contains the desired sample to be analyzed. Depending the type of sensing to be made, the dimension of the chamber have tougher restrictions. The proposed LoC has been configured for a silicon sensor, Fig. 3.32. The silicon sensor is not single-use chip, it is thought to be reusable. Due to the LoC platform is single-use, an auxiliary PCB is used where the chip is integrated. This auxiliary PCB is connected to the Lab on Chip PCB after the fabrication and afterward can be disconnected. The auxiliary PCB is round and has a square milling in the center with the same size than the silicon chip. This auxiliary PCB and has pads and tracks, the pads are connected to the sensor by wire bonding and this pads are connected by tracks to thru-hole semi-vias at the edge of the PCB. The semi-vias are soldered to the tracks of the backside of the LoC PCB, sealing the auxiliary PCB with the LoC PCB. In this case, a dummy sensor is used, that is, a silicon die without sensing components and with a side of 3 mm. The chamber has to be big enough to contains the sample, and it is only needed that the sample gets in contact with the silicon chip. However, different sensing can be developed. In the next section, a glucose sensing is developed for being able to integrate in this LoC platform.

3.4.3 Fabrication Process

The fabrication process of the complete system is detailed, Fig. 3.33. The system is manufactured using SU-8 and PCB in the same manner than the microvalve and the impulsion system.

The process starts with a commercial PCB with a 5 μm-thick copper layer PCB where the electrical copper lines are fabricated by using the typical wet etching of the PCB process. These copper lines define the electrical connections, the copper fuse of the microvalve, a microheater and also a male PCI connector. The female connector is placed in the electronic device. Once the copper lines are manufactured, the PCB is cut following the shape of the male PCI connector.

The typical SU-8 process is performed to fabricate the microfluidic circuit. The process starts with the manufactured PCB as a substrate, step a. A SU-8 layer of 5 μm (SU-8 2005, Microchem Corp.), is manufactured over the whole PCB for improving the adhesion between the PCB and the SU-8. The thin layer is spin coated at 3000 rpm for 1 min. Then, the SU-8 is baked for 5 min at 65°C and during 15 min at 95°C in a hot plate, step b. In the step c, the baked SU-8 is exposed to UV light for 8 steps of 20 s. The source of light used is a mask

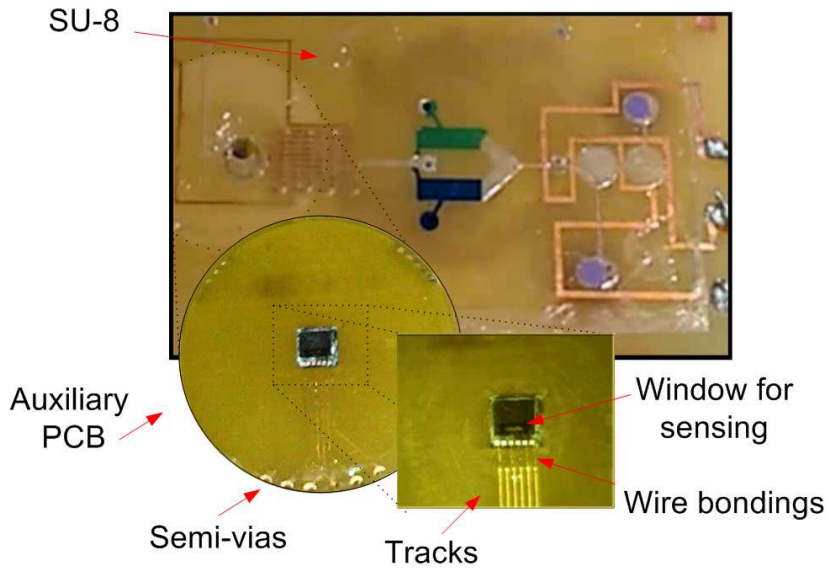

Figure 3.32: Example of silicon Chip integrated in the detection chamber.

aligner with UV light power density of 7 mW/cm^2. Then, a post exposure bake of 2 min at 65°C and 5 min at 95°C is performed. Subsequently, in step d, two layers of 150 μm are spin coated to obtain the final thickness of 300 μm. The first layer is deposited using SU-8 2050 (Microchem Corp.) at 700 rpm for 1 min. A short soft bake is made for 5 min at 65°C and 10 min at 95°C in order to harden enough the 150 μm SU-8 layer before doing the second deposition. The PCB is cooled down at room temperature before depositing the second layer. Later on, the second layer is deposited in the same way and it is baked for 5 min at 65°C and 2 h at 95°C. During this long soft bake, the solvent for the 300 μm SU-8 layer is removed. In step e, the SU-8 is exposed to UV light for 6 steps of 20 s using the mask which define the microchannels, chambers, and the SU-8 wall. After that, a post exposure bake of 3 min at 65°C and 5 min at 95°C is performed. After this step, the SU-8 exposed to the UV light is crosslinked, and the unexposed ones are ready for being developed. When the PCB is at room temperature, it is immersed in developer mr 600 Developer (MicroChem Corp.) for 7 min, step f. The uncrosslinked SU-8 is removed remaining the desired SU-8 structure. Finally, the structure is cleaned with isopropanol.

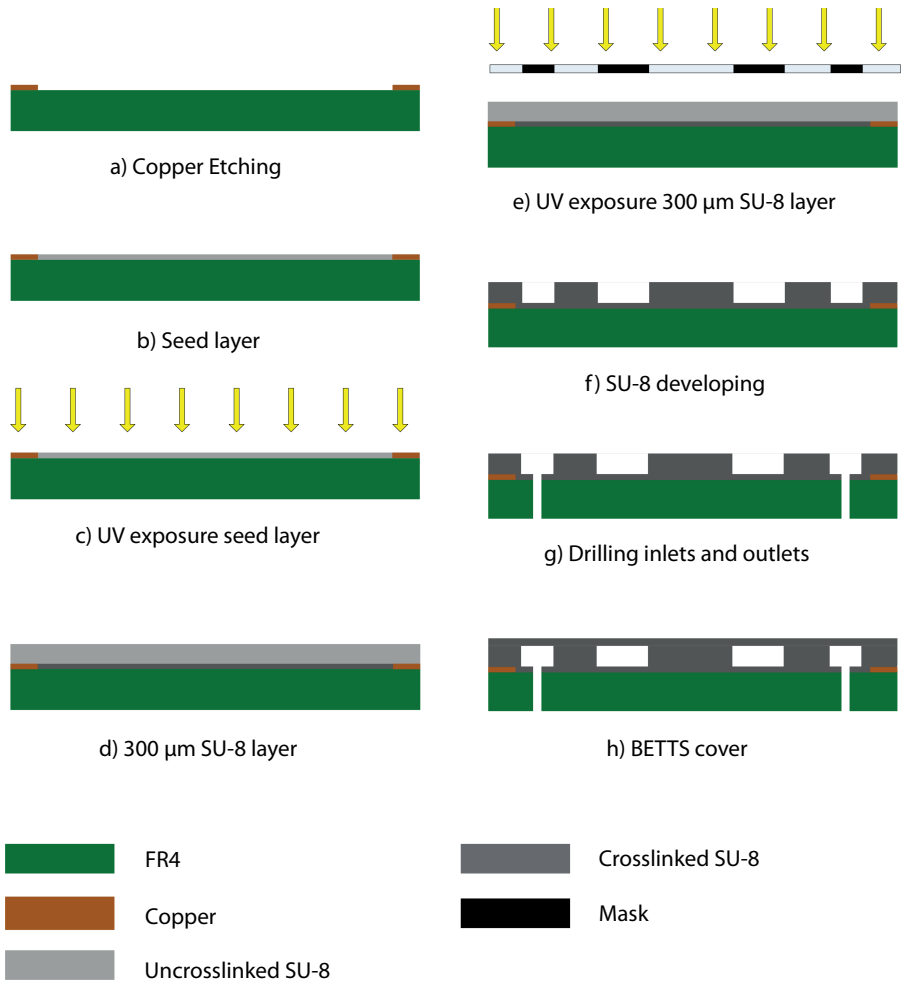

Figure 3.33: Fabrication process of the microfluidic circuit with the impulsion system.

Once the SU-8 structure is manufactured and before putting the cover, the holes for the inlets, outlets, pressurization system and the cavity for the sensor are drilled, step g.

The last phase of the fabrication process is to create a cover, step h. It will be created using SU-8 by means of the BETTS technique [200]. After that, the microfluidic platform of the LoC system is manufactured and ready for being used. A picture of the fabricated device can be observed in Fig. 3.34.

3.4.4 Electronic Design and Operation

The presented microfluidic circuit is activated electronically by means of the microvalve. This activation is developed in a controlled and autonomous way with the help of an electronic reader. The electronic reader is developed using a microcontroller to control the activation of the microvalves. The proposed device takes advantage of the PCB substrate of the microfluidic platform for the implementation of the connection with the reader. In this section, the description of this electronic device is proposed.

The electronic device is developed for acting as the smart part, it is in charge of the activation of the microfluidic platform. The activation is carried out with the iteration of the user. The microcontroller acts as an intermediary between the complete system and the user. The communication with the user is accomplished by an LCD inserted in the electronic device. This LCD display shows information about instructions and state of the process. The final electronic device can be seen in Fig. 3.35, where apart from the LCD there are a push button, a switch and a PCI port. The PCI port is the female connector where the microfluidic platform is inserted, the microfluidic platform contains the pads with the female connector as it was commented. The switch handle the the flow operation of the system and the push button is pressed by the user for the beginning of the process.

There are two energy sources in the system, the first one needed for the activation of the microvalve and another one for the power supply of the electronic circuit. The switch has three different position, as can be seen in Fig. 3.35,"O" ("OPERATION"), "N" ("NEUTRAL") and "E" ("ENERGY"). The "E" position is the position where the energy is store for the impulsion of the microvalve. The "O" state is used for the activation of the system, the electronic control begins and the instruction for operation and the state of the operation is displayed in the LCD. Finally, the "N" state is a state for not operation of the system. A chrono-

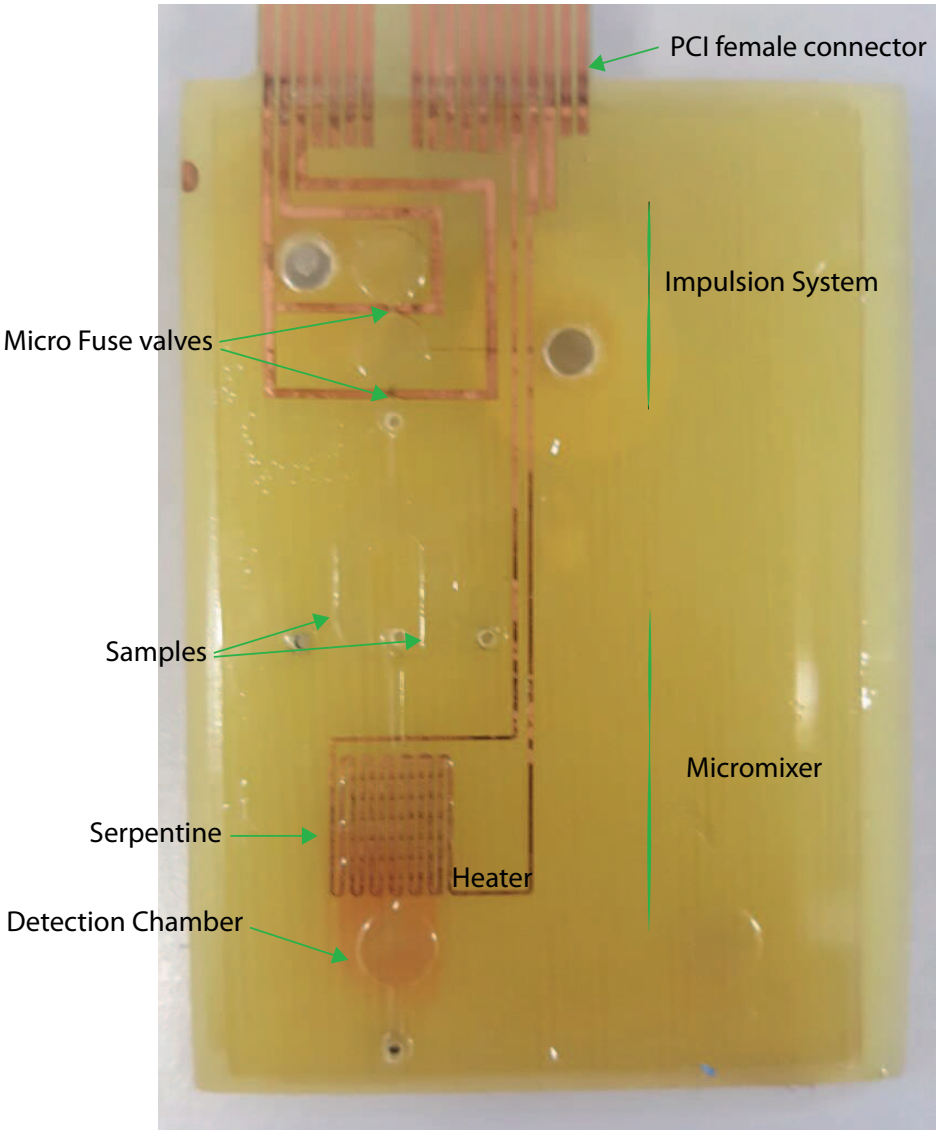

Figure 3.34: Fabricated microfluidic circuit with the impulsion system.

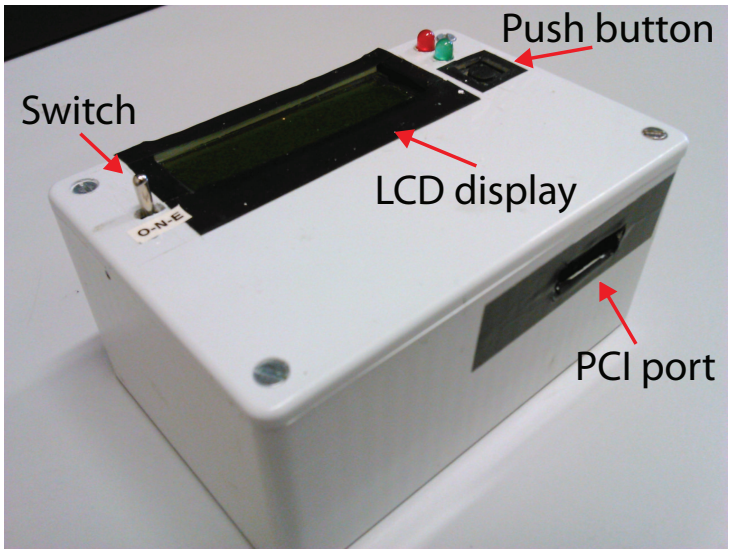

Figure 3.35: Electronics device for the activation and handle of the microfluidic circuit.

logical diagram of the working of the system can be seen in Fig. 3.36 to explain the operation flow.

There are two phases in the operation of the system, the first phase is controlled by the user. This phase is the start-up of the system. The process starts with the charge of the capacitors which will provide the energy for activating the microvalve. The charge is performed by moving the switch to the "E" position for a few seconds. Afterward, the switch is change to "O" to begin with the operation of the system. In that state, the LCD is switched on and it will appear "push to initialize", this will be the last action of the user, the next steps will be performed by the system. The second phase consists on the activation. After pushing the button, the first impulsion is activated. In that moment, the LCD will display "impulsion 1/2" during the whole time. Then, the second impulsion is carried out and the LCD will change to "impulsion 2/2" and the fluids are moved from the serpentine to the detection chamber. Finally, when the process ends, the LCD shows "End of the process" during a short time, and then the device is ready for a new process showing "push to initialize". If no other activation is made, the switcher must be change to neutral "N".

The electronic module is designed regarding the specifications of the system. In addition, it is going to be designed for being portable, providing the LoC system

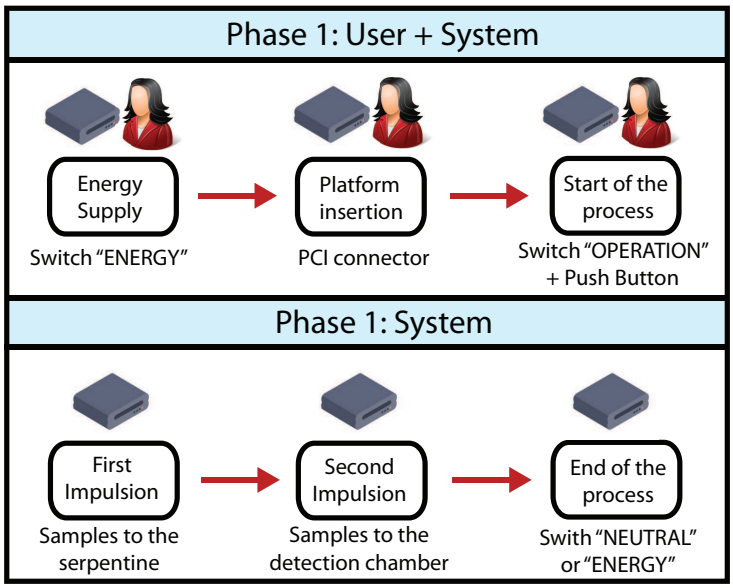

Figure 3.36: Chronological scheme of the working of the complete system.

a great versatility in the general applications. Taking into account that the system requires a great and quick source of energy to activate the microvalves, a group of capacitors are chosen for providing the energy due to high response. These capacitors are connected through the switch to batteries, the batteries charge the capacitors when the switch is set to "E" energy. The control is given to the system when the switch is change to "O" operation, in that moment the microcontroller handles the operation and the different steps of the system are displayed via LCD. The activation of the microvalves is carried out by two power MOSFET (M1 and M2) (IRFB4227PBF), as can be seen in Fig. 3.37. These MOSFETs are connected to the capacitors and ground of the system, and the gate of the MOSFETs is connect to a driver, this driver is needed to activated the transistor. The driver of the transistor is connected to two port of the microcontroller P2_3 and P2_4, given the control of the activation to the microcontroller. These transistors support a repetitive peak current compatible with the activation of the microvalves. These components require 15V to operate adequately. The MOSFETs let the current goes through the microvalves, when the microprocessor switches them "on", and avoid the pass of current when they are switched "off".

The rest part of the electronic module is the microcontroller and its connection to the LCD, LEDs and driver of the MOSFETs. The schematic is shown in

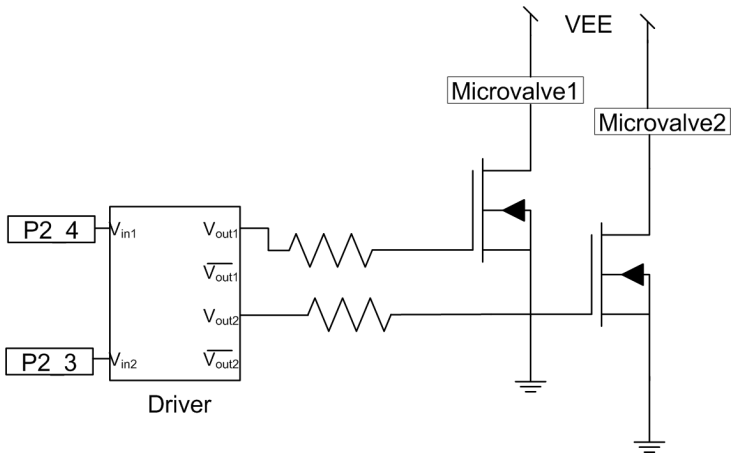

Figure 3.37: Electronics scheme of the MOSFETs in charge of the activation. These are connected to the microcontroller (Pin P2_3 and P2_4) via the driver.

Fig. 3.38. The red LED will be on while the first impulsion is carried out and the green one while the second impulsion. The ports SCL, SDA and CONTRAST are on charge of the control of the LCD. In addition, the push button is connected to one of the ports of the microcontroller, to give to the microcontroller the order of starting the process. The final electronic assembly inside the electronic device can be observed in Fig. 3.39

In conclusion, a portable, low cost and easy-to-used electronic system is developed. The system is designed to cover the requirements of the LoC platform. This system is versatile for implementing new functions like more activations or sensing.

3.4.5 Characterization and results

The fabricated microfluidic platform together with the electronic system is tested to evaluate its behavior. The intended purpose is the management of fluids along the microfluidic platform. The way of proceeding starts by filling the sample chambers with the samples through the inlets, in this case a green and blue color ink diluted in water is used. The reasons of using diluted ink are the similarity in physical properties with the water based chemical samples and the clear visibility of the colors to monitor their behavior. It is filled with the help of a pipette. Later on, the inlets are closed by an adhesive tape. The next step in the set up is the pressurization of the impulsion system, this is achieved by introducing the

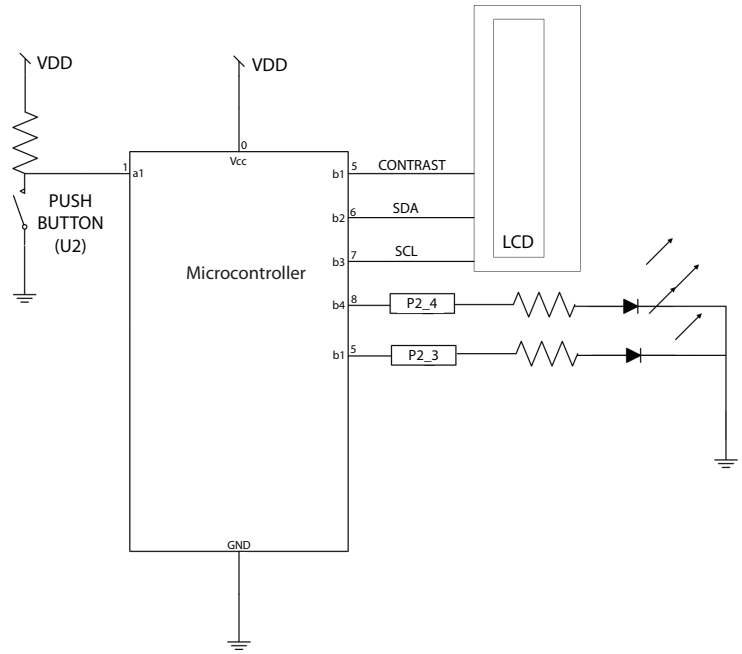

Figure 3.38: Schematic of the microcontroller and the PINs connection.

putty material inside the tubes which are glued in the PCB above the pressurized chambers, as it could see in section 3.3.2. Once the samples are filled and the chambers are pressurized, the microfluidic platform is inserted in the electronic device for being activated, as can be observed in Fig. 3.40.

The electrical activation starts by moving the switch to "ENERGY" for a few seconds and the capacitors are getting charged. Later on, the switch is changed to "OPERATION" and the LCD will be turned "on", the sentence "Push to start" will be displayed and the reader is ready to be used. When the push button is pushed by the user, the activation is carried out 1 s later, and the LCD will display the process. In the first impulsion, the pressure and time are established to move the liquids from the samples chambers to the serpentine channel, Fig. 3.41. In Fig. 3.41.a), the liquids are in repose before the aperture of the first microvalve. In Fig. 3.41.b), the precise moment in which the microvalve is open. In Fig. 3.41.c), the liquids are moving from the store chambers to the serpentine microchannel, mixing the liquids and in Fig. 3.41.d), the first impulsion has already finished and the liquids are stored in the serpentine.

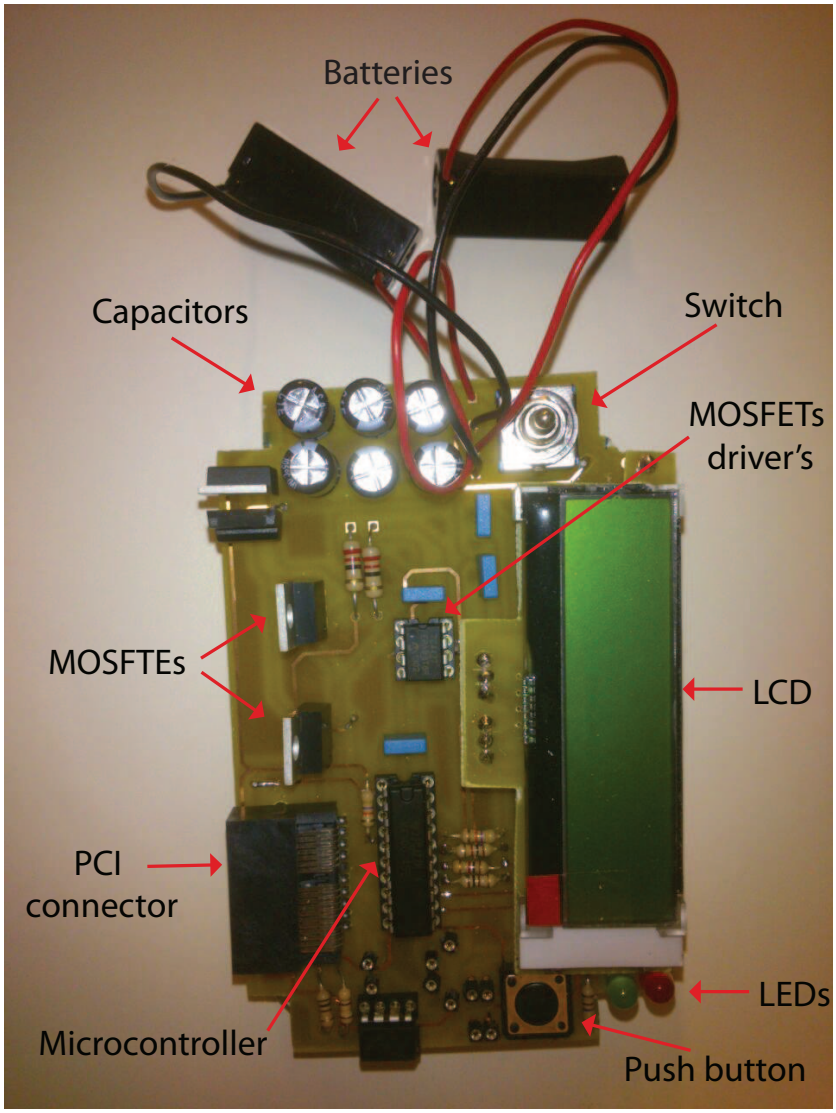

Figure 3.39: Fabricated PCB of the electronic device.

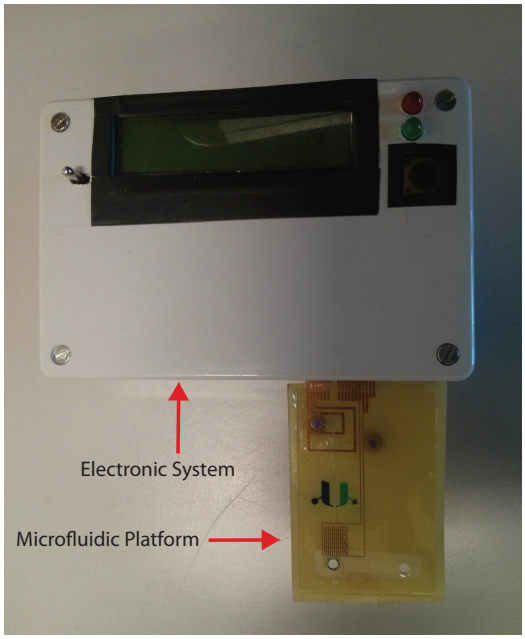

Figure 3.40: Complete system before the electronic activation.

In the second impulsion, the liquids are moved from the serpentine to the detection chamber. In the Fig. 3.42 an evolution of the second impulsion process can also be observed. It is noticeable the precision in the movements of the liquids, the liquids after the first impulsion remain centering in the serpentine and in the second are stored in the chamber, as it was designed. For the particular experiment, the difference in time between impulsions is 6 s, because it was set to a media parameter between the possible time of discharge seeing in Fig. 3.31. However, it can not be enough for the discharged, it is related to the microfluidic resistance of the microvalve. In order to ensure the total discharge, the slowest time can be programmed in the microcontroller.

Moreover, an electrical study of the activation of the microvalves is made in order to analyze the behavior of the microvalves. The study was done with the help of an oscilloscope as it was made in the characterization of the microvalve, and the voltage and the current in the moment of melting were acquired. The graphics are shown in Fig. 3.43 for both microvalves. It is remarkable the fact that the melting time of the microvalves are different. Nevertheless, It is know that this is due to the tolerance of the microvalve in the fabrication process. The consumption

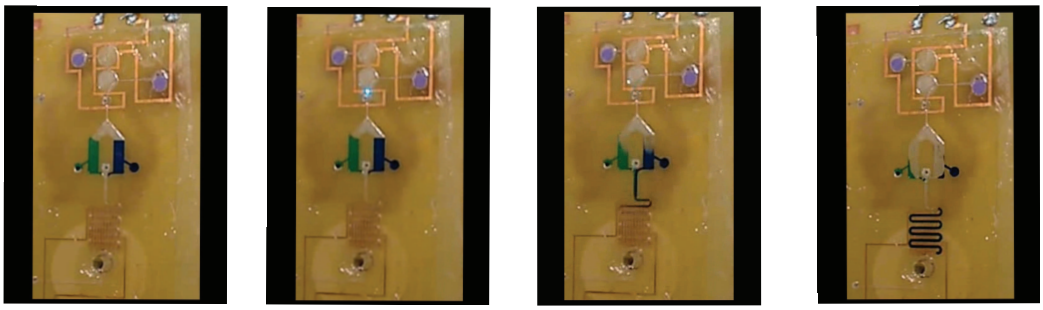

Figure 3.41: Screen capture from a video of the first impulsion. The liquids are stored in the sample chambers and reach the serpentine.

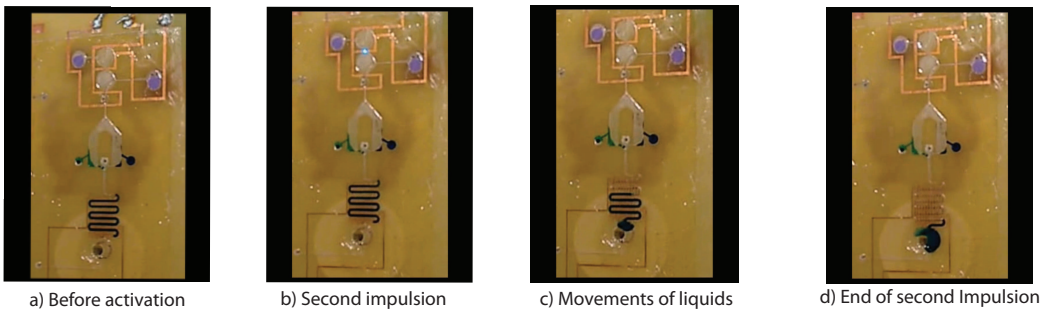

Figure 3.42: Second impulsion sequence, the liquids are stored in the serpentine and reach the detection chamber.

Table 3.7: Main parameters of the characterized LoC.

Characteristics of the System	
Dimensions	**W x L x H (cm)**
Electronic Box	12 x 8 x 6
LoC Platform	4.5 x 7.5 x 1.5
Volumes	**μ L**
Samples	9.66
First Impulsion	10
Second Impulsion	10
Pressure	**MPa**
Pressurized Chambers	0.3
Time	**s**
First Impulsion	1.4
Second Impulsion	15.2
Energy Consumption	**mJ**
First Microvalve	14.1
Second Microvalve	17.9

of the microvalves in the activation was calculated using these graphics. These parameters and another that summarized the system tested are in Table. 3.7.

In addition to the microfluidic characterization, the heating is an additional actuation which can be used with the help of a microheater. The microheater is a resistor connected to the microcontroller, regarding the desired application, the temperature can be different. In the proposed system the microheater is fabricated in the microfluidic platform and controlled by the microcontroller. For these colored samples, the microheater is not used because it does not take part in the fluid movement. Nevertheless, the characterization is carried out. The microheater copper line has a value of resistance of 2.7 Ω. This value is very high for a single copper line due to its thickness, 5μm. This high resistance makes possible the use of a reasonable value of current and time to reach the temperature by Joule effect. In order to do so, different voltages has been applied between the appropriate pads. The temperature of the microheater as a function of the applied voltage are shown in Fig.3.44. The limit of operation of the microheater is related with the glass transition temperature of the PCB, in this case 135 °C for $Vh = 2.65V$.

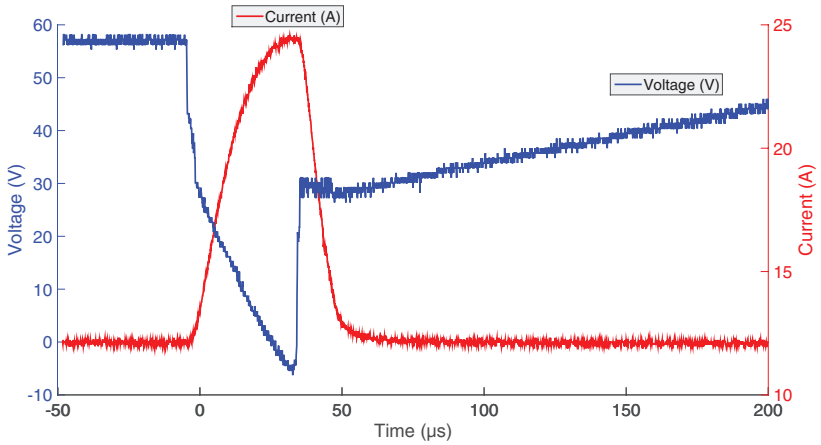

a) Opening of the first microvalve

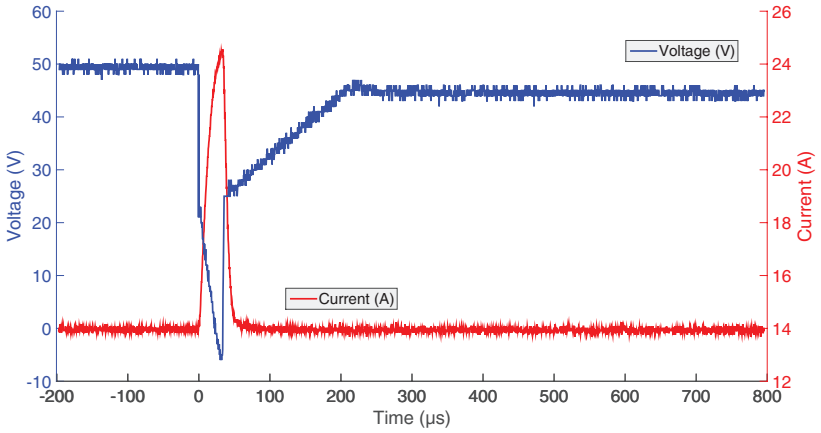

b) Opening of the second microvalve

Figure 3.43: Voltage and current of the two microvalves during the opening, the difference in time is related with the tolerances in the fabrication.

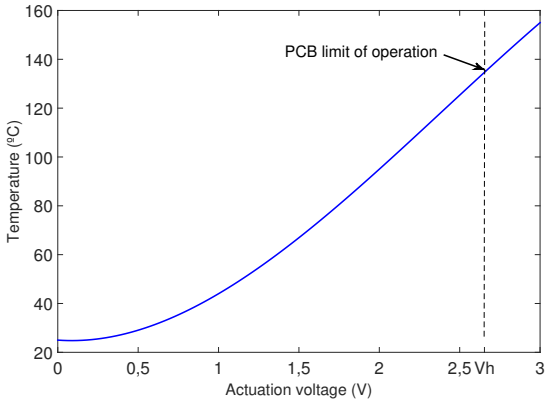

Figure 3.44: Temperature curve of the microheater designed in the LoC system as function of the applied voltage.

The sensing in the system has not been implemented yet because this section was focused on handling of fluids in a microfluidic platform. However, a particular sensing in an application of glucose detection will be analyzed in the next section. Moreover, due to versatility of the system an silicon chip can be easily integrated and different type of sensing can be performed. In the Appendices at the end of the document can be found the integration of a silicon chip in the microfluidic platform.

The system is designed for the impulsion of two fluids of a particular volume and pressure. However, if the application requires the design could be modify increasing the number of impulsion systems, adding more samples, detection chambers or integrating other components like filters or fluid multiplexer.

3.5 Detection chamber for glucose sensing application

3.5.0.1 Introduction

In this section a glucose sensing platform is presented, this platform is designed for being compatible with the fabrication process of the developed LoC system. The glucose sensing is based on the absorbance of light. A kinetic reaction is applied to the samples, giving a red colored liquid with an intensity of color related

to the level of glucose in the sample. A green light beam is applied to the sample, and the non absorbance light is detected and, consequently, sensing the glucose in the sample. The platform developed for glucose detection is designed, fabricated and characterized. Moreover, the electronic module integrated for the light beam is designed for this particular application. To sum up, despite this platform is designed for being integrated in the pneumatic platform developed, due to its integrability and its easy sensing, it can be integrated in any other platform.

3.5.0.2 Glucose Detection

The glucose detection is an important issue for the human society, is the most common metabolic disorder world-wide, with more than 300 million affected people. In recent years, a number of approaches have been raised toward the development of glucose sensors because several areas such as clinical diagnostics, biotechnology and the food industry are involved. The most popular sensors are based on the enzyme glucose oxidase (GOx) using different transduction mechanisms as electrochemical signal transduction, fluorescence and absorvance [206–208]. However, the nonenzymatic methods are gaining ground as an alternative.

In this platform the sensing developed is based on the the colorimetric enzyme-kinetic principle. A glucose Trinder GOD-POD (Spinreact, S.A) [209] is used. The reaction is summarized in the reactions (3.25) and (3.26). The glucose oxidase catalyzes the oxidation of glucose to gluconic acid (3.25) and the hydrogen peroxide generated is detected by a chromogenic oxygen acceptor, phenol-aminophenazone in the presence of peroxidase (3.26). The kit contains a context with enzymes, a buffer of phenol and a glucose cal, Glucose aqueous primary standard 100 mg/dL. The method is developed by preparing the working reagent which is made by dissolving the context of enzymes with the buffer (phenol). The reagent is mixed with the glucose sample in different volume ratios, depending on the dilution factors (DF) (3.27). The reaction of glucose with the working reagent generates a red colored quinoneimine, which has an absorbance peak at 505 nm. The intensity of that color is proportional to the glucose concentration in the sample, Fig. 3.45.

$$\beta - D - Glucose + H_2O \rightarrow Gluconic Acid + H_2O \tag{3.25}$$

$$H_2O_2 + Phenol + Aminophenazone \rightarrow Quinone + H_2O \tag{3.26}$$

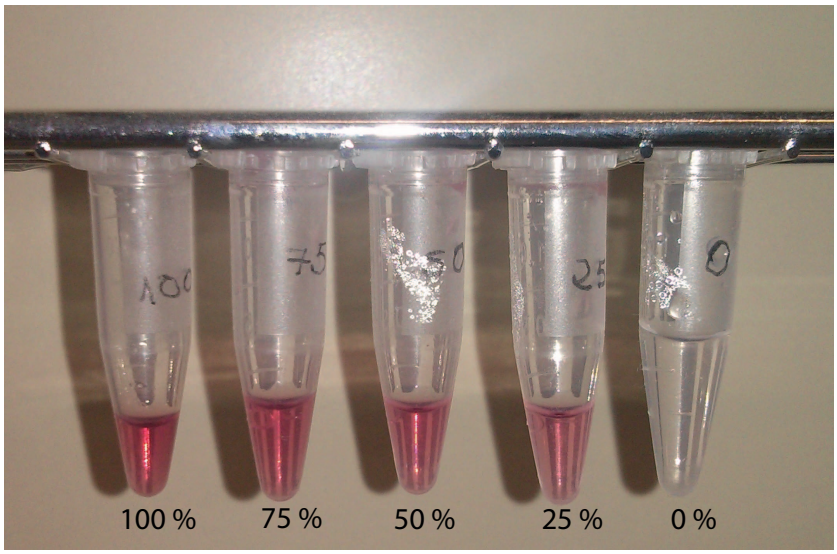

Figure 3.45: Different concentration of the reaction products.

$$DF = \frac{Vsolution}{Vsolute} \tag{3.27}$$

3.5.0.3 Design

The way of doing the detection of glucose is based on light absorbance. The kinetic reaction of glucose produces a red color in the liquids, the more glucose concentration has the reaction, the more colored is the reaction. The absorbance of the light to that color has the peak at 505 nm, which is blue-green color, as can be expected because it is the complementary color to the red. A beam of green light pass through the colored liquid and a 505 nm photodetector receives the light that the liquid lets pass. An scheme of the absorbance sensing can be observed in Fig. 3.46.

The designed glucose platform is composed by a microfluidic circuit and an electronic module where the LEDs are assembled. An scheme of the detection platform can be observed in Fig. 3.47. As being part of the LoC platform, the microfluidic circuit is designed to be easily integrated in the LoC. Taking into account this premise, the system is being manufactured in PCB and SU-8, as the LoC platform and will contain a glass integrated for the pass of light. Moreover,

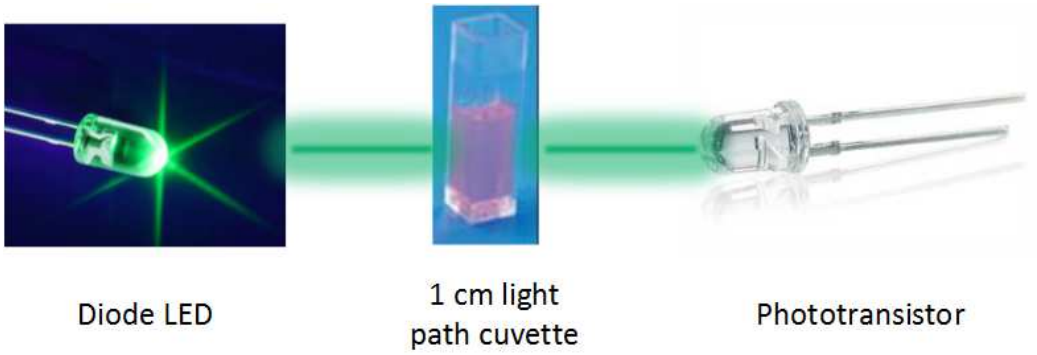

Figure 3.46: Scheme of the glucose detection by absorvance.

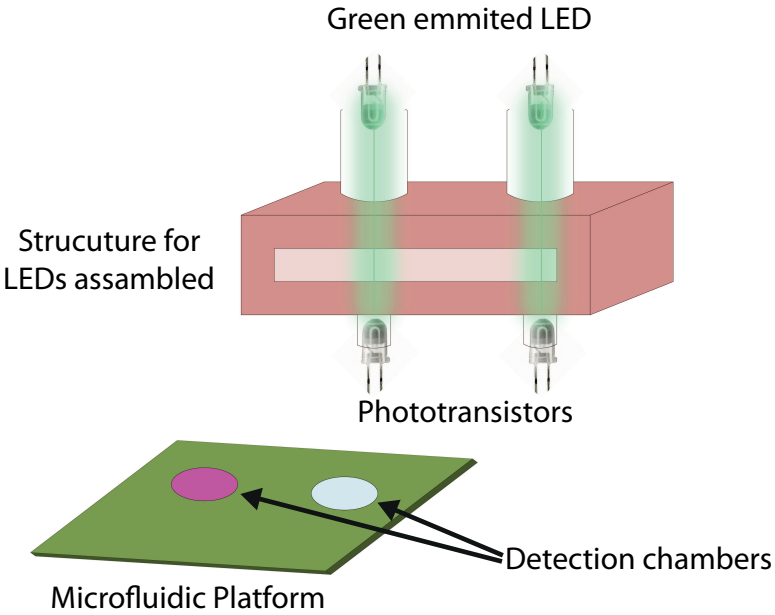

Figure 3.47: Proposed scheme of the glucose sensing platform.

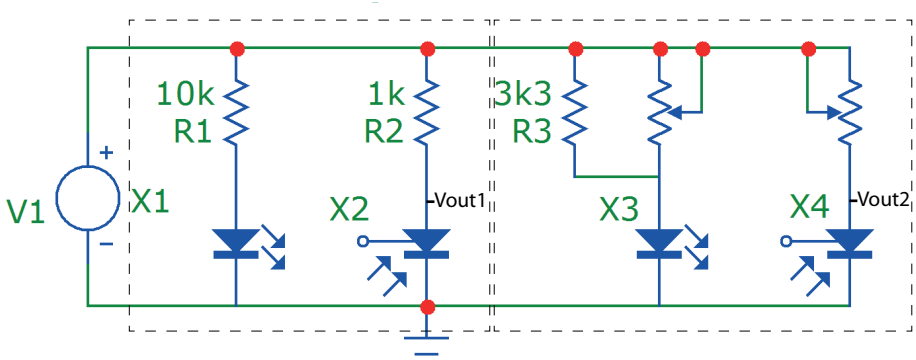

Figure 3.48: Electronics schematic of the LEDs and photodetectors.

the system is thought to work in differential mode to avoid external noise in the measurement. As a result, the microfluidic circuit is composed of one PCB with two holes. A thin layer of glass is completely embedded in the PCB, over this substrate a layer of SU-8 of 300 μm is manufactured with two circular chambers with the same size than the holes in the PCB and completely aligned. One of this chamber will correspond to the detection chamber of the LoC platform. The other chamber is used as a reference, to work in differential mode and avoid external noise, as commented.

In addition to the microfluidic circuit, the system contains the electronic module responsible of the sensing part. Moreover, this electronic module is assembled in a structure because the LEDs and the phototransistors have to be faced. The beam of light is generated by a green light emitting diode (Nichia NEPE510JS), that light goes through a detection chamber and reachs the phototransistor (Vishay TEPT4400). The electronic design for the polarization of the LED and phototransistor is shown in Fig. 3.48. According to the schematic, the more red is the glucose assay, the more light is absorbed by the liquid, and therefore the output voltage (Vout1) will be increased. As the electronic system works in differential mode, in parallel with the reaction chamber, there are a replicated microfluidic and an electronic circuit using X3 and X4 amplified. The output voltage of this system is proportional to the difference Vout1-Vout2. The polarization system will provide an output signal (Vout1 and Vout2) between 0 a 370 mV for a range of glucose from 0 mg/dL to 100 mg/dL.

3.5.0.4 Fabrication Process

There are two different fabrication process, on one hand the microfluidic circuit and the electronic module on the other. The microfluidic circuit is manufactured in PCB, glass and SU-8. Firstly, the fabrication process is very similar to the previously presented. However, the integration of the glass has not been developed yet. The microfluidic circuit is composed of two chambers over glass, these two chambers have a diameter of 5 mm and a depth of 300 μm. The top and the bottom of the designed microfluidic circuit is shown in In Fig. 3.49 A) and B). The fabrication process is detailed in Fig. 3.49 C). The process begins with 1 mm thick glass and a single PCB, step a). In the next step b), the FR4 is milled with the same dimensions of the glass in depth and area. In order to do so, an automatic CNC milling machine is used. After milling, in the step c), two holes of 5 mm are drilled where the chambers will be located on. After that, in the step d), the glass is integrated into the milled area of the PCB, the glass is glued to ensure the permeability and stability. The typical SU-8 process is performed above the glass and the FR4 to fabricate the microfluidic circuit. Moreover, the SU-8 polymer avoids any leakage between the glass and the PCB. In step e), a layer of 300 μm of SU-8 2050 (MicroChem Corp.) is deposited over the FR4 and the glass in order to fabricate the two chambers. To do this task, a deposition of 150 μm -thick SU-8 layer is carried out at 700 rpm during 60 s and a softbake of 5 min at 65°C and then at 95°C during 15 min. Then, an additional deposition of a layer of 150 μm is performed, with the same spin speed but with a softbake of 5 min at 65°C and 2 h at 95°C is carried out to achieve the desired thickness of 300 μm. Subsequently, in step f), the photoresist is exposed to UV light for 2 min using a mask to define the chambers. Later on, in step g), the uncrosslinked SU-8 is developed by immersion and stirring in Mr600 Developer (MicroChem Corp.) during 7 min. Finally, the whole structure is cleaned with IPA. In this way, the entire manufactured microfluidic structure is defined, Fig. 3.50. In this process a mayor concern is the cleaning, if the microfluidic structure is not clean enough, because if there is any uncrosslinked SU-8 in the chambers, it will affect significantly the measure of glucose.

Secondly, the electronic module is form by two pairs of LED and photodetectors and the electronics of signal processing. The LEDs and the photodetector have to be faced and aligned. Moreover, the electronics has to be connected to both. On this basis, the adopted solution was the fabrication of the structure shown in Fig. 3.47 with a 3D printer. The fabrication process with a 3D printer is

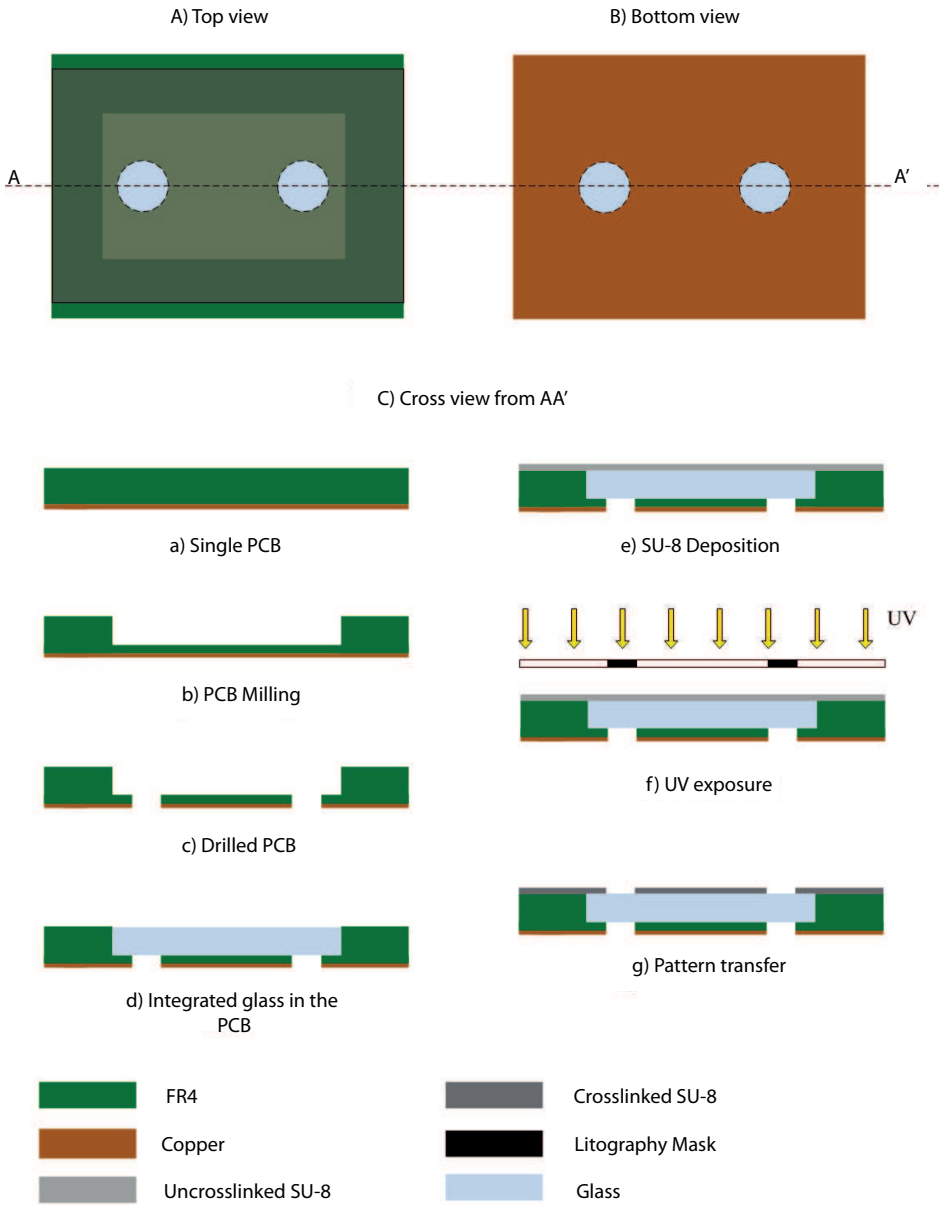

Figure 3.49: Fabrication process of the microfluidic circuit.

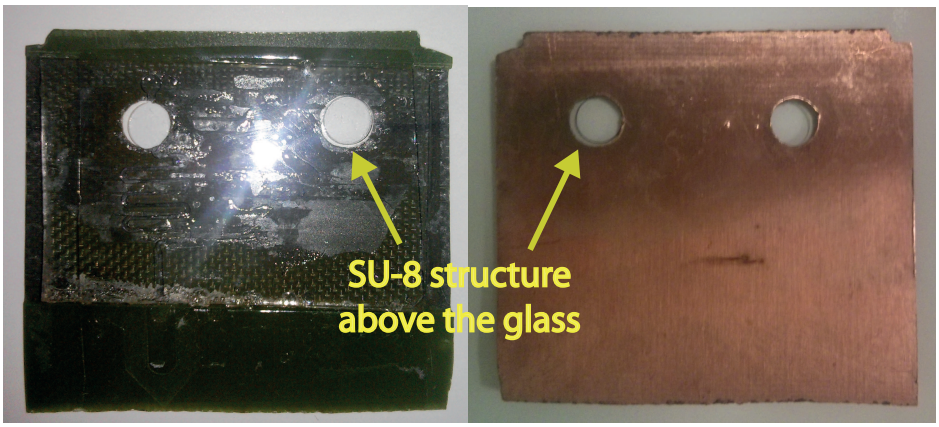

Figure 3.50: Fabricated microfluidic circuit.

very simple, the design plans are drawn in a CAD software and are read by the 3D printer. The design plans and the final device are shown in Fig. 3.51. The structure has a dimensions of 55 x 35 x 15 mm and there is an aperture of 5 mm where the microfluidic PCB will be assembled. Moreover, in the aperture, there is a small aperture of 1,60 mm that will act as a rail system for the alignment of the PCB. This PCB will be exactly assembled 30 cm, the device is designed with a stop, as can be observed. Consequently, the PCB will be perfectly aligned. The holes in the PCB are designed to be in the exact position than the cavities in the device. Moreover, the cavities have dimensions adjusted to the LEDS and photodetector. Lastly, the signal processing electronics is soldered in a PCB and this PCB is fixed to the plastic structure.

Finally, the glucose sensing platform can be observed in Fig. 3.52.

3.5.0.5 Characterization and results

The characterization of the experiments for the glucose detection is divided in two parts: calibration of the optical detection and characterization of the complete platform.

In a first set of experiments, the focus is on the validation of the calibration of the optical circuit. The calibration aims to prove the validation and repetitiveness

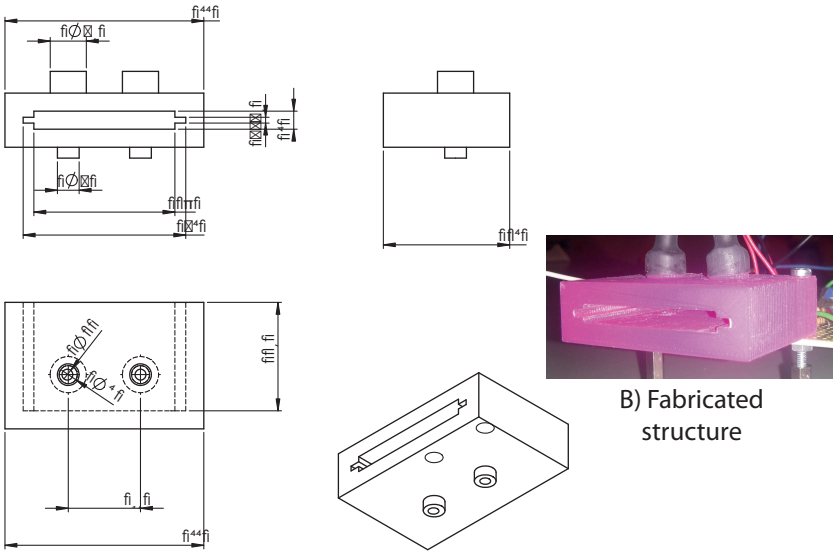

A) Drawing of the plastic structure

B) Fabricated structure

Figure 3.51: A) Design plans for the structure for the LEDs and photodetector. B) Fabricated structure in a 3D printer.

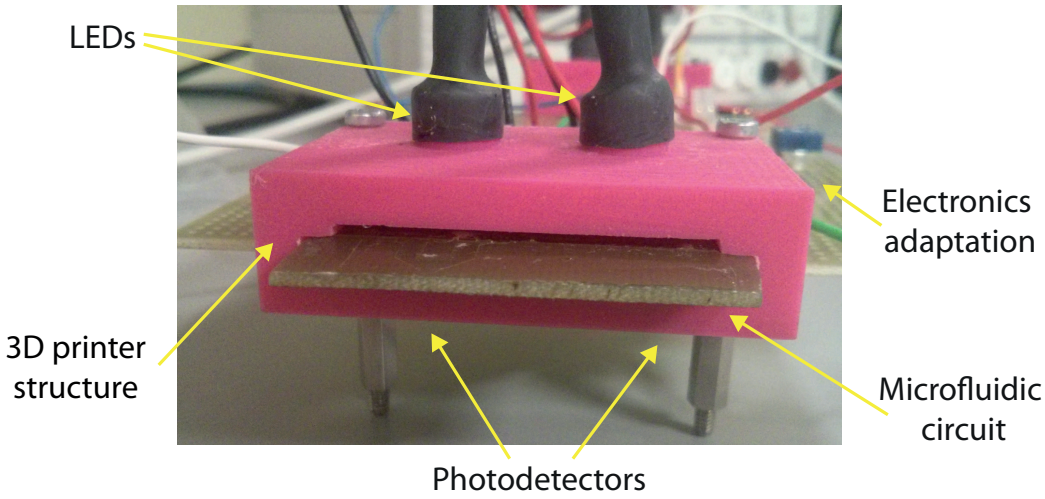

Figure 3.52: Complete glucose detection platform. The different components that compound the system can be observed: LEDs, photodetector, electronics adaptation, microfluidic circuit and 3D printer structure.

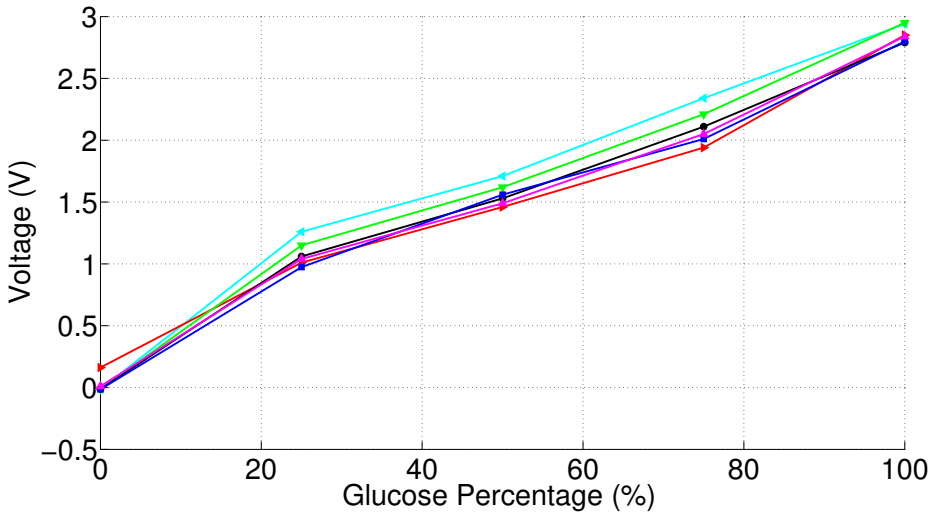

Figure 3.53: Output voltage for 1 cm light path cuvette as a function of glucose concentration.

of the system. A standard cuvette of 1 cm light path is used as microfluidic circuit as previously presented in Fig. 3.46. The dilution factor used to prove the system is 100. This has been chosen for being the most typical for 1 cm light path. The electronic circuit for this volume of liquid is adapted and assembled and in a protoboard with the same LEDs and phototransistors.

The glucose assay is performed filling five different concentration of glucose in a cuvette with 1 mL of reagent, Fig. 3.45. Then, these are mixed for 10 min at 37 ^{o}C. In order to do the detection, the cuvettes are always placed in the protoboard between the LED and the phototransistor in the same position and orientation. It is important to highlight because any change in the relative position of the detection chamber respect to the LEDs, significantly modifies the measure. All experiments were performed at room temperature and data were acquired 30 s after the cuvettes are placed between the LED and the phototransistor. The result shows six different experiments for five glucose concentrations, Fig. 3.53. The experiments show a good repetitiveness and linearity. However, the data dispersion in the measurement for one glucose concentration are justified for the use of a manual set up, which does not guarantee a reproducible optical geometry.

The proposed device will overcome the problem of the geometry by using the mechanical device designed with the 3D printer, which determines an accuracy

geometric between LED, phototransistor and chamber. The use of the mechanical structure for alignment will increase the stability of the signal, as it will be explained.

Finally, the second set of experiments is focused in the characterization of the complete platform. One of the chambers of the microfluidic circuit is filled with reagent liquid and the other is filled with the glucose assay. The two chambers have a volume of 5.89 μL. One small glass is put above the chamber, acting like a cover to ensure that the chamber is completely filled, and to avoid a curved interface liquid-air which can affect the measure. Five different glucose concentration assays have been done with a dilution factor (DF) of 5, which is smaller than those used in typical colorimetric sensors (DF = 100). The reason for not using DF = 100 is for improving the absorbance and avoid any external noise. The experiments consist in measuring the different voltage in the phototransistor for different solutions. Special care should be taken in the cleanness of the LoC, since any disturbance will have an impact on the measurement. Nevertheless, the platform is thought to be integrated in the pneumatic LoC platform developed in this thesis which is single use. Moreover, the microfluidic PCB is manually inserted in the reader structure since the alignment is assure with the rails. In spite of the safeguards, after cleaning the PCB and before filling the chambers, it is inserted and measured to validate the zero output. In addition, the diameter of the chambers (5 mm) was chosen bigger than the phototransistors diameter (3mm) to solve the problem of the manually PCB insertion.

Five different concentrations of glucose (0%, 25%, 50%, 75%, 100%) are pipetted to the chambers in four different experiments. The output for four experiments is shown in Fig. 3.54. The results show very similar behavior for the four different experiments. Moreover, it can be observed the non linearity in the slope of these curves in comparison with Fig. 3.53. It is caused by the difference between the dilution factors, from 100 to 5. However, the similarity between the experiments has improved significantly.

3.6 Conclusions

In this chapter a Lab on Chip platform for multipurpose applications has been presented. The main goals for the development of the system were the reliability, the integrability, the autonomy and the low consumption. Concerning these purposes, the proposed device has been designed, fabricated and characterized.

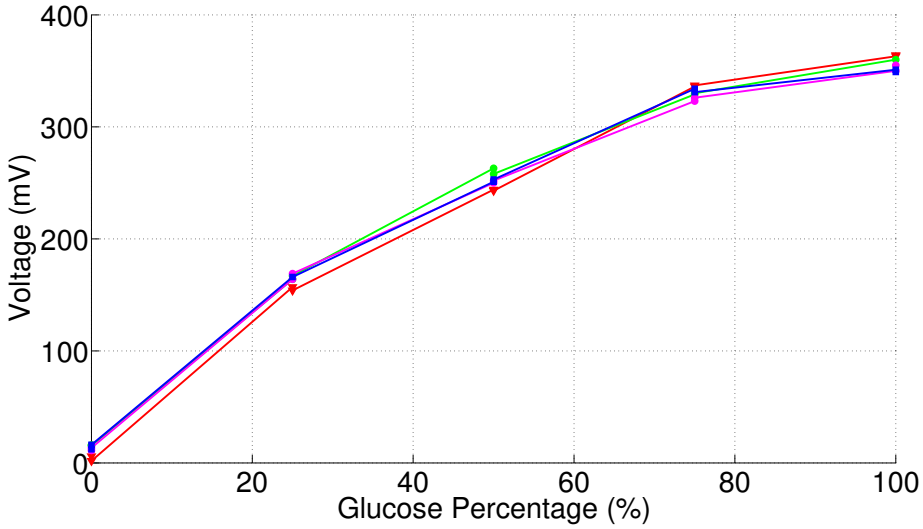

Figure 3.54: Output voltage of the proposed device for four different experiment as a function of glucose concentration.

The chapter starts with the more important and, at the same time, complex part of the system, the microvalve. This has been developed with electrical activation, a track of copper is used as a fuse and the aperture is electronically controlled. The results have shown a quick and controlled response and a low consumption of energy, due to the fact that only needs electrical energy, not pneumatic energy like most of the microvalves in the state of art. Moreover, because of non pneumatic energy is required for the activation, the microvalve is very versatile for any impulsion system backwards. In addition, the only fluidic parameters that define the microvalve is the fluidic resistance after the gap left by the opening. The flow rate of the microvalve will depend on the fluidic resistance and also the pressure applied, that is independent on the microvalve, which makes the microvalve more versatile for being integrable in any platform.

The second component studied has been the impulsion system. The biggest challenged was the complete autonomy of the system and the integrability with the fuse microvalve. With these premises, the developed impulsion system consists on two chambers connected each other, one of them is filled with a particular volume, impulsing the air through the other chamber and pressurizing it. The volume displaced and the volume of the chamber is totally controlled, obtaining a controlled pressure in the system. The system is manufactured using a similar fab-

rication process than the one with the microvalve. In addition, the characterization is developed with the microvalve. The experiments showed a controlled volume displacement, regarding the amount of volume manage in the applications of LoC platforms. Additionally, an study of the permeability of the system is made, the results show that the system is able to bear the pressure for one hour with a leakage of 2.5%, which is acceptable because the system is thought to be pressurized in the moment of use.

The third component is the microfluidic circuit, the idea of the microfluidic circuit is to test the developed impulsion system. In this case the microfluidic circuit consists of two stages: a stage for mixing and other for sensing. However, any other typology can be applied. It was thought as a general circuit where two fluids are mixed and reach a detection chamber. Several design where studied because the asymmetries of the tolerance in the fabrication process, and finally, the chosen model was the one that absorbs this matter. A mathematical model of the system was developed to choose the best values of the parameters, taking into account the aperture of the microfuse valve and different pressure applied into the impulsion system. Moreover, in this section the electronics system that would monitor the system is built, making it autonomous to the user. The only iteration with the system is to switch it on and to decide the starting point of the process, making it suitable for a non expert user.

Finally, a possible application for the circuit is manufactured. A totally integrable glucose detection platform is carried out. The idea is to create a glucose sensor to be used in the detection chambers of the presented microfluidic circuit. The detection is based on the absorbance of the light. A first calibration is made with the use of cuvettes of 1 cm light pass to migrate to 300 μm light pass. The results show even better results that the one with the cuvettes, thanks to the structure manufacture to improve the alignment of the fluidic circuit with the light.

In conclusion, a microfluidic platform for multipurpose application is manufactured. This is thought as a prototype, due to the use of SU-8 polymer that is very versatile material for manufacture structures. However, the fabrication process and the design of the different components have been done concerning the migration to other technologies more industrial. The idea of using Printed Circuit Board (PCB) as a substrate provides a good option for the connection to any electronics device, making this LoC platform closer to Point-of-care-testing (POCT).

The results obtained within this chapter has been published in high impact scientific journals [201, 210, 211] and in two conferences in the area of research [212, 213].

4

TOWARDS MASS PRODUCTION

4.1 Introduction

In this chapter the migration of the self-contained multipurpose lab on chip in SU-8 towards a mass production technology is described. The SU-8 is a suitable polymer for prototyping due to its high accuracy and the versatile fabrication process. Moreover, it can be easily performed in an university clean room. However, it is not appropriate for mass production due to the amount of steps that can not be done automatically. As a result, it was decided to change the SU-8 for a thermoplastic where the channels and chambers are transferred by more industrial fabrication process, Hot Embossing. On the contrary, the PCB remains as substrate because it is integrable with any electronics components.

In contrast to the SU-8, the adhesion between the thermoplastic and the PCB is not trivial, an intermediate layer which bonds the two surfaces must be included. The layer must assure the sealing between the two surfaces but at the same time, it can not collapse the channels and chambers of the microfluidic circuit. In consequence, the bond between these two components is an important challenge in this migration towards massive production.

The chapter is organized as follow, the first section of the chapter is devoted to the fabrication process, the manufacturing of the microfluidic circuit in the thermoplastic and the gluing technique used to bond the PCB and the plastic. Secondly, the next section is focused in the integration of the fuse microvalve into this new technology. Finally, the complete multipurpose lab on chip is developed and characterized with a new autonomous impulsion system.

4.2 Fabrication Process

The material selected for the implementation of the developed lab on chip in mass production is PMMA and PCB. The reasons for using the PMMA instead of any thermoplastics is the good mechanical properties for molding and mechanizing. Moreover, the high transparency of PMMA makes it very suitable for the use of optical detectors. The channels, chambers and walls are going to be located in the PMMA. On the contrary, the PCB remains as a substrate for the high integrability and connectivity with the electronic reader. The PMMA is manufactured by hot embossing by means of a mold and the copper lines of the PCB are fabricated by photolithography and wet etching.

4.2.1 PMMA manufacturing

The PMMA microfluidic circuit has been performed by hot embossing, as previously said, so a mold with the negative design of the systems is needed. The mold is manufactured in aluminum by micromilling. The hot embossing is made in a hydraulic press 4120 CARVER® with temperature. The process stars over the negative design of the desired microfluidic structure, some examples can be seen in Fig. 4.1 a) and b). The design can be done in L-Edit software or any other drawing program as AutoCAD. Then, this design must be loaded in a software for the NC code generator. In this case, the software is Cut2D which is a software that generates the routes and deepness for milling the desired structure. In this two examples two different structures are designed, in the left part of the image there is a design of two chamber and a microchannel, the chambers are separated by a wall where the microfuse valve is located. In the right part of the image is drawn the design of a microfluidic system with two impulsion systems. These designs will be explained in detail further down. The outside part of the designs is a grid of channels designed to release the air during the hot embossing process and improve the adhesion between the PMMA and the FR4. The route lines of the automatic milling machine are designed for a tool of a certain diameter, the bigger the tool is, the faster the machine goes. However, the accuracy is lower, the chosen tool would depend on the requirements of the design. Once the design with the routes is done, this is transferred to the milling machine software. In this software, the NC code for each tool is loaded and the zero level of the tool in the three coordinates (x,y,z) must be set. Moreover, for each used tool, the parameters of speed and z deepness have to be set. In the particular case of the microvalve, the critical parameter is the wall of the microvalve, which is a channel in the mold, it is done with a 400 μm tool, the rest of the circuit is done with a tool of 1 mm diameter. Once the routes and the tools are configured for the desired milling, the aluminum piece is placed in the milling machine and the design is transferred. The results for both can be seen in Fig. 4.2.

Once the mold is design, the next step is the fabrication of the thermoplastic structure by hot embossing. Hot embossing is a technique of hot stamping a pattern into a polymer by means of pressure and temperature above the glass transition temperature of the thermoplastics, 2. In this case, the PMMA glass transition temperature is the 105°C, so the hot embossing must be done at higher temperatures to achieve the stamping. In our case a hydraulic press with a temperature controller plates are used, Fig. 4.3. The process starts over a piece of PMMA

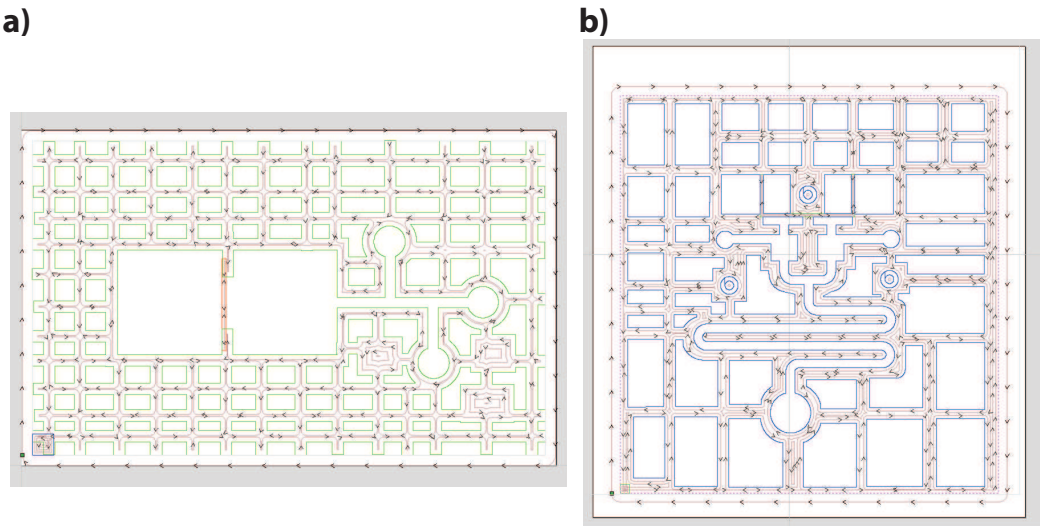

Figure 4.1: Different designs for the milling machine.

smaller than the mold, to assure than the stamping is done inside the mold and the release of air can be performed. The process chosen to do the hot embossing is based on a work studied in the state of the art and our experience working with this particular hydraulic press machine. The press is previously set to a temperature of 130° in the bottom plate and at 80° in the top plate. The mold with the piece of PMMA over it are placed in the center of the bottom plate, to assure the distribution of pressure. Afterward, the two plates are closed until the top plate touches the PMMA structure but without applying any pressure. In this moment the plates temperature drops a few degrees, due to the PMMA and mold were at room temperature, so it must be wait until the plates reach the set temperature, 80° and 130°. When the plates achieve the temperature, a pressure of 5.8 MPa must be applied to the mold and PMMA. However, the machine does not have a pressure indicator, only the applied weight m, so the weight in Kg must be calculated following (4.1)

$$m = \frac{F}{g} = \frac{P \cdot A}{g} \tag{4.1}$$

Being F the force applied in Newton, P the pressure in Pascal and A the area in m^2. Depending the area to be printed, the weight must be calculated. This weight must be applied for 3 min, assuring that the pressure does not go down.

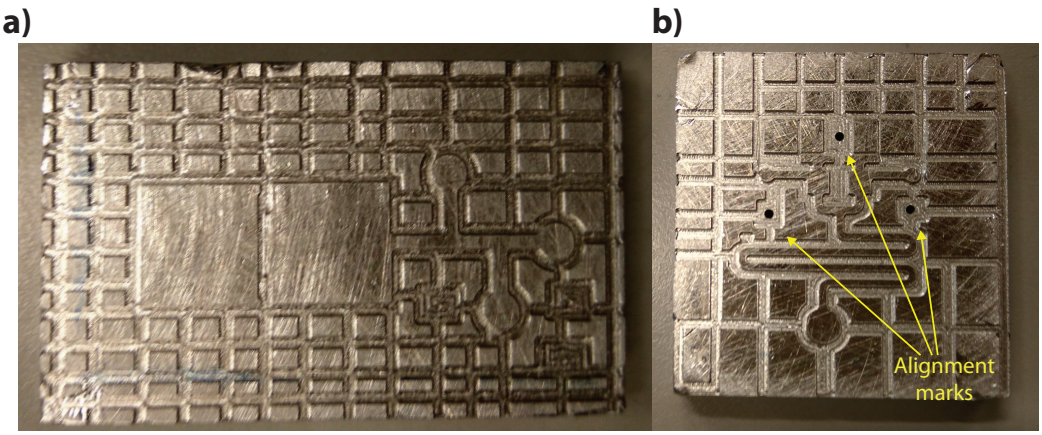

Figure 4.2: Micromolds designs.

After that, the temperature must be turn off and the pressure is dropping until the piece reaches room temperature or a temperature below 70°, well below the transition temperature of PMMA. Since that moment the hydraulic press can be open and the piece and mold can be took off. The piece can be unmold only at room temperature, if the mold and piece had been taken off from the hydraulic press before, it should be waited until reaches room temperature to avoid any stress in the unmolding process of the PMMA. The unmolding of the piece is carefully without applying any bending force. The result from the pieces is shown in Fig. 4.4.

4.2.2 Gluing

The next step in the fabrication process is the gluing of the PCB with the PMMA structure. This has been the main challenge in the development of this work thesis towards the mass production. The join of PMMA and PCB is not a great deal, the problem comes when there are small channels that must be sealed but without glue inside the channels. In addition, another important restriction has been the integration of the microvalve in the structure. With these premises, several trials have been done until reaching the best option. The first considered option was gluing via dip coating, it was developed in Jade University (Deutschland) during a stay with Prof. Gassmann. The glue used was epoxy and the result was not satisfactory because after the gluing the PMMA structure suffered stress and it cracked the layer of glue. One decision adopted was to sand down the surface to

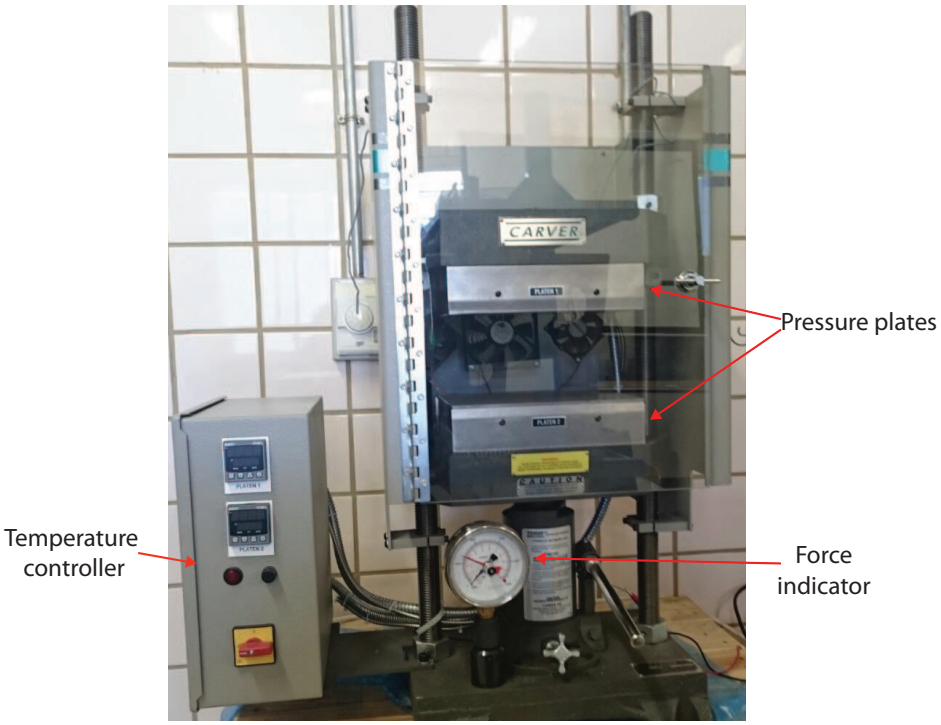

Figure 4.3: Hyadraulic press with temperature controller.

improve the mechanical bonding of the PMMA with the layer of glue. With this solution the two parts stayed bonded, however the channels were collapsed. Other option considered was using an adhesive tape as a bonding layer. The results for the channel was excellent, sealing them but without collapsing those [214]. However, the microvalve does not work properly, it was open only for a short period of time, not enough to impulse the desired volume. The next considered glue was a UV glue Loctite 3922 [215]. This is an anaerobic glue which presents an inconvenience, the excess glue in the surfaces of the channels does not cure and when the microvalve is open this liquid glue closed the microvalve. Finally, the glue chosen was EPO-TEK 301 [216]. This glue is a two components epoxy with very low viscosity and biocompatible, which is something very important for lab on chips. The results of the microfluidics channels were very satisfactory, sealing the components without collapsing. Moreover, the integration of the microvalve was also acceptable, as it will be explained further on. In Fig. 4.5 can be seen an example of a channel and chambers sealed with the epoxy glue.

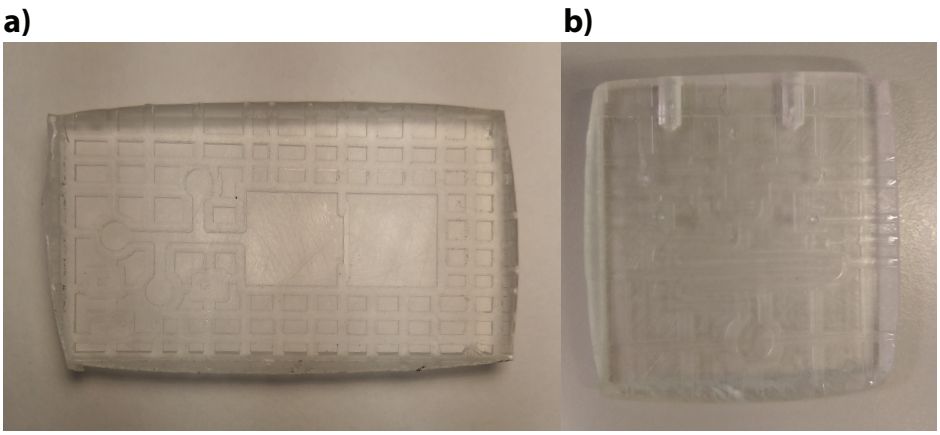

Figure 4.4: Fabricated structures in PMMA via Hot Embossing.

The fabrication process for gluing the PMMA and the PCB starts over the two manufactured pieces. The PCB is manufactured with the typical wet etching for copper pattering and the PMMA through hot embossing, as it has been commented. The PMMA piece is sanded with a fine sand paper P240, to improve the mechanical adhesion between the layer of glue and the PMMA. After that, the two pieces are cleaned, the PCB with acetone and Isopropanol and the PMMA with water and soap, if it were necessary the PMMA can be washed into an ultrasonic bath. Later on, the pieces are introduced in an oven at 35° for 1 hour, to eliminate all the humidity of the pieces. Meanwhile the pieces are in the oven, the glue is prepared mixing the two parts that contains the glue in a proportion by weight of 4:1. This mixture is introduced in a vacuum chamber to 10 min for removing the bubbles that could appear in the mixing. After the preconditioning of the materials and the glue, the gluing process starts using stamping [217–219]. A layer of glue is deposited with the help of a roller for 86 μm thickness on a flat clean surface, in our case a copper sheet. The PMMA is carefully dropped on the layer of glue and it is waited until the glue cover all the surfaces in contact with the glue. Then, the PMMA is lifted up from glue and placed into the PCB. It is important to highlight that instead of applying a layer of glue over the PCB, the stamping process avoids the excess of glue and the collapsing of channels.

Finally, once the PMMA and the PCB are joined by the glue, the glue needs heat to cure and also weight to keep the structures joined. In our case, the pieces are heated at 50° for 2 hour and with a weight of 20 kg, after that time, the heat is switched off without taking the pieces from hot plate. When the pieces reach

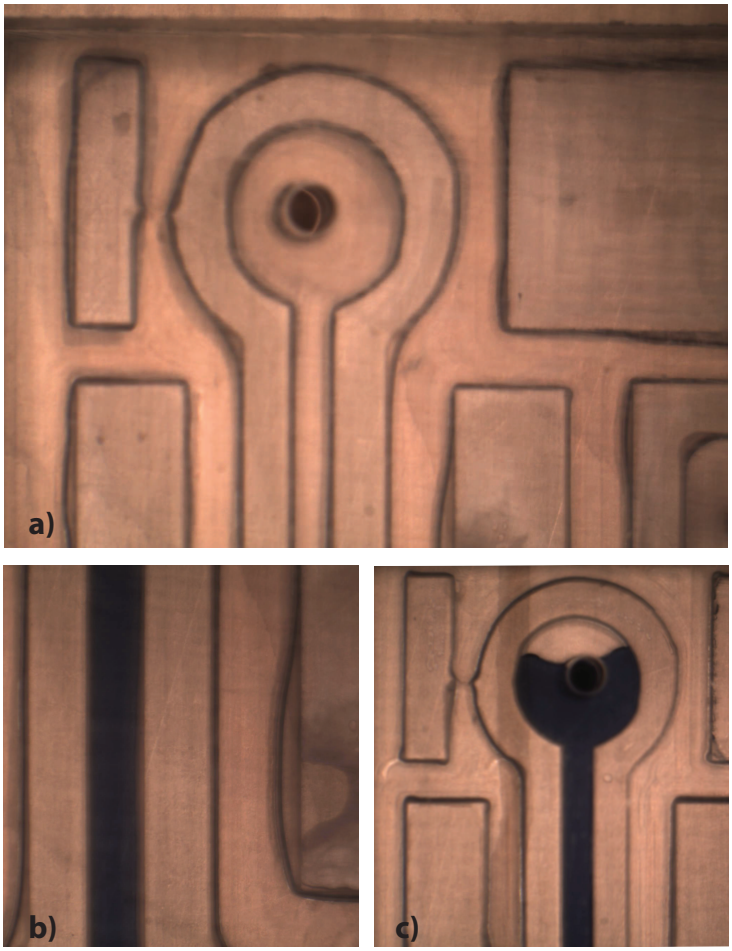

Figure 4.5: Example of glued channel with the EPO-TEK 301 glue. a) The PMMA structure after glued, b) and c) the glued structure with a blue ink to test the sealing of the gluing process.

room temperature, weight is taken away and the pieces remain glued. It should be emphasized that the weight applied is based in our experience gluing pieces of the same area approximately. If a bigger piece is wanted to be glued, the process should be characterized. The complete fabrication process can be seen in Fig. 4.6. Finally, the repetitiveness of the fabrication process has been evaluated, several Lab on Chip has been manufactured with a repetitiveness of 87 %, which adds value to this mass production technology.

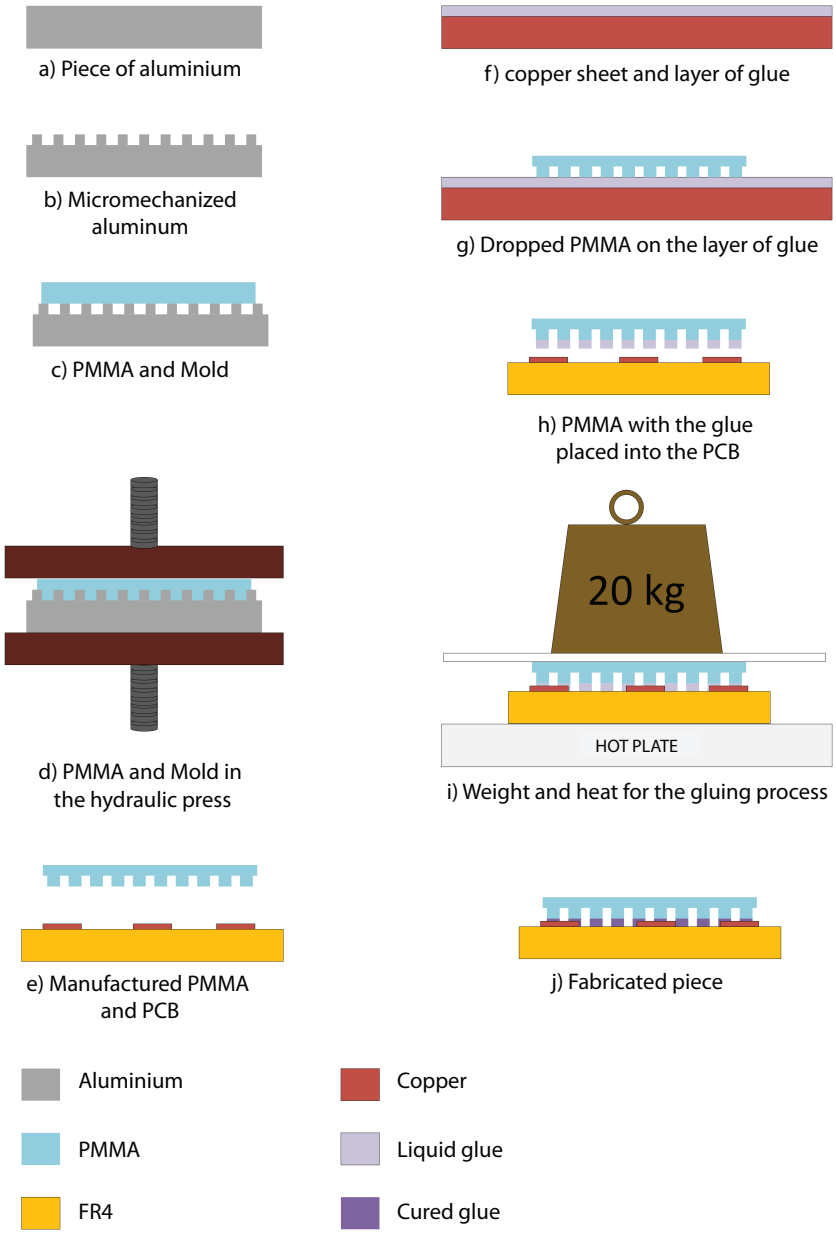

Figure 4.6: Fabrication process for PMMA and PCB structures.

4.3 Microvalve

Once the fabrication process is characterized and tested, the next step towards the mass production is the integration of the fuse microvalve in the fabrication process. The idea of integration the microvalve was always present to obtain an autonomous LoC. As it was said, it was a mayor challenge in the development of the fabrication process. The experience gained along the progress of gluing helps us to realize that the glue must perform hard after the curing. When the fuse microvalve is destroyed, it opens a channel where the fluid passes. If the glue remains liquid or semi liquid, the temperature achieves during the microvalve opening is enough to melt the glue and collapse the channel where the fluid passes. It could be instantly or gradually, but this time could not be enough to impulse all the fluid desired. As a results, the requirement was a glue that remains totally hard after the cured process.

4.3.1 Design and fabrication of the microvalve

The design of the microvalve was done following requirement of the fabrication process of hot embossing. A design was done in an aluminum mold that is transferred in a PMMA piece. Moreover, the PCB is a 5 μm copper where the microfuse is patterned. In the prototype design of the microvalve in SU-8, the microvalve was composed of a thin layer of copper and a wall of SU-8 over it, dividing two microfluidic circuits. When the layer of copper was melted, the wall of SU-8 was lifted off and the air pass through one microfluidic circuit to other. For this new fabrication process, this configuration can not be done because the minimum width of PMMA wall is around 200 μm and the electric fuse width is 100 μm, together with the layer of glue, the copper melting is not able to open a channel. The adopted solution cab be seen in Fig. 4.7, the copper track and the wall of the microvalve are perpendicular, so when the fuse it is melted, a channel is created in the wall of PMMA, creating a way out. The microvalve needs a difference of pressure between the inlet and the outlet of the microvalve for the movement of liquids. This difference is created using a pressurized chamber in the inlet of the microvalve, this chamber is pressurized using the same method than the use for the impulsion system in SU-8 3.3. In conclusion, the design realized to test the microvalve is composed of one chamber to be pressurized, the wall of the microvalve and a channel where a liquid is inserted to do a monitorization the movement of the fluid to be impulsed. The fabrication process is mostly the same

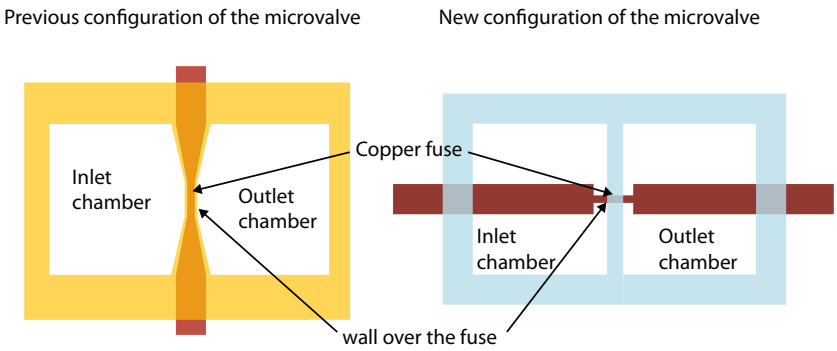

Figure 4.7: Schematic design of the new configuration of the microvalve.

as explained previously but there is one step more, in the process of placing the PMMA over the PCB the two pieces must be aligned. The wall of PMMA and the track of copper of the microfuse must match. In this case the alignment is done with the help of a microscope, because the tolerance allowed is big. However, for more complex structure alignment marks are used. The design for the mold can be seen in Fig. 4.1 a), the fabricated mold in Fig. 4.2 a) and the fabricated microvalve by hot embossing in Fig. 4.3 a). The final fabricated device is shown in Fig. 4.8, where the different parts that compound the microvalve are pointed and the microchannel has been filled with a diluted ink for the further characterization.

4.3.2 Characterization and results

In the same way it was done in section 3.2.5.3, a characterization of the working of the microvalve is carried out. As it was explained in the fabrication process, the opening of the microvalve was assured in the choice of the glue, so the purpose in this section is the microfluidic characterization of the microvalve, the pass of a fluid when the microvalve is activated. The first step is the pressurization of the inlet chamber by means of the putty material. The pressurized system is design to impulse around 4 μL which means a pressure of approx 300 mbar. This calculation are not really important because the intended goal was to evaluate the microfluidic behaviour of the microvalve, if the microvalve works under laminar or turbulent. In the first test, the outlet chamber of the microvalve was in the same order of the channel size and, as it was suspected, when the microvalve was opened, the pressurized air breaks the ink sample. The theoretical calculation of the behaviour can not be done easily, because the gap leave after the opening is

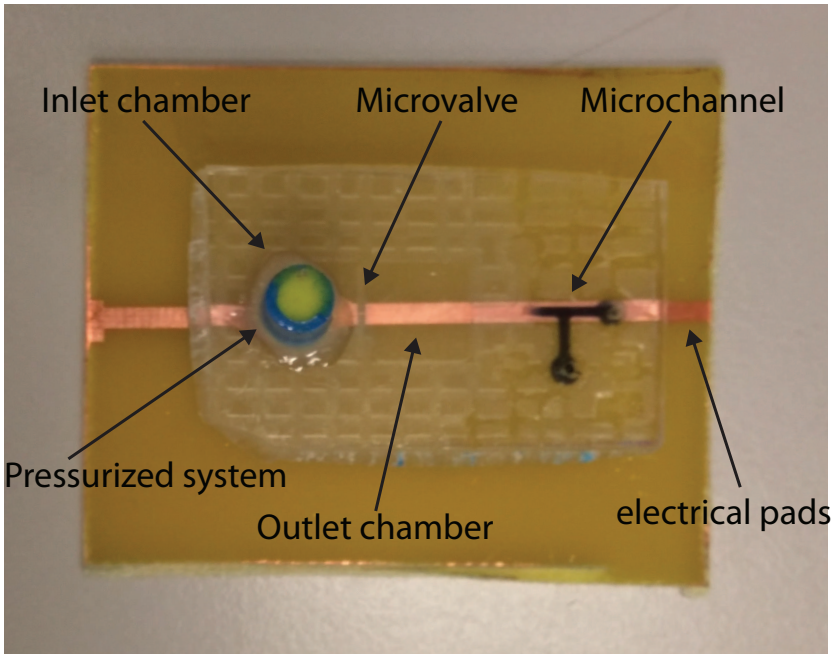

Figure 4.8: Fabricated microvalve for the microfluidics characterization.

unknown. However, assuming the results it can be supposed the behaviour of the fluid is under turbulent flow. After that experiment, it was decided to use silicone oil as a buffer because it reduces the dynamic of the impulsion due to the high viscosity of the oil, and therefore laminar flow is expected when the microvalve is open. Although it solved the problem, the residual left by the oil was not very suitable for a Lab on Chip. As a result, the proposed solution was to increase the outlet chamber giving the same results as the oil buffer. The different test carried out can be seen in Fig. 4.9.

4.4 Lab on Chip

The final step in this work thesis is the fabrication of the prototype lab on chip in PMMA and PCB. It means the integration of the microvalve in a microfluidic circuit with an autonomous impulsion system. The autonomous impulsion system follows the impulsion developed for the prototype in SU-8 of one pressurized chamber in the moment of impulsion, to avoid any possible leakage. However,

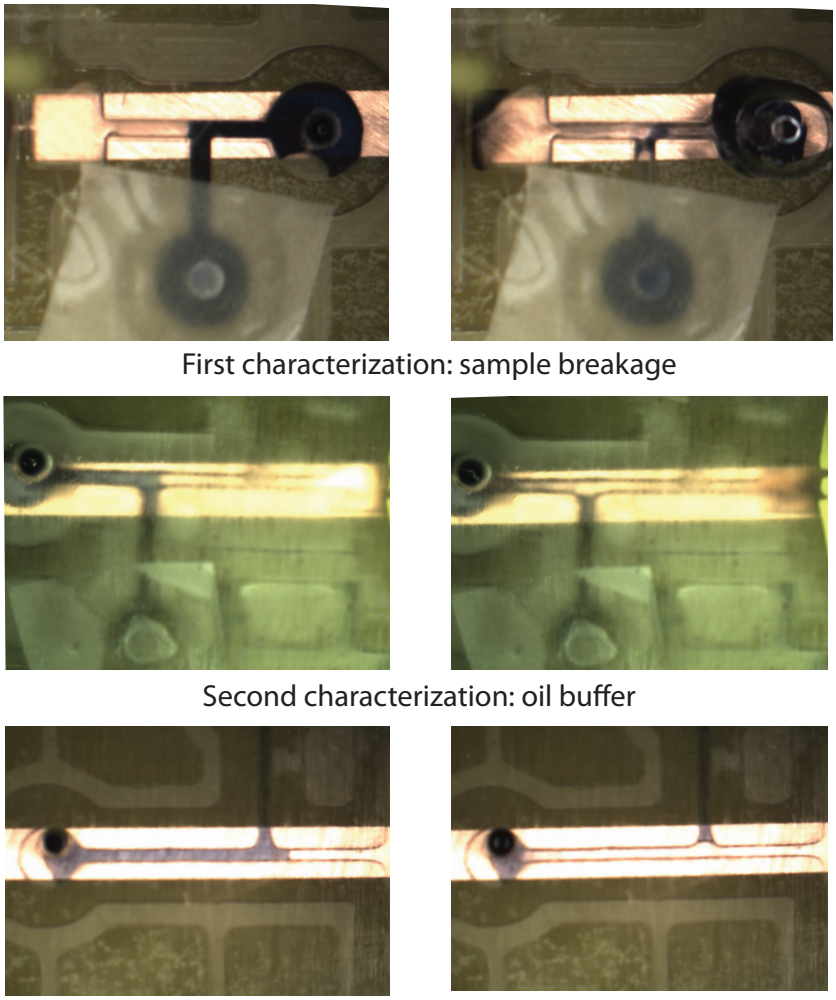

Figure 4.9: Three different characterization perform for the microvalve.

the pressurization is not carried out via a putty material, this is going to be carried out with two plungers. The microfluidic circuit is designed as a general multi-impulsion system to mix and transport two liquids towards a detection chambers. The objective is the migration towards an industrial production the lab on chip developed in this work thesis, a general purpose lab on chip platform. In this section the new impulsion system is described, the integration of the microvalves

with the impulsion system is detailed and the final design of the general purpose microfluidic circuit is designed, manufactured and characterized.

4.4.1 Impulsion system based on plungers

In the design of the impulsion system for the prototype LoC in SU-8 and PCB, the main goal was the design of an autonomous impulsion system based on pressurized chambers with zero leakages. The pioneering characteristic was the pressurization of the chamber at the moment of activation and this characteristic, in this new design was also primordial. Instead of using a flexible material to pressurized the chamber, a syringe plunger is used. The syringe plungers have a head rubber that ensure the fluids do not scape backwards, moving it through the barrel to the tip. The operation method is very similar than the syringe operation, it is summarized in Fig. 4.10. In this case the syringe plunger is introduced in a cylinder shape cavity of a diameter slightly smaller than the head rubber of the plunger. This cavity has two holes, one is connected to the pressurized chamber and the other is connected to the outside, Fig. 4.10 a). The hole connected to the outside acts as a purge, when the plunge passes it, the air does not find way out and the pressure starts to rise, Fig. 4.10 b). Finally, when the plunger reaches the end of the cavity, the pressurized chamber achieves the desire pressure. These calculation are done considering constant temperature, following Boyle's Law (4.2). Where P_{co} and V_T are the initial pressure and volume of the pressurized chamber, the hole connecting the two chambers and the rectangular cavity. P_{cf} and V_c are the volume of the pressurized chamber and the hole and the pressure final achieved. As it was defined in this work thesis, the aim is the design of a multipurpose lab on chip with management of fluids. In consequence, this impulsion system can be seen as a volume displacement, where the volume introduced by the plunge is the same that is going to be impulsed with the pressurized chamber. This volume introduced V_i is proportional to the distance between the holes s, and the diameter of the plunge D_p (4.3). As a result, the impulsed volume would depend of the space between the holes and the diameter of the plunger used, which there are a great variety in the market. This impulsion system is integrated with the fuse microvalve as part of the lab on chip.

$$P_{co}V_T = P_{cf}V_c = k \tag{4.2}$$

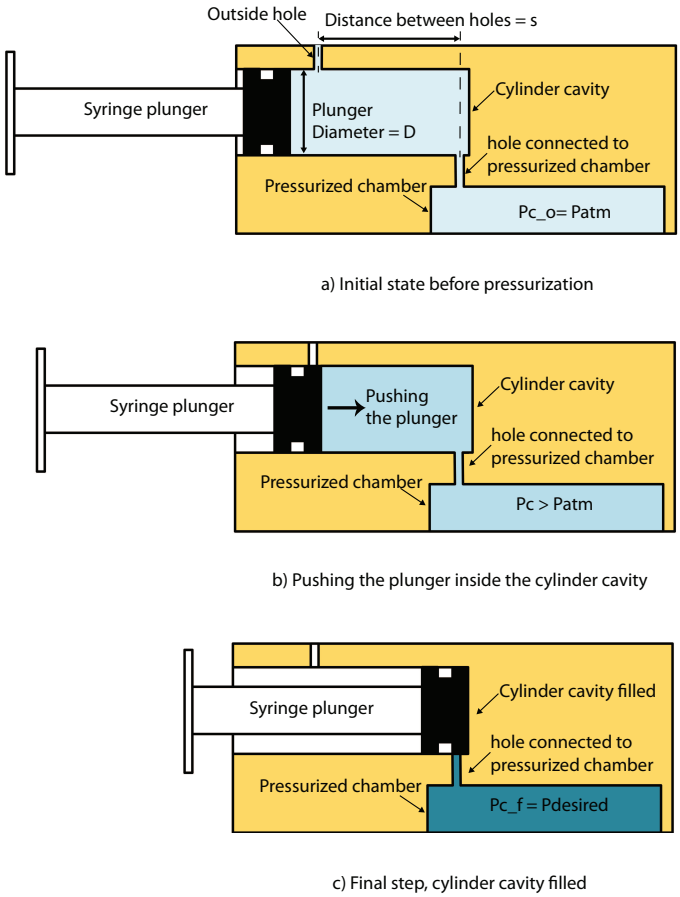

Figure 4.10: Plunger operation process.

$$V_i = \pi \cdot (\frac{D_p}{2})^2 \cdot s \tag{4.3}$$

4.4.2 Design and fabrication of the lab on chip

As it was commented, the new Lab on Chip is designed as a self-contained general multipurpose lab on chip, where the management of microfluidics is guaranteed. For this purpose, the lab on chip will contain two impulsion systems based on plungers with four microvalves, two chamber to store the two samples, a serpentine microfluidic channel where the samples are mixed and one detection chamber.

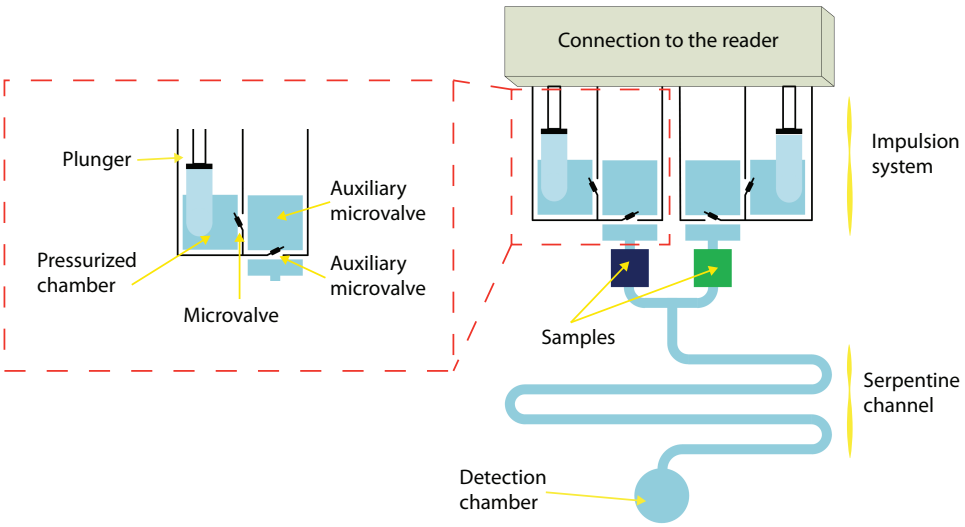

Figure 4.11: Schematic of the lab on chip in PCB and PMMA

A complete schem of the proposed design can be seen in Fig. 4.11. The first part of the circuit is the connection to the reader, where the electrical signals and plungers are connected. Secondly, there are two impulsion systems. These impulsion systems are detailed in a dash square on the left. As it was explained above, every plunger is connected to one pressurized chamber which is, likewise, connected to the fuse microvalve. However, the design differs a little bit from the plungers design. In order to avoid the breakage of the liquids backwards the microvalve, the big chamber solution of the microvalve is changed for a secondary small chamber with another microvalve, auxiliary microvalve. These auxiliary microvalves are opened before the microvalves connected to the pressurized chamber. When the microvalve connected to the pressurized chamber is opened, the pressurized air leaves the chamber through the microvalve towards the secondary chamber. In the secondary chamber, the air finds the way out for the small channel leaves for the secondary microvalve. With this configuration the speed of the pressurized air decreases and avoids the breakage of the sample liquids. This solution has been adopted instead of the big microchamber used in the characterization of the microvalve because it occupies less space. The impulsion system is design to transport a volume of 10 μL each, 20 μL in total.

After the impulsion systems, there are the two chambers to store the samples with volume of each sample of 5,4 μL. Under the two samples, there is a channel with a Y junction and a long serpentine channel of 29,7 μL, where the liquids

are mixed by diffusion after the two impulsions. Finally, there is a chamber for a possible detection which in this case is not accomplished because the goal is focused in the management of fluids.

The fabrication of this device is based on the fabrication process described above in section (4.2). The total system contains one PCB where are the microfuses and the tracks of copper and one PMMA piece where all the microfluidic components are stamped. The process is mainly the same as the general process described with the particularity of the plungers and the alignment marks. The plungers in our system are designed to impulse a volume of 10 μL. As previously said the volume displaced by the plungers will depend on the diameter of the cylinder where the syringe plunger is introduced and the distance between the purge hole and the hole connected to the pressurized chamber. The plunger used is from a syringe of 0.3 mL which the head rubber has a measured diameter of 2.7 mm, so the diameter where the plunger is introduced is set to 2.7 mm, to assure the sealing. The distance between holes to obtain the 10 μL is 1.74 mm and it is obtained from the equation (4.3). This cylinder and the two holes are manufactured with a drill of 2.7 mm and 0.3 mm respectively. Other variation adds to the fabrication process is the alignment, in the microvalve the alignment was made by visual observation but in this case, with four microvalves the alignment has to be more accurate. The solution was to introduced in the aluminum mold three drills so during the process of hot embossing those creates a bump in the PMMA, these drills can be seen in Fig. 4.2 b). These drills are also made in the PCB assuring the complete alignment of both parts, achieving a fast and automatic alignment for mass production. The fabrication process is summarized in Table 4.1.

The micromold used was shown in the fabrication process in Fig. 4.2 b). The fabricated and glue device can be shown in Fig. 4.12 where are the different components integrated are pointed. Before proceeding with the activation of the system, the auxiliary microvalves must be opened. These microvalves avoid the breakage of the sample liquids after the impulsion. These are individually opened applying voltage between the terminals and the electrical characteristics is the same as in Fig. 3.43. The opening of the microvalve creates a microchannel which acts as a filter, slowing down the pressurized air that impulses the fluids. Once the auxiliary microvalves are opened, the system is ready to be used.

Table 4.1: Fabrication process of the LoC system in PMMA and PCB.

Step	Description	Material and Equipment
1	**PCB Manufacturing**	
1.1	PCB cut and drills	5 μm PCB and CNC micromilling
1.2	PCB pattering	Mask, etching solution and UV aligner
1.3	PCB cleaning	IPA and Acetone
2	**Mold Manufacturing**	
3.1	Mold manufacturing	Al and CNC micromilling
3.2	Mold cleaning	Water and soap
3	**PMMA Manufacturing**	
3.1	PMMA cut	PMMA and CNC micromilling
3.2	PMMA pattering	PMMA and hydraulic press
3.3	Plungers fabrication	Drills and CNC micromilling
3.4	PMMA sand down	Sand paper
4.4	PMMA cleaning	Water and soap
4	**PMMA, PCB pretreatment and glue preparation**	
4.1	PMMA drying	PMMA and Owen
4.2	PCB drying	PCB and Owen
4.3	Glue preparation	EPO-TEK 301
4.3	Glue preparation	EPO-TEK 301 and Vacuum chamber
5	**PMMA and PCB gluing**	
5.1	Glue deposition	EPO-TEK 301, 86 μm roller
5.2	PMMA stamping	PMMA and glue
5.3	PMMA and PCB junction	PMMA, glue, PCB and alignment marks
5.4	Curing for 2 h 50°	PMMA, glue, PCB, heat and weight
5.5	Cooling down	PMMA, glue, PCB and weight

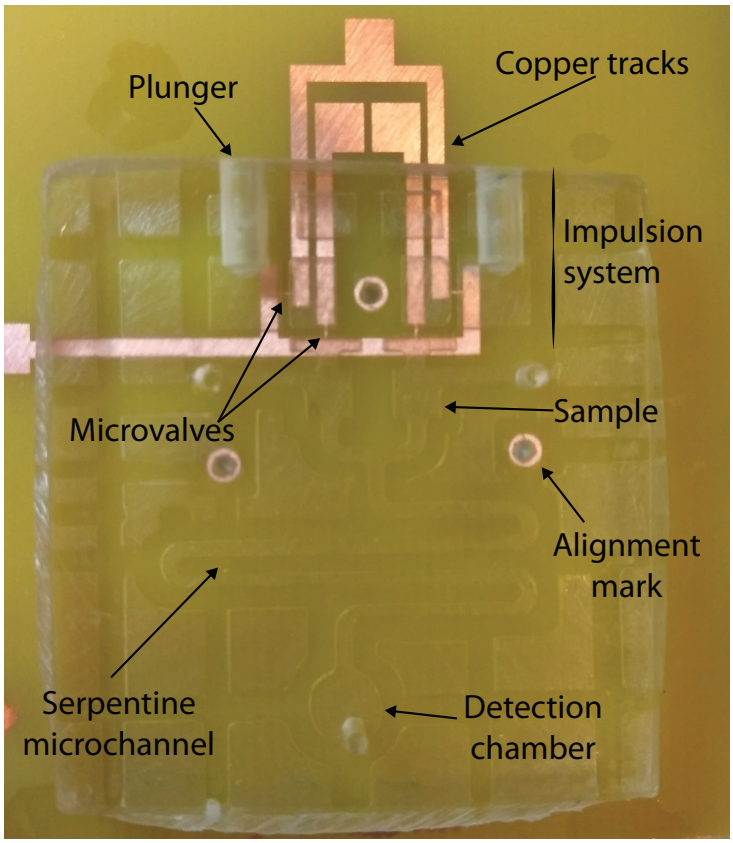

Figure 4.12: Fabricated LoC system in PCB and PMMA.

4.4.3 Characterization of the Lab on Chip

As it was done in 3.4.5, the LoC system is tested to evaluate its behaviour and see if the management of fluids along the microfluidic circuit is achieved. The way of proceeding starts by filling the samples chamber through the inlets. The samples are filled with diluted inks due to its similarity in chemical properties with water based chemical samples. The 5,4 μL of each sample is filled with the help of a pipette. Afterward, the inlets are closed with adhesive tape. For this set up, the syringe plunges are introduced in the cylinder cavities and fitted before the purge hole, just before pressurization. Then, the plunges are pushed forward until reaching the end of the cavity, pressurizing the chambers. In this moment, the microvalves are activated and the pressurized air leaves the chambers, impulsing the samples. The activation is carried out via the two microvalves connected

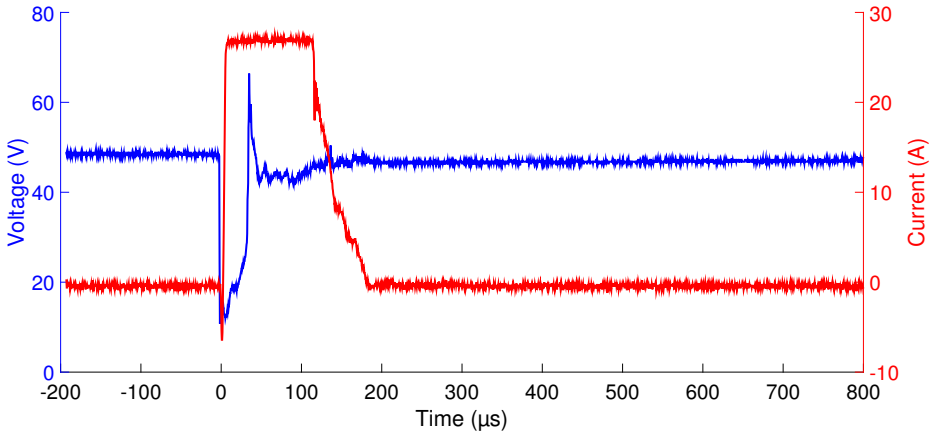

Figure 4.13: Electrical characteristic of the activation of two parallel microfuses.

to the pressurized system. Since the objective in the transport and mixed of the two samples, the two microvalves must be opened at the same time. For that purpose, the two microvalves are connected in parallel, as it can be seen in Fig. 4.12, so the voltage is applied between the pads and the two fuses are melted. One microfuse is, of course, opened before the other, the one with lower resistance. However, the difference in time is so small that it is negligible for the microfluidic behaviour. Moreover an electrical study of this double impulsion is made to analyze the behaviour. The results of the current and the voltage in the melting of the two parallel microvalves is shown in Fig. 4.13. In this figure there are differences with the previous electrical characteristic of single microfuses, the current needed for the melting is higher, as it could be expected and also the time of melting, in this case the time is almost 200 μs. However, these 200 μs is fast enough to be negligible for being noticed in the impulsion of the fluids, as it will be observed further down.

The lab on chip system is designed to impulse the two samples 20 μL. If the serpentine microchannel contains a volume of 29,7 μL, the sample liquids must remain after the impulsion inside the serpentine. The reason for designing the system to place the sample in the serpentine and not in the detection chamber is the accuracy in the visualization of the results. The section of the channel is smaller than the detection chamber and it is easier to detect any deviation from the theoretical impulsed volume and the experimental impulsed one. The process starts with the samples filled in with the inks and the plungers connected, pressurizing the

chambers, and the auxiliary chamber opened. After that, the parallel microvalves are opened, and the pressurized air of the chambers is released, impulsing the fluids. The process is captured showing different stages, Fig. 4.14. Looking at the images it is important to highlight that as it can be seen in t=0.03 s the samples are impulsed instantly and the 200 μs of difference between the electrical opening of each do not interfere in the impulsion. Moreover, it is observed that the liquids do not break, the auxiliary chamber and microvalve fulfill their purpose using less space in the LoC. Finally, the two samples are mixed and moved in 17 s, which compares with the 200 ms of the difference between the opening of the two microvalves is negligible. The experimental displaced volume is 22.6 μL which is a variation of 13 % from the theoretical volume. The variation between the theoretical impulsed volume and the real volume is due to the tolerances in the fabrication process, the mold contains differences in the channel deepness due to the slight tilt of the micromilling structure. Moreover, the biggest tolerance comes from the drill for the hole of the plunger. The hole is made with a drill of 2.7 mm diameter, as it was mentioned in the fabrication process, 2.6 μL more in total means 1.3 μL more per plunger. Assuming the same error for the two plungers, it means the impulsed volume of 11.3 μL and using the equation (4.3) the radio of the drill for this volume is 87.7 μm bigger, with means a 6.49 % from the 2.7 mm. The results obtains are good from the point of view of a prototype, the error obtained can be easily improved with a more accurate process in the fabrication of the PMMA, to absorb and decrease the error of tolerances.

4.5 Conclusions

In conclusion, in this chapter the migration of a self-contained multipurpose lab on chip for the management of fluids in a more industrial technology has been illustrated. Firstly, the new fabrication process has been defined, with materials and process that are reproducible in mass production technology. Moreover, the different active components of the lab on chip platform has been integrated, the microvalve and the impulsion system. The fuse microvalve has been designed for this new process and characterized. In addition, a new impulsion system based on syringe plungers is designed. This new design is also based on a pressurized chamber just before activation, in this way, any possible leakage is avoided. Finally, a microfluidic circuit with two simultaneous impulsions and mixing of two samples is carried out, showing the adaptability of the platform developed.

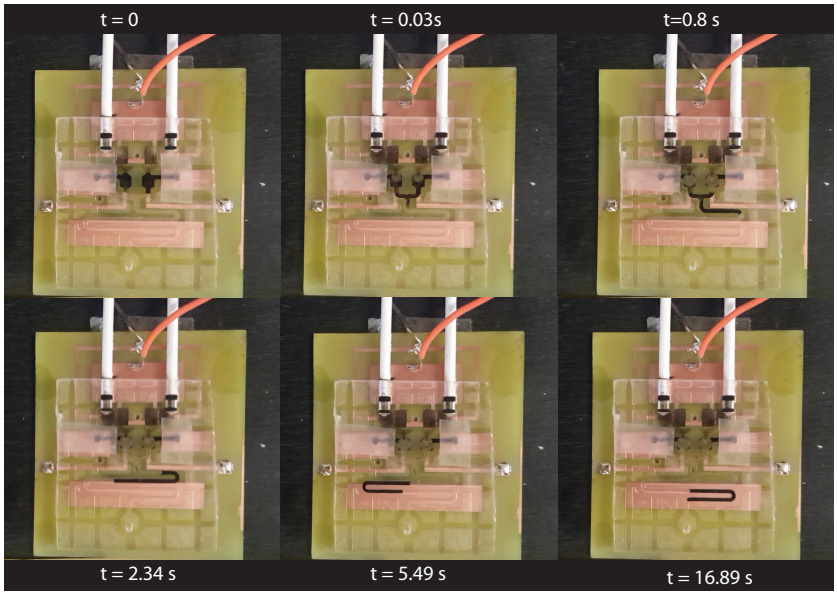

Figure 4.14: Fabricated LoC system in PCB and PMMA.

The results obtained within this chapter are planning to be published in a high impact scientific journal and in a conference in the area of research.

5

CONCLUSIONS AND FUTURE WORK

5.1 Conclusions

This thesis has resulted in a self-contained microfluidic platform for general purpose Lab-on-Chip using an industrial level technology. This new Lab on Chip involves the development of several active components with great repercussion in the state of the art. The main contribution of this thesis are summarized as follows:

Development of a single use microfuse microvalve

- A single-use thermoelectric active microvalve is presented. The main novelty of the system lies on the simple activation method based on a fuse. An electrical current is in charge of the activation, avoiding pneumatic forces like most of the microvalves. The microvalve activation is characterized in terms of time of opening and energy consumption, being very competitive with an opening of less than 1 ms and energy consumption of 30 mJ.
- In addition, the design of the microvalve is thought to be easily integrable in many microfluidic platform. The horizontal structure of the microvalve with the two chambers and the wall makes it very simple to fabricate and integrate. In the Table 5.1, the main contribution of the microvalve are summarized.

Table 5.1: Comparative of the single used microvalves in the state of the art.

Microvalve	Activation Time(ms)	Energy (mJ)	Fabrication complexity	Integrability
Guerin [136]	1200	400	Medium	Medium
McDonald [137]	1000	150	Low	High
Ahn [138]	700	28	Medium	High
Li [141]	100	2.5	Medium	Low
Pitchaimani [142]	7000	350	Medium	High
Moreno [5]	2000	350	Medium	High
Aracil [4]	2500	700	Low	High
Perdigones [6]	1000	188	Medium	Very high
This work	**0.1**	**30**	**Low**	**Very high**

Development of an impulsion system

- The impulsion system has been developed for being autonomous and versatile in the amount of volume impulsed. The main new feature, compared to other similar systems, is the pressurization at the time of use. In this way, any possible leakage due to material porosity at high pressure is avoided.
- The impulsion system has been characterized for different volume showing the feasibility of the system, with errors between the introduced volume and the impulsed volume around 4 %.
- The integration of this pressurized system has been tested for two different technologies SU-8, PMMA and PCB, showing the versatility of the proposed system.
- The permeability of the system is studied to evaluate the pressure over an hour, resulting in leakages of less than 3 %.

Development of microfluidic platform as a proof of context

- A new microfluidic technology more oriented towards mass production in PMMA and PCB is developed. A gluing technique has been developed, assuring the tightness at high pressure and, at the same time, the flooding of glue inside the channels.
- A microfluidic platform integrating the microvalve and the impulsion system has been developed demonstrating the control and management of fluids. This microfluidic platform has been fabricated in the two technologies of this work thesis SU-8/PCB and PMMA/PCB, showing the integrability of the system.
- A portable electronic reader for the system is developed. This electronic reader contains a programmable microcontroller to give autonomy and control to the platform. In addition, it will provides an easy-to-use and reliable handling of a microfluidic platform to non-expert users. This electronic reader will contain wireless connection to the microfluidic platform.
- A detection platform based on light absorbancy has been performed. The system presents a great stability due to the structure where the LEDs are assembled. In addition, due to the differential mode in the signal acquisition the sensitivity has improved 10 times.

5.2 Future work

The variety of approaches reached in this thesis contributes with several open lines in the area of Lab on Chips. This open lines are oriented towards the continuation of the research work and, towards the commercialization of one Lab on Chip system. The next items of future are described below:

- Integration of a more complex microfluidic circuit. In line with the mass production already started in this thesis, the microfluidic circuit will contain more features, as injectors, extractors and systems of continuous transport. The Lab on Chip will be able to accommodate different applications according to the requirements.

- Integration of several detection sensors in the platform. Due to the integrability of the fabrication process, the integration of silicon sensors has become more affordable.

- Development of an electronic reader with total control of the platform. The reader must perform the control of the whole platform, including activation of the different active components and the data acquisition from the sensors. The electronic reader must be an user interface between the microfluidic platform and the non-expert users. This electronic reader will contain wireless connection with the reader.

- Standardization of the microfluidic building blocks and the development of a design package to automate the manufacturing process of LoCs that will implement future Point of Care applications.

- Technology transfer to a production system. Thanks to the results obtained with this work thesis, this research has been getting closer towards the development of a product. This work could result on the basis for the creation of a company on Lab on Chips systems.

Appendices

A

FABRICATION PROCESS DEVELOPED IN JADE UNIVERSITY

A.1 Introduction

In this appendix the different gluing techniques acquired during a stay in University of Jade in 2015 are presented. The collaboration was made with Prof. Gassmann who is full professor in that University and he researches in the field of MEMS, microfluidics and electronics. He and his laboratory team, leaded by the Engineer Helmut Schütte, are focused in the fabrication of microfluidic devices in PMMA and PCB. In this stay was expecting to acquired the fabrication technology from the host University and being able to integrate it in our designs in SU-8. At that time, the lab on chip is SU-8 had been already developed and it was looking for the migration towards a massive production technology. From these premises, it was a good opportunity to learn the technology.

The appendix focuses on the gluing technologies learned in Jade University, these technologies would be the base of the migration towards the Lab on Chip in PCB and PMMA.

A.2 Gluing structures with acrylic adhesive tape of 50 μm

The first trial for the bonding of PCB and PMMA structures was with an acrylic adhesive transfer tape of 50 μm (3M^{TM}). This fabrication techniques was already tested in small channels by the Electronics Department in the University of Jade with successful results [220]. However, the main purpose of this stay was the integration of the fuse microvalve, until then no active component had been integrated. The process of gluing is easy and intuitive, as it is carefully explained down below. The first phase is the preparation of the materials, the PCB and the PMMA structure have to be designed in a template. This template is designed for fitting the pressing plates which would be used for bonding. In this particular case, the template is a square of 200 mils width and two alignment holes of 3.1 mm diameter, fiducials, Fig. A.1 a). The pieces needs to be carefully cleaned, the PCB with Alcohol or Acetone and the PMMA with water and soap, and if it is needed with an ultrasonic bath in water. Once the materials are prepared, the tape is transfer to the PCB and it is pressed with a roller. With the aid of a cutter, the places for the fiducials are released and the Kraft paper that covers the tape is peeled. The PCB is placed in the plates structured and the thermoplastic piece is located on the PCB and the upper iron plate is putted on, see Fig. A.1 b). The next

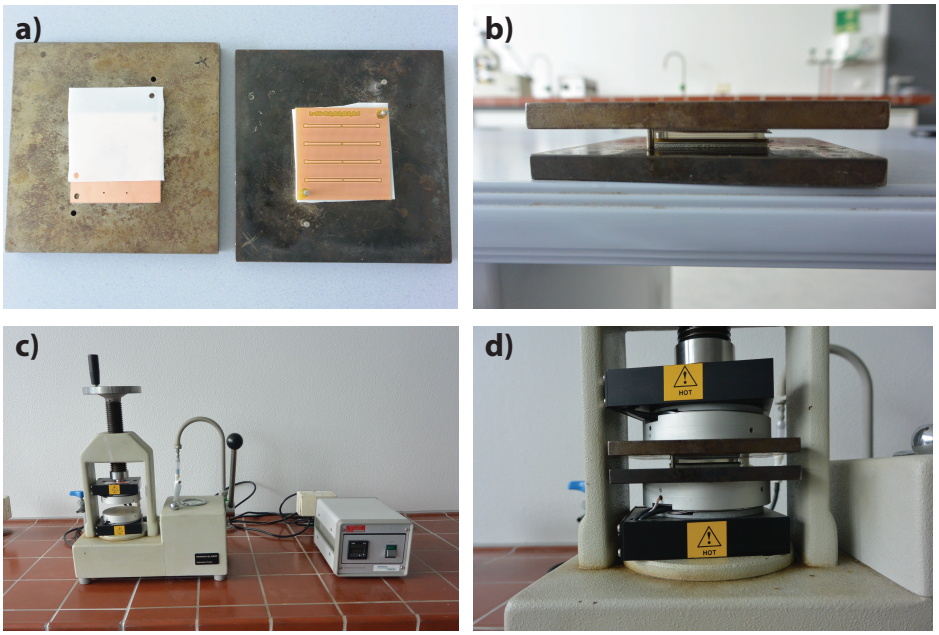

Figure A.1: Gluing process with acrylic adhesive tape: Structure plates a), b) and hydraulic press c), d).

step is the cure of the adhesive tape glue, the metal structure with the PCB and the PMMA is introduced in a hydraulic press with a weigh of 250 kg and a temperature of 60 °C for 45 min, Fig. A.1 c) and d). When the room temperature is reached, the hydraulic press is opened and the PCB and the thermoplastic, already glued, are released from the plate structures. However, result was not the one expected because the microvalve after activation is opened for a short period of time and then the microvalve is closed. Even, the action of closing after opening, it is not a bad news. This is the operation of a peristaltic valve. Unfortunately, the time that remained open was not enough to impulse the desired fluid. The result from the opening of the microvalve is shown in Fig. A.2.

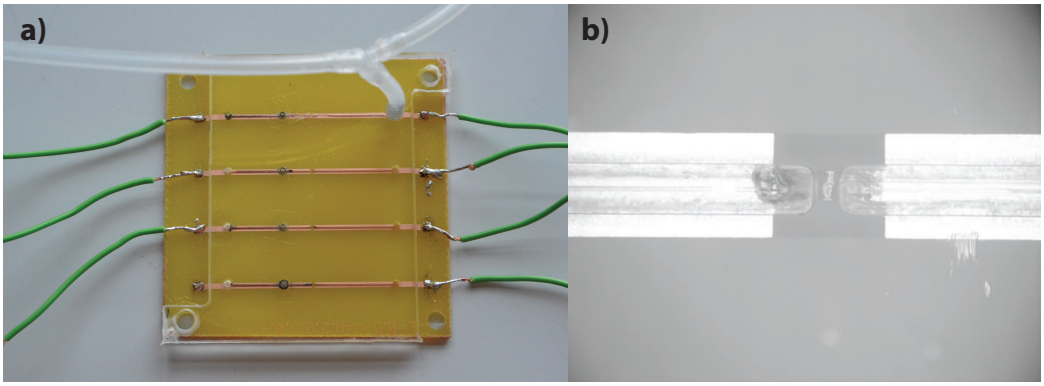

Figure A.2: Result of the gluing process with adhesive tape: Channels glued a) and open microvalve b).

A.3 Gluing structures with acrylic adhesive tape of 25 μm

After the results obtained with the 50 μm adhesive tape, it was decided to test the system with a thinner tape, 25 μm. The properties of the tape was the same than the 50 μm thickness, so it was expected to have the same results in the gluing and improve the microvalve opening. The fabrication process used was the same as were previously and the fabrication results was also satisfactory. In the characterization of the microvalves different design of the copper fuse were carried out, this is summarized in Table A.1. The microvalve were opened enough time to impulse the fluids in all cases except for a length of 500 μm and a width of 250μm. As the length decreases the electric resistance increases and the electric current is not able to open the microvalve.

A.4 Pattern transfer process in adhesive tape of 25 μm

During the gluing process, a pressure is applied to improve the bonding between the PMMA and the PCB. Due to the pressure, some glue goes to the channels, changing the volume inside those. In order to avoid this amount of glue inside the channels, it was consider to pattern the microfluidic design in the adhesive tape.

Table A.1: Microvalve characterization for 25 μm

Different copper fuse dimensions		
Length	**Width**	**Results**
1 mm	110 μm	Opened enough time for the fluid displacement
	148 μm	Opened enough time for the fluid displacement
	255 μm	Opened enough time for the fluid displacement
500 μm	46 μm	Opened enough time for the fluid displacement
	86 μm	Opened enough time for the fluid displacement
	250 μm	The microfuse was not melted

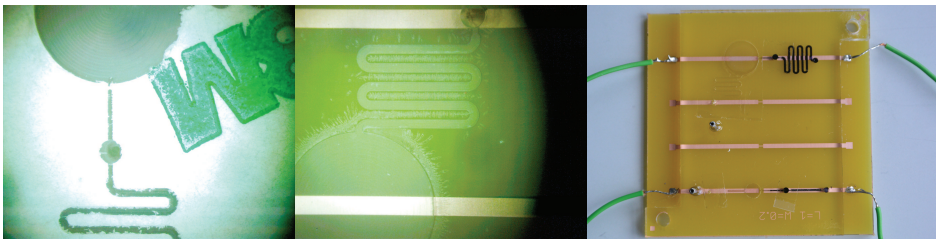

Figure A.3: Pattering transfer tape.

The tape is transferred to the virgin PMMA without peeling the Kraft paper and these two parts are milled. Then, the Kraft paper is peeled off and it is glue in the PCB with the same fabrication process. This arrangement improves the control of volume because any glue that may appears during the gluing is much less. In Fig. A.3 is shown the pattern transfer process.

A.5 Gluing structures using Dip Coating

Dip Coating is an immersion technique to achieve thin coats over a surface. A substrate is dipping into the solution coat and it is withdrawn at a constant speed. The thickness of the coat in the material would depend on the speed and the con-

centration of the solution. This fabrication technique has already been used for the creation of microfluidic channels gluing two PCBs in Rostock University by the research group headed by Prof. Pagel where Prof. Gassmann developed his PhD. The objective with this stay was to apply this fabrication technique for gluing PMMA and PCB. The fabrication process used for the creating of the coat was the same as the fabrication used in Rostock University for gluing two PCBs. The glue used was EPOXY due to its probed adhesion to the PCB. In order to reduced the viscosity of the glue and obtain a thin coat, the EPOXY is diluted in ethanol. This glue is introduced in a bucket, and a tow machine is used to set the speed of dipping and withdraw of the PCB, Fig. A.4. After that, the PCB is introduced in a oven to eliminate the Ethanol, and the PCB with the coat of glue and the PMMA are placed on the iron plates and glued with pressure and heat.

The different steps and parameters for a glue coat of 2-3 μm are detailed:

1. PCB and the PMMA are manufactured and cleaned.
2. The glue is diluted with a relation of 7 g EPOXY, 2.8 g Hardener and 10.2 g Ethanol.
3. The glue is mixed thoroughly for two minutes and introduced in the bucket of the tow device.
4. The speed of the tow is set to 10 cm/min and the PCB is hung in the tow.
5. The tow is switched on and the PCB is going down until it is introduced in the bucket, the PCB must remain in the bucket for 30 s.
6. The PCB is gone up and taken out from the tow.
7. The PCB is introduced in an oven for 10 min at 80 °C, at that time the Ethanol is evaporated.
8. The PCB is cooled down at room temperature.
9. The PCB and the PMMA are placed in the iron plates.
10. Those are introduced in the hydraulic press with a weight of 250 kg and the temperature is set to 80 °C.
11. When the temperature is reached, the heater is turned off and the structure is left in the pressing machine for 16-18 h.

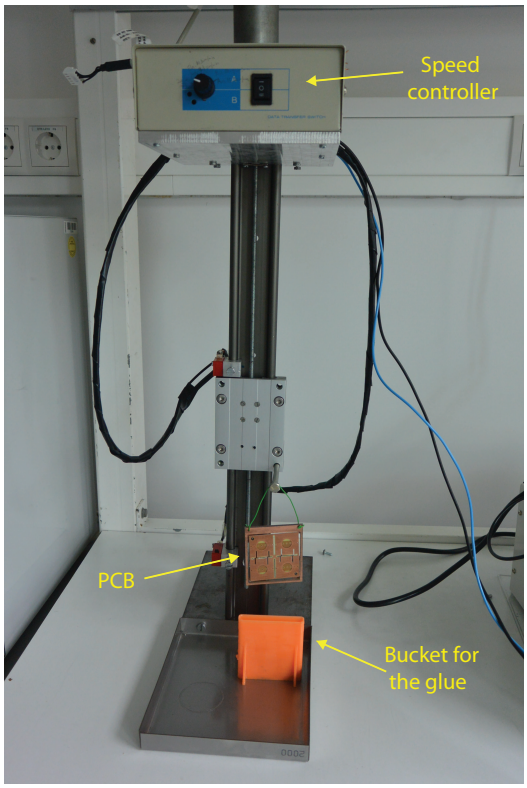

Figure A.4: Tow device for the glue coat.

12. After that time, the hydraulic press is opened and the PCB and the PMMA are carefully released from the iron plates.

With this fabrication process the result obtained was not satisfactory, the glue adheres to the PCB but not to the PMMA. In order to improve the process different modification were done:

- Cleaning the surface of the PMMA with plasma to improve the adhesion of the Epoxy.
- Using flexible plates to avoid the stress. The plates that were used to press between the two iron plates were two Teflon plates. Two softer plates are used to avoid the stress caused by pressing.
- Increasing the glue layer. It can be increased by increasing the speed in the tow or by reducing the amount or Ethanol.

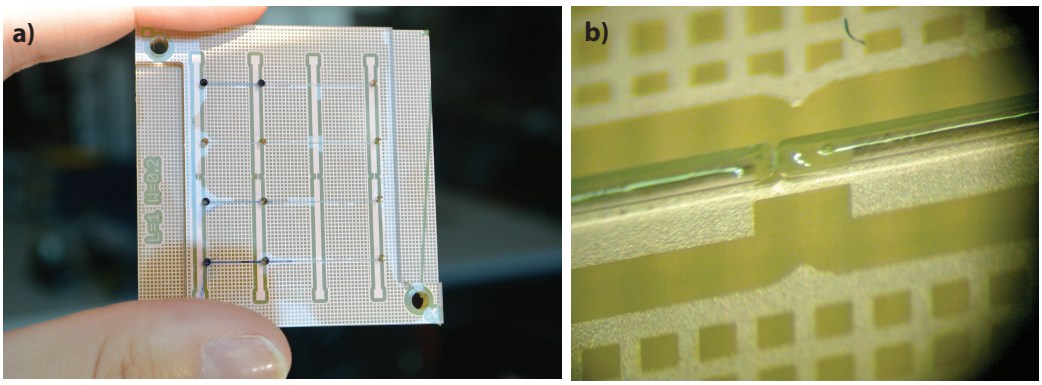

Figure A.5: Results using Dip coating fabrication process: a) the PMMA is not glued to the PCB, due to stresses produced during the curing. b) the two devices remain glued but the channels are collapsed.

- Reducing the temperature in the pressing machine.
- Sanding the PMMA.

After different evidences in the fabrication process, the conclusion achieved was that the Epoxy does not glue the PMMA or thermoplastics. Having a bonding between PCB and PMMA is only possible if the PMMA is sanded and there is a thick layer of glue. Thanks to the scratches of the sanding, there is a mechanical bonding that helps the junction. However, it presents problems caused by the amount of glue between the scratches that collapse the channels. Some fabricated devices can been seen in Fig. A.5

B

PUBLICATIONS

B.1 Journals articles and conference contributions

In this appendix are detailed the scientific contributions published upon the development ot this thesis. There have been published so far there articles in a high impact scientific journal and one more in progress. Furthermore, two contributions have been made in conferences in the field of this thesis.

- **International Journal Articles**
  - Flores, G., Aracil, C., Perdigones, F., & Quero, J. M. (2014). Low consumption single-use microvalve for microfluidic PCB-based platforms. Journal of Micromechanics and Microengineering, 24(6), 065-013.
  - Aracil, C., Perdigones, F., Moreno, J. M., Luque, A., Flores, G., & Quero, J. M. (2014). Depressurised reservoirs for portable fluid extraction in SU-8-based microfluidic systems. Micro & Nano Letters, 9(11), 821-824.
  - Flores, G., Perdigones, F., Aracil, C., & Quero, J. M. (2015). Pressurization method for controllable impulsion of liquids in microfluidic platforms. Microelectronic Engineering, 140, 11-17.
- **Conferences contribution**
  - Flores, G., Perdigones, F., & Quero, J. M. (2013, February). Pressurized microvalve with SMD-based activation to drive fluid in low-cost and autonomous MEMS. In Electron Devices (CDE), 2013 Spanish Conference on (pp. 147-150). IEEE.
  - Flores, G., Perdigones, F., Aracil, C., Cabello, M., & Quero, J. M. (2015, February). Microfluidic platform with absorbance sensor for glucose detection. In Electron Devices (CDE), 2015 10th Spanish Conference on (pp. 1-4). IEEE.

IOP Publishing Journal of Micromechanics and Microengineering
J. Micromech. Microeng. 24 (2014) 065013 (6pp) doi:10.1088/0960-1317/24/6/065013

Low consumption single-use microvalve for microfluidic PCB-based platforms

G Flores, C Aracil, F Perdigones and J M Quero

Department of Electronics Engineering, University of Seville, Av. Descubrimientos s/n, E-41092, Seville, Spain

E-mail: gflores@zipi.us.es

Received 18 December 2013, revised 3 April 2014
Accepted for publication 11 April 2014
Published 6 May 2014

Abstract
In this paper, a single-use and unidirectional microvalve with low consumption of energy for PCB-based microfluidic platforms is reported. Its activation is easy because it works as a fuse. The fabrication process of the device is based on PCB technology and a typical SU-8 process, using the PCB as a substrate and SU-8 for the microfluidic channels and chambers. The microvalve is intended to be used to impulse small volumes of fluids and it has been designed to be highly integrable in PCB-based microfluidic platforms. The proposed device has been fabricated, integrated and tested in a general purpose microfluidic circuit, resulting in a low activation time, of about 100 μs, and a low consumption of energy, with a maximum of 27 mJ. These results show a significant improvement because the energy consumption is about 84% lower and the time response is about four orders of magnitude shorter if compared with similar microvalves for impulsion of fluids on PCB-based platforms.

Keywords: microvalve, PCB–MEMS, SU-8

(Some figures may appear in colour only in the online journal)

1. Introduction

The development of microfluidic platforms has experienced a significant increase in recent decades due to its application in fields such as biomedicine and environment [1–3]. An important effort has been made to improve microfluidic components in order to increase the functionality and reliability of the microfluidic platforms. A highlighted element in these platforms is the microvalve. Its functionality plays different roles since it can be on charge to regulate the flow of microchannels, or to isolate regions and be the active element of an impulsion system. Many groups have focused their research on designing and evaluating microvalves using different materials and technologies [4–8]. In that way, a low-cost fabrication technology called PCB–MEMS has been considered. Printed circuit boards (PCBs) are a long-standing electronic technology and have been applied to a variety of applications. The substrate used in this technology is the FR4 layer of the PCB. The copper layer can be used as a structural material of the microfluidic circuit, and as electronic connections of the device, [9–11]. In this manner microelectromechanical systems (MEMS) can be manufactured with a low-cost and a high integration with electronic components. Moreover, they are compatible with other materials such as, for example, SU-8. This material can be used as the structural material of the microfluidic circuit, and the copper layer can also be used as a sacrificial layer. Many structures can be fabricated by the combination of both a PCB and SU-8.

In the literature, several actuation principles have been adopted as an operation method in microvalves. Taking into account the characteristic of the technology, thermo-pneumatical activation is considered the most suitable. Microvalves reported by other research groups include [12–16].

In this work, the mechanism of operation is based on passing current through an element that acts as a fuse. This kind of activation opens the connections between chambers, which is set by different pressures. The release of pressure can be used to impulse the fluid.

Previous research based on the combination of SU-8 and PCB–MEMS has given rise to the fabrication of several microvalves [17–19]. They are characterized by a high consumption and a complex fabrication. Firstly, the

J. Micromech. Microeng. **24** (2014) 065013 G Flores *et al*

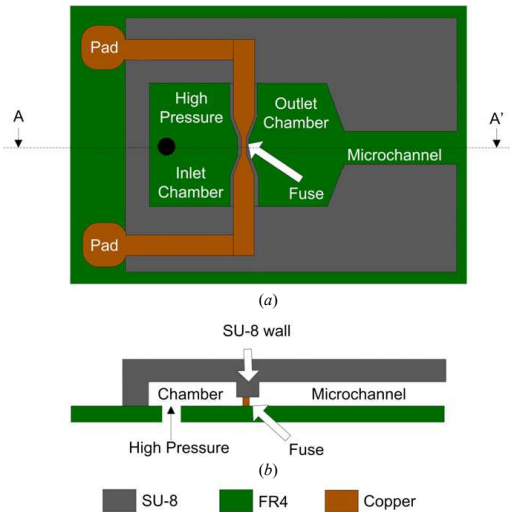

Figure 1. (*a*) Top view. Microvalve integrated with a microchannel and a chamber set at high pressure. (*b*) Cross section view (AA) of the microvalve.

fabrication of out-of-plane devices, in [17] and [18], implies the manufacture of very high aspect-ratio walls by means of photolithography. Since the activation involves a mechanical effect that depends on both wall thickness and height, the tolerance has to be signif cantly decreased. This fact poses a challenge from a fabrication point of view. Finally, in the third case [19], the tolerance is related to the thickness of the membrane. A very small variation in this parameter implies an important difference in the activation.

Keeping in mind the advantages of the technology, the aim of this work is the design of a microvalve based on PCB–MEMS technology. The most important requirements are a low-cost and a high-reliability fabrication process and a reduction of energy consumption.

This paper is organized as follows: section 2 describes the device, including its parts and behavior. In section 3, the fabrication process f ow is described. The device characterization and experimental results are presented in section 4. Finally, in section 5, a discussion is included. Finally, the main conclusions of the research are summarized in section 6.

2. Microvalve structure and working

The proposed microvalve is a single-use device fabricated using a PCB and SU-8. The copper layer of the PCB is used to construct the microvalve and the electronic connections at the same time. The FR4 is the substrate for both microf uidic circuit and microvalve. The microf uidic circuit is manufactured using SU-8 over the PCB. Therefore, the proposed device is highly integrable in microf uidic platforms, as much in the f uidic part as the electronic one.

The microvalve structure is shown in f gure 1. It is composed of a thin copper line working as a fuse. This copper line separates the inlet chamber set at high pressure from the rest of the microf uidic circuit.

The SU-8 wall located over the fuse is used in the fabrication process as a mask to def ne the width of the fuse, as will be commented later. The adhesion between SU-8 and copper is robust enough to support the difference of pressure and to avoid leakage between the high and low pressure chambers of the circuit. In addition, this wall works as a link between the microf uidic and electrical circuits to achieve complete integration between the SU-8 and PCB parts of the microvalve. In order to activate the device, it is connected to a power supply.

The fuse demands a short-circuit current, destroying the fuse in a very short time. The melting time is an important parameter in the design of the microvalve and depends on the fuse section. In this particular case, the fuse section is rectangular with the height f xed from the copper layer of the PCB. The smaller the section is, the lower the time. For this reason, a PCB copper layer with a thickness of 18 μm-height has been chosen. The fuse width is a parameter to be characterized subsequently.

The consumption of energy takes place during this short melting time. So, although the current is large, the consumption energy is low. This electrical energy can be applied by a battery or by using a power supply. Once the fuse has been destroyed, the liquid of the microf uidic circuit is propelled along the platform due to the pressure difference between the inlet chamber, which set at high pressure, and the outlet chamber, which is set at atmospheric pressure.

3. Fabrication process

The combination of polymer technology with a PCB is an attractive research f eld that may result in the widespread adoption of integrated MEMS devices. As previously explained, the key of this process consists of using an 18 μm thick copper layer to reach the melting point in the minimum time. The fabrication process is shown in f gure 2. The process starts over a PCB, which is used as a substrate (step (*a*)). The electrical part of the microvalve is def ned using copper etching (step (*b*)). The copper pattern created includes the bonding pads, alignment marks and copper lines. To def ne the structure of the microvalve, two layers of SU-8 are consecutively spin coated (SU-8 2050 formulation, Microchem) with the following spinning conditions: 400 rpm for 10 s followed by 700 rpm for 50 s. A thickness of 300 μm is obtained (step (*c*)). Then the SU-8 is baked for 15 min at 65 °C, and for 1 h 45 min at 95 °C on a hot plate. Once the photoresist is cooled down at room temperature, it is exposed to UV light for 1 min 40 s using an appropriate mask in order to def ne the channel and the chamber of the microvalve (step (*d*)). Then, a post-exposure bake step (PEB) is carried out, baking for 5 min at 65 °C and for 7 min at 95 °C in order to crosslink the SU-8. After that, the wafers are immersed in the SU-8 developer (Microchem.Corp) for 7 min. Finally, the SU-8 is rinsed in IPA (step (*e*)).

The remaining copper is etched away to achieve the desired fuse width (step (*f*)). This process is carried out

J. Micromech. Microeng. **24** (2014) 065013 G Flores *et al*

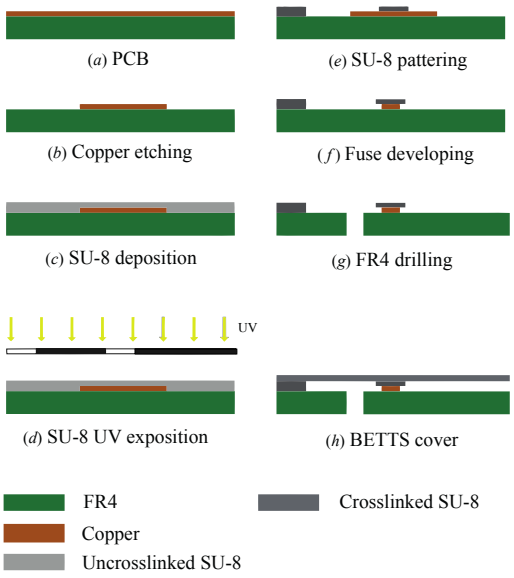

Figure 2. Fabrication process f ow step by step.

through an immersion in an etchant with a proportion of 10% of hydrogen peroxide and hydrochloric acid, and 80% of water. This low concentration improves the control of the wet etching process by carrying out immersions for 5 min and controlling the process by visual inspection. In order to manufacture several fuses in the same process, a range of widths is obtained with this proportion of water.

After that, as can be seen in step (*g*), a 1 mm diameter orif ce is drilled in the center of the inlet chamber through the FR4 to connect an external pressure source. The last step in the fabrication of the microvalve is the transfer of the top cover. The cover bonding process is carried out with BETTS [20]. The chamber and channels are hermetically closed, due to the bonding of SU-8/SU-8 and the high adhesion of SU-8/f lm. A 100 μm layer of polydimethylsiloxane (PDMS) layer is spin coated over a f exible, transparent acetate f lm previously cleaned with acetone. Then the PDMS is baked in a hot plate at 85 $^{\circ}$C for 20 min. Once the PDMS is cured, a 30 μm layer of SU-8 (SU-8 2025 formulation, Microchem Corp) is spin coated with the following spinning conditions: 400 rpm for 10 s followed by 2800 rpm for 50 s. The uncrosslinked SU-8 layer over the f lm is f ipped and placed over the SU-8 microvalve structure and exposed to UV light for 2 min. Then, the PEB is carried out, baking the board for 4 min at 75 $^{\circ}$C to achieve the crosslinking of SU-8. After the PEB process, the device is cooled at room temperature and the acetate with the PDMS is easily peeled off, releasing the SU-8 layer which remains bonded to the structure (step (*h*)). The fabricated microvalve can be seen in f gure 3.

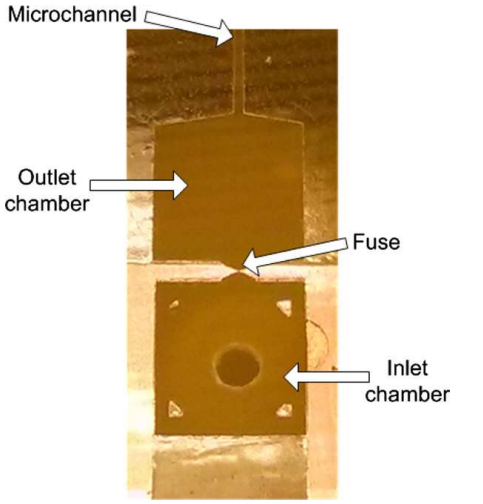

Figure 3. Fabricated microdevice. The main parts of the microvalve can be seen: the inlet chamber with the inlet port, the fuse, the outlet chamber and the microchannel.

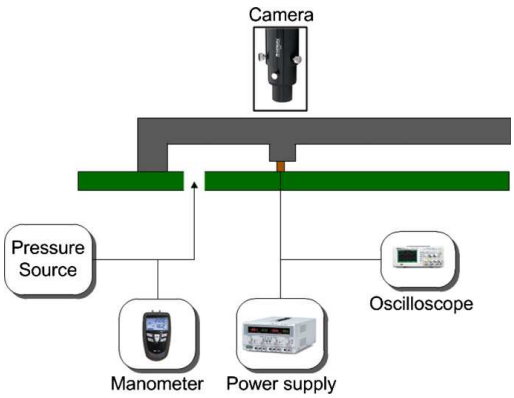

Figure 4. Set up used for performing the experiments. A power supply and a pressure source are used for activation. A camera, an oscilloscope and a manometer for controlling the working out are shown.

4. Experimental results

For evaluation of the experimental results, three different studies have been carried out: electrical phenomena, energy consumption and working out of the whole microvalve. The main purpose was to evaluate them separately in order to be able to better characterize each phenomena.

The experiment set up can be seen in f gure 4. A microscope has been used for recording videos and images of the activation and an oscilloscope for acquiring voltage and current data. A pressure system is needed to be able to drive any f uid through the channel. To evaluate the activation, a commercial power supply has been used to supply the current

J. Micromech. Microeng. **24** (2014) 065013 G Flores *et al*

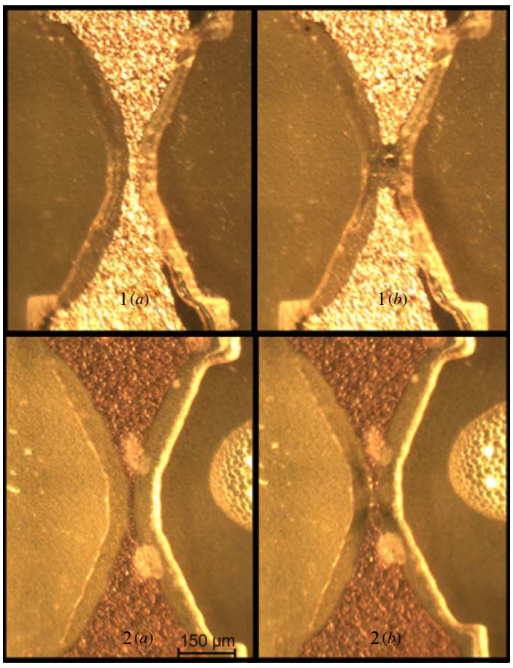

Figure 5. Two microvalves with different widths before ((1*a*) and (2*a*)) and after activation, ((1*b*) and (2*b*)). It is important to emphasize the fuse breakage without destroying the SU-8 and the amount of copper melting depending on fuse width.

necessary for the electrical activation and a pressure source for the pressure system.

The first test was performed to characterize the electrical phenomena. Several microdevices were manufactured and tested, varying their working conditions and design parameters in order to determine their behavior and the activation voltage. In figures 5(1*a*) and (2*a*) two fabricated microfuses with different widths before being activated are shown. Figures 5(1*b*) and (2*b*) shows those microfuses already activated. As can be expected, the wider the fuse is, the bigger the melted copper is. Tests have shown that fuses with less than 50 μm width do not destroy the top cover and the energy consumption is enough to open the microvalve. Fuses with values over 50 μm in width can result in a too-abrasive attack that could break the SU-8 cover of the microvalve.

If several microvalves are manufactured in the same fabrication process, the range of widths that can be obtained depends on the wet etching parameters, as previously commented. In this case, the voltage used to perform the activation is imposed by the highest width of the fabricated fuse. Therefore, this voltage assures the working of the fabricated microvalves.

The characterization of the microdevice is performed from the point of view of the energy consumed. To illustrate this issue, the voltage and the current are measured using an oscilloscope, and it is instantly captured when the fuse is

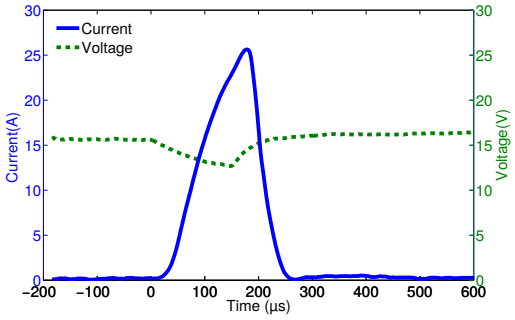

Figure 6. Voltage and current during the electrical working out: voltage at the output of the power supply and current passing through the fuse.

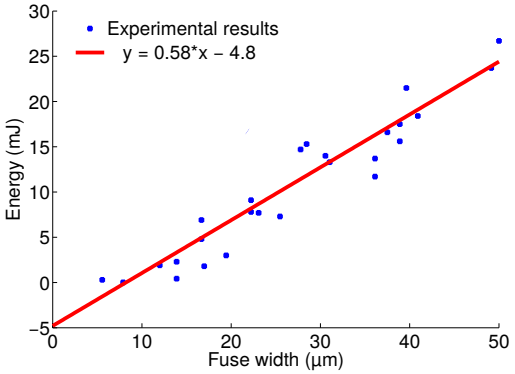

Figure 7. Consumption of energy as a function of the width of the fuse.

open, figure 6. These plots show the moment at which the connection of the supply power is carried out, so the voltage decreases and current increases, until the fuse breaks. Data from the oscilloscope are treated and analyzed to obtain the energy consumed by the microdevice. The energy is calculated by integrating the product of voltage and current in time (1)

$$E(t) = \int V(t)I(t)\,\mathrm{d}t \qquad (1)$$

where $E(t)$, $V(t)$ and $I(t)$ are the energy, voltage and current as a function of the time, respectively.

The rupture time is considered from the beginning of the activation, that is, the instant in which the voltage starts to fall, to the destruction of the fuse in which case the voltage increases. As can be seen in figure 6 the activation time to destroy the fuse is 100 μs. It is important to highlight that this peak of current of 25 A can be achieved with a current voltage supply or by using charged capacitors.

The effect of the width has been studied in different experiments and several energies have been obtained; the results can be seen in figure 7. It is important to comment that energy increases when the fuse width increases. The maximum

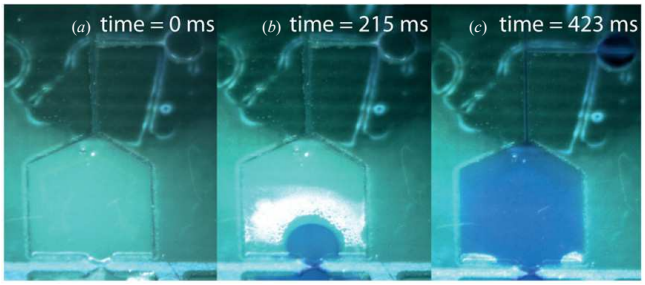

Figure 8. Three different frames of a video showing the liquid flow process. (*a*) Starting time 0 ms: the liquid is located in the inlet chamber. (*b*) Step time 215 ms: the microvalve is already open, the liquid is passing through the fuse to the outlet chamber. (*c*) Step time 423 ms: the outlet chamber and microchannels are filled with liquid.

energy obtained is about 27 mJ. It will be compared with previous reported microvalves in section 5.

Once the electrical phenomena and the energy consumption has been characterized, the complete activation of the microvalve is carried out. The stiffness of the top cover of the microdevice allows the chamber to be pressurized up to 1 bar over the atmospheric pressure. A color liquid is injected through the drilled orifice of the inlet chamber to test the working of the microvalve during activation. Air from the pressure source is injected through the inlet chamber until reaching the desired pressure, in this case 0.1 bar. The value of the selected pressure and the microfluidic circuit will determine the flow rate. It is important to highlight that the pressure in the chamber does not depend on the activation time. However, once the fuse is open, the speed of the liquid through the channel relies on the pressure of the inlet chamber. Three images captured from a video where the whole activation process can be seen are illustrated in figure 8.

In figure 8(*a*), the fuse, outlet chamber and microchannel can be seen. Once the microdevice is activated, the liquid passes through the gap left by the fuse (figure 8(*b*)). Finally, in figure 8(*c*), the liquid fills the outlet chamber and the microchannel. The experimental results show that the liquid is driven through the channel, as expected.

5. Discussion

The microvalve reported in this work has an activation time of about 100 μs and a maximum consumption energy of 27 mJ. These characteristics are compared with other reported microvalves for fluid impulsion, even though some of them are fabricated using different materials and processes. It is important to pay special attention to the comparison with other PCB-based microvalves for integration in microfluidic platforms.

As can be seen in table 1, the order of magnitude of the consumption energy and the activation time of the reported device are the same as reported in [16, 21, 22]. However, these values are much lower than the ones for microvalves based on PCBs for microfluidic applications [11, 18, 19, 23]. In particular, the time is about 10 000 times shorter and the required energy is about 12 times lower. The microvalve of Li [16] has very low energy consumption but higher activation time. Also, this microvalve is more difficult to integrate in PCB platforms. A study of the role that the width of the fuse plays in the consumption of energy has been performed. These experimental results show a nearly linear behavior for a fuse with a thickness of 18 μm and several values of width. The fabrication process of the proposed microvalve is compatible with the fabrication of pressurized SU-8 microchambers [24]. Therefore, if necessary, the inlet chamber could be pressurized to obtain a complete platform that is independent of the external pressure sources. Finally, the proposed microvalve fulfils the requirements of low consumption energy and cost, short time of activation and high integrability in a PCB based microfluidic platform.

6. Conclusions

A single-use and unidirectional microvalve for PCB-based microfluidic platforms has been reported. The activation of the microvalve is related with the destruction of a copper line in the PCB, which works as a fuse. The rest of the device is fabricated using SU-8—integrating it in the microfluidic platform in a monolithic manner. The device is electrically actuated with a maximum consumption of energy of about 27 mJ and an activation time of about 100 μs. These results show a significant improvement because the consumption of energy is about 84% lower and the time response is about four orders of magnitude shorter if compared with similar microvalves for impulsion of fluids on PCB-based platforms. Thanks to these values, the impulsion device proposed in this paper can be considered as a low consumption and rapid response device if compared with other microvalves for impulsion in PCB-based platforms. The fabrication process to build the microvalve comprises standard copper wet etching for PCB fabrication and the typical photolithographic process of an SU-8 resist, avoiding the gold wires used in other PCB-based microvalves. The use of a PCB as substrate makes possible the integration of microfluidic and electronic connections on the same platform. Therefore sensing, actuating or signal processing could be performed

Table 1. Comparison between existing single-use microvalves and the device presented in this paper.

	Pitchaimani [11]	McDonald [21]	Ahn [22]	Li [16]
Activation time (ms)	7000	1000	700	100
Required energy (mJ)	350	150	28	2.5
Fabrication complexity	Medium	Low	Medium	Medium
Integrability	High	High	High	Low
	Aracil [19]	Moreno [23]	Perdigones [18]	This work
Activation time (ms)	2000	2500	1000	0.1
Required energy (mJ)	350	700	188	27
Fabrication complexity	Low	Low	Low	Low
Integrability	High	High	Very high	Very high

on the same substrate if necessary, completing the lab-on-chip platforms where microvalves are integrated. These characteristics make the reported device cost-effective and highly integrable in PCB-based microfluidic platforms.

Acknowledgments

This work was supported by the Spanish Ministry of Science and Innovation (project TEC2011-29045-C04-02, ISILAB).

References

[1] Oh K W and Ahn C H 2006 Topical review: a review of microvalves *J. Micromech. Microeng.* **16** 13

[2] Cardenas-Valencia A M, Dlutowski J, Bumgarner J, Muñoz C, Wang W, Popuri R and Langebrake L 2007 Development of various designs of low-power, MEMS valves for fluidic applications *Sensors Actuators* A **136** 374–84

[3] Li X T and Wang A Q 2012 High-sealing microvalves for PCR *Adv. Mater. Res.* **383** 2025–30

[4] Calvo V, Ezkerra A, Elizalde J, Fernández L J, Berganzo J, Mayora K and Ruano-López JM 2011 A highly integrated vertical SU8 valve for stepwise in-series reactions *J. Micromech. Microeng.* **21** 065037

[5] Luo C, Liu X, Poddar R, Garra J, Gadre A P, Keuren E V, Schneider T, White R, Currie J and Paranjape M 2006 Thermal ablation of pmma for water release using a microheater *J. Micromech. Microeng.* **16** 580

[6] Bu M, Perch-Nielsen I R, Sun Y and Wolff A 2011 A microfluidic control system with re-usable micropump/valve actuator and injection moulded disposable polymer lab-on-a-slide *TRANSDUCERS'11: 16th IEEE Int. Solid-State Sensors, Actuators and Microsystems Conf.* pp 1244–7

[7] Yoo J-C, Moon M-C, Choi Y J, Kang C J and Kim Y-S 2006 A thermopneumatic-actuated polydimethylsiloxane microfluidic system *NEMS'06: 1st IEEE Int. Conf. on Nano/Micro Engineered and Molecular Systems* pp 1379–83

[8] Sánchez-Ferrer A, Fischl T, Stubenrauch M, Albrecht A, Wurmus H, Hoffmann M and Finkelmann H 2011 Liquid-crystalline elastomer microvalve for microfluidics *Adv. Mater.* **23** 4526–30

[9] Merkel T, Graeber M and Pagel L 1999 A new technology for fluidic microsystems based on PCB technology *Sensors Actuators* A **77** 98–105

[10] Gaßmann S, Ibendorf I and Pagel L 2007 Realization of a flow injection analysis in PCB technology *Sensors Actuators* A **133** 231–5

[11] Pitchaimani K, Sapp B C, Winter A, Gispanski A, Nishida T and Fan Z H 2009 Manufacturable plastic microfluidic valves using thermal actuation *Lab Chip* **9** 3082–7

[12] Guerin L J, Dubochet O, Zeberli J-F, Clot P and Renaud P 1998 Miniature one-shot valve *MEMS'98: Proc. 11th Annu. Int. Workshop on Micro Electro Mechanical Systems* pp 425–8

[13] Debray A, Shibata M and Fujita H 2007 A low melting point alloy as a functional material for a one-shot micro-valve *J. Micromech. Microeng.* **17** 1442

[14] Bejhed J, Rangsten P and Köhler J 2007 Demonstration of a single use microsystem valve for high gas pressure applications *J. Micromech. Microeng.* **17** 472

[15] Madou M J and Tierney M J 1994 Micro-electrochemical valves and method *US Patent No* 5368704 A www.google.com/patents/us5368704

[16] Li P-Y, Givrad T K, Holschneider D P, Maarek J-M I and Meng E 2009 A parylene MEMS electrothermal valve *J. Microelectromech. Syst.* **18** 1184–97

[17] Moreno J M and Quero J M 2010 A novel single-use SU-8 microvalve for pressure-driven microfluidic applications *J. Micromech. Microeng.* **20** 015005

[18] Perdigones F, Aracil C, Moreno J M, Luque A and Quero J M 2014 Highly integrable pressurized microvalve for portable SU-8 microfluidic platforms *J. Microelectromech. Syst.* **23** 398–405

[19] Aracil C, Quero J M, Luque A, Moreno J M and Perdigones F 2010 Pneumatic impulsion device for microfluidic systems *Sensors Actuators* A **163** 247–54

[20] Aracil C, Perdigones F, Moreno J M and Quero J M 2010 BETTS: bonding, exposing and transferring technique in SU-8 for microsystems fabrication *J. Micromech. Microeng.* **20** 035008

[21] McDonald J C, Metallo S J and Whitesides G M 2001 Fabrication of a configurable, single-use microfluidic device *Anal. Chem.* **73** 5645–50

[22] Ahn C H, Choi J-W, Beaucage G, Nevin J H, Lee J-B, Puntambekar A and Lee J Y 2004 Disposable smart lab on a chip for point-of-care clinical diagnostics *Proc. IEEE* **92** 154–73

[23] Moreno J M and Quero J M 2010 A novel single-use SU-8 microvalve for pressure-driven microfluidic applications *J. Micromech. Microeng.* **20** 015005

[24] Moreno J M, Perdigones F and Quero J M 2011 Fabrication process of a SU-8 monolithic pressurized microchamber for pressure driven microfluidic applications *CDE'11: Proc. IEEE 8th Spanish Conf. on Electron Devices* pp 1–4

Depressurised reservoirs for portable fluid extraction in SU-8-based microfluidic systems

Carmen Aracil, Francisco Perdigones, J. Miguel Moreno, Antonio Luque, Guadalupe Flores, José Manuel Quero

Departamento de Ingeniería Electrónica, Escuela Superior de Ingenieros, Universidad de Sevilla, Avenida de los Descubrimientos S/N, Sevilla 41092, Spain
E-mail: caracil@gte.esi.us.es

Published in Micro & Nano Letters; Received on 12th August 2014; Revised on 12th September 2014; Accepted on 13th October 2014

A depressurisation method to build SU-8 chambers as pneumatic energy reservoirs is described. The method consists in a combination of injection/extraction of uncrosslinked SU-8 and its exposure in different steps, intended to set the pressure of a chamber below atmospheric. These chambers are intended to be integrated with an actuation system to perform the extraction of fluids from the outside to the inside of a microfluidic SU-8 lab-on-a-chip. This method improves the portability of the platform because external pumps used to impulse the fluids can be avoided.

1. Introduction: The handling of small volumes of fluids is an important issue in the development of lab-on-a-chip (LOC) devices. There are many methods to achieve fluids flow [1]. However, in general, the motion of fluids is generated by external pumps connected to the microfluidic platform, making portable devices not possible because of the size of those pumps. Many micropumps have been reported for fluid impulsion in LOC applications [2], allowing the transport of controlled small volumes of fluids. When pumps are integrated, different methods of activation having been reported [3], they usually have high power consumption and require a large area of the LOC platform [4], which increases the cost and makes integration difficult. Therefore, incorporation of these devices into the market is a hard task [5].

To overcome these problems, the design of devices that include storage of pneumatic energy is proposed. Thanks to this approach, external pumping is not necessary because the system provides portable reservoirs of energy, as for example, in [6–10]. In all these cases, the stored pressure is above atmospheric. However, many LOC devices need the extraction of fluids from an external location to obtain the sample to be analysed. Among others, the methods of extraction are based on the Venturi effect [11–13], piezoelectric effect [14–17] or expanding polydimethylsiloxane (PDMS) composite [18]. In general, these methods provide a good approach to extract small volumes of fluids. However, integration of these devices with SU-8 microfluidic platforms is not easy. The fabrication of the depressurised chambers proposed in this Letter, as energy reservoirs, can be considered a good solution for this purpose.

Previous work has set a simple and inexpensive method of fabrication to construct easily integrable pressurised microchambers for the impulsion in a microfluidic SU-8 platform [19]. However, this method is only valid for design pressures above the atmospheric one. In this Letter, a depressurisation method that allows the fabrication of SU-8 chambers at pressures lower than atmospheric is developed. A prototype has been fabricated using SU-8 on a printed circuit board substrate.

The method reported in this Letter can be easily parallelised to depressurise several chambers at the same level. This is an important issue if taking into account the mass production of devices.

The rest of the Letter is structured as follows. In Section 2, the concept of depressurisation is summarised. Section 3 describes the depressurisation method. In Section 4, the fabrication process is commented upon. In Section 5, experimental results are reported and discussed. Finally, conclusions relating to this research is contained in Section 6.

2. Concept of depressurisation: The concept of depressurisation is based on the relationship between the pressure and the volume of an ideal gas which evolves in a closed chamber, which is as in the following

$$\frac{P_1 V_1}{T_1} = \frac{P_2 V_2}{T_2} \quad (1)$$

where P_1, V_1 and T_1 are the initial pressure, volume and temperature, respectively, and P_2, V_2 and T_2 are the pressure, volume and temperature, respectively, in final conditions. It can be deduced that, at constant temperature, the pressure of a chamber can be fixed controlling its volume. This is the main idea behind the proposed depressurisation system. The pressure of a chamber is set by means of the control of the volume of an auxiliary microfluidic circuit using a syringe pump, Fig. 1.

The whole circuit is initially filled with air, and its volume varies if liquid SU-8 is injected/extracted through the inlet port. The auxiliary microfluidic circuit is composed of an inlet port, an outlet port and a control microchannel. The aim is that the final pressure is

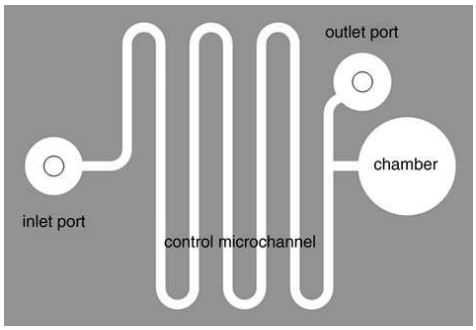

Figure 1 Microfluidic structure for depressurisation of chambers
Parts of the circuit can be seen

below atmospheric, so the final volume must be larger than the initial one. For this purpose, an outlet port is also required to purge the system and allow air to flow out at the right moment. Once the outlet port is blocked, the extraction of the uncrosslinked SU-8 makes the air volume to increase.

The design of the depressurisation method is governed by the following equation

$$P_2(x) = P_1 \frac{V_c}{V_c + hwx} \quad (2)$$

where P_1 is the initial pressure, V_c is the volume of the chamber and h, w and x are the height, width and length of the extracted SU-8 in the control microchannel, respectively, that is, the increment of the volume.

3. Method of depressurisation: Now the concept of depressurisation has been explained, it can be studied in detail. The complete method is summarised in Fig. 2. It consists of filling the microchannel with SU-8 using a syringe pump until the SU-8 goes out through the open outlet port (step (a) in Fig. 2). The aim of this step is to fill the microfluidic system avoiding an increase of air pressure, as it has previously been explained.

Then, in step (b), the SU-8 is crosslinked by UV light in the short microchannel and in the outlet port. It is important that the SU-8 in the control microchannel and in the inlet chamber continue being uncrosslinked. To do so, an appropriate photomask must be used. Once the outlet port has been blocked by crosslinked SU-8 and the microfluidic circuit is completely filled with uncrosslinked SU-8, the initial values of pressure and volume are defined. The initial volume, V_1, is the one in the pressurised chamber and the initial pressure, P_1, is the atmospheric pressure.

The next step, step (c), consists in extracting the liquid SU-8 using the syringe pump again. While SU-8 is being extracted, air expands in the microfluidic circuit and the pressure in the pressurised chamber decreases, as it can be deduced using equation (2). The final pressure in the chamber will be P_2, lower than atmospheric pressure, and the final volume will be V_2 higher than V_1.

Finally, in step (d), the SU-8 in the control microchannel and in the inlet chamber is crosslinked, isolating the pressure chamber at P_2.

4. Fabrication process: The fabrication process of the microfluidic circuit for depressurisation is shown in Fig. 3. The cross-section of this Figure corresponds to section AA′ of Fig. 2.

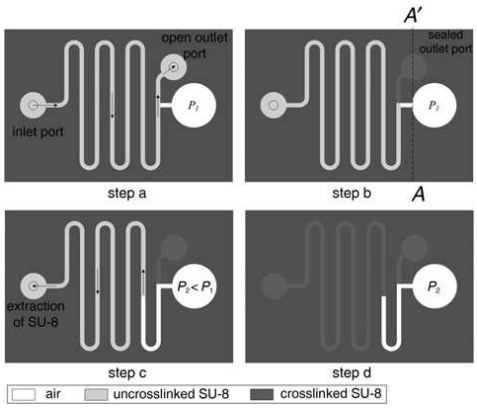

Figure 2 Top view of the microfluidic circuit where the method of depressurisation is summarised in four steps

The process starts by cleaning an FR4 substrate, (step 1). Then, a 25 μm-thick SU-8 2025 layer (Microchem Corp.), with a density of 1.219 g/ml and viscosity of 4500 cSt, is deposited by spin coating to improve the adherence between the SU-8 and the FR4 substrate. After that, the SU-8 is baked for 3 min at 65°C and for 7 min at 95°C on a hotplate and it is exposed to UV light for 60 s. Then, a post-exposure bake step (PEB) is carried out, baking for 2 min at 65°C and for 5 min at 95°C to achieve the crosslinking of the SU-8 layer (step 2).

The next step is the deposition of a 200 wm SU-8 2025 layer over the last deposited layer. Next, the soft-bake of this SU-8 layer is performed by baking for 10 min at 65°C and for 60 min at 95°C. This SU-8 layer is exposed to UV light for 2 min with a mask that defines the microfluidic structure. After that, a PEB step is performed for 5 min at 65°C and for 10 min at 95°C. Later, the developing is performed, this consists in removing the uncrosslinked SU-8 by immersion in Mr 600 Developer (Microchem Corp.) for 4 min and then the SU-8 is rinsed in isopropyl alcohol. The structure of the microfluidic circuit has already been manufactured (step 3).

Once the SU-8 has been cleaned, 0.6 mm diameter orifices are drilled, one of them in the centre of the inlet chamber through the FR4, to connect the syringe pump, and the other corresponding to the outlet port. After that, the structure is cleaned with N_2 to remove the dust because of the drilling. The result of this step can be in seen in Fig. 4, where the outlet port is shown on the left and the pressurised chamber on the right. Finally, an SU-8 2025 (MicroChem Corp.) layer of 50 wm is transferred as the top cover using the BETTS process [20] (step 4).

The next step consists in injecting SU-8 2005 (MicroChem Corp.), with a density of 1.164 g/ml and viscosity of 45 cSt, through the inlet port to the control microchannel. The inlet port is connected to a manometer and a syringe pump that impulses the liquid SU-8 through the control microchannel to the outlet port. When the SU-8 has reached the outlet port, the SU-8 in this port is exposed to UV light during 15 min and baked in order to block the outlet port, (step 5).

In the fabricated prototype, the control microchannel has a length of 11 cm, with a height of 200 wm and a width of 500 wm; the volume of the pressure chamber is 1.5 wl.

5. Results of fabrication: The results of fabrication and pressurisation can be seen in Fig. 5, where the structure before and after depressurisation is shown.

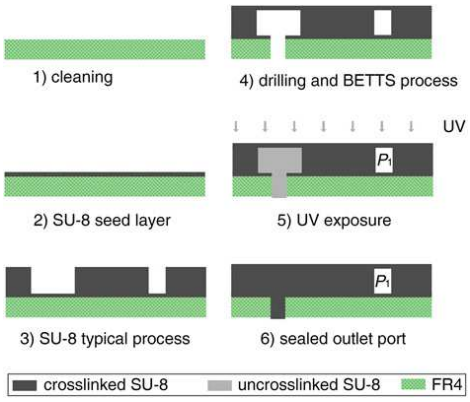

Figure 3 Fabrication process step-by-step to fabricate the depressurised chambers
Cross-section corresponds to section AA′ of Fig. 2

Micro & Nano Letters, 2014, Vol. 9, Iss. 11, pp. 821–824
doi: 10.1049/mnl.2014.0481

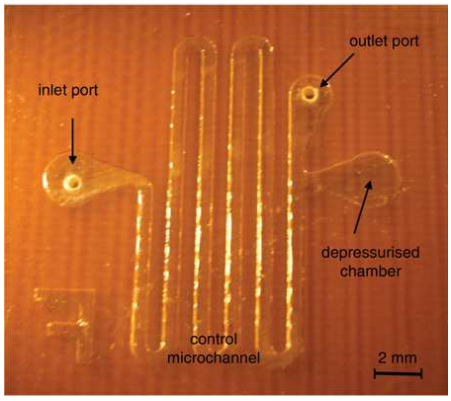

Figure 4 SU-8 microfluidic structure fabricated to perform the depressurisation method
Inlet and outlet ports, the chamber and the control microchannel can be seen Height of the SU-8 walls is 200 µm; the microchannel width is 500 µm and the radius of the outlet chamber is 900 µm and 1200 µm in the case of the depressurised chamber

Although the top cover has to be rigid in a real working device, the depressurised chamber cover has been selected in this case as a thin membrane of about 50 µm, in order to visualise the deformation because of the depressurisation. In this example, the fixed pressure was 500 mbar, lower than atmospheric pressure, demonstrating the validity of this method of depressurisation. The pressure in the chamber is known by an experimental procedure using a manometer. As can be seen from Fig. 6, where the setup is depicted, the syringe pump extracts the liquid SU-8 that is connected by a tube to the manometer. Once the desired pressure is reached in the chamber, the syringe pump is stopped and when the pressure is equal on both sides, the fluid stops. At that moment, the manometer shows the pressure inside the chamber.

The reported method can be multiplexed easily. The parallel depressurisation can be performed using a common inlet chamber, and different control microchannels and pressure chambers. All the pressure chambers are therefore fixed at the same pressure using this method.

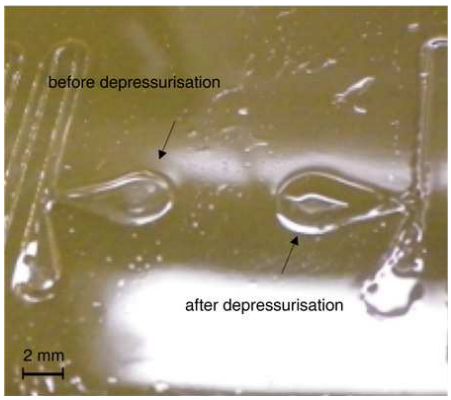

Figure 5 SU-8 chambers at atmospheric pressure before depressurisation on the left and depressurised under atmospheric pressure on the right are shown
As can be seen on the right, the membrane is deflected because of the value of the pressure in the chamber

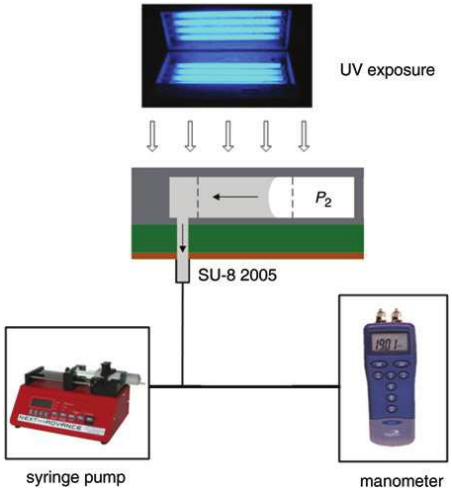

Figure 6 Setup to perform the depressurisation of the chamber
The syringe pump and the manometer are connected to the microfluidic circuit UV light to crosslink liquid SU-8 is depicted

6. Conclusions: The concept, design and procedure of fabrication of depressurised chambers have been reported, their characteristics being fast and inexpensive fabrication, simplicity and robustness. The method is based on the injection/extraction of liquid SU-8 for varying the volume of the system, so that the pressure in the depressurised chamber is set at a desired value. First the system, except the chamber, is filled with liquid SU-8 to block the outlet port. Then, the extraction of the SU-8 implies a controllable decrement of pressure inside the chamber, which is fixed after UV exposure.

The experimental results have shown that depressurisation of the chamber is achieved, and that the chamber is monolithically integrable in SU-8 microfluidic circuits, as a component of a system on charge of the movement of fluids by aspiration. The depressurised chambers are designed to build extraction systems for portable microfluidic SU-8 platforms, for example, a system with microneedles, to aspirate a certain amount of volume after activation. To do so, microvalves can be integrated, which connect the chamber to a working microfluidic circuit. When the valves are activated, aspiration effect occurs in the circuit and a fluid is extracted from outside.

7. Acknowledgment: This work was supported by the Spanish Ministry of Science and Innovation under grant TEC2011-29045-C04-02, ISILAB.

8 References

[1] Lim Y.C., Kouzani A.Z., Duan W.: 'Lab on chip: a component view', Microsyst. Technol., 2010, 16, pp. 1995–2015
[2] Laser D.J., Santiago J.G.: 'A review of micropumps', J. Micromech. Microeng., 2004, 14, pp. R35–R64
[3] Zhang C., Xing D., Li Y.: 'Micropumps, microvalves, and micromixers within PCR microfluidic chips: advances and trends', Biotechnol. Adv., 2007, 25, (5), pp. 483–514
[4] Jeong O.C., Park S.W., Yang S.S., Pak J.J.: 'Fabrication of a peristaltic PDMS micropump', Sens. Actuators A, Phys., 2005, 123–124, pp. 453–458

[5] Lee S.J., Lee S.Y.: 'Micro total analysis system (μTAS) in biotechnology', Appl. Microbiol. Biotechnol., 2004, 64, pp. 289–299
[6] Hong C.-C., Choi J.-W., Ahn C.H.: 'An on-chip air bursting detonator for driving fluids on disposable lab-on-a-chip systems', J Micromech. Microeng., Las Vegas, NV, USA, 2007, 17, pp. 410–417
[7] Hong C.-C., Choi J.-W., Ahn C.H.: 'Disposable air-bursting detonators as an alternative on-chip power source'. 15th IEEE Int. Conf. on Micro Electro Mechanical Systems, Las Vegas, NV, USA, 2002, pp. 240–243
[8] Hong C.-C., Choi J.-W., Ahn C.H.: 'A disposable on chip air detonator for driving fluids on point-of-care systems', Micro Total Anal. Syst., 2002, 17, (2), pp. 949–951
[9] Ahn C.H., Choi J.-W., Beaucage G., ET AL.: 'Disposable smart lab on a chip for point-of care clinical diagnostics', Proc. IEEE, 2004, 92, (1), pp. 154–173
[10] Hong C.-C., Murugesan S., Kim S., Beaucage G., Choi J.-W., Ahn C. H.: 'A functional on-chip pressure generator using solid chemical propellant for disposable lab-on-a-chip', Lab Chip, 2003, 3, pp. 281–286
[11] Perdigones F., Luque A., Quero J.M.: 'PDMS microdevice for precise liquid aspiration in the submicroliter range based on the Venturi effect', Microelectron. Eng., 2010, 87, (11), pp. 2103–2109
[12] Koo K.-I., Jeong M.-J., Park S., Choi H.M., Kim G.-S., Cho D.D.: 'Novel valveless micro suction pump using a solid chemical propellant'. Proc. World Congress on Medical Physics and Biomedical Engineering 2006, COEX, Seoul, Korea, 2007, Vol. 14, pp. 310–313
[13] Chang D.S., Langelier S.M., Burns M.A.: 'An electronic Venturi-based pressure microregulator', Lab Chip, 2007, 7, (12), pp. 1791–1799
[14] Szita N., Buser R.A., Dual J.: 'Aspiration and dispensing of biological liquids in the micro- and submicroliter range with high precision', Biomed. Microdev., 2001, 3, pp. 175–182
[15] Zhang B., Foret F., Rejtar T., Karger L.: 'Parallel sample loading and injection device for multichannel microfluidic devices'. US Patent Number 6,939,452 B2, September 2005
[16] Hodac A., Ingenhoven N., Schmid N.: 'Device and system for dispensing or aspirating/dispensing liquid samples'. US Patent Number 7,055,723 B2, June 2006
[17] Tsuchiya K., Nakanishi N., Uetsuji Y., Nakamachi E.: 'Development of blood extraction system for health monitoring system', Biomed. Microdev., 2005, 7, pp. 347–353
[18] Samel B., Sandstrom N., Griss P., Stemme G.: 'Liquid aspiration and dispensing based on an expanding PDMS composite', J. Microelectromech. Syst., 2008, 17, (5), pp. 1254–1262
[19] Moreno J.M., Perdigones F., Quero J.M.: 'Fabrication process of a SU-8 monolithic pressurized microchamber for pressure driven microfluidic applications'. Proc. 8th Spanish Conf. on Electron Devices. Palma de Mallorca, Spain, 2011, pp. 1–7
[20] Aracil C., Perdigones F., Moreno J.M., Quero J.M.: 'BETTS: bonding, exposing and transferring technique in SU-8 for microsystems fabrication', J. Micromech. Microeng., 2010, 20, p. 035008

Micro & Nano Letters, 2014, Vol. 9, Iss. 11, pp. 821–824
doi: 10.1049/mnl.2014.0481

Microelectronic Engineering 140 (2015) 11–17

Contents lists available at ScienceDirect

Microelectronic Engineering

journal homepage: www.elsevier.com/locate/mee

Pressurization method for controllable impulsion of liquids in microfluidic platforms

G. Flores *, F. Perdigones, C. Aracil, J.M. Quero

Dpto. Ingeniería Electrónica, Universidad de Sevilla, Spain

article info

Article history:
Received 9 January 2015
Received in revised form 14 April 2015
Accepted 22 May 2015
Available online 29 May 2015

Keywords:
Integration
PCB
Impulsion
Microfluidic platform

abstract

In this paper, a pressurization method for manufacturing an independent impulsion system is proposed. The method consists in inserting a deformable material filling a microchamber, leading to its pressurization, which will be on charge of the movement of fluid. The reached pressure involves a wide range of positive values which match well for its application in microfluidic systems, such as Lab on a Chip. It has to be highlighted that the portability of microfluidic platforms is improved due to the fact that the use of external pumps to impulse the fluids can be avoided. So, the paper is focused on the displacement of fluid from one part of the microfluidic circuit to another, with the minimum error, in steady state. The control on the impulsion of liquids only depends on the volume of material which has been inserted. This method is intended to be used with an actuation system, in order to perform the impulsion of fluids in a controllable manner. The permeability of the system has been also studied. The experiments have shown good impermeability during 1 h, time enough to perform the subsequent activation after pressurization. A microfluidic circuit, including the pressurized system, has been implemented for testing and as an example of a certain application.

1. Introduction

The handling of small volumes of fluids is an important issue in the development of Lab on a Chip (LOC) devices. There are many methods to achieve fluid flow [1]. However, in general, the motion of fluids is generated by external pumps connected to the microfluidic platform, making portable devices not possible due to the size of those pumps. Many micropumps have been reported for fluid impulsion in LOC applications [2], allowing the transport of controlled small volume of fluids. Different methods of activation are reported [3], but they usually present high power consumptions and require large areas of the LOC platform [4], increasing the cost and making the integration difficult. Therefore, the incorporation of these devices into the market is a hard task [5].

In order to overcome these problems, one of the strategies found in the state of the art, is the design of devices that incorporate a pneumatic system to store pneumatic energy [6–9]. Thanks to this approach, external pumping is not necessary, since there are provided portable reservoirs that can be integrated in small areas of the chip. The main problem in these cases is related to packaging, since pressure sealing increases drastically its cost [10]. So, an important requirement of our design was low cost fabrication. A convenient solution in order to solve this problem is using PCB as a substrate. Moreover, its versatility for integration with electronics and polymers makes it very beneficial. Many devices have been reported in this field using PCB MEMS technology [11–15].

The starting point of this method was a previous work [16] related to the fabrication of pressurized chambers. It was based on the injection of SU-8 through a long channel connected to a chamber to compress the air in the chamber. The dimensions of the channel and the chamber are calculated to achieve the desired pressure in the chamber. When the desired pressure is reached, the SU-8 is crosslinked blocking the chambers. However, the complex set-up made quite difficult the control of pressure in most cases, a syringe pump is needed with a rough connection to the device to avoid any leakage. So, an important aim is to minimize the required set-up.

In this paper, an improvement of this method is proposed in order to construct chambers at pressures over atmospheric one. If it is compared with the previous work, the current setup does not need syringe pumps, external tubes and pressure sources, avoiding possible leakages of the system. In addition, it reduces significantly the dimension of the microfluidic circuit because the auxiliary circuit for pressurization is reduced. Moreover, the method presented in this paper can be easily parallelized in order to pressurize several chambers at different pressures to move different volumes of fluids. This is an important issue if taking into account the mass-production of devices. An SU-8 general purpose microfluidic circuit is fabricated to demonstrate the working of the proposed method. However, this method does not depend on the fabrication material and process. For testing the working of the system, a SU-8 microfluidic circuit will be performed. Also, a study of the

* Corresponding author.
E-mail address: gflores@zipi.us.es (G. Flores).

http://dx.doi.org/10.1016/j.mee.2015.05.002
0167-9317/

permeability of this pressurization method for SU-8 based microfluidic platform is carried out.

The rest of the paper is structured as follows. In Section 2, the concept of the pressurization is commented. In Section 3, the fabrication process to construct the microfluidic circuit is described. In Section 4, the experimental results are reported and discussed. Finally, the conclusion of this research is commented in Section 5.

2. Pressurization system

The concept of pressurization is based on the Boyle's Law

$$P_1V_1 = P_2V_2 = \text{constant} \quad (1)$$

This expression states that, at constant number of moles and temperature, pressure and volume are inversely proportional. Where P_1 and V_1 are the initial pressure and volume, and P_2 and V_2 are the pressure and volume in final conditions. Boyle's Law explains how the volume of a gas varies with the surrounding pressure.

Applying this concept, the difference of initial volume and final volume brings about a change of pressure. So, the pressure of a chamber can be controlled by means of the change of volume. The impulsion system is based on the use of an auxiliary chamber, where the gas is compressed when a deformable material is inserted. The part of the microfluidic circuit to be pressurized will be connected to the auxiliary chamber through a small microchannel. When the pressure of this chamber is released, by means of an actuator, the impulsed volume is the same than the injected one. Therefore, the proposed system could be completed with a microvalve to activate the system in a controllable manner. This method is designed to be single-use. Even though the advantages of continuous operation devices are wider in general applications, single-use devices provide interesting advantages on biological and chemical applications. These are disposables, low-cost and highly integrable due to the fact that these do not need a cleaning circuit that assures its sterilization. The generic system can be seen in Fig. 1.

The method is summarized in Fig. 2, where a cross view from Fig. 1 is detailed. The initial pressure in the chamber is atmospheric one (P_1) (step a). The procedure consists in inserting a putty-like modeling material as a filler in the auxiliary chamber through the hole of the substrate. In this case we used plasticine, however any material with similar properties can be used. During the process the pressure increases meanwhile the material is being inserted (step b). Finally, the auxiliary chamber is filled in and the final pressure is reached (step c). The microchannel acts as a filter defining the amount of putty injected. As it was commented before, the pressure on the pressurized chambers depends on the volume of those chambers, and the injected material following Eq. (1), where P_1, P_2, V_1 and V_2 are the atmospheric pressure, the final pressure on the pressurized chamber, the initial volume (auxiliary chamber, pressurized chamber, microchannel and hole

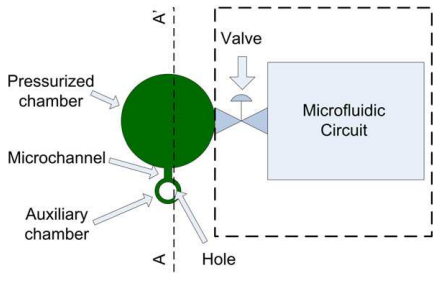

Fig. 1. Microfluidic structure. The parts of the microfluidic structure can be seen.

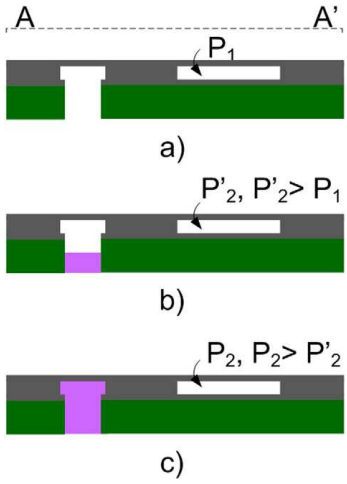

Fig. 2. Pressurization method, step by step, from the cross view AA' of Fig. 1.

substrate) and pressurized chamber volume, respectively. The theoretical inserted volume V_{ha} is the sum of the volumes of hole substrate and the auxiliary chamber, that will be the impulsed volume after the activation.

Therefore, the design parameters are the diameter of the hole, the substrate thickness and the chamber dimensions because the volume of the microchannel is designed to be negligible if compared with V_{ha}. Finally, the expressions of V_{ha} and P_2 can be written as a function of the chambers and hole dimensions as follows:

$$V_{ha} = \frac{\pi D^2 H_{substrate}}{4} + V_{aux} \quad (2)$$

$$P_2 = P_1 \frac{V_1}{V_2} = P_1 \frac{V_{ha} + V_{pc}}{V_{pc}} \quad (3)$$

where D is the diameter of the substrate hole, $H_{substrate}$ is the substrate thickness, V_{aux} is the auxiliary chamber volume and V_{pc} is the pressurized chamber one. The volume of the microchannel has been neglected.

The ratio (inserted volume/total volume) has to be less than one because the inserted one has to be always smaller than the volume of the circuit. Otherwise, the samples would be transported out the device. The inserted volume has to be designed as a function of the volume to be moved, in order to transport the samples towards the desired place in the device. Therefore, this ratio depends on the designer.

The minimum inserted volume depends on the machining of the substrate, that is, on the diameter of the drilling tool used to perform the hole through a PCB substrate of 1.5 mm. The diameter has to be large enough to insert the filler material manually filling the chamber and to avoid the tool breaking. In our case, the minimum drilling tool has a diameter of 600 μm, to fulfill these issues. Therefore, the minimum volume is 0.42 μL, if the volume of the auxiliary chamber is reduced to zero.

Regarding the minimum pressure, it has to be enough to move the samples, that is, higher than the one due to the friction with the walls. In the proposed approach, the sample is colored water and the material is SU-8. The friction on the circuit can be considered negligible due to the hydrophobic nature of the SU-8.

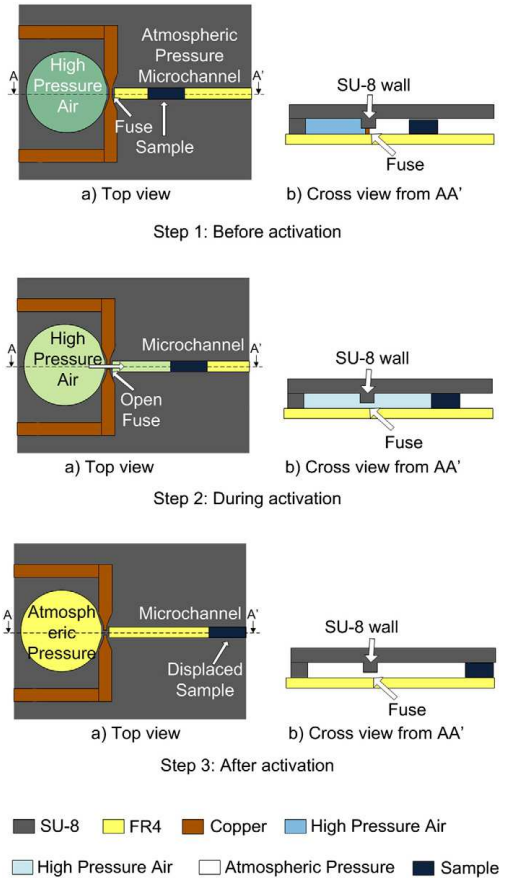

Fig. 3. Working of the microvalve.

The design is based in the steady state of the system. However, some transient parameters could be necessary if the application requires. The temporal parameters, as the velocity, can be obtained with simulations, for example with Simulink, as reported in [17]. A similar Simulink model has been used to simulate the dynamic behavior of this impulsion, where the average velocity is 41 mm/s and the time response is about 400 ms.

The method can be readily integrable with thermo-mechanical microvalves [18–22] to achieve a portable pneumatic system. In that way, the storage of air is easily undertaken in a controlled manner. In this paper, the PCBMEMS-based microvalve reported in [18] is chosen. The working of the microvalved is based on a fuse. A thin layer of copper is melted, releasing the air compressed in a chamber, as can be seen in Fig. 3. A simple microfluidic circuit is also included. It is composed by a microchannel with a sample, an inlet port to introduce the sample, two purge chambers and an outlet port. However, its application is not limited to this example. The complete system to be manufactured can be seen in Fig. 4.

3. Fabrication process

For proving the pressurized method, a complete system has been implemented. The fabrication process is shown in Fig. 5, from the cross view AA' of Fig. 1. It starts from the manufactured microvalve, (step a). Then, a 5 μm of SU-8 2005 (Microchem Corp.) is deposited by spin coating in order to improve the adherence between the SU-8 and the FR4 substrate (step b). After that, the SU-8 is baked for 5 min at 65 °C and for 15 min at 95 °C in a hotplate and it is exposed to UV light for 40 s (step c). Then, a post exposure bake step (PEB) is carried out, baking for 2 min at 65 °C and for 3 min at 95 °C in order to achieve the crosslinking of the SU-8 layer. The next step, (step d) is the deposition of a 300 μm SU-8 layer over the last deposited layer. Then, the softbake of this SU-8 layer is performed baking for 5 min at 65 °C and for 120 min at 95 °C. This SU-8 layer is exposed to UV light for 2 min with a mask that defines the microfluidic structure (step e). After that, a PEB step is performed for 3 min at 65 °C and for 5 min at 95 °C.

Then, the developing is performed. It consists in removing the uncrosslinked resist by immersion in Mr 600 Developer (Microchem Corp.) for 5 min and then, the SU-8 is carefully rinsed in isopropyl alcohol (IPA) (step f). Once the structure has been cleaned, the substrate is drilled through the FR4. The corresponding hole for the auxiliary chamber with a diameter D, and the rest of the orifices are drilled to perform the outlet

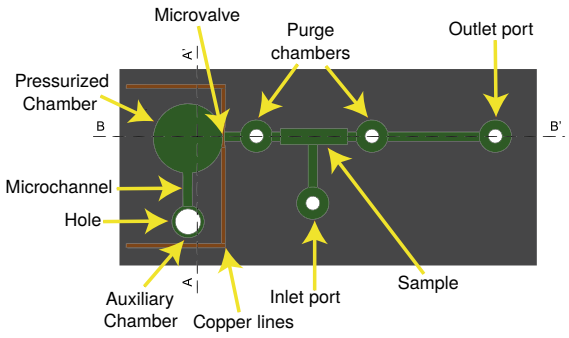

Fig. 4. Complete system composed by a pressurized chamber, the auxiliary chamber, the selected microvalve and microfluidic circuit for testing.

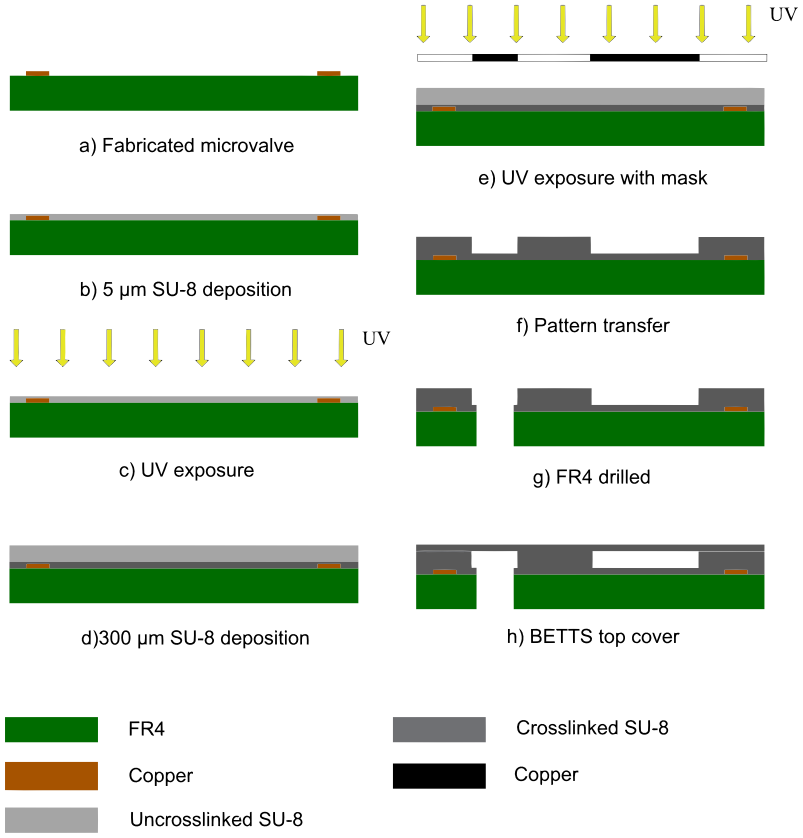

Fig. 5. Fabrication process step by step to fabricate the general purpose microfluidic circuit.

and inlet ports with a diameter of 800 μm (step g). After that, the structure is cleaned with N_2 in order to remove the dust due to the drilling. Then, a 50 μm layer (SU-8 2025) is transferred as top cover by BETTS process [23], (step h) where the acetate used in this process is not removed.

The results of fabrication can be seen in Fig. 6 where the inlet and outlet ports, and the chambers are shown. The sample is already inserted in the center of the microchannel and the pressurization is already done.

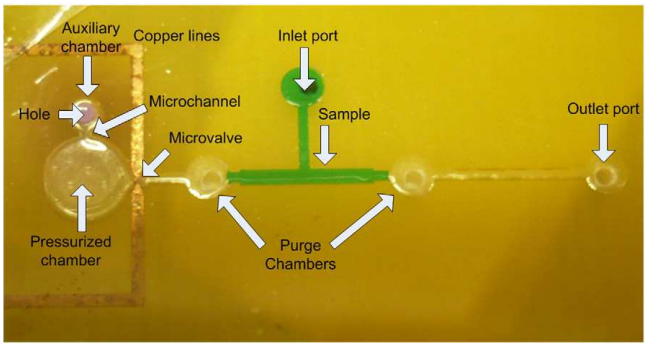

Fig. 6. General purpose microfluidic circuit for impulsion. It can be seen, that the sample that will be used in the operation is already inserted in the center of the microchannel.

Table 1
Theoretical impulsion parameters.

Experiment	Hole diameter (μm)	Aux. chamber volume (μL)	Theoretical volume (μL)
A	600	0.46	0.88
B	800	0.60	1.35
C	1500	1.25	3.90

4. Results and discussion

4.1. Impulsion results

An electronic circuit is connected to the microvalve to activate it and release the stored air. After activation, when the pressure return to atmospheric pressure, the volume which leaves the pressurized chamber is the same than the one injected through the drilled hole of the auxiliary chamber. It is important to highlight that after impulsion, the behavior of the plasticine was correct, and there is not any change in the material.

The impulsed volume can be easily measured with the microscope and P_2 will be deducted by Eq. (1) using the experimental impulsed volume. This pressure is not measured by a sensor, in this case, since the value of the total volume will be modified by the sensor volume. This change of volume implies that the pressure reached would not be the same than in the original system. Because of that the pressure P_2 is deduced.

In this section, the validity of the method is demonstrated for several impulsions. Once the method of pressurization is experimentally checked, a study of the permeability of the fabricated chambers is performed.

The volume of the sample to impulse is 0.68 μL in case A and 1.35 μL in cases B and C. The theoretical calculated impulsion parameters can be seen in Table 1. The microchannel volume, 0.02 μL, has not been considered in the calculated parameters, as previously said in Section 2, because it is negligible in comparison with the impulsed volume. The percentage of extra volume added would be 2.55% 1.66% and 0.5753% in cases A, B, and C respectively. The total volume for the experiments is 10.41 μL in case A, 13.58 μL in case B and 18.5 μL in case C. The ratio between the inserted volume and the total volume of the system is 8.4% 9.94% and 21.08% for the three cases respectively. However, as previously said, these parameters depend on the design of the circuit, and do not affect the pressurization.

The results of the experiments can be seen in Fig. 7 for the impulsions described in Table 1. Fig. 7-A1 corresponds to the circuit before impulsion, and Fig. 7-A2 is the same circuit after a theoretical impulsion of 0.88 μL. In this case, the experimental impulsed volume is 0.91 μL, and therefore the error in this impulsion is 3.4% Fig. 7-B1 and Fig. 7-B2 correspond to the circuit before and after a theoretical impulsion of 1.35 μL, respectively. The experimental impulsed volume is 1.4 μL, and the error is 3.7% Finally, Fig. 7-C1 and Fig. 7-C2 correspond to the circuit before and after a theoretical impulsion of 3.9 μL. The experimental impulsed volume is 4.3 μL, and the error is 10.3% These results are summarized in Table 2. The errors are due to tolerances of the fabrication process. The highest tolerance is due to the drilling, i.e., the higher diameter of the hole implies the higher value of tolerance.

Taking into account that the volume of pressurized chamber is 3.77 μL, the values of pressures obtained from the measured volume are 0.02 MPa, 0.04 MPa and 0.11 MPa for experiments A, B and C, respectively. These values of pressure only affect to the dynamic behavior of the system. The velocity of the fluid depends on the pressure, that is, the higher the values of the stored pressure, the higher the values of velocity. However, the impulsed volume is independent of that pressure; it depends only on the volume of the injected material in both, the auxiliary chamber and the drilled hole. Therefore, the impulsed volume of air which pushes the liquid sample has the same steady state independent of the pressure for a fixed volume.

The required volume in many microfluidic applications involves microliter range. For these values the proposed system is designed. However, if a larger value is required, different strategies can be

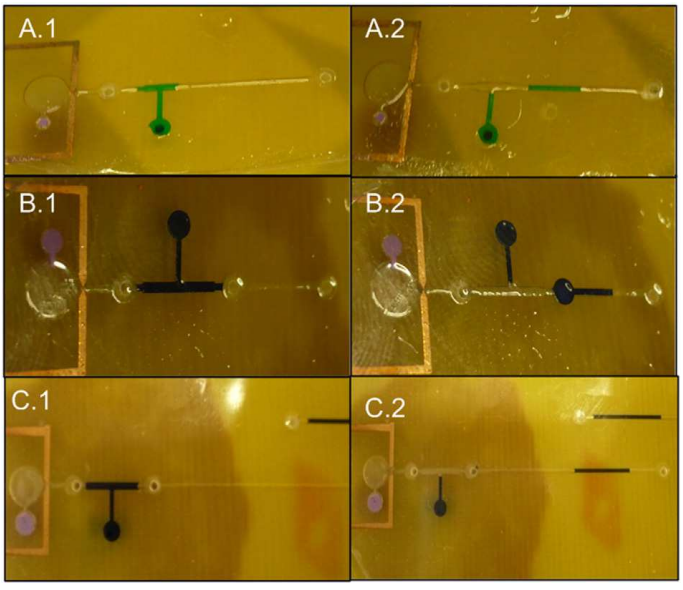

Fig. 7. Experimental results for three different impulsions.

Table 2
Comparison of the values obtained experimentally with the theoretical.

Experiment	Theoretical volume (μL)	Experimental volume (μL)	Error (%)
A	0.88	0.91	3.4
B	1.35	1.4	3.7
C	3.90	4.30	10.3

performed. One possible approach is to enlarge the auxiliary chamber diameter. Other strategy consists on designing several systems (chamber–microvalve) in series, that is, the impulsions performed sequentially, and finally a combination of both them.

4.2. Permeability results

Polymers are several orders of magnitude more permeable to gas leakage than other materials like glass or metals. However, the epoxy resins are characterized by low gas permeability and therefore can be used for package sealing [24–26]. A study of the permeability of the pressurized chamber is performed due to the porosity of the polymers is important especially in the long-term. The aim is to secure that there are not leakages large enough to reduce the pressure in the operation time.

Taking into account that the impulsion system is only composed of SU-8 chambers, the study of permeability inside these chambers is just required. However, the method is designed to be integrable with other components so it is also carried out in the study of the permeability of the complete system. Then, there are two different experiments, the first one studies the permeability of the chamber with no microvalve, and the second one studies the complete system chamber–microvalve.

In this section, the measurement of pressure inside the chamber is carried out by the pressure sensor (40PC015G1A from Honeywell) because it is necessary to monitor its value along the time. The target is to validate that the pressure keeps stable enough to perform the impulsion. The results are plotted in Fig. 8.

As can be seen, there are two plots; each plot corresponds to a pair of experiments with microvalve and without microvalve for a particular pressure. In this case 200 mbar and 120 mbar have been used. The leakages of the complete system, chamber–microvalve, are considerably higher than the ones with no microvalve. However, the decrease of pressure in the first case lies from 185 to 180 mbar for 1 h, that is, 2.7% In the second case, for 120 mbar, the pressure decreases to 117 mbar, 2.5%in 1 h. For both cases, there are leakages but they are low enough to perform the activation after pressurization. Even 1 h later, the variation in the measured pressure is approximately 2.5% This range of time is enough to perform the activation after pressurization, since the method is designed to be carried out when the system is going to be activated. All the same, the top cover of the device could be fabricated thicker, in order to improve the permeability, or a thin film of aluminum can be deposited over the top cover [27]. These solutions do not affect significantly the permeability in this case because the main leakage is due to the thin wall of the SU-8 microvalve.

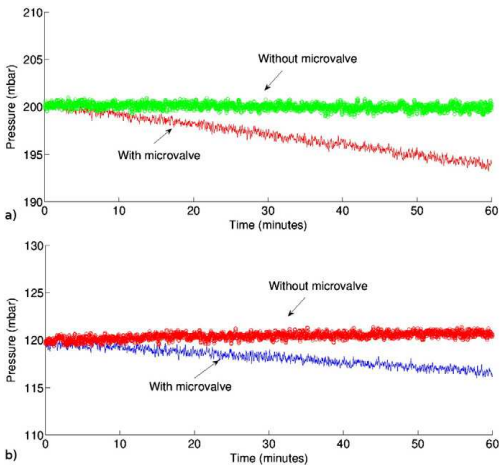

Fig. 8. Permeability experiments. Pressure as a function of the time for chambers with and without microvalve.

It is important to highlight that this method is independent of the selected microvalve and the manufactured materials. A study of permeability to characterize the operation time is convenient if different materials and designs are used.

5. Conclusion

A pressurization method to fabricate an impulsion system, as a component of a microfluidic platform has been designed, fabricated, and tested in the laboratory. It consists in inserting a certain volume of material through a hole, filling a chamber and using a narrow microchannel as a stop of filling. The injected volume in the chamber is the same than the one to be impulsed on the circuit. Then, the stored volume can be released using, for example, a microvalve. The experimental results showed a good control on the impulsed volume of liquids with errors of about 3% Also, the studies of permeability prove the low permeability of the chamber, being the main leakages through the selected microvalve. However, in this case, these leakages are low enough to impulse the liquids after the pressurization step. Assuming the maximum operation time between activation and impulsion could be 1 h, an error of about 2.5%on the stored pressure could be expected. In addition, the area of the wafer used for pressurizing is a low percentage of the whole microfluidic circuit area. The proposed impulsion system is manufactured in SU-8, which is a material for rapid prototyping, but other materials of industrial production can be used, for example plastic injection. In this case, it is not necessary to use a putty for the pressurization, the same plastic injection could be used to insert the material for pressurization. Finally, the proposed pressurization method does not depend on the microfluidic structure material, and therefore it can be integrated on platforms fabricated using different materials or fabrication technologies.

Acknowledgment

This work was supported by the Spanish Ministry of Science and Innovation under grant TEC2011-29045-C04-02, ISILAB.

References

[1] Y.C. Lim, A.Z. Kouzani, W. Duan, Lab-on-a-chip: a component view, Microsyst. Technol. 16 (2010) 1995–2015.
[2] D.J. Laser, J.G. Santiago, A review of micropumps, J. Micromech. Microeng. 14 (2004) R35.
[3] Chunsun Zhang, Da Xing, Yuyuan Li, Micropumps, microvalves, and micromixers within PCR microfluidic chips: advances and trends, Biotechnol. Adv. 25 (5) (2007) 483–514.
[4] Ok Chan Jeong, Sin Wook Park, Sang Sik Yang, James Jungho Pak, Fabrication of a peristaltic PDMS micropump, Sensors Actuators A Phys. 123–124 (2005) 453–458.
[5] S.J. Lee, S.Y. Lee, Micro total analysis system (μ-TAS) in biotechnology, Appl. Microbiol. Biotechnol. 64 (2004) 289–299.
[6] Chien-Chong Hong, Jin-Woo Choi, Chong H. Ahn, An on-chip air-bursting detonator for driving fluids on disposable lab-on-a-chip systems, J. Micromech. Microeng. 17 (2007) 410–417.
[7] C.H. Ahn, Jin-Woo Choi, G. Beaucage, J.H. Nevin, Jeong-Bong Lee, A. Puntambekar, J.Y. Lee, Disposable smart lab on a chip for point-of-care clinical diagnostics, Proc. IEEE 92 (1) (2004) 154–173.

[8] Changlin Pang, Yu-Chong Tai, Joel W. Burdick, Richard A. Andersen, Electrolysis-based diaphragm actuators, Nanotechnology 17 (4) (2006) S64.
[9] Niclas Roxhed, Susanna Rydholm, Björn Samel, Wouter van der Wijngaart, Patrick Griss, Göran Stemme, A compact, low-cost microliter-range liquid dispenser based on expandable microspheres, J. Micromech. Microeng. 16 (12) (2006) 2740.
[10] Yong-Kook Kim, Eun-Kyung Kim, Soo-Won Kim, Byeong-Kwon Ju, Low temperature epoxy bonding for wafer level MEMS packaging, Sensors Actuators A Phys. 143 (2) (2008) 323–328.
[11] Tobias Merkel, Michael Graeber, Lienhard Pagel, A new technology for fluidic microsystems based on PCB technology, Sensors Actuators A Phys. 77 (2) (1999) 98–105.
[12] Stefan Gaßmann, Ingo Ibendorf, Lienhard Pagel, Realization of a flow injection analysis in PCB technology, Sensors Actuators A Phys. 133 (1) (2007) 231–235.
[13] Konstatinos Kontakis, Anastasios Petropoulos, Grigoris Kaltsas, Thanassis Speliotis, Evangelos Gogolides, A novel microfluidic integration technology for PCB-based devices: application to microflow sensing, Microelectron. Eng. 86 (4) (2009) 1382–1384.
[14] Anastasios Petropoulos, Dimitris N. Pagonis, Grigoris Kaltsas, Flexible PCB-MEMS flow sensor, Procedia Eng. 47 (2012) 236–239.
[15] D.N. Pagonis, A. Petropoulos, G. Kaltsas, A pumping actuator implemented on a PCB substrate by employing water electrolysis, Microelectron. Eng. 95 (2012) 65–70.
[16] JM. Moreno, F. Perdigones, J.M. Quero, Fabrication process of a SU-8 monolithic pressurized microchamber for pressure driven microfluidic applications, Electron Devices (CDE), 2011 Spanish Conference on feb. 2011, pp. 1–4.
[17] C. Aracil, F. Perdigones, J.M. Moreno, A. Luque, J.M. Quero, Portable lab-on-pcb platform for autonomous micromixing, Microelectron. Eng. 131 (2015) 13–18.
[18] G. Flores, C. Aracil, F. Perdigones, J.M. Quero, Low consumption single-use microvalve for microfluidic PCB-based platforms, J. Micromech. Microeng. 24 (6) (2014) 065013.
[19] J.M. Moreno, C. Aracil, J.M. Quero, High-integrated microvalve for lab-on-chip biomedical applications, Biomedical Circuits and Systems Conference, 2008. BioCAS 2008. IEEE Nov. 2008, pp. 313–316.
[20] J.M. Moreno, J.M. Quero, A novel single-use SU-8 microvalve for pressure-driven microfluidic applications, J. Micromech. Microeng. 20 (2010) 015005.
[21] Carmen Aracil, José M. Quero, Antonio Luque, J. Miguel Moreno, Francisco Perdigones, Pneumatic impulsion device for microfluidic systems, Sensors Actuators A Phys. 163 (1) (2010) 247–254.
[22] A.M. Cardenas-Valencia, J. Dlutowski, J. Bumgarner, C. Munoz, W. Wang, R. Popuri, L. Langebrake, Development of various designs of low-power, MEMS valves for fluidic applications, Sensors Actuators A Phys. 136 (1) (2007) 374–384 (25th Anniversary of Sensors and Actuators A: Physical).
[23] Carmen Aracil, Francisco Perdigones, J.M. Moreno, J.M. Quero, BETTS: bonding, exposing and transferring technique in SU-8 for microsystems fabrication, J. Micromech. Microeng. 20 (2010) 035008.
[24] Gonzalo Murillo, Zachary J. Davis, Stephan Keller, Gabriel Abadal, Jordi Agusti, Alberto Cagliani, Nadine Noeth, Anja Boisen, Nuria Barniol, Novel SU-8 based vacuum wafer-level packaging for MEMS devices, Microelectron. Eng. 87 (5–8) (2010) 1173–1176.
[25] A. Gerlach, W. Keller, J. Schulz, K. Schumacher, Gas permeability of adhesives and their application for hermetic packaging of microcomponents, Microsyst. Technol. 7 (2001) 17–22.
[26] Cheng Pang, Zhan Zhao, Lidong Du, Zhen Fang, Adhesive bonding with SU-8 in a vacuum for capacitive pressure sensors, Sensors Actuators A Phys. 147 (2) (2008) 672–676.
[27] H.S. Ko, C.W. Liu, C. Gau, Micropressure sensor fabrication without problem of stiction for a wider range of measurement, Sensors Actuators A Phys. 138 (1) (2007) 261–267.

Pressurized Microvalve with SMD-Based Activation to Drive Fluid in Low-Cost and Autonomous MEMS

G. Flores, F. Perdigones, J.M. Quero
Dept. of Electronic Engineering, Universidad of Seville
Sevilla, Spain
gflores@gte.esi.us.es

***Abstract*— This paper reports an inexpensive and simple method to impulse fluid in PCB-based Lab on a Chip (LOC) MEMS devices. This method consists on using pressurized SU-8 chambers, with membranes as cover. The membrane is burst thank to the increase of pressure in the chamber due to the increase of temperature, at constant volume. The increase of temperature is achieved supplying voltage to a Surface-Mounted-Device (SMD) resistor. This method is intended for fabricating autonomous and inexpensive LOC devices.**

Keywords*— *Microfluidics, LOC, SU-8, MEMS

I. INTRODUCTION

Lab on Chip devices have been gained momentum during the last two decades [1]. The development of devices fabrication has rapidly increased. High costs and restrictions in silicon processing have driven interest in alternative technologies focused on MEMS offering inexpensive and simple fabrication processes, such as polymers. Many spin-coated amorphous polymers such as polyimides, benzocyclobutene (BCB), parylene, and photoresists [2] have been investigated as intermediate layers for wafer bonding. One of these polymers is the negative photoresist SU-8 [3]. It is a highly crosslinked epoxy-type photo-patternable polymer. These properties and his low cost, make SU-8 a very suitable material for building rigid mechanical structures for various applications. Despite this advancement, there are numerous drawbacks that need to be addressed to achieve a completely autonomous and portable LOC. Consequently, different techniques have been proposed to package LOC devices [4-6] to address issues like liquid leakage or pressure for wide range of applications and especially in the biomedical field [6]. There is an approach to overcome these issues [7]. The method proposed here allows an easy integration between electronic and microfluidics in the same platform includes an inexpensive pressurization system, and it is driven using a different working principle than reported in [7]. In spite of most valves are propel by mechanical process, there are other ways of impulsion such as thermal. The proposed system is activated using both, mechanical and thermal effects. Previously, a pressurized microchamber is fabricated to be finally broken out using a SMD resistor that is embedded in the substrate.

II. WORKING PRINCIPLE

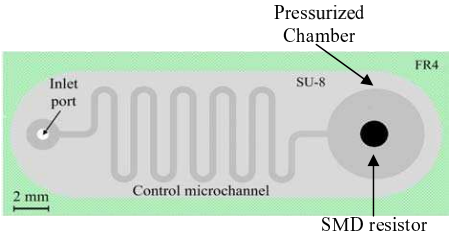

Fig.1 Top view of the proposed design

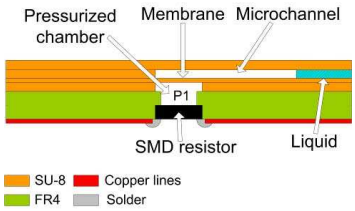

Fig.2 Cross view of the proposed design

The proposed design is shown in Fig 1 and Fig. 2. The system consists in an inlet port, a control microchannel, a chamber to store the pneumatic energy and a SMD resistor. The microvalve is activated by means of two simultaneous and different phenomena: thermal and mechanical. Firstly, air volume trapped inside the channel at atmospheric pressure is pushed by low viscous SU-8. Consequently, it increases the air pressure in the chamber, following Boyle-Mariotte Law:

$$P_1 V_1 \quad P_2 V_2 \tag{1}$$

where P1 and V1 are the fluid atmospheric pressure and volume, respectively ; and P2 and V2 are the same properties

after pressurization and before actuation. P2 is set to be higher than the pressure which breaks the membrane (P0). Once the chamber has already been pressurized, the microvalved is activated by thermal phenomenon, following Charles-Gay Lussac law:

$$\frac{P_2}{T_2} = \frac{P_3}{T_3} \tag{2}$$

where T2 is the room temperature and T3 will be the necessary temperature reached by the SMD to break the membrane. The pressure P3 is the pressure that breaks the membrane: P3 = P0. The voltage to be applied is obtained using the characteristics curve of SMD resistor which relates the applied voltage to the resistor and its superficial temperature, Fig.3.

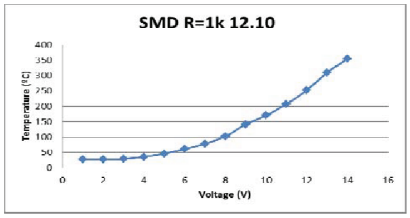

Fig.3 SMD temperature as a function of the applied voltage

III. FABRICATION PROCESS

The fabrication process is illustrated in Fig. 4. A single Printed Circuit Board (PCB) is selected as a substrate due to its low cost and good adherence with SU-8 [3], (step a). Fabrication starts by pattering the copper layer using standard photolithography process typically used in printed circuit electronics (step b). After copper removal, SU-8 is going to be deposited on the back side of the single PCB. In order to assure adherence with the FR4, this will be carried out in three steps. Firstly, a 33 µm-thick SU-8 layer (Microchem Corp. 2025 formulation) is deposited. After this, the SU-8 is baked for 2 min at 65 ºC and for 5 min at 95ºC in a hotplate. Once the resist is cooled down at room temperature, it is exposed to UV light for 1 min 40 s. Then, a post-exposure bake step is carried out, baking the board for 2 min at 65 ºC and for 3 min at 95 ºC in order to cross-link the SU-8 (step c). The next step is the deposition of a 200 µm SU-8 layer over the board. This is going to be done in two layers of 100 µm. Firstly, one layer of 100 µm deposited and baked for 3 min at 65º and for 9 min at 95º. Secondly, 100µm layers is deposited and baked for 3 min at 65 ºC and for 30 min at 95 ºC. Finally, SU-8 is then exposed to UV light for 2 min with a mask that defines the device layout, and a post-exposure back of 2 min at 65º and 5 min at 95º, as previosly (step d). After a relaxation step of 10 min at room temperature, the following stage is to immerse the board with the polymerized resist in the SU-8 developer, mr 600 Developer (Microchem Corp) for 4 min. Then, the patterned SU-8 is carefully rinsed in isopropyl alcohol (IPA) to clean the inlet port, the control microchannel and the pressure chamber (step e).

Once the structure is done, 0.8 mm and 2mm diameter orifices are drilled, the first one is located in the center of the inlet port through the FR4 to connect an external pressure source and a the second orifice is located in the center of the chamber to connect the chamber with the SMD resistor (step f). Now, the device is covered by a 33 µm SU-8 layer using BETTS [8] technique. The thickness of the SU-8 layer over the acetate is selected to avoid undesirable displacements into the cavities of the resist in contact with the device walls, and specifically to prevent the control microchannel from obstruction. The cover bonding process is carried out in the absence of pressure applied over the acetate, and the SU-8 diffuses uniformly on the structure walls, ensuring the device enclosure and preventing possible pressure leakages in the chamber. The bonding is carried out by means of an UV exposure step of 3 min over the whole device and 4 min in a hot plate at 75ºC, achieving the bonding between both SU-8 resists (step g). The next step is to join the SMD resistor by soldering it to the PCB. Moreover, it is trapped with glue to avoid leakages (step h).

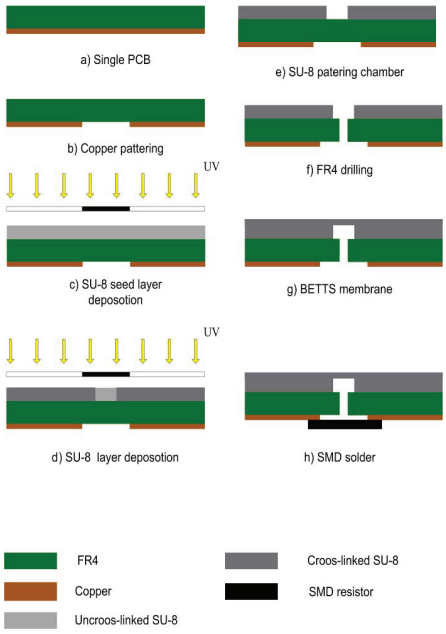

Fig.4. Fabrication process.

IV. IMPULSION METHOD

Fig.5 Final device without activating

When the system has already been built, Fig. 5, the activation of the microvalve is carried out by means of the two physical phenomenons, as explain above, (1) and (2). A mechanical activation is achieved by injecting SU-8 (2005 formulation) through the inlet port to the control microchannel Fig. 6. The inlet port is externally connected to a pressure gauge through a tube previously full of SU-8. The SU-8 2005 is chosen as the impulsion liquid due to its low viscosity, making easier the control flow from the tube through the microchannel. When the desired pressure is achieved inside the device according to the pressure gauge calculation mentioned in (1), the syringe pump is fixed and the board is exposed to UV light for 10 min. This process is made in controlled steps of 5 min in order to avoid an appreciable increment of the chamber temperature which would produce an undesired pressure increment and the uncontrolled breakages of the membrane as a result. After the UV exposure step, with the SU-8 cross-linked, the chamber has already been pressurized. Now, the thermal system will be the responsible for the breakage of the membrane. The SMD resistor is connected to a power supply and the temperature of the SMD will be increased following Ohm's Law. Consequently, the necessary chamber temperature will be increased to reach P0, the pressure needed to break the membrane.

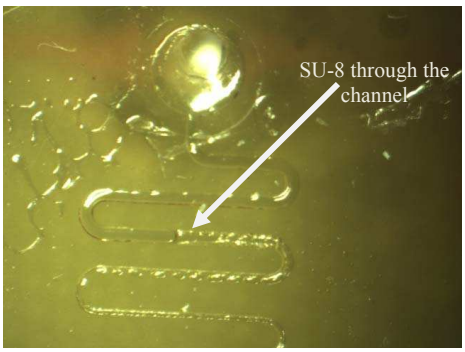

Fig .6. SU-8 through the channel

V. EXPERIMENTAL RESULTS

Several experiments demonstrate the validity of the proposed method. The membrane fabricated has a radius of 1500 µm and a thickness of about 40 µm, channels have a width of 450µm, length of 11.79 cm. The complete system has a high of 200 µm. SMD resistor is CRCW1210 Vishay. P2 was set to 2300 mbar and P1 was set to 650 mbar over atmospheric pressure, T1 is 298 K (25ºC) and atmospheric pressure is about 1000 mbar. Therefore, T2 is 596K (323ºC). This temperature corresponds to a voltage of 60 V. It is important to highlight that every calculation has been done taking into account no to reach the breakage pressure of the membrane. Fig. 7 shows a microvalve that has already been activated. In Table I, the results of several experiments are shown.

Table I. Experimental results for several broken microvalves

	Experiment 1	Experiment 2	Experiment 3	Experiment 4
Pressure	660 mbar	630 mbar	760 mbar	761 mbar
Voltage	64 V	64 V	64 V	64 V
Time	6 s	6 s	5 s	5 s

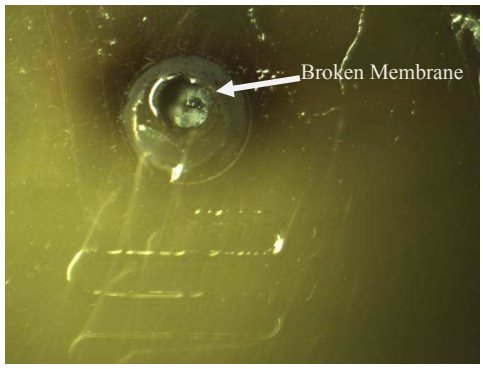

Fig. 7. Activated microvalve

VI. CONCLUSION

An inexpensive fluid impulsion method for microfluidics platforms such as lab on a chip has been proposed and its validity demonstrated. The device can be easily integrated in both microfluidic and electronic circuits thanks to the use of

PCB as substrate. The proposed device as energy reservoir is portable, autonomous and electrically controllable. Therefore, the external pumps to drive the fluids can be avoided. The same method can be use to integrate other SMD components, e.g., NTC resistors which can be used a temperature sensors.

ACKNOWLEDGMENT

This work was supported by the Spanish Ministry of Science and Innovation under grants TEC2011-29045-C04-02, ISILAB.

REFERENCES

[1] Y. C. Lim, A. Z. Kouzani and W. Duan, "Lab-on-a-chip: a component view", Microsyst Technol 16, 2010, pp. 1995–2015.

[2] David C. Duffy, J. Cooper McDonald, Olivier J. A. Schueller , and George M. Whitesides "Rapid Prototyping of Microfluidic Systems in Poly (dimethylsiloxane)," Anal. Chem., vol. 70, no. 23 (1998), pp. 4974-4984

[3] F. Perdigones, J. M. Moreno, A. Luque and J. M. Quero,"Characterisation of the fabrication process of freestanding SU-8 microstructures integrated in printing circuit board in microelectromechanical systems", Micro and Nano Letters 5, 2010, pp. 7–13.

[4]. F. Niklaus, P. Enoksson, P. Griss, E. Kälvesten, and G. Stemme, "Low-temperature wafer-level transfer bonding," J. Microelectromechanical Syst., vol. 10, no. 4 (2001), pp. 525-531.

[5] Y.K. Kim, E.K. Kim, S.W. Kim and B.K. Ju, "Low temperature epoxy bonding for wafer level MEMS packaging", Sensors and Actuators: A Physical 143, 2008, pp. 323–328.

[6] G. Murillo, Z. Davis, S. Keller, G. Abadal, J. Agusti, A. Cagliani, N. Noeth, A. Boisen and N. Barniol, "Novel SU-8 based vacuum wafer-level packaging for MEMS devices", Microelectronic Engineering 87, 2010, pp. 1173–1176.

[6] J. M. Moreno, C. Aracil and J. M. Quero, "High-integrated microvalve for lab-on-chip biomedical applications", IEEE Biomedical Circuits and Systems Conf., 2008, pp. 313–6.

[7] J. M. Moreno and J. M. Quero. "A novel single-use SU-8 microvalve for pressure-driven microfluidic applications", Journal of Micromechanics and Microengineering 20: 015005, 2010.

[8] Aracil, F. Perdigones, J. M. Moreno and J. M. Quero, "BETTS: bonding, exposing and transferring technique in SU-8 for microsystems fabrication", Journal of Micromechanics and Microengineering 20: 035088, 2010.

2015 10th Spanish Conference on Electron Devices (CDE)

Microfluidic Platform with Absorbance Sensor for Glucose Detection

G. Flores, F Perdigones, C. Aracil, M. Cabello and 1.M. Quero
University of Seville
Seville, Spain
Email: gf ores@gte.esi.us.es

Abstract- In this paper, a microfuidic Lab on Chip (LOC) platform for clinical diagnosis of glucose is proposed. The method is based on measuring the amount of glucose in a sample using a colorimetric enzyme-kinetic method. The colorimetric changes are detecting using an absorbance system consisting of a light emitting diode and a phototransistor working on the wavelength of 505 nm. The proposed platform is intended to be integrated with microfuidic PCB-based platforms for portable use. The experiments have shown good stability of the measure due to the use of a differential measurement circuit.

I. INTRODUCTION

The glucose detection in human physiological fuids is an important issue in the biomedical feld. Diabetes is the most common metabolic disorder world-wide, with more than 300 million affected people. In recent years, a number of ap proaches have been raised toward the development of glucose sensors. This employs different transduction mechanisms as well as recognition elements. The glucose biosensors reported in the bibliography mainly utilize electrochemical signal trans duction [1]- [3], fuorescence [4], [5] and absorbance [6].

Lab on Chip (LOC) devices are an alternative method towards the glucose detection. They offer many advantages over macroscopic systems, including low volume of samples and low reagents consumption, low waste production, high levels of throughput, automation and portability. The target of microfuidic lab-on-a-chip (LOC) systems is focused on integrating a complete analytical process into a single device capable to perform sampling, sample pre-treatment, analytical separation, bio-chemical reaction, analyze detection and data analysis operations. There have been several approaches [7], [8] in glucose assay. However, these are not easily integrable in a multifunction microfuidic circuits due to the complexity in the fabrication process.

In this paper, an absorbance MEMS platform is developed and characterized. This is an approach toward a LOC glucose detection system which is thought to be a component of a microfuidic circuit for impulsion, mixing, heating and sensing. The proposed platform is highly portable and integrable with other microfuidic components due to the fabrication materials, that is, SU-8, PCB and glass. Moreover, its optical detection electronic circuit is robust since it uses the differential measure mode, and the stability of an assembly system, avoiding any mechanical disturbance.

II. GLUCOSE DETECTION

The method of glucose detection in our system is based on the colorimetric enzyme-kinectic principle. A glucose Trinder

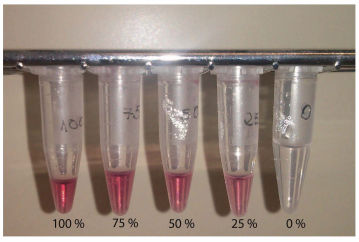

Fig. 1. Different concentration of the reaction products.

GOD-POD (Spinreact, S.A) [9] is used. In this reaction, the glucose oxidase catalyzes the oxidation of glucose to gluconic acid (1). The hydrogen peroxide generated is detected by a chromogenic oxygen acceptor, phenol-aminophenazone in the presence of peroxidase (2). The preparation method consists of a working reagent and a glucose cal, Glucose aqueous primary standard 100 mg/dL. A working reagent is prepared dissolving the context of enzymes, which will react with the glucose, and with a buffer (phenol). The reagent is mixed with the glucose sample in different volumen ratios, depending on the dilution factors (DF) (3). The reaction of glucose with the working reagent generates a red colored quinoneimine, which has an absorbance peak at 505 nm. The intensity of that color is proportional to the glucose concentration in the sample, Fig. 1.

f. D. Glucose + H20 - GluconicAcid + H20 (1)

H20 2+ Phenol + Aminophenazone- Quinone+ H20 (2)

$$DF = \frac{\text{Vsolution}}{\text{Vsolute}} \quad (3)$$

III. MICROFLUIDIC SYSTEM FOR GLUCOSE REACTION

The purpose of this paper is to develop a microfuidic platform for glucose detection. The fabrication process is designed to integrate different microfuidics components in that platform. In the paper, the mixure of reagents and sample is going to be done manually. However, several active and passive components have been already developed for PCB based platforms [10], [11].

978-1-4799-8108-3/151$31.00 ©2015 IEEE

2015 10th Spanish Conference on Electron Devices (CDE)

Fig. 2. Schematic system of the optoelectronic system detection.

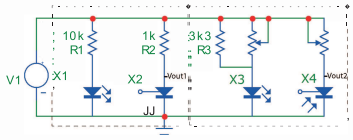

Fig. 3. Schematic circuit for the optoelectronic system detection.

IV. OPTOELECTRONIC SYSTEM FOR DETECTION

The optical detection system consists of a green light emitting diode (Nichia NEPE51QJS), which generates light that goes through a detection chamber, and reachs a phototransistor (Vishay TEPT4400), as can be seen in Fig. 2.

The absorbance for the reaction products reduces the amount of light intensity detected by the phototransistor. According to the polarization of the phototransistor Fig. 3, the redder is the glucose assay, the more light is observed by the liquid, and therefore the output voltage (Voutl) will be increased.

The electronic system works in dif erential mode to avoid any disturbance from ambient noise. In parallel with the reaction chamber, there are a replicated microf uidic and an electronic circuit using X3 and X4 amplif ed. The output voltage of this system is proportional to the difference Vout1-Vout2. The polarization system will have a signal output (Voutl and Vout2) between 0 a 370 mV for a range of glucose from o mg/dL to 100 mg/dL.

V. FABRICATION PROCESS AND SETUP

The Lab on Chip is manufactured in PCB, glass and SU-S. The schematic of the platform consists of a PCB, as a substrate where the microf uidic circuit is fabricated, and a plastic (PLA) structure where the electronic system is assembled. The PCB with the microf uidic circuits contains two chambers with 5 mm of diameter where the different concentrations are located, Fig. 4 A) schematic top view, and B) schematic bottom view.

The fabrication process can be observed in Fig. 4 C). In the step (a), the process begins with 1 mm thick glass and a single PCB. Then, in the step (b), the FR4 is milled with the same dimensions of the glass. In order to do so, a automatic CNC milling machine is used. Af er milling, in the step (c), two holes of 5 mm are drilled. The chambers will be located over these two holes. After that, in the step (d), the glass is placed into the milled area of the PCB, and glued to ensure the permeability and stability. The typical SU-S process is performed above the glass and the FR4 to fabricate

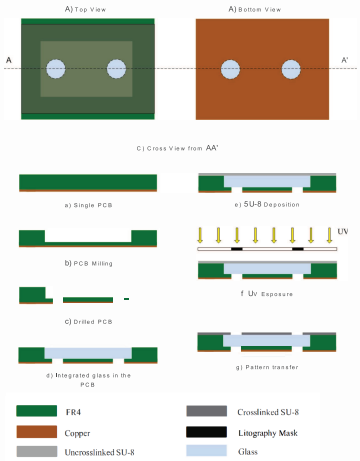

Fig. 4. A) Top view and B) Bottom view of the microf uidic PCB. C) Fabrication process from cross view A N .

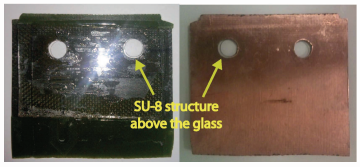

Al Top view Bl Bottom view

Fig. 5. A) Top view and B) Bottom view of the fabricated microf uidic PCB.

the microf uidic circuit. Also, the SU-S polymer avoids any leakage between the glass and the PCB. In step (e), a layer of 300 { m of SU-S 2050 (MicroChem Corp.) is deposited over the FR4 and the glass in order to fabricate the two chambers. To do this task, a deposition of 150 / m -thick SU-8 layer is carried out at 700 rpm during 60 s and a sof bake of 5 min at 65° C and then at 95° C during 15 min. Then, an adittional deposition of a layer of 150 / m is performed, with the same spin speed but with a softbake of 5 min at 65° C and 2 h at 95° C is carried out to achieve the desired thickness of 300 / m. Subsequently, in step (f , the photoresist is exposed to UV light for 2 min using a mask to def ne the chambers. Later on, in step (g), the uncrosslinked SU-S is developed by immersion and agitation in Mr600 Developer (MicroChem Corp.) during 7 min. Finally, the whole structure is cleaned with IPA. In this way, the entire structure is def ned, Fig. 5. In this process, the main concern is the cleaning of the structure, because if there is any uncrosslinked SU-S in the chambers, it will af ect signif cantly the measure of glucose.

Af erward, the complete Lab on Chip is inserted in a

2015 10th Spanish Conference on Electron Devices (CDE)

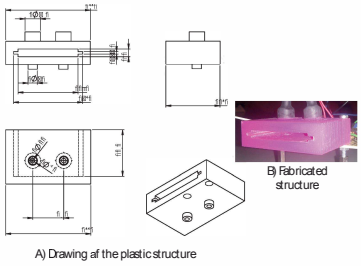

Fig. 6. Plastic structure for the optical reader detection electronic system.

plastic reader which was manufactured using a 3D printer, Fig. 6. The plastic structure of the reader contains two LEDs and photodetectors completely aligned and faced with one another, and an aperture. The microfluidic circuit will be introduced in that aperture, and it is found between the LEDs and phototransistor. Finally, this plastic structure is fixed to a new PCB where the detection electronic system is assembled.

VI. EXPERIMENTAL RESULTS

A. Optical detection

In a first bunch of experiments, the focus is on the validation of the calibration of the optical circuit. A calibration with a standard cuvette of 1 cm light path is done to prove the validation and linearity of the system, as previously presented in Fig. 2. The dilution factor used to prove the system is 100. This has been chosen for being the most typical for 1 cm light path. A electronic circuit adapted to this volume of liquid is assembled in a protoboard with the same LEDs and phototransistors.

The glucose assay is performed filling five cuvettes with 1 mL of reagent. Different concentration of glucose are manually pipette in each cuvette. Then, they are mixed for 10 min at 37° C. These cuvettes are always placed in the protoboard between the LED and the phototransistor in the same position and orientation. It is important to highlight that any change in the relative position of the detection chamber, respect to the LEDs, significantly modifies the measure. All experiments were performed at room temperature and data were acquired 30 s after the reagent and glucose are mixed. The result shows six different experiments for five glucose concentrations, Fig. 7. The experiments show a good repetitiveness and linearity.

The data dispersion in the measurement for one glucose concentration are justified for the use of a manual set up, which does not guarantee a reproducible optical geometry.

As will be explained in the next section, the proposed device will increase the stability of the signal by using a mechanical structure, which determines an accuracy geometric between LED, phototransistor and chamber.

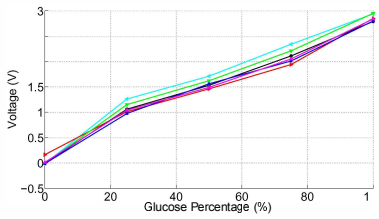

Fig. 7. Output voltage for 1 cm light path cuvette as a function of glucose concentration.

B. Experimental procedure

In the second bunch of experiments, the complete set up have been carried out. One of the chambers is filled with reagent liquid and the other is filled with glucose assay. The two chambers have a volume of 5.89 µL. One small glass is put above the chamber, acting like a cover to ensure that the chamber is completely filled, and to avoid a curved interface liquid-air which can affect the measure. Five different glucose concentration assays have been done with a dilution factor (DF) of 5, which is smaller than those used in typical colorimetric sensors (DF = 100). The reason for not using DF = 100 is for improving the absorbance and avoid any external noise. The experiments consist in measuring the different voltage in the phototransistor for different solutions. Special care should be taken in the cleanness of the LOC, since any disturbance will have an impact on the measurement. Moreover, the microfluidic PCB is introduced in the reader structure manually, any deviation in the led position will change the output voltage. In order to avoid these problems, after cleaning the PCB and before filling the chambers, it is inserted and measured to validate the zero output. In addition, the diameter of the chambers (5 mm) was chosen smaller than the phototransistors diameter (3mm) to solve the problem of the manually PCB insertion.

The same volume of sample and reagent are mixed in 5 cuvettes with different concentrations of glucose (0%, 25%, 50%, 75%, 100%) and pippeted to the chambers. The output for 4 experiments is shown in Fig. 8. The results show very similar behavior for the four different experiments. Moreover, it can be observed the non linearity in the slope of these curves in comparison with Fig. 7. It is caused by the differential in the dilution factor, from 100 to 5. However, the similarity between the experiments has improved significantly.

VII. CONCLUSION

An integrable microfluidic platform for photometric glucose sensor has been reported. The reported device is steady due to the differential mode of measurement and the plastic structure used to integrate the whole system. The values for a glucose assay concentrations have an average variation of only 13 mV from an output of 350 mV, which means an error of 3.7%. In addition, the decive is highly integrable in a more complex microfluidic circuit due to his fabrication process. The future work will be to include a detection system in a

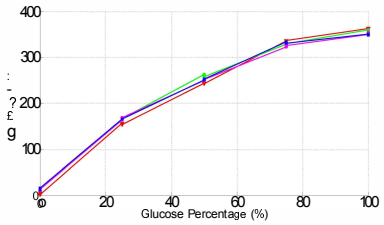

Fig. 8. Output voltage of the proposed device for four different experiment as a function of glucose concentration.

general multipurpose microf uidic platform using microvalves, impulsion system, mixers and heaters. It will be managed automatically and sensed with the electronic reader.

A CKNOWLEDGMENT

This work was supported by the Spanish Ministry of Science and Innovation under grants TEC2011-29045-C04-02, ISILAB.

REFERENCES

[I] Joseph Wang. Electrochemical glucose biosensors. Chemical reviews, 108(2):814-825, 2008.

[2] Sejin Pa k, Taek Dong Chung, and Hee Chan Kim. Nonenzymatic glucose detection using mesoporous platinum. Analytical chemist , 75(13):3046-3049, 2003.

[3] X iangjie Bo, Jean Chrysostome Ndar anisha, l ing Bai, and L iping Guo. Nonenzymatic amperometric sensor of hydrogen peroxide and glucose based on pt nanoparticles/ordered mesoporous ca bon nanocomposite. Talanta, 82(1):85-91, 2010.

[4] Elizabeth A Moschou, Bethel V Sha ma, Sapna K Deo, and Sylvia Daunert. Fluorescence glucose detection: advances towa d the ideal in vivo biosensor. *Journal of fluorescence*, 14(5):535-547, 2004.

[5] Ryan J Russell, Michael V Pishko, Christopher C Gefrides, Michael J McShane, and Gerard L Cote. A f uorescence-based glucose biosensor using concanavalin a and dextran encapsulated in a poly (ethylene glycol) hydrogel. Analytical Chemistry, 71(15):3126-3132, 1999.

[6] Wenbing Shi, Qinlong Wang, Yijuan L ong, Zhiliang Cheng, Shihong Chen, H uzhi Zheng, and Yuming H uang. Carbon nanodots as perox idase mimetics and their applications to glucose detection. Chemical Communications, 47(23):6695-6697, 2011.

[7] Saeedeh L ott Mohammad A bad and Keivan Maghooli. Dif erent approaches for detecting glucose. I n Bioinj rmatics and Biomedical Engineering, 2008. TCBBE 2008. The 2nd Tnternational Conference on, pages 1535-1538. IEEE, 2008.

[8] Joseph Wang, A lfredo I banez, and M adhu Prakash Chatrathi. On-chip integration of enzyme and immunoassays: simultaneous measurements of insulin and glucose. Journal of the A merican Chemical Societ , 125(28):8444-8445, 2003.

[9] Glucosa-TR: Trinder. GOD-POD S CT, www.spinreact.com

[10] Carmen A racil, Francisco Perdigones, Jose Miguel Moreno, A ntonio L uque, and Jose Manuel Quero. Portable lab-on-PCB platform for autonomous micromixing. M icroelectronic Engineering, 2014.

[I I] G Flores, C A racil, F Perdigones, and JM Quero. L ow consumption single-use microvalve for microf uidic PCB-based platforms. Journal of M icromechanics and M icroengineering, 24(6):065013, 2014.

C

ACRONYMS AND ABBREVIATIONS. SIMBOLS AND UNITS. PHYSIC CONSTANTS

C.1 Acronyms and abbreviations

Acronyms	Definition
BETTS	A Bonding, Exposing and Transferring Technique in SU-8
CTE	Coefficient ot thermal expansion
CE	Electrophoresis capillar
CNC	Computer numerical control
COC	UCyclic olefin copolymer
DEP	Dielectrophoresis capillar
DNA	Deoxyribonucleic acid
DPI	Dots per inch
DRIE	Deep reactive ion etching
EWOD	Electrowetting on Dielectric
FR4	Flame Retardant 4
IPA	Isopropanol
LCD	Liquid Cristal Display
LED	Light-emitting diode
LIGA	Litographym electroplating and molding
LoC	Lab-on-chip
LPCVD	Low pressure chemical vapor deposition
MEMS	Microelectromechanical systems
MOSFET	Metal-oxide-semiconductor Field-effect transistor

Acronyms	Definition
PC	Polycarbonate
PCB	Printed circuit board
PCBMEMS	Printed circuit board for Microelectromechanical systems
PCI	Peripheral Component Interconnect
PDMS	Polidimetilsiloxano
PEB	Post exposure bake
PMMA	Poly methyl methacrylate
PP	Polypropylene
RIE	Reactive ion etching
HV	Ultra-high-vacuum
UV	Ultra-violet
μTAG	Micro total analysis systems

C.2 Symbols and Units

Symbols	Definition
ρ	Density
τ	Stress tensor
$\vec{f_m}$	Vector of the mass forces per unit volume
ε	Thermodynamic internal energy
k	Temperature coefficient

Symbols	Definition
T	Temperature
Φ_ν	Work of forces in the deformation of a particle
Q_r	Radiative heating
Q_q	Viscous heating
Re	Reynolds Number
ν	Velocity of a fluid
L	Characteristic length
μ	Viscosity
D_h	Hydraulic Diameter
Pe	Peclet number
D	Diffusion coefficient
Ca	Capillar number
σ	Surface or interfacial tension between the two fluid phases
We	Weber number
ΔP	Increased pressure in the channel
Q	Flow rate in the channel
R_f	Fluidic resistance
P	Pressure
V	Volume
n	Number of moles
R	Gas constant
H	Heat released

Symbols	Definition
I	Current
t	Time
E	Energy
Deq	Equivalent Diameter
v	Speed
P_a	Atmospheric pressure
m	Mass
F	Force
A	Area
D_p	Plunge diameter

C.3 Physic constants

Constant	Definition	Value
μ_{air}	Air viscosity at 20°	$1.003{\cdot}10^{-3}\ N \cdot s \cdot m^2$
μ_{water}	Water viscosity at 20°	$1.8{\cdot}10^{-5}\ N \cdot s \cdot m^2$
ρ_{air}	Air density	1.2979 kg / m^3
ρ_{water}	Water density	998 kg / m^3
R	Universal gas constant	$8.314\ J \cdot K^{-1} \cdot mol^{-1}$
P_a	Atmospheric pressure	101325 Pa

See [221].

Bibliography

[1] Y. Lim, A. Kouzani, and W. Duan, "Lab-on-a-chip: a component view," *Microsystem Technologies*, vol. 16, no. 12, pp. 1995–2015, 2010.

[2] A. Luque, F. A. Perdigones, J. Esteve, J. Montserrat, A. M. Gañán-Calvo, and J. M. Quero, "Silicon microdevice for emulsion production using three-dimensional flow focusing," *Journal of Microelectromechanical Systems*, vol. 16, no. 5, pp. 1201–1208, 2007.

[3] F. Perdigones, A. Luque, and J. M. Quero, "Novel structure for a pneumatically controlled flow regulator with positive gain," *Journal of Microelectromechanical Systems*, vol. 19, no. 5, pp. 1070–1078, 2010.

[4] A. Luque, J. M. Quero, C. Hibert, P. Flückiger, and A. M. Gañán-Calvo, "Integrable silicon microfluidic valve with pneumatic actuation," *Sensors and Actuators A: Physical*, vol. 118, no. 1, pp. 144–151, 2005.

[5] C. Aracil, J. M. Quero, A. Luque, J. M. Moreno, and F. Perdigones, "Pneumatic impulsion device for microfluidic systems," *Sensors and Actuators A: Physical*, vol. 163, no. 1, pp. 247–254, 2010.

[6] J. M. Moreno and J. M. Quero, "A novel single-use su-8 microvalve for pressure-driven microfluidic applications," *Journal of Micromechanics and Microengineering*, vol. 20, no. 1, p. 015005, 2009.

[7] F. Perdigones, C. Aracil, J. M. Moreno, A. Luque, and J. M. Quero, "Highly integrable pressurized microvalve for portable su-8 microfluidic platforms," *Journal of Microelectromechanical Systems*, vol. 23, no. 2, pp. 398–405, 2014.

[8] C. Aracil, F. Perdigones, J. M. Moreno, A. Luque, and J. M. Quero, "Portable lab-on-pcb platform for autonomous micromixing," *Microelectronic Engineering*, vol. 131, pp. 13–18, 2015.

[9] R. Ghodssi and P. Lin, *MEMS materials and processes handbook*, vol. 1. Springer Science & Business Media, 2011.

[10] G. M. Rebeiz, *RF MEMS: theory, design, and technology*. John Wiley & Sons, 2004.

[11] *An introduction to MEMS*. Prime Faraday Partnership, 2002.

[12] R. P. Feynman, "There's plenty of room at the bottom," *Engineering and science*, vol. 23, no. 5, pp. 22–36, 1960.

[13] K. E. Petersen, "Silicon as a mechanical material," *Proceedings of the IEEE*, vol. 70, no. 5, pp. 420–457, 1982.

[14] M. Shimbo, K. Furukawa, K. Fukuda, and K. Tanzawa, "Silicon-to-silicon direct bonding method," *Journal of Applied Physics*, vol. 60, no. 8, pp. 2987–2989, 1986.

[15] Y. Kanda, "A graphical representation of the piezoresistance coefficients in silicon," *IEEE Transactions on electron devices*, vol. 29, no. 1, pp. 64–70, 1982.

[16] M. Gad-el Hak, *MEMS: applications*. CRC press, 2005.

[17] S. Nihtianov and A. Luque, *Smart sensors and MEMS: Intelligent devices and microsystems for industrial applications*. Woodhead Publishing, 2014.

[18] Y. Developpement, "Mems market analysis." urlhttp://www.yole.fr/ash, 2016.

[19] M. J. Madou, *Fundamentals of microfabrication: the science of miniaturization*. CRC press, 2002.

[20] G. W. Neudeck and R. F. Pierret, "Introduction to microelectronic fabrication," *Modular Series on Solid State Devices*, vol. 5, 2002.

[21] P. Rai-Choudhury, *Handbook of microlithography, micromachining, and microfabrication: microlithography*, vol. 1. Iet, 1997.

[22] M. J. Madou, *Manufacturing techniques for microfabrication and nanotechnology*, vol. 2. CRC Press, 2011.

[23] H. Miyajima and M. Mehregany, "High-aspect-ratio photolithography for mems applications," *Journal of microelectromechanical systems*, vol. 4, no. 4, pp. 220–229, 1995.

[24] G. Engelmann, O. Ehrmann, J. Simon, and H. Reichl, "Fabrication of high depth-to-width aspect ratio microstructures," in *Micro Electro Mechanical Systems, 1992, MEMS'92, Proceedings. An Investigation of Micro Structures, Sensors, Actuators, Machines and Robot. IEEE*, pp. 93–98, IEEE, 1992.

[25] G. T. Kovacs, N. I. Maluf, and K. E. Petersen, "Bulk micromachining of silicon," *Proceedings of the IEEE*, vol. 86, no. 8, pp. 1536–1551, 1998.

[26] R. Oosterbroek, J. Berenschot, S. Schlautmann, G. Krijnen, T. Lammerink, M. Elwenspoek, and A. Van den Berg, "Designing, simulation and realization of in-plane operating micro valves, using new etching techniques," *Journal of Micromechanics and Microengineering*, vol. 9, no. 2, p. 194, 1999.

[27] H. Ohji and P. French, "Single step electrochemical etching in ammonium fluoride," *Sensors and Actuators A: Physical*, vol. 74, no. 1, pp. 109–112, 1999.

[28] J. C. Love, K. E. Paul, and G. M. Whitesides, "Fabrication of nanometer-scale features by controlled isotropic wet chemical etching," *Advanced Materials*, vol. 13, no. 8, pp. 604–607, 2001.

[29] C. Merveille, "Surface quality of $\{111\}$ side-walls in koh-etched cavities," *Sensors and Actuators A: Physical*, vol. 60, no. 1, pp. 244–248, 1997.

[30] J. D. Johnson, S. R. Zarabadi, J. C. Christenson, and T. A. Noll, "Single crystal silicon low-g acceleration sensor," tech. rep., SAE Technical Paper, 2002.

[31] Y.-H. Wang, C.-P. Chen, C.-M. Chang, C.-P. Lin, C.-H. Lin, L.-M. Fu, and C.-Y. Lee, "Mems-based gas flow sensors," *Microfluidics and nanofluidics*, vol. 6, no. 3, pp. 333–346, 2009.

[32] J. GARRA, S. BRIDA, L. FERRARIO, and M. PARANJAPE, "Application of dual-doped tmah silicon etchant in the fabrication of a micromachined aluminum flexing beam actuator," *Sensors and materials*, vol. 13, no. 6, pp. 351–358, 2001.

[33] E. Stern, J. F. Klemic, D. A. Routenberg, P. N. Wyrembak, D. B. Turner-Evans, A. D. Hamilton, D. A. LaVan, T. M. Fahmy, and M. A. Reed, "Label-free immunodetection with cmos-compatible semiconducting nanowires," *Nature*, vol. 445, no. 7127, pp. 519–522, 2007.

[34] S. Kurth, R. Hahn, C. Kaufmann, K. Kehr, J. Mehner, U. Wollmann, W. Dötzel, and T. Gessner, "Silicon mirrors and micromirror arrays for spatial laser beam modulation," *Sensors and Actuators A: Physical*, vol. 66, no. 1, pp. 76–82, 1998.

[35] S. Tanzi, P. F. Østergaard, M. Matteucci, T. L. Christiansen, J. Cech, R. Marie, and R. Taboryski, "Fabrication of combined-scale nano-and microfluidic polymer systems using a multilevel dry etching, electroplating and molding process," *Journal of Micromechanics and Microengineering*, vol. 22, no. 11, p. 115008, 2012.

[36] N. Dhindsa, A. Chia, J. Boulanger, I. Khodadad, R. LaPierre, and S. S. Saini, "Highly ordered vertical gaas nanowire arrays with dry etching and their optical properties," *Nanotechnology*, vol. 25, no. 30, p. 305303, 2014.

[37] J. M. Bustillo, R. T. Howe, and R. S. Muller, "Surface micromachining for microelectromechanical systems," *Proceedings of the IEEE*, vol. 86, no. 8, pp. 1552–1574, 1998.

[38] S. R. Oh, K. Yao, and F. E. H. Tay, "Fabrication of piezoelectric p (vdf-trfe) microcantilevers by wafer-level surface micromachining," *Journal of Micromechanics and Microengineering*, vol. 23, no. 9, p. 095023, 2013.

[39] M. Alexe and U. Gösele, *Wafer bonding: applications and technology*, vol. 75. Springer Science & Business Media, 2013.

[40] K. Derendorf, S. Essig, E. Oliva, V. Klinger, T. Roesener, S. P. Philipps, J. Benick, M. Hermle, M. Schachtner, G. Siefer, *et al.*, "Fabrication of gainp/gaas//si solar cells by surface activated direct wafer bonding," *IEEE Journal of Photovoltaics*, vol. 3, no. 4, pp. 1423–1428, 2013.

[41] E. Higurashi, D. Chino, T. Suga, and R. Sawada, "Au–au surface-activated bonding and its application to optical microsensors with 3-d structure," *IEEE Journal of Selected Topics in Quantum Electronics*, vol. 15, no. 5, pp. 1500–1505, 2009.

[42] A. Shigetou, T. Itoh, M. Matsuo, N. Hayasaka, K. Okumura, and T. Suga, "Bumpless interconnect through ultrafine cu electrodes by means of surface-activated bonding (sab) method," *IEEE transactions on advanced packaging*, vol. 29, no. 2, pp. 218–226, 2006.

[43] V. Dragoi, G. Mittendorfer, C. Thanner, and P. Lindner, "Wafer-level plasma activated bonding: new technology for mems fabrication," *Microsystem Technologies*, vol. 14, no. 4-5, pp. 509–515, 2008.

[44] M. Wiemer, D. Wuensch, J. Braeuer, and T. Gessner, "Plasma-activated bonding," *Handbook of Wafer Bonding*, pp. 101–118, 2011.

[45] T. Rogers and J. Kowal, "Selection of glass, anodic bonding conditions and material compatibility for silicon-glass capacitive sensors," *Sensors and Actuators A: Physical*, vol. 46, no. 1, pp. 113–120, 1995.

[46] S. M. Langelier, L. Y. Yeo, and J. Friend, "Uv epoxy bonding for enhanced saw transmission and microscale acoustofluidic integration," *Lab on a Chip*, vol. 12, no. 16, pp. 2970–2976, 2012.

[47] S. Gassmann, A. Trozjuk, J. Singhal, H. Schuette, M. L. Miranda, and O. Zielinski, "Pcb based micro fluidic system for thermal cycling of seawater samples," in *Industrial Technology (ICIT), 2015 IEEE International Conference on*, pp. 3365–3369, IEEE, 2015.

[48] K. Kim, S. Park, J.-B. Lee, H. Manohara, Y. Desta, M. Murphy, and C. H. Ahn, "Rapid replication of polymeric and metallic high aspect ratio microstructures using pdms and liga technology," *Microsystem Technologies*, vol. 9, no. 1-2, pp. 5–10, 2002.

[49] E. Becker, W. Ehrfeld, P. Hagmann, A. Maner, and D. Münchmeyer, "Fabrication of microstructures with high aspect ratios and great structural heights by synchrotron radiation lithography, galvanoforming, and plastic moulding (liga process)," *Microelectronic engineering*, vol. 4, no. 1, pp. 35–56, 1986.

[50] C. Rusch, M. Börner, J. Mohr, T. Zwick, Y. Chen, and J. Héctor, "Electrical tuning of dielectric resonators with liga-mems," in *Microwave Integrated Circuits Conference (EuMIC), 2013 European*, pp. 316–319, IEEE, 2013.

[51] D. Haluzan, *Electrostatically actuated LIGA-MEMS structures with high aspect ratio beams for RF applications and mechanical property extraction*. PhD thesis, University of Saskatchewan, 2014.

[52] H. Becker and U. Heim, "Hot embossing as a method for the fabrication of polymer high aspect ratio structures," *Sensors and Actuators A: Physical*, vol. 83, no. 1, pp. 130–135, 2000.

[53] L. Peng, Y. Deng, P. Yi, and X. Lai, "Micro hot embossing of thermoplastic polymers: a review," *Journal of Micromechanics and Microengineering*, vol. 24, no. 1, p. 013001, 2013.

[54] G. M. Whitesides, "The origins and the future of microfluidics," *Nature*, vol. 442, no. 7101, pp. 368–373, 2006.

[55] G. M. Whitesides, "What comes next?," *Lab on a Chip*, vol. 11, no. 2, pp. 191–193, 2011.

[56] A. C. Martínez, *Mecánica de fluidos*. Editorial Paraninfo, 2006.

[57] L. D. Landau, J. Bell, M. Kearsley, L. Pitaevskii, E. Lifshitz, and J. Sykes, *Electrodynamics of continuous media*, vol. 8. elsevier, 2013.

[58] P. Tabeling, *Introduction to microfluidics*. Oxford University Press on Demand, 2005.

[59] H. Bruus, "Theoretical microfluidics. oxford master series in condensed matter physics," 2008.

[60] P. Day, A. Manz, and Y. Zhang, *Microdroplet technology: principles and emerging applications in biology and chemistry*. Springer Science & Business Media, 2012.

[61] O. Geschke, H. Klank, and P. Telleman, *Microsystem Engineering of Lab-on-a-chip Devices*, vol. 100. Wiley Online Library, 2008.

[62] R. E. Sonntag, C. Borgnakke, G. J. Van Wylen, and S. Van Wyk, *Fundamentals of thermodynamics*, vol. 6. Wiley New York, 1998.

[63] G. J. Van Wylen, R. E. Sonntag, and C. Borgnakke, *Fundamentals of classical thermodynamics*, vol. 1. John Wiley & Sons, 1994.

[64] P. Abgrall and A. Gue, "Lab-on-chip technologies: making a microfluidic network and coupling it into a complete microsystem a review," *Journal of Micromechanics and Microengineering*, vol. 17, no. 5, p. R15, 2007.

[65] K. Ren, J. Zhou, and H. Wu, "Materials for microfluidic chip fabrication," *Accounts of chemical research*, vol. 46, no. 11, pp. 2396–2406, 2013.

[66] H. Becker and L. E. Locascio, "Polymer microfluidic devices," *Talanta*, vol. 56, no. 2, pp. 267–287, 2002.

[67] MicroChem. urlhttp://www.microchem.com/ash.

[68] H. Lorenz, M. Despont, N. Fahrni, N. LaBianca, P. Renaud, and P. Vettiger, "Su-8: a low-cost negative resist for mems," *Journal of Micromechanics and Microengineering*, vol. 7, no. 3, p. 121, 1997.

[69] A. del Campo and C. Greiner, "Su-8: a photoresist for high-aspect-ratio and 3d submicron lithography," *Journal of Micromechanics and Microengineering*, vol. 17, no. 6, p. R81, 2007.

[70] K. V. Nemani, K. L. Moodie, J. B. Brennick, A. Su, and B. Gimi, "In vitro and in vivo evaluation of su-8 biocompatibility," *Materials Science and Engineering: C*, vol. 33, no. 7, pp. 4453–4459, 2013.

[71] V. Kumar and N. Sharma, "Su-8 as hydrophobic and dielectric thin film in electrowetting-on-dielectric based microfluidics device," *Journal of Nanotechnology*, vol. 2012, 2012.

[72] M. Hopcroft, T. Kramer, G. Kim, K. Takashima, Y. Higo, D. Moore, and J. Brugger, "Micromechanical testing of su-8 cantilevers," *Fatigue & Fracture of Engineering Materials & Structures*, vol. 28, no. 8, pp. 735–742, 2005.

[73] MicroChem. urlhttp://www.microchem.com/ash.

[74] T. Merkel, M. Graeber, and L. Pagel, "A new technology for fluidic microsystems based on pcb technology," *Sensors and Actuators A: Physical*, vol. 77, no. 2, pp. 98–105, 1999.

[75] L. Pagel and S. Gabmann, "Microfluidic systems in pcb technology," in *31st Annual Conference of IEEE Industrial Electronics Society, 2005. IECON 2005.*, pp. 4–pp, IEEE, 2005.

[76] A. Petropoulos, D. N. Pagonis, and G. Kaltsas, "Flexible pcb-mems flow sensor," *Procedia Engineering*, vol. 47, pp. 236–239, 2012.

[77] M. Souilah, A. Chaabi, F. Perdigones, J. M. Quero, G. Flores, and M. R. Lain, "Fabrication process for pcbmems capacitive pressure sensors using the cu layer to define the gap," *IEEE Sensors Journal*, vol. 16, no. 5, pp. 1151–1157, 2016.

[78] F. T. Moreira, M. J. M. Ferreira, J. R. Puga, and M. G. F. Sales, "Screen-printed electrode produced by printed-circuit board technology. application to cancer biomarker detection by means of plastic antibody as sensing material," *Sensors and Actuators B: Chemical*, vol. 223, pp. 927–935, 2016.

[79] B. Salvador, E. Franco, F. Perdigones, and J. M. Quero, "Fabrication process for inexpensive, biocompatible and transparent pcbs. application to a flow meter," *Microelectronic Engineering*, vol. 173, pp. 6–12, 2017.

[80] F. A. Perdigones, C. Aracil, J. M. Moreno, A. Luque, and J. M. Quero, "Highly integrable pressurized microvalve for portable SU-8 microfluidic platforms," *Microelectromechanical Systems, Journal of*, vol. 23, no. 2, pp. 398–405, 2014.

[81] J. N. Palasagaram and R. Ramadoss, "Mems-capacitive pressure sensor fabricated using printed-circuit-processing techniques," *IEEE Sensors Journal*, vol. 6, no. 6, pp. 1374–1375, 2006.

[82] B. A. Cetiner, J. Qian, H. Chang, M. Bachman, G. Li, and F. De Flaviis, "Monolithic integration of rf mems switches with a diversity antenna on pcb substrate," *IEEE transactions on microwave theory and techniques*, vol. 51, no. 1, pp. 332–335, 2003.

[83] S. Schumacher, J. Nestler, T. Otto, M. Wegener, E. Ehrentreich-Förster, D. Michel, K. Wunderlich, S. Palzer, K. Sohn, A. Weber, *et al.*, "Highly-integrated lab-on-chip system for point-of-care multiparameter analysis," *Lab on a Chip*, vol. 12, no. 3, pp. 464–473, 2012.

[84] J. Gong and C.-J. Kim, "Direct-referencing two-dimensional-array digital microfluidics using multilayer printed circuit board," *Journal of microelectromechanical systems*, vol. 17, no. 2, pp. 257–264, 2008.

[85] R. E. Pawinanto, J. Yunas, B. Majlis, and A. Hamzah, "Design and fabrication of compact mems electromagnetic micro-actuator with planar microcoil based on pcb," *TELKOMNIKA (Telecommunication Computing Electronics and Control)*, vol. 14, no. 3, pp. 856–866, 2016.

[86] A. Wego, S. Richter, and L. Pagel, "Fluidic microsystems based on printed circuit board technology," *Journal of Micromechanics and Microengineering*, vol. 11, no. 5, p. 528, 2001.

[87] A. Wego and L. Pagel, "A self-filling micropump based on pcb technology," *Sensors and Actuators A: Physical*, vol. 88, no. 3, pp. 220–226, 2001.

[88] S. Gaßmann, I. Ibendorf, and L. Pagel, "Realization of a flow injection analysis in pcb technology," *Sensors and Actuators A: Physical*, vol. 133, no. 1, pp. 231–235, 2007.

[89] W. Wang and S. A. Soper, *Bio-MEMS: technologies and applications*. CRC press, 2006.

[90] D. V. Rosato and M. G. Rosato, *Injection molding handbook*. Springer Science & Business Media, 2012.

[91] L. E. Locascio, M. Gaitan, J. Hong, and M. Eldefrawi, "Plastic microfluid devices for clinical measurements," in *Micro Total Analysis Systems*, pp. 367–370, Springer, 1998.

[92] H. Becker, W. Dietz, and P. Dannberg, "Microfluidic manifolds by polymer hot embossing for μ-tas applications," in *Micro Total Analysis Systems*, pp. 253–256, Springer, 1998.

[93] L. Martynova, L. E. Locascio, M. Gaitan, G. W. Kramer, R. G. Christensen, and W. A. MacCrehan, "Fabrication of plastic microfluid channels by imprinting methods," *Analytical chemistry*, vol. 69, no. 23, pp. 4783–4789, 1997.

[94] D. Benvegnu and R. M. McCormick, "Method for sample injection in microchannel device," May 4 1999. US Patent 5,900,130.

[95] M. Heckele and W. Schomburg, "Review on micro molding of thermoplastic polymers," *Journal of Micromechanics and Microengineering*, vol. 14, no. 3, p. R1, 2003.

[96] K. W. Oh and C. H. Ahn, "A review of microvalves," *Journal of micromechanics and microengineering*, vol. 16, no. 5, p. R13, 2006.

[97] S. C. Terry, J. H. Jerman, and J. B. Angell, "A gas chromatographic air analyzer fabricated on a silicon wafer," *IEEE Transactions on Electron Devices*, vol. 26, no. 12, pp. 1880–1886, 1979.

[98] A. Meckes, J. Behrens, O. Kayser, W. Benecke, T. Becker, and G. Müller, "Microfluidic system for the integration and cyclic operation of gas sensors," *Sensors and Actuators A: Physical*, vol. 76, no. 1, pp. 478–483, 1999.

[99] B. Bae, H. Kee, S. Kim, Y. Lee, T. Sim, Y. Kim, and K. Park, "In vitro experiment of the pressure regulating valve for a glaucoma implant," *Journal of Micromechanics and Microengineering*, vol. 13, no. 5, p. 613, 2003.

[100] C. Fu, Z. Rummler, and W. Schomburg, "Magnetically driven micro ball valves fabricated by multilayer adhesive film bonding," *Journal of Micromechanics and microengineering*, vol. 13, no. 4, p. S96, 2003.

[101] K. Sato and M. Shikida, "An electrostatically actuated gas valve with an s-shaped film element," *Journal of micromechanics and microengineering*, vol. 4, no. 4, p. 205, 1994.

[102] L. Yobas, D. M. Durand, G. G. Skebe, F. J. Lisy, and M. A. Huff, "A novel integrable microvalve for refreshable braille display system," *Journal of microelectromechanical systems*, vol. 12, no. 3, pp. 252–263, 2003.

[103] H. Li, D. Roberts, J. Steyn, K. Turner, O. Yaglioglu, N. Hagood, S. Spearing, and M. Schmidt, "Fabrication of a high frequency piezoelectric microvalve," *Sensors and Actuators A: Physical*, vol. 111, no. 1, pp. 51–56, 2004.

[104] T. Rogge, Z. Rummler, and W. Schomburg, "Polymer micro valve with a hydraulic piezo-drive fabricated by the amanda process," *Sensors and Actuators A: Physical*, vol. 110, no. 1, pp. 206–212, 2004.

[105] Q. S. Pan, L. G. He, F. S. Huang, X. Y. Wang, and Z. H. Feng, "Piezoelectric micropump using dual-frequency drive," *Sensors and Actuators A: Physical*, vol. 229, pp. 86–93, 2015.

[106] P. W. Barth, "Silicon microvalves for gas flow control," in *Solid-State Sensors and Actuators, 1995 and Eurosensors IX.. Transducers' 95. The 8th International Conference on*, vol. 2, pp. 276–279, IEEE, 1995.

[107] D. Reynaerts, J. Peirs, and H. Van Brussel, "An implantable drug-delivery system based on shape memory alloy micro-actuation," *Sensors and Actuators A: Physical*, vol. 61, no. 1, pp. 455–462, 1997.

[108] H. Takao, K. Miyamura, H. Ebi, M. Ashiki, K. Sawada, and M. Ishida, "A mems microvalve with pdms diaphragm and two-chamber configuration of thermo-pneumatic actuator for integrated blood test system on silicon," *Sensors and Actuators A: Physical*, vol. 119, no. 2, pp. 468–475, 2005.

[109] X. Yang, C. Grosjean, and Y.-C. Tai, "Design, fabrication, and testing of micromachined silicone rubber membrane valves," *Journal of microelectromechanical systems*, vol. 8, no. 4, pp. 393–402, 1999.

[110] D. Baechi and R. Buser, "Suspension handling system," *Sensors and Actuators B: Chemical*, vol. 63, no. 3, pp. 195–200, 2000.

[111] C. Goll, W. Bacher, B. Buestgens, D. Maas, W. Menz, and W. Schomburg, "Microvalves with bistable buckled polymer diaphragms," *Journal of Micromechanics and Microengineering*, vol. 6, no. 1, p. 77, 1996.

[112] S. Böhm, G. Burger, M. Korthorst, and F. Roseboom, "A micromachined silicon valve driven by a miniature bi-stable electro-magnetic actuator," *Sensors and Actuators A: Physical*, vol. 80, no. 1, pp. 77–83, 2000.

[113] M. T. Guler, P. Beyazkilic, and C. Elbuken, "A versatile plug microvalve for microfluidic applications," *Sensors and Actuators A: Physical*, 2017.

[114] S. Z. Hua, F. Sachs, D. X. Yang, and H. D. Chopra, "Microfluidic actuation using electrochemically generated bubbles," *Analytical chemistry*, vol. 74, no. 24, pp. 6392–6396, 2002.

[115] T. Watanabe, G. Biswas, E. Carlen, and H. Suzuki, "An autonomous electrochemically-actuated microvalve for controlled transport in stand-alone microfluidic systems," *RSC Advances*, vol. 7, no. 62, pp. 39018–39023, 2017.

[116] D. T. Eddington and D. J. Beebe, "A valved responsive hydrogel microdispensing device with integrated pressure source," *Journal of microelectromechanical systems*, vol. 13, no. 4, pp. 586–593, 2004.

[117] Y. Liu, C. B. Rauch, R. L. Stevens, R. Lenigk, J. Yang, D. B. Rhine, and P. Grodzinski, "Dna amplification and hybridization assays in integrated plastic monolithic devices," *Analytical Chemistry*, vol. 74, no. 13, pp. 3063–3070, 2002.

[118] R. Pal, M. Yang, B. N. Johnson, D. T. Burke, and M. A. Burns, "Phase change microvalve for integrated devices," *Analytical chemistry*, vol. 76, no. 13, pp. 3740–3748, 2004.

[119] L. Gui and J. Liu, "Ice valve for a mini/micro flow channel," *Journal of Micromechanics and Microengineering*, vol. 14, no. 2, p. 242, 2004.

[120] K. Yoshida, M. Kikuchi, J.-H. Park, and S. Yokota, "Fabrication of micro electro-rheological valves (er valves) by micromachining and experiments," *Sensors and Actuators A: Physical*, vol. 95, no. 2, pp. 227–233, 2002.

[121] H. Hartshorne, C. J. Backhouse, and W. E. Lee, "Ferrofluid-based microchip pump and valve," *Sensors and Actuators B: Chemical*, vol. 99, no. 2, pp. 592–600, 2004.

[122] K. W. Oh, C. Park, and K. Namkoong, "A world-to-chip microfluidic interconnection technology with dual functions of sample injection and sealing for a multichamber micro pcr chip," in *18th IEEE International Conference on Micro Electro Mechanical Systems, 2005. MEMS 2005.*, pp. 714–717, IEEE, 2005.

[123] T. Hasegawa, T. Hasegawa, K. Ikuta, K. Ikuta, K. Nakashima, K. Nakashima, and T. Hasegawa, "10-way micro switching valve chip with rotary mechanism for multi-directional flow control," in *The Seventh International Symposium on Micro Total Analysis System*, pp. 215–218, 2003.

[124] H. Takao and M. Ishida, "Microfluidic integrated circuits for signal processing using analogous relationship between pneumatic microvalve and mosfet," *Journal of microelectromechanical systems*, vol. 12, no. 4, pp. 497–505, 2003.

[125] E. Lagally, I. Medintz, and R. Mathies, "Single-molecule dna amplification and analysis in an integrated microfluidic device," *Analytical chemistry*, vol. 73, no. 3, pp. 565–570, 2001.

[126] J. Ulrich and R. Zengerle, "Static and dynamic flow simulation of a koh-etched microvalve using the finite-element method," *Sensors and Actuators A: Physical*, vol. 53, no. 1, pp. 379–385, 1996.

[127] K.-S. Yun, I.-J. Cho, J.-U. Bu, C.-J. Kim, and E. Yoon, "A surface-tension driven micropump for low-voltage and low-power operations," *Journal of microelectromechanical systems*, vol. 11, no. 5, pp. 454–461, 2002.

[128] G.-H. Feng and E. S. Kim, "Micropump based on pzt unimorph and one-way parylene valves," *Journal of micromechanics and microengineering*, vol. 14, no. 4, p. 429, 2004.

[129] N.-T. Nguyen and T.-Q. Truong, "A fully polymeric micropump with piezoelectric actuator," *Sensors and Actuators B: Chemical*, vol. 97, no. 1, pp. 137–143, 2004.

[130] O. Jensen and P. Gravesen, "Flow characteristics of a micromachined diaphragm valve designed for liquid flows above 1 ml min-1," *Journal of Micromechanics and Microengineering*, vol. 3, no. 4, p. 236, 1993.

[131] V. L. Gott, D. E. Alejo, and D. E. Cameron, "Mechanical heart valves: 50 years of evolution," *The Annals of thoracic surgery*, vol. 76, no. 6, pp. S2230–S2239, 2003.

[132] C. Schabmueller, M. Koch, M. Mokhtari, A. Evans, A. Brunnschweiler, and H. Sehr, "Self-aligning gas/liquid micropump," *Journal of Micromechanics and Microengineering*, vol. 12, no. 4, p. 420, 2002.

[133] J.-H. Tsai and L. Lin, "A thermal-bubble-actuated micronozzle-diffuser pump," *Journal of microelectromechanical systems*, vol. 11, no. 6, pp. 665–671, 2002.

[134] C. J. Morris and F. K. Forster, "Low-order modeling of resonance for fixed-valve micropumps based on first principles," *Journal of Microelectromechanical Systems*, vol. 12, no. 3, pp. 325–334, 2003.

[135] M. Yamada and M. Seki, "Nanoliter-sized liquid dispenser array for multiple biochemical analysis in microfluidic devices," *Analytical chemistry*, vol. 76, no. 4, pp. 895–899, 2004.

[136] L. G. Puckett, E. Dikici, S. Lai, M. Madou, L. G. Bachas, and S. Daunert, "Investigation into the applicability of the centrifugal microfluidics platform for the development of protein-ligand binding assays incorporating enhanced green fluorescent protein as a fluorescent reporter," *Analytical chemistry*, vol. 76, no. 24, pp. 7263–7268, 2004.

[137] L. Guerin, O. Dubochet, J.-F. Zeberli, P. Clot, and P. Renaud, "Miniature one-shot valve," in *Micro Electro Mechanical Systems, 1998. MEMS 98. Proceedings., The Eleventh Annual International Workshop on*, pp. 425–428, IEEE, 1998.

[138] J. C. McDonald, S. J. Metallo, and G. M. Whitesides, "Fabrication of a configurable, single-use microfluidic device," *Analytical chemistry*, vol. 73, no. 23, pp. 5645–5650, 2001.

[139] C. H. Ahn, J.-W. Choi, G. Beaucage, J. H. Nevin, J.-B. Lee, A. Puntambekar, and J. Y. Lee, "Disposable smart lab on a chip for point-of-care clinical diagnostics," *Proceedings of the IEEE*, vol. 92, no. 1, pp. 154–173, 2004.

[140] A. Cardenas-Valencia, J. Dlutowski, J. Bumgarner, C. Munoz, W. Wang, R. Popuri, and L. Langebrake, "Development of various designs of low-power, mems valves for fluidic applications," *Sensors and Actuators A: Physical*, vol. 136, no. 1, pp. 374–384, 2007.

[141] A. Debray, M. Shibata, and H. Fujita, "A low melting point alloy as a functional material for a one-shot micro-valve," *Journal of Micromechanics and Microengineering*, vol. 17, no. 8, p. 1442, 2007.

[142] P.-Y. Li, T. K. Givrad, D. P. Holschneider, J.-M. I. Maarek, and E. Meng, "A parylene mems electrothermal valve," *Journal of Microelectromechanical Systems*, vol. 18, no. 6, pp. 1184–1197, 2009.

[143] K. Pitchaimani, B. C. Sapp, A. Winter, A. Gispanski, T. Nishida, and Z. H. Fan, "Manufacturable plastic microfluidic valves using thermal actuation," *Lab on a Chip*, vol. 9, no. 21, pp. 3082–3087, 2009.

[144] Z. Khaji, P. Sturesson, L. Klintberg, K. Hjort, and G. Thornell, "Manufacturing and characterization of a ceramic microcombustor with integrated oxygen storage and release element," *Journal of Micromechanics and Microengineering*, vol. 25, no. 10, p. 104006, 2015.

[145] C.-C. Hong, S. Murugesan, S. Kim, G. Beaucage, J.-W. Choi, and C. H. Ahn, "A functional on-chip pressure generator using solid chemical propellant for disposable lab-on-a-chip," *Lab on a Chip*, vol. 3, no. 4, pp. 281–286, 2003.

[146] J.-w. Ban, K.-i. Koo, S. Park, G. Kim, *et al.*, "Micro-injection system for localized drug delivery using embedded solid chemical propellant," in *Frontiers in the Convergence of Bioscience and Information Technologies, 2007. FBIT 2007*, pp. 567–571, IEEE, 2007.

[147] C. R. Neagu, J. G. Gardeniers, M. Elwenspoek, and J. J. Kelly, "An electrochemical microactuator: principle and first results," *Journal of Microelectromechanical systems*, vol. 5, no. 1, pp. 2–9, 1996.

[148] A. R. Wheeler, H. Moon, C.-J. C. Kim, J. A. Loo, and R. L. Garrell, "Electrowetting-based microfluidics for analysis of peptides and proteins by matrix-assisted laser desorption/ionization mass spectrometry," *Analytical Chemistry*, vol. 76, no. 16, pp. 4833–4838, 2004.

[149] S. Srigunapalan, I. A. Eydelnant, C. A. Simmons, and A. R. Wheeler, "A digital microfluidic platform for primary cell culture and analysis," *Lab on a Chip*, vol. 12, no. 2, pp. 369–375, 2012.

[150] R. Sista, Z. Hua, P. Thwar, A. Sudarsan, V. Srinivasan, A. Eckhardt, M. Pollack, and V. Pamula, "Development of a digital microfluidic platform for point of care testing," *Lab on a Chip*, vol. 8, no. 12, pp. 2091–2104, 2008.

[151] A. Renaudin, J.-P. Sozanski, B. Verbeke, V. Zhang, P. Tabourier, and C. Druon, "Monitoring saw-actuated microdroplets in view of biological applications," *Sensors and Actuators B: Chemical*, vol. 138, no. 1, pp. 374–382, 2009.

[152] Z. Guttenberg, H. Müller, H. Habermüller, A. Geisbauer, J. Pipper, J. Felbel, M. Kielpinski, J. Scriba, and A. Wixforth, "Planar chip device for pcr and hybridization with surface acoustic wave pump," *Lab on a Chip*, vol. 5, no. 3, pp. 308–317, 2005.

[153] M. Borgatti, N. Bianchi, I. Mancini, G. Feriotto, and R. Gambari, "New trends in non-invasive prenatal diagnosis: Applications of dielectrophoresis-based lab-on-a-chip platforms to the identification and manipulation of rare cells (review).," *International journal of molecular medicine*, vol. 21, no. 1, p. 3, 2008.

[154] C.-C. Hong, J.-W. Choi, and C. H. Ahn, "An on-chip air-bursting detonator for driving fluids on disposable lab-on-a-chip systems," *Journal of Micromechanics and Microengineering*, vol. 17, no. 2, p. 410, 2007.

[155] J. Moreno, F. Perdigones, and J. Quero, "Fabrication process of a su-8 monolithic pressurized microchamber for pressure driven microfluidic applications," in *Electron Devices (CDE), 2011 Spanish Conference on*, pp. 1–4, IEEE, 2011.

[156] S. N. Pei, J. K. Valley, Y.-L. Wang, and M. C. Wu, "Distributed circuit model for multi-color light-actuated opto-electrowetting microfluidic device," *Journal of Lightwave Technology*, vol. 33, no. 16, pp. 3486–3493, 2015.

[157] P.-Y. Chiou, Z. Chang, and M. C. Wu, "Droplet manipulation with light on optoelectrowetting device," *Journal of Microelectromechanical Systems*, vol. 17, no. 1, pp. 133–138, 2008.

[158] D. C. Duffy, H. L. Gillis, J. Lin, N. F. Sheppard, and G. J. Kellogg, "Microfabricated centrifugal microfluidic systems: characterization and multiple enzymatic assays," *Analytical Chemistry*, vol. 71, no. 20, pp. 4669–4678, 1999.

[159] S. Z. Andreasen, D. Kwasny, L. Amato, A. L. Brøgger, F. G. Bosco, K. B. Andersen, W. E. Svendsen, and A. Boisen, "Integrating electrochemical detection with centrifugal microfluidics for real-time and fully automated sample testing," *RSC Advances*, vol. 5, no. 22, pp. 17187–17193, 2015.

[160] L. Shui, J. C. Eijkel, and A. van den Berg, "Multiphase flow in microfluidic systems–control and applications of droplets and interfaces," *Advances in Colloid and Interface Science*, vol. 133, no. 1, pp. 35–49, 2007.

[161] R. Bodén, M. Lehto, U. Simu, G. Thornell, K. Hjort, and J.-Å. Schweitz, "A polymeric paraffin actuated high-pressure micropump," *Sensors and Actuators A: Physical*, vol. 127, no. 1, pp. 88–93, 2006.

[162] R. H. Liu, J. Bonanno, J. Yang, R. Lenigk, and P. Grodzinski, "Single-use, thermally actuated paraffin valves for microfluidic applications," *Sensors and Actuators B: Chemical*, vol. 98, no. 2, pp. 328–336, 2004.

[163] S. C. Terry, J. H. Jerman, and J. B. Angell, "A gas chromatographic air analyzer fabricated on a silicon wafer," *IEEE Transactions on Electron Devices*, vol. 26, no. 12, pp. 1880–1886, 1979.

[164] A. Manz, N. Graber, and H. á. Widmer, "Miniaturized total chemical analysis systems: a novel concept for chemical sensing," *Sensors and actuators B: Chemical*, vol. 1, no. 1-6, pp. 244–248, 1990.

[165] A. Manz, Y. Miyahara, J. Miura, Y. Watanabe, H. Miyagi, and K. Sato, "Design of an open-tubular column liquid chromatograph using silicon chip technology," *Sensors and actuators B: Chemical*, vol. 1, no. 1, pp. 249–255, 1990.

[166] S. C. Jacobson, R. Hergenröder, A. W. Moore Jr, and J. M. Ramsey, "Precolumn reactions with electrophoretic analysis integrated on a microchip," *Analytical Chemistry (Washington);(United States)*, vol. 66, no. 23, 1994.

[167] C. S. Effenhauser, A. Paulus, A. Manz, and H. M. Widmer, "High-speed separation of antisense oligonucleotides on a micromachined capillary electrophoresis device," *Analytical Chemistry*, vol. 66, no. 18, pp. 2949–2953, 1994.

[168] A. T. Woolley and R. A. Mathies, "Ultra-high-speed dna fragment separations using microfabricated capillary array electrophoresis chips," *Proceedings of the National Academy of Sciences*, vol. 91, no. 24, pp. 11348–11352, 1994.

[169] G. Fuhr, T. Schnelle, and B. Wagner, "Travelling wave-driven microfabricated electrohydrodynamic pumps for liquids," *Journal of Micromechanics and Microengineering*, vol. 4, no. 4, p. 217, 1994.

[170] E. M. Verpoorte, B. Van Der Schoot, S. Jeanneret, A. Manz, H. Widmer, and N. De Rooij, "Three-dimensional micro flow manifolds for miniaturized chemical analysis systems," *Journal of Micromechanics and Microengineering*, vol. 4, no. 4, p. 246, 1994.

[171] D. Daniel and I. G. Gutz, "Electronic micropipettor: A versatile fluid propulsion and injection device for micro-flow analysis," *Analytica chimica acta*, vol. 571, no. 2, pp. 218–227, 2006.

[172] J. Steigert, M. Grumann, T. Brenner, K. Mittenbühler, T. Nann, J. Rühe, I. Moser, S. Haeberle, L. Riegger, J. Riegler, *et al.*, "Integrated sample preparation, reaction, and detection on a high-frequency centrifugal microfluidic platform," *JALA: Journal of the Association for Laboratory Automation*, vol. 10, no. 5, pp. 331–341, 2005.

[173] B. Jung, K. Fisher, K. D. Ness, K. A. Rose, and R. P. Mariella Jr, "Acoustic particle filter with adjustable effective pore size for automated sample preparation," *Analytical chemistry*, vol. 80, no. 22, pp. 8447–8452, 2008.

[174] S. Choi and J.-K. Park, "Microfluidic system for dielectrophoretic separation based on a trapezoidal electrode array," *Lab on a Chip*, vol. 5, no. 10, pp. 1161–1167, 2005.

[175] P. Sabounchi, A. M. Morales, P. Ponce, L. P. Lee, B. A. Simmons, and R. V. Davalos, "Sample concentration and impedance detection on a microfluidic polymer chip," *Biomedical Microdevices*, vol. 10, no. 5, p. 661, 2008.

[176] R. B. Brown and J. Audet, "Current techniques for single-cell lysis," *Journal of the Royal Society Interface*, vol. 5, no. Suppl 2, pp. S131–S138, 2008.

[177] J. Waterval, H. Lingeman, A. Bult, and W. J. Underberg, "Derivatization trends in capillary electrophoresis," *Electrophoresis*, vol. 21, no. 18, pp. 4029–4045, 2000.

[178] H. Suzuki, C.-M. Ho, and N. Kasagi, "A chaotic mixer for magnetic bead-based micro cell sorter," *Journal of Microelectromechanical Systems*, vol. 13, no. 5, pp. 779–790, 2004.

[179] Z. Yang, S. Matsumoto, H. Goto, M. Matsumoto, and R. Maeda, "Ultrasonic micromixer for microfluidic systems," *Sensors and Actuators A: Physical*, vol. 93, no. 3, pp. 266–272, 2001.

[180] A. P. Sudarsan and V. M. Ugaz, "Fluid mixing in planar spiral microchannels," *Lab on a Chip*, vol. 6, no. 1, pp. 74–82, 2006.

[181] H. Chen and J.-C. Meiners, "Topologic mixing on a microfluidic chip," *Applied Physics Letters*, vol. 84, no. 12, pp. 2193–2195, 2004.

[182] A. V. Pattekar and M. V. Kothare, "A microreactor for hydrogen production in micro fuel cell applications," *Journal of Microelectromechanical Systems*, vol. 13, no. 1, pp. 7–18, 2004.

[183] Z. T. Cygan, J. T. Cabral, K. L. Beers, and E. J. Amis, "Microfluidic platform for the generation of organic-phase microreactors," *Langmuir*, vol. 21, no. 8, pp. 3629–3634, 2005.

[184] H. Aran, D. Salamon, T. Rijnaarts, G. Mul, M. Wessling, and R. Lammertink, "Porous photocatalytic membrane microreactor (p2m2): a new reactor concept for photochemistry," *Journal of Photochemistry and Photobiology A: Chemistry*, vol. 225, no. 1, pp. 36–41, 2011.

[185] Q. Ramadan, V. Samper, D. P. Poenar, and C. Yu, "An integrated microfluidic platform for magnetic microbeads separation and confinement," *Biosensors and Bioelectronics*, vol. 21, no. 9, pp. 1693–1702, 2006.

[186] M. D. Vahey and J. Voldman, "An equilibrium method for continuous-flow cell sorting using dielectrophoresis," *Analytical chemistry*, vol. 80, no. 9, pp. 3135–3143, 2008.

[187] J. Pipper, Y. Zhang, P. Neuzil, and T.-M. Hsieh, "Clockwork pcr including sample preparation," *Angewandte Chemie International Edition*, vol. 47, no. 21, pp. 3900–3904, 2008.

[188] L. Zhu, C. Lee, and D. DeVoe, "Integrated microfluidic uv absorbance detector with attomol-level sensitivity for bsa," *Lab on a Chip*, vol. 6, no. 1, pp. 115–120, 2006.

[189] X. Fan, I. M. White, H. Zhu, J. D. Suter, and H. Oveys, "Overview of novel integrated optical ring resonator bio/chemical sensors," in *Lasers and Applications in Science and Engineering*, pp. 64520M–64520M, International Society for Optics and Photonics, 2007.

[190] Y. Yang, C. Li, J. Kameoka, K. H. Lee, and H. Craighead, "A polymeric microchip with integrated tips and in situ polymerized monolith for electrospray mass spectrometry," *Lab on a Chip*, vol. 5, no. 8, pp. 869–876, 2005.

[191] E. Ghafar-Zadeh and M. Sawan, "Charge-based capacitive sensor array for cmos-based laboratory-on-chip applications," *IEEE Sensors Journal*, vol. 8, no. 4, pp. 325–332, 2008.

[192] J. Fu, R. B. Schoch, A. L. Stevens, S. R. Tannenbaum, and J. Han, "A patterned anisotropic nanofluidic sieving structure for continuous-flow separation of dna and proteins," *Nature nanotechnology*, vol. 2, no. 2, pp. 121–128, 2007.

[193] S. Schumacher, J. Nestler, T. Otto, M. Wegener, E. Ehrentreich-Förster, D. Michel, K. Wunderlich, S. Palzer, K. Sohn, A. Weber, *et al.*, "Highly-integrated lab-on-chip system for point-of-care multiparameter analysis," *Lab on a Chip*, vol. 12, no. 3, pp. 464–473, 2012.

[194] D. Moschou and A. Tserepi, "The lab-on-pcb approach: tackling the μtas commercial upscaling bottleneck," *Lab on a Chip*, vol. 17, no. 8, pp. 1388–1405, 2017.

[195] C.-Y. Liu, J. Rick, T.-C. Chou, H.-H. Lee, and G.-B. Lee, "Integrated microfluidic system for electrochemical sensing of urinary proteins," *Biomedical microdevices*, vol. 11, no. 1, p. 201, 2009.

[196] S. W. Park, J. H. Lee, H. C. Yoon, B. W. Kim, S. J. Sim, H. Chae, and S. S. Yang, "Fabrication and testing of a pdms multi-stacked hand-operated loc for use in portable immunosensing systems," *Biomedical microdevices*, vol. 10, no. 6, pp. 859–868, 2008.

[197] Y.-F. Lee, K.-Y. Lien, H.-Y. Lei, and G.-B. Lee, "An integrated microfluidic system for rapid diagnosis of dengue virus infection," *Biosensors and Bioelectronics*, vol. 25, no. 4, pp. 745–752, 2009.

[198] S. Schumacher, J. Nestler, T. Otto, M. Wegener, E. Ehrentreich-Förster, D. Michel, K. Wunderlich, S. Palzer, K. Sohn, A. Weber, *et al.*, "Highly-integrated lab-on-chip system for point-of-care multiparameter analysis," *Lab on a Chip*, vol. 12, no. 3, pp. 464–473, 2012.

[199] Y. Yu, J. Chen, and J. Zhou, "Parallel-plate lab-on-a-chip based on digital microfluidics for on-chip electrochemical analysis," *Journal of Micromechanics and Microengineering*, vol. 24, no. 1, p. 015020, 2013.

[200] C. Aracil, F. Perdigones, J. M. Moreno, and J. M. Quero, "BETTS: bonding, exposing and transferring technique in SU-8 for microsystems fabrication," *Journal of Micromechanics and Microengineering*, vol. 20, no. 3, p. 035008, 2010.

[201] G. Flores, C. Aracil, F. Perdigones, and J. Quero, "Low consumption single-use microvalve for microfluidic PCB-based platforms," *Journal of Micromechanics and Microengineering*, vol. 24, no. 6, p. 065013, 2014.

[202] G. Murillo, Z. J. Davis, S. Keller, G. Abadal, J. Agusti, A. Cagliani, N. Noeth, A. Boisen, and N. Barniol, "Novel su-8 based vacuum wafer-level packaging for mems devices," *Microelectronic engineering*, vol. 87, no. 5, pp. 1173–1176, 2010.

[203] A. Gerlach, W. Keller, J. Schulz, and K. Schumacher, "Gas permeability of adhesives and their application for hermetic packaging of microcomponents," *Microsystem Technologies*, vol. 7, no. 1, pp. 17–22, 2001.

[204] C. Zhang, D. Xing, and Y. Li, "Micropumps, microvalves, and micromixers within pcr microfluidic chips: advances and trends," *Biotechnology advances*, vol. 25, no. 5, pp. 483–514, 2007.

[205] S. Choi, "Powering point-of-care diagnostic devices," *Biotechnology advances*, vol. 34, no. 3, pp. 321–330, 2016.

[206] J. Wang, "Electrochemical glucose biosensors," *Chemical reviews*, vol. 108, no. 2, pp. 814–825, 2008.

[207] R. J. Russell, M. V. Pishko, C. C. Gefrides, M. J. McShane, and G. L. Cote, "A fluorescence-based glucose biosensor using concanavalin a and dextran encapsulated in a poly (ethylene glycol) hydrogel," *Analytical Chemistry*, vol. 71, no. 15, pp. 3126–3132, 1999.

[208] W. Shi, Q. Wang, Y. Long, Z. Cheng, S. Chen, H. Zheng, and Y. Huang, "Carbon nanodots as peroxidase mimetics and their applications to glucose detection," *Chemical Communications*, vol. 47, no. 23, pp. 6695–6697, 2011.

[209] G.-T. T. GOD-POD. urlhttp://www.spinreact.com/ash.

[210] C. Aracil, F. Perdigones, J. M. Moreno, A. Luque, G. Flores, and J. M. Quero, "Depressurised reservoirs for portable fluid extraction in su-8-based microfluidic systems," *Micro & Nano Letters*, vol. 9, no. 11, pp. 821–824, 2014.

[211] G. Flores, F. Perdigones, C. Aracil, and J. Quero, "Pressurization method for controllable impulsion of liquids in microfluidic platforms," *Microelectronic Engineering*, 2015.

[212] G. Flores, F. Perdigones, and J. Quero, "Pressurized microvalve with smd-based activation to drive fluid in low-cost and autonomous mems," in *Electron Devices (CDE), 2013 Spanish Conference on*, pp. 147–150, IEEE, 2013.

[213] G. Flores, F. Perdigones, C. Aracil, M. Cabello, and J. Quero, "Microfluidic platform with absorbance sensor for glucose detection," in *Electron Devices (CDE), 2015 10th Spanish Conference on*, pp. 1–4, IEEE, 2015.

[214] J. Singhal, D. Pinho, R. Lopes, P. C Sousa, V. Garcia, H. Schütte, R. Lima, and S. Gassmann, "Blood flow visualization and measurements in microfluidic devices fabricated by a micromilling technique," *Micro and Nanosystems*, vol. 7, no. 3, pp. 148–153, 2015.

[215] "Loctite website." urlhttp://www.loctite.co.uk.

[216] "Epotek website." urlhttp://www.epotek.com.

[217] N. Halonen, J. Kilpijärvi, M. Sobocinski, T. Datta-Chaudhuri, A. Hassinen, S. B. Prakash, P. Möller, P. Abshire, E. Smela, S. Kellokumpu, *et al.*, "Low temperature co-fired ceramic package for lab-on-cmos applied in cell viability monitoring," *Procedia Engineering*, vol. 120, pp. 1079–1082, 2015.

[218] S.-M. Kuo and C.-H. Lin, "Fabrication of aspherical su-8 microlens array utilizing novel stamping process and electro-static pulling method," *Optics express*, vol. 18, no. 18, pp. 19114–19119, 2010.

[219] S. Satyanarayana, R. N. Karnik, and A. Majumdar, "Stamp-and-stick room-temperature bonding technique for microdevices," *Journal of Microelectromechanical Systems*, vol. 14, no. 2, pp. 392–399, 2005.

[220] J. Singhal, D. Pinho, R. Lopes, P. C Sousa, V. Garcia, H. Schütte, R. Lima, and S. Gassmann, "Blood flow visualization and measurements in microfluidic devices fabricated by a micromilling technique," *Micro and Nanosystems*, vol. 7, no. 3, pp. 148–153, 2015.

[221] D. Fenna, *Elsevier's Encyclopedic Dictionary of Measures*. Elsevier Press, 1998.